GET OVER THE GUT: APICOMPLEXAN PARASITE INTERACTION, SURVIVAL AND STAGE PROGRESSION IN VERTEBRATE AND INVERTEBRATE DIGESTIVE TRACTS

EDITED BY: Chandra Ramakrishnan, Robert Sinden and Nicholas Charles Smith
PUBLISHED IN: Frontiers in Cellular and Infection Microbiology

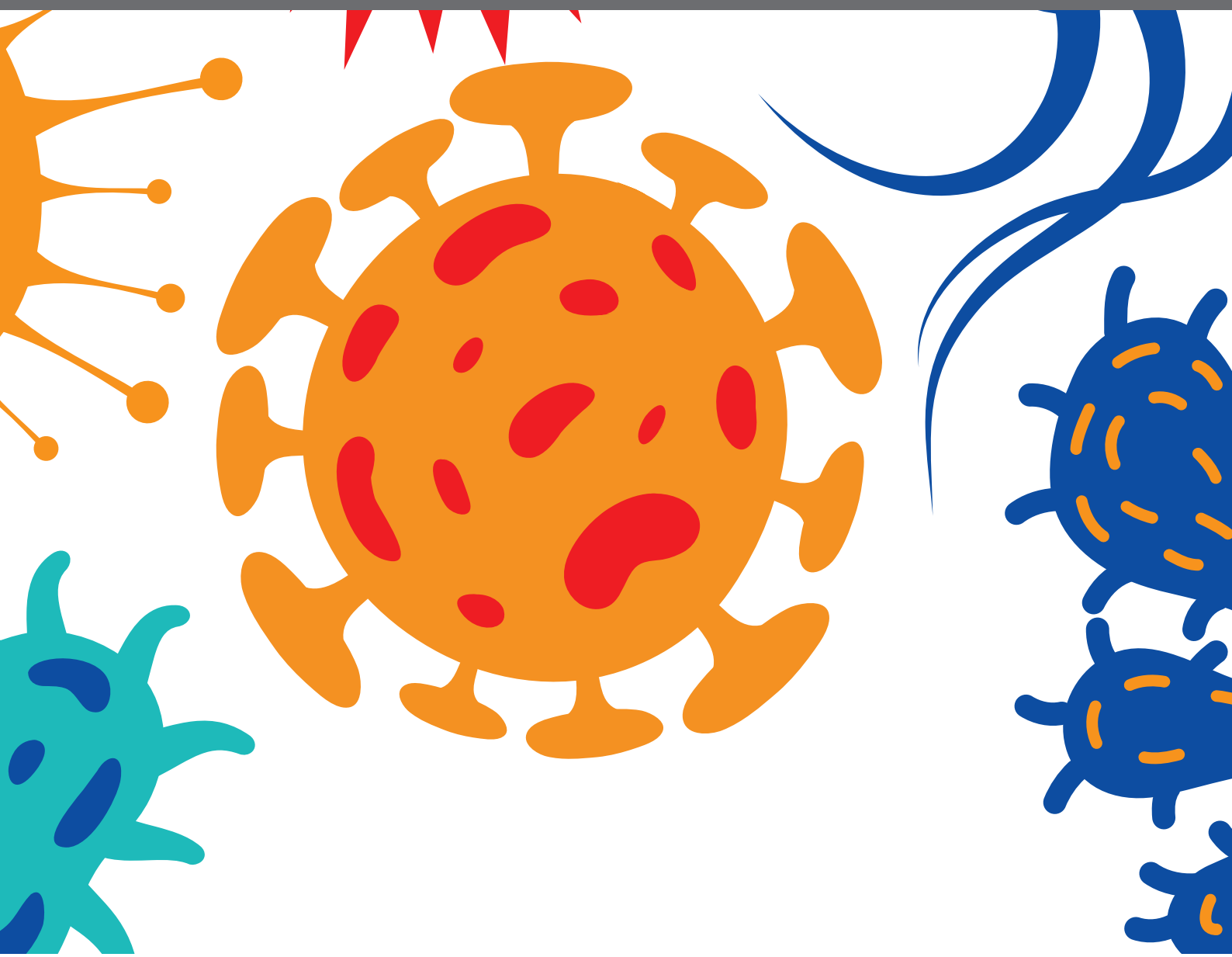

frontiers Research Topics

frontiers

ISSN 1664-8714
ISBN 978-2-88966-926-4
DOI 10.3389/978-2-88966-926-4

About Frontiers

Frontiers is more than just an open-access publisher of scholarly articles: it is a pioneering approach to the world of academia, radically improving the way scholarly research is managed. The grand vision of Frontiers is a world where all people have an equal opportunity to seek, share and generate knowledge. Frontiers provides immediate and permanent online open access to all its publications, but this alone is not enough to realize our grand goals.

Frontiers Journal Series

The Frontiers Journal Series is a multi-tier and interdisciplinary set of open-access, online journals, promising a paradigm shift from the current review, selection and dissemination processes in academic publishing. All Frontiers journals are driven by researchers for researchers; therefore, they constitute a service to the scholarly community. At the same time, the Frontiers Journal Series operates on a revolutionary invention, the tiered publishing system, initially addressing specific communities of scholars, and gradually climbing up to broader public understanding, thus serving the interests of the lay society, too.

Dedication to Quality

Each Frontiers article is a landmark of the highest quality, thanks to genuinely collaborative interactions between authors and review editors, who include some of the world's best academicians. Research must be certified by peers before entering a stream of knowledge that may eventually reach the public - and shape society; therefore, Frontiers only applies the most rigorous and unbiased reviews.
Frontiers revolutionizes research publishing by freely delivering the most outstanding research, evaluated with no bias from both the academic and social point of view. By applying the most advanced information technologies, Frontiers is catapulting scholarly publishing into a new generation.

What are Frontiers Research Topics?

Frontiers Research Topics are very popular trademarks of the Frontiers Journals Series: they are collections of at least ten articles, all centered on a particular subject. With their unique mix of varied contributions from Original Research to Review Articles, Frontiers Research Topics unify the most influential researchers, the latest key findings and historical advances in a hot research area! Find out more on how to host your own Frontiers Research Topic or contribute to one as an author by contacting the Frontiers Editorial Office: frontiersin.org/about/contact

GET OVER THE GUT: APICOMPLEXAN PARASITE INTERACTION, SURVIVAL AND STAGE PROGRESSION IN VERTEBRATE AND INVERTEBRATE DIGESTIVE TRACTS

Topic Editors:
Chandra Ramakrishnan, University of Zurich, Switzerland
Robert Sinden, Imperial College London, United Kingdom
Nicholas Charles Smith, University of Technology Sydney, Australia

Citation: Ramakrishnan, C., Sinden, R., Smith, N. C., eds. (2021). Get over the Gut: Apicomplexan Parasite Interaction, Survival and Stage Progression in Vertebrate and Invertebrate Digestive Tracts. Lausanne: Frontiers Media SA. doi: 10.3389/978-2-88966-926-4

Table of Contents

04 ***Editorial: Get Over the Gut: Apicomplexan Parasite Interaction, Survival and Stage Progression in Vertebrate and Invertebrate Digestive Tracts***
Nicholas C. Smith, Robert E. Sinden and Chandra Ramakrishnan

07 ***The Growth of* Eimeria tenella*: Characterization and Application of Quantitative Methods to Assess Sporozoite Invasion and Endogenous Development in Cell Culture***
Virginia Marugan-Hernandez, Georgia Jeremiah, Kelsilandia Aguiar-Martins, Alana Burrell, Sue Vaughan, Dong Xia, Nadine Randle and Fiona Tomley

20 ***Crypto-Currency: Investing in New Models to Advance the Study of* Cryptosporidium *Infection and Immunity***
N. Bishara Marzook and Adam Sateriale

27 ***Midgut Mitochondrial Function as a Gatekeeper for Malaria Parasite Infection and Development in the Mosquito Host***
Shirley Luckhart and Michael A. Riehle

35 ***A Hetero-Multimeric Chitinase- Containing* Plasmodium falciparum *and* Plasmodium gallinaceum *Ookinete-Secreted Protein Complex Involved in Mosquito Midgut Invasion***
Kailash P. Patra, Hargobinder Kaur, Surendra Kumar Kolli, Jacob M. Wozniak, Judith Helena Prieto, John R. Yates III, David J. Gonzalez, Chris J. Janse and Joseph M. Vinetz

55 ***From Initiators to Effectors: Roadmap Through the Intestine During Encounter of* Toxoplasma gondii *With the Mucosal Immune System***
Lindsay M. Snyder and Eric Y. Denkers

65 ***The Absence of Gut Microbiota Alters the Development of the Apicomplexan Parasite* Eimeria tenella**
Pauline Gaboriaud, Guillaume Sadrin, Edouard Guitton, Geneviève Fort, Alisson Niepceron, Nathalie Lallier, Christelle Rossignol, Thibaut Larcher, Alix Sausset, Rodrigo Guabiraba, Anne Silvestre, Sonia Lacroix-Lamandé, Catherine Schouler, Fabrice Laurent and Françoise I. Bussière

74 ***A Protective and Pathogenic Role for Complement During Acute* Toxoplasma gondii *Infection***
Patricia M. Sikorski, Alessandra G. Commodaro and Michael E. Grigg

83 ***Harmonization of Protocols for Multi- Species Organoid Platforms to Study the Intestinal Biology of* Toxoplasma gondii *and Other Protozoan Infections***
David Holthaus, Estefanía Delgado-Betancourt, Toni Aebischer, Frank Seeber and Christian Klotz

101 ***Using scRNA-seq to Identify Transcriptional Variation in the Malaria Parasite Ookinete Stage***
Kathrin Witmer, Farah Aida Dahalan, Tom Metcalf, Arthur M. Talman, Virginia M. Howick and Mara K. N. Lawniczak

114 ***Identification of Three Novel* Plasmodium *Factors Involved in Ookinete to Oocyst Developmental Transition***
Chiamaka V. Ukegbu, George K. Christophides and Dina Vlachou

frontiers in Cellular and Infection Microbiology

EDITORIAL
published: 28 April 2021
doi: 10.3389/fcimb.2021.680555

Editorial: Get Over the Gut: Apicomplexan Parasite Interaction, Survival and Stage Progression in Vertebrate and Invertebrate Digestive Tracts

Nicholas C. Smith[1,2], *Robert E. Sinden*[3] *and Chandra Ramakrishnan*[4*]

[1] School of Life Sciences, University of Technology Sydney, Sydney, NSW, Australia, [2] Research School of Biology, Australian National University, Canberra, ACT, Australia, [3] Department of Life Sciences, Imperial College London, London, United Kingdom, [4] Institute of Parasitology, University of Zurich, Zurich, Switzerland

Keywords: Apicomplexa, barrier, gut, immune system, microbiota, host, model system

Editorial on the Research Topic

Get Over the Gut: Apicomplexan Parasite Interaction, Survival and Stage Progression in Vertebrate and Invertebrate Digestive Tracts

OPEN ACCESS

Edited and reviewed by:
Tania F. De Koning-Ward, Deakin University, Australia

***Correspondence:**
Chandra Ramakrishnan
chandra.ramakrishnan@uzh.ch

Specialty section:
This article was submitted to Parasite and Host, a section of the journal Frontiers in Cellular and Infection Microbiology

Received: *14 March 2021*
Accepted: *08 April 2021*
Published: *28 April 2021*

Citation:
Smith NC, Sinden RE and Ramakrishnan C (2021) Editorial: Get Over the Gut: Apicomplexan Parasite Interaction, Survival and Stage Progression in Vertebrate and Invertebrate Digestive Tracts. Front. Cell. Infect. Microbiol. 11:680555. doi: 10.3389/fcimb.2021.680555

INTRODUCTION

For endoparasites, invasion of their hosts represents the greatest challenge to survival; for many it is the gut of the host/vector that present this barrier. Those barriers are increasingly being recognized as optimal targets for intervention strategies (Sinden, 2010; Smith et al., 2014; Sinden, 2017). The phylum Apicomplexa embraces thousands of species of parasites of vertebrates and invertebrates, many of major veterinary/medical importance including important agents of zoonoses. Whilst certain parasites are monoxenous (*e.g.*, *Eimeria*, *Cryptosporidium*), others are heteroxenous (*e.g. Plasmodium*, *Toxoplasma gondii*) with distinct developmental pathways in each host. All Apicomplexans are thought to undergo critical developmental phases within intestinal tracts; thus, infection or transition of a gut is crucial for their survival. In this Research Topic, we present contributions on mechanisms of gut infection and traversal; the gut as a barrier to parasites; model systems for parasite development, and the impact of gut microbiota upon the infection process.

THE GUT: AN ENTRANCE AND A BARRIER

The gut is a parasite entry point, but also a significant host barrier to infection. In the case of *T. gondii* infecting intermediate hosts, the gut offers several routes by which to reach the lamina propria and beyond: direct infection of epithelial cells and replication before moving further; intercellular traversal; or subversion of immune cells to become 'Trojan horses'. These processes

trigger immune responses, and cells serving as Trojan horses can also be involved in combatting parasites (reviewed by Snyder and Denkers). Additionally, whilst parasites may need to protect themselves from the complement system, there may be an advantage if they stimulate a certain level of protective immunity to avoid killing their hosts *via* unchecked proliferation (reviewed in Sikorski et al.). Moreover, host and parasite are rarely alone; the 'environmental' microbiota play an important role in regulation of immunity and inflammation (reviewed by Snyder and Denkers and Sikorski et al.).

Plasmodium encounters the gut after having been taken up by the mosquito in a blood meal. Gametogenesis and fertilization happen rapidly after arrival in the midgut, being triggered by the changes in environment. The midgut lumen is a hostile place for *Plasmodium*, with factors from both the blood and the mosquito targeting the parasite. To escape this attack, the fertilized parasite transforms into a motile ookinete, which immediately faces the obstacle of a chitin-rich peritrophic matrix. To overcome this barrier, *Plasmodium* is thought to use a complex comprised of proteins that mediate recognition and attachment and a chitinase to digest chitin (Patra et al.). Additionally, mitochondrial function of the midgut epithelial cells is dynamic and thought to be involved in resistance to pathogens (reviewed in Luckhart and Riehle).

Using loss-of-function mutants, a large number of genes involved in ookinete motility, invasion and differentiation have been identified in *Plasmodium*. However, not only the absence or presence of a gene, but the fine-tuning of its expression may play a role in the parasite's capacity to overcome the gut and differentiate. Witmer et al. hypothesize that genes may be differentially regulated among different individual ookinetes as a potential 'bet-hedging' strategy. Using single-cell RNA sequencing, they show that transcriptional variations occur within inbred populations and propose candidate genes involved in bet-hedging. Once the parasite gets to the other side of the midgut, differentiation to oocysts takes place; Ukegbu et al. have identified three genes that are important in the transition of ookinetes to oocysts, likely operating downstream of midgut traversal.

MODEL SYSTEMS TO STUDY PARASITE-GUT INTERACTION

Studying the interplay between parasite and the gut is not straightforward because either *in vitro* systems or *in vivo* models have not yet been established or do not support all stages of development. *In vitro* systems are also commonly a prerequisite for high through-put screening of anti-parasitic drugs and may be useful for the identification of vaccine candidates.

In the case of a major agent of chicken coccidiosis, *Eimeria tenella*, *in vitro* systems only support the development of early asexual stages or produce very low yields of sexual stages and oocysts. However, innovative use of Madin-Darby Bovine Kidney (MDBK) epithelial cells has enabled researchers to mimic sporozoite invasion *in vitro* and even obtain first generation merozoites (Marugan-Hernandez et al., 2020). Additionally, this *in vitro* platform enables screening of anticoccidial drugs. Several *in vitro* platforms using multiple cell types have shown that sexual development of coccidia may be better supported in such systems (Chen et al., 2013; Worliczek et al., 2013; Martorelli Di Genova et al., 2019). The situation is similar for *Cryptosporidium*, for which two- and three-dimensional cell culture systems supporting sexual development have been established recently (reviewed by Marzook and Sateriale). Additionally, an *in vivo* mouse model for human cryptosporidiosis, using the genetically tractable *Cryptosporidium tyzzeri*, is now available (reviewed by Marzook and Sateriale). Holthaus et al. have achieved harmonized protocols for cultures of human, mouse, pig and chicken intestinal cells that are important hosts for protozoan infections. Using the example of *T. gondii* tachyzoites and *Giardia duodenalis*, the authors also demonstrate the potential utility of their system for co-infection studies.

All these *in vitro* platforms utilize complex media and cellular environments but, whilst more sophisticated than monolayer cultures, they lack important players in the interaction of the host with the parasite, namely, immune cells and microbiota. Introducing bacteria and fungi into these systems is desirable because experiments without microbiota may lead to conclusions that are insecure, as exemplified by a recent *in vivo* study on *E. tenella* showing that, in the absence of intestinal microbiota, parasite replication is altered (Gaboriaud et al.). However, developing *in vitro* systems that incorporate microbiota is challenging because these systems require more complex media to support the growth of diverse cell types, and lack important host factors that control/suppress growth of the replicating bacteria/fungi.

PERSPECTIVES

This Research Topic, with examples from four genera of Apicomplexa, documents the innovative research currently being performed to address interactions between gut and parasite and highlights the fact that the interplay between the two is complex, with both parties having well-developed strategies for their own survival. Novel tools and methodologies are being developed, state-of-the-art techniques expanded, and many new insights gained. As knowledge gaps are being closed, doors are being opened to develop novel intervention strategies against these parasites.

AUTHOR CONTRIBUTIONS

NS, RS and CR have written the editorial. All authors contributed to the article and approved the submitted version.

FUNDING

NS is grateful for research support from the National Health and Medical Research Council (NHMRC) of the Australian Government (Project Grant GNT1128911). These funders played no role in interpretation of data and information researched for this article, its writing, or the decision to submit it for publication.

REFERENCES

Chen, H., Wiedmer, S., Hanig, S., Entzeroth, R., and Kurth, M. (2013). Development of *Eimeria Nieschulzi* (Coccidia, Apicomplexa) Gamonts and Oocysts in Primary Fetal Rat Cells. *J. Parasitol Res.* 2013, 591520. doi: 10.1155/2013/591520

Martorelli Di Genova, B., Wilson, S. K., Dubey, J. P., and Knoll, L. J. (2019). Intestinal delta-6-desaturase Activity Determines Host Range for *Toxoplasma* Sexual Reproduction. *PLoS Biol.* 17, e3000364. doi: 10.1371/journal.pbio.3000364

Sinden, R. E. (2010). A Biologist's Perspective on Malaria Vaccine Development. *Hum. Vaccin* 6, 3–11. doi: 10.4161/hv.6.1.9604

Sinden, R. E. (2017). Targeting the Parasite to Suppress Malaria Transmission. *Adv. Parasitol* 97, 147–185. doi: 10.1016/bs.apar.2016.09.004

Smith, R. C., Vega-Rodríguez, J., and Jacobs-Lorena, M. (2014). The *Plasmodium* Bottleneck: Malaria Parasite Losses in the Mosquito Vector. *Mem Inst Oswaldo Cruz* 109, 644–661. doi: 10.1590/0074-0276130597

Worliczek, H. L., Ruttkowski, B., Schwarz, L., Witter, K., Tschulenk, W., and Joachim, A. (2013). *Isospora Suis* in an Epithelial Cell Culture System - an In Vitro Model for Sexual Development in Coccidia. *PLoS One* 8, e69797. doi: 10.1371/journal.pone.0069797

Conflict of Interest: The authors declare that the research was conducted in the absence of any commercial or financial relationships that could be construed as a potential conflict of interest.

frontiers in Cellular and Infection Microbiology

ORIGINAL RESEARCH
published: 08 October 2020
doi: 10.3389/fcimb.2020.579833

The Growth of *Eimeria tenella*: Characterization and Application of Quantitative Methods to Assess Sporozoite Invasion and Endogenous Development in Cell Culture

Virginia Marugan-Hernandez[1]*, *Georgia Jeremiah*[1], *Kelsilandia Aguiar-Martins*[1], *Alana Burrell*[2], *Sue Vaughan*[3], *Dong Xia*[1], *Nadine Randle*[4] and *Fiona Tomley*[1]

[1] The Royal Veterinary College, University of London, London, United Kingdom, [2] Electron Microscopy Science Technology Platform, The Francis Crick Institute, London, United Kingdom, [3] Department of Biological and Medical Sciences, Oxford Brookes University, Oxford, United Kingdom, [4] Department of Infection Biology, Institute of Infection & Global Health, University of Liverpool, Liverpool, United Kingdom

OPEN ACCESS

Edited by:
Robert Sinden,
Imperial College London,
United Kingdom

Reviewed by:
Renato Augusto DaMatta,
State University of the North Fluminense Darcy Ribeiro, Brazil
Rita Tewari,
University of Nottingham,
United Kingdom

***Correspondence:**
Virginia Marugan-Hernandez
vhernandez@rvc.ac.uk

Specialty section:
This article was submitted to Parasite and Host, a section of the journal Frontiers in Cellular and Infection Microbiology

Received: 03 July 2020
Accepted: 07 September 2020
Published: 08 October 2020

Citation:
Marugan-Hernandez V, Jeremiah G, Aguiar-Martins K, Burrell A, Vaughan S, Xia D, Randle N and Tomley F (2020) The Growth of Eimeria tenella: Characterization and Application of Quantitative Methods to Assess Sporozoite Invasion and Endogenous Development in Cell Culture. Front. Cell. Infect. Microbiol. 10:579833. doi: 10.3389/fcimb.2020.579833

In vitro development of the complete life cycle of *Eimeria* species has been achieved in primary cultures of avian epithelial cells with low efficiency. The use of immortalized cell lines simplifies procedures but only allows partial development through one round of parasite invasion and intracellular replication. We have assessed the suitability of Madin-Darby Bovine Kidney (MDBK) cells to support qualitative and quantitative studies on sporozoite invasion and intracellular development of *Eimeria tenella*. Analysis of parasite ultrastructure by transmission electron microscopy and serial block face—scanning electron microscopy proved the suitability of the system to generate good quality schizonts and first-generation merozoites. Parasite protein expression profiles elucidated by mass spectrometry corroborated previous findings occurring during the development of the parasite such as the presence of alternative types of surface antigen at different stages and increased abundance of proteins from secretory organelles during invasion and endogenous development. Quantitative PCR (qPCR) allowed the tracking of development by detecting DNA division, whereas reverse transcription qPCR of sporozoite- and merozoite-specific genes could detect early changes before cell division and after merozoite formation, respectively. These results correlated with the analysis of development using ImageJ semi-automated image analysis of fluorescent parasites, demonstrating the suitability and reproducibility of the MDBK culture system. This systems also allowed the evaluation of the effects on invasion and development when sporozoites were pre-incubated with anticoccidial drugs, showing similar effects to those reported before. We have described through this study a series of methods and assays for the further application of this *in vitro* culture model to more complex studies of *Eimeria* including basic research on parasite cell biology and host-parasite interactions and for screening anticoccidial drugs.

Keywords: *Eimeria tenella*, cell culture, endogenous development, electron microscopy, quantitative PCR, anticoccidial inhibition

INTRODUCTION

Eimeria tenella is a host- and tissue-specific parasite, replicating *in vivo* only in the epithelial cells that line the caeca of the domestic chicken. This parasite together with six other species (*E. acervulina, E. brunetti, E. maxima, E. mitis, E. necatrix,* and *E. praecox*) is responsible for chicken coccidiosis, an enteric disease characterized by malabsorption, diarrhea, and/or hemorrhage with a significant impact on chicken meat and egg production worldwide. Unlike other *Eimeria* species that infect chickens, purified sporozoites of *E. tenella* invade and undergo some endogenous development in avian and mammalian cells *in vitro*. There was early optimism that avian cells might support the whole developmental life cycle when small numbers of male and female gametocytes were observed several days following sporozoite infection (Strout and Ouellette, 1969). However, despite many efforts and technical innovations the best results achieved to date have come from using primary embryonic chick kidney cells where small numbers of unsporulated oocysts can be produced ($\sim 10^2$ oocysts from an inoculation of 10^4 to 10^5 sporozoites), which sporulate very poorly compared to oocysts produced in chickens (Doran, 1971; Doran and Augustine, 1973; Hofmann and Raether, 1990).

The use of immortalized mammalian cell lines, which are simpler to maintain than primary avian cells, has proven useful to study the early part of the *E. tenella* developmental cycle. Non-avian cells support a single round of asexual growth (schizont development and the release of first-generation merozoites) and for this they are at least as efficient as primary chick cell cultures (Patton, 1965). Several studies agree that many mammalian cell lines are susceptible to sporozoite invasion however they differ widely in their capacity to support schizogony and merozoite formation (Doran and Vetterling, 1967; Tierney and Mulcahy, 2003). The most reliable cells used to date for the study of *E. tenella* sporozoite invasion and intracellular growth are Madin-Darby Bovine Kidney (MDBK) epithelial cells (Brown et al., 2000; Bumstead and Tomley, 2000; Tierney and Mulcahy, 2003). These have been used to examine phenotypes of transgenic *E. tenella* parasites generated by transfection (Clark et al., 2008; Marugan-Hernandez et al., 2017b) and to test the impacts of anticoccidial drugs (Zhu et al., 1994; Jenkins et al., 2014; Thabet et al., 2015, 2017), antibodies (Whitmire et al., 1988), cytokines (Kogut and Lange, 1989), natural compounds (Allen, 2007; Alnassan et al., 2015), and competition with other organisms (Tierney et al., 2004).

In this study, we have used this MDBK cell culture system to develop reliable quantitative *in vitro* assays that measure parasite replication and gene expression during the first round of intracellular schizogony of *E. tenella*. The assays incorporate the use of quantitative PCR (qPCR) as well as reverse transcription qPCR (RT-qPCR) that targets expression of stage-specific (sporozoite and merozoite) genes, combined with semi-automated image analysis. We demonstrate the utility of these combined assays for development of high throughput *in vitro* systems to evaluate anti-parasitic effects of novel treatments and identify by mass spectrometry potential targets expressed at different time points during first generation schizogony.

MATERIALS AND METHODS

Parasites and Birds

The *E. tenella* Wisconsin (Wis) strain (McDougald and Jeffers, 1976) and a transgenic population, *E. tenella* YFPmYFP, derived from this strain (Clark et al., 2008) were propagated in 3-week-old White Leghorn chickens reared under specific pathogen free conditions as previously described (Shirley, 1995). Oocyst purification, excystation and sporozoite purification were performed as described previously (Pastor-Fernandez et al., 2019). Freshly purified sporozoites were used to infect cell monolayers.

Cell Culture

The NBL-1 line of MDBK cells (NBL-1; ECACC-Sigma-Aldrich, Salisbury, UK) was used throughout. Cells were passaged twice weekly by trypsinization of confluent monolayers and maintained in T75 (10×10^6 cells/well) flasks at 37°C, 5% CO_2 in Advanced DMEM (Gibco, Leicestershire, UK) supplemented with 2% fetal bovine serum (FBS; Sigma, Suffolk, UK) and 100 U/ml penicillin/streptomycin (Fisher, Leicestershire, UK). For sporozoite infections, freshly trypsinized MDBK cells were seeded into 24-well plates (0.3×10^6 cells/well).

In vitro Endogenous Development

Freshly seeded MDBK monolayers were infected with sporozoites (1×10^6 sporozoites/well, 3 h after seeding) and incubated at 41°C, 5% CO_2. At 4, 20, 24, 28, 44, 48, 52, and 68 h post infection (hpi) infected monolayers (3 wells/time point, technical replicates) were recovered by pipetting into 0.35 ml of RTL buffer (Qiagen, West Sussex, UK) and stored at −20°C. These experiments were performed in triplicate for both *E. tenella* Wis (three biological replicates) and *E. tenella* YFPmYFP (three biological replicates). Alternately, monolayers (3 wells/time point, technical replicates) were washed gently in phosphate-buffered saline (PBS; 3×1 ml) and fixed in 3% paraformaldehyde in PBS solution followed by a further wash in PBS and storage at 4°C. This experiment was performed in triplicate for *E. tenella* YFPmYFP (three biological replicates).

Anticoccidial Drugs Assay

Sporozoites (1×10^6 per replicate) of *E. tenella* Wis strain were pre-incubated for 1 h at 41°C, 5% CO_2 with a selection of anticoccidial compounds [amprolium (AMP), robenidine (ROB), and salinomycin (SAL)] or with cytochalasin D (CYT); all compounds were suspended to a final concentration of 5 μg/ml in PBS just before use, made from stock concentrations of 10 mg/ml in dimethyl sulfoxide (DMSO). DMSO alone was also included as a control (0.05% final volume). After incubation, sporozoites were washed with PBS, resuspended in DMEM and added to MDBK monolayers (3 wells/time point/condition, technical replicates). After 2, 24, 44, and 52 hpi cells were recovered using 0.35 ml of RTL buffer (Qiagen) for further DNA extraction. This experiment was performed in duplicate for *E. tenella* Wis (two biological replicates).

Isolation of Nucleic Acids and Synthesis of Complementary DNA (cDNA)

Genomic DNA (gDNA) and RNA were isolated from the samples stored in RTL buffer (Qiagen) using the AllPrep DNA/RNA Mini Kit (Qiagen) following manufacturer's instructions. Complementary DNA (cDNA) was synthesized from total RNA following the procedure described by Marugan-Hernandez et al. (2016).

Real Time Quantitative PCR (qPCR) and Reverse Transcription qPCR (RT-qPCR)

Real time quantitative PCR (qPCR) was performed in a CFX96 Touch® Real-Time PCR Detection System (Bio-Rad, Hertfordshire, UK) following the procedures described previously (Marugan-Hernandez et al., 2016). For parasite quantification, the number of haploid genomes (equivalent to single sporozoites or merozoites) per well (3 wells/sample, technical replicates) was determined for each time point using gDNA specific primers for *Eimeria* spp. 5S rDNA (Fw_5S: TCATCACCCAAAGGGATT, Rv_5S: TTCATACTGCGTCTAATGCAC) (Clark et al., 2008) and a standard curve of sporozoite gDNA extracted by the same methods.

For the evaluation of the endogenous development, transgene transcription was quantified from cDNA (RT-qPCR) using specific primers for the sporozoite (SP25: Fw_SP25: AGGCTCTTTACTATGTCCA, Rv_SP25: CAAAAAACACATACAGACGC) and merozoite-specific (MZ80: Fw_MZ80: TTTCGCCGCATGATCATAT, Rv_MZ80: CGATGTCTCCTCTCCAATT) genes from the *esf2* family described by Reid et al. (2014); together with actin (Fw_Actin: TTGTTGTGGTCTTCCGTCA, Rv_Actin: GAATCCGGGGAACATAGTAG). Transcript levels were compared with serial dilutions of DNA standard templates for each transgene (pGEM®-T Easy plasmid (Promega, Hampshire, UK) containing the SP25, MZ80 or actin coding sequences). Transcript numbers along a time-course of intracellular schizont development were normalized to the number of parasite genomes. Data were analyzed with the Bio-Rad CFX Manager software (Bio-Rad).

Light and Fluorescent Microscopy

Digital images from fixed cell monolayers infected with fluorescent *E. tenella* YFPmYFP along the endogenous development time course were captured using a Leica DMI300 B microscope equipped with a high-speed camera DCF365FX (Leica Microsystems, Milton Keynes, UK). Transgenic *E. tenella* YFPmYFP expressing the yellow fluorescent protein (YFP) were detected with the fluorescein isothiocyanate filter (FITC). Exposure, gain, gamma and resolution were adjusted remotely through the Leica application suite software v4.0.0.

ImageJ Semi-Automated Image Analysis

Semi-automated image analysis of representative micrographs taken at each stage during the infection time-course (4, 20, 24, 28, 44, 48, 52, and 68 hpi) was accomplished using a custom script designed to utilize existing ImageJ components, implement new functionality and greatly increase data output.

Digital images of a given resolution comprise a fixed number of pixels determined by their dimensions. Each pixel is assigned a value ranging from 0 to 255 in an 8-bit image, dependent upon the intensity of light detected by the microscope camera at the time of capture. The original pixel values are altered when color channels are applied, leading to an unwanted loss of data integrity. Therefore, each captured image was stored as an 8-bit depth TIF file for continuity purposes and lookup tables (LUTs) were applied to give the illusion of color without altering core pixelation data. Using the ImageJ scripting language, a program was created to load an image, apply LUTs, identify and threshold structures of interest (sporozoite or schizont), mask, map and measure each structure before summarizing individual perimeter and area data.

A LUT is a customizable color map, in which a user can define an array of display colors for given grayscale values between 0 and 255. LUTs allow the user to distinguish between the two different structures with similar light intensities and the "Green Fire Blue" LUT was applied to loaded images, staining sporozoites bright green and schizonts deep blue. Threshold values were hard-coded to maintain consistency between images. Threshold masks were applied separately to duplicate images for sporozoites and schizonts before being converted to binary images with two possible pixel values—black and white. Particle analysis was then conducted by identifying edges at the juxtaposition of white and black pixels to produce structure outlines, record perimeter data and calculate the particle area using ImageJ's inbuilt mathematical library. Perimeter and area data collected from processed images was recorded for analysis.

Samples for Election Microscopy

One-hundred microliters of 25% electron microscopy grade glutaraldehyde were added to MDBK monolayers after 48 hpi in 1 ml of cell-culture medium. Fifteen minutes after the addition of glutaraldehyde, cell-culture medium was removed and replaced by 1 ml of primary fix [20% freshly-prepared formaldehyde solution (10%), 10% electron microscopy grade glutaraldehyde (25%), and 50% sodium cacodylate buffer (0.2 M) in double distilled (dd)H_2O]. Monolayers were washed five times in 0.1 M cacodylate buffer followed by a 60 min incubation in 500 µl of 4% osmium tetroxide and 500 µl of 0.2 M sodium cacodylate buffer. Fixed cells were washed five times in ddH_2O followed by an overnight incubation in 2% freshly-filtered aqueous uranyl acetate (at 4°c and in the dark). Cells were washed three times in ddH_20. Cells were then dehydrated by a series of 20 min incubations in increasing concentration of ethanol in ddH_20. Dehydration steps consisted of 30% ethanol, 50% ethanol, 70% ethanol, 90% ethanol, and 100% ethanol. One milliliter of propylene oxide (TAAB) was added to each well and left for 30 s. Agitating the solution using a Pasteur pipette resulted in detachment of the monolayer which could then be transferred to a 1.5 ml microcentrifuge tube. Detached monolayers were then incubated in three changes of 100% anhydrous acetone, each for 10 min. Cells were incubated in 25% TAAB 812 resin in acetone for 2 h, 50% resin overnight; 75% resin for 6 h; 100% resin

overnight and two changes of 100% resin, each for 2 h. Infected-monolayer pellets were centrifuged for 20 min in fresh 100% resin and polymerized by incubation at 60°C for 24 h.

Transmission Electron Microscopy (TEM)

All two-dimensional electron microscopy imaging was performed using a Hitachi™ H-7560 transmission electron microscope with bottom mount camera (2k CCD, Advanced Microscopy Techniques) and manual tilt and rotation capabilities. Digital images were captured using either 1 or 4 integrations depending on sample stability.

Serial Block Face—Scanning Electron Microscopy (SBF-SEM)

SBF-SEM data was collected using a Zeiss™ Merlin scanning electron microscope with Gatan™ 3View™ automated sectioning and image capture system. The block-face was imaged using a scanning electron beam with 3–5 kV accelerating voltage. Pixel size was between 3 and 7 nm with a section thickness from 60 to 100 nm. Dwell time was ∼2 s per pixel with a scan area of around 4,000 × 4,000 pixels. SBF-SEM data was processed using IMOD™ software, run through Cygwin™ command line interface.

Mass Spectrometry (MS)

MDBK cells infected with *E. tenella* sporozoites at a 4:1 in ratio in T25 flasks (two per time point to generate enough material) were harvested at 4, 24, 36, and 48 hpi. Three biological replicates were prepared per time point. Sample preparation, trypsin digestion and analysis using an LCMS/MS system comprising an Ultimate 3000 nano system coupled to a Q-Exactive mass spectrometer (Thermo Fisher Scientific, Waltham, MA, USA) was performed as described by Horcajo et al. (2018). Spectral data were transformed into.mgf files with Progenesis QI and exported for peptide identification using the Mascot (version 2.3, Matrix Science, London, UK) search engine and the database ToxoDB-26 (version 26, ToxoDB). Protein abundance (iBAQ) was calculated as the sum of all the peak intensities (from the Progenesis output) divided by the number of theoretically observable tryptic peptides for a given protein. Heat maps from MS data were generated Morpheus software (https://software.broadinstitute.org/morpheus/) using hierarchical clustering (one-minus Pearson correlation) to cluster proteins showing similar patterns along the intracellular development.

Data Analysis

Dataset distributions were ascertained using Shapiro-Wilk and D'Agostino-Pearson omnibus normality tests. The skewed 5S, SP25, MZ80, and actin qPCR/RT-qPCR datasets were analyzed using a Friedman's test for each set of triplicate repeats per time point, whilst normally distributed data obtained from the custom ImageJ script were analyzed using a repeated measures one-way ANOVA with a Geisser-Greenhouse correction. Comparisons across contrasting datasets were first normalized (0% = smallest mean, 100% = largest mean per dataset) before using parametric Pearson Coefficient or non-parametric Spearman's Rank tests based on the presence or absence of a Gaussian distribution. Statistically significant differences were established using a $p < 0.05$ and all analyses, including calculation of arithmetic parameters and normalization of comparative datasets were performed using Graphpad Prism software v7.0b (California, USA).

The normality of data for the anticoccidial drug assay was evaluated using Kolmogorov-Smirnov test. Comparison of groups evaluating one factor was performed using One-way Anova for parametric data and Kruskal-Wallis test for non-parametric. Both analyses were followed by Dunnett's multiple comparisons as a *post-hoc* test using Graph Pad Prism 8.0 (California, USA) or SPSS Statistics 22 (New York, USA). Two-way Anova was used to compare two factors among groups. The relative level of inhibition of *E. tenella* between groups treated with anticoccidial drugs was additionally assessed by a method adapted from Thabet et al. (2017). For this, the proportion of invasion or reproduction of parasites was calculated by normalizing samples to DMSO controls to characterize the inhibition level:

$$\text{Level of Inhibition (\%)} = 100 * \left(1 - \frac{\text{Average number of E. tenella genomes in treated sample}}{\text{Average number of E. tenella genomes in sample treated with DMSO}}\right)$$

Ethical Statement

This study was carried out in strict accordance with the Animals (Scientific Procedures) Act 1986, an Act of Parliament of the United Kingdom. All animal studies and protocols were approved by the Royal Veterinary College Ethical Review Committees and the United Kingdom Government Home Office under specific project licenses. The laboratory work involving GMO was conducted under authorization GM9708.1, administered by the UK Health and Safety Executive. The animal facilities for GMO are classified derogated containment level 3.

RESULTS

In vitro MDBK Cell Culture Supported the Endogenous Development of *E. tenella* Leading to Fully Formed First-Generation Merozoites

Cell culture conditions were optimized for an optimal rate of invasion and development of *E. tenella* sporozoites without damaging the MDBK monolayers. In monolayers with over 70% of infected cells (**Figure 1A**) parasites were left for spontaneous development into schizonts. Since first generation schizont development of *E. tenella* in cell culture (from sporozoite infection to the release of first-generation merozoites) is not easily visualized by bright field, we used transgenic parasites expressing a tandemly inserted double copy of YFP under control of the 5'UTR of the *E. tenella* microneme gene *EtMIC1* (*E. tenella* YFPmYFP; Clark et al., 2008) to track parasite development *in vitro*. Micrographs of bright field supported by fluorescence

microscopy at different time points (**Figure 1**) showed the progressive appearance and development of mature schizonts from 44 h post infection (hpi) (**Figures 1M–O**) until the release of first-generation merozoites from 52 hpi (**Figures 1P–U**). Since YFPmYFP is regulated by the EtMIC1 promoter mature merozoites showed a reduced fluorescence (Marugan-Hernandez et al., 2017b).

Transmission electron microscopy (TEM) confirmed the presence of schizonts within MDBK cells and provided fine detail for some of the structures. For example, at 48 h post-infection, host cell endoplasmic reticulum and mitochondria were easily visualized in MDBK cells (**Figure 2A**). At this time, maturing schizonts containing multiple nuclei were observed within parasitophorous vacuoles, delineated by a parasitophorous vacuole membrane (**Figures 2B,C**). Immature merozoite structures were visible including newly formed conoid structures that could be seen budding from the periphery of some schizonts (**Figure 2D**) as well as intra-schizont structures including microtubules, situated just under the schizont multi-layered membrane and several multi-laminar apicoplasts (**Figures 2E,F**). Mature schizonts were also visualized by TEM at 68 hpi revealing the presence of multiple fully formed first generation merozoites contained within the parasitophorous vacuole membrane (**Figure 2G**). Inside the merozoites, apical complex structures including micronemes and fully formed conoids (**Figure 2H**) were seen. These observations confirmed the suitability of this *in vitro* cell system to support the development of good quality schizonts and first-generation merozoites.

Serial block face-scanning electron microscopy (SBF-SEM) was carried out to obtain sequential serial sections of whole individual MDBK cells containing intracellular parasites. A total of 836 sequential serial sections were captured and vacuoles containing schizonts were identified. The parasitophorous vacuole membrane, schizont nuclei and single refractile body were segmented for each schizont (**Figure 3A**). Of the three schizonts imaged by this technology, one of the schizonts contained two nuclei, one contained four nuclei and one contained 16 nuclei (**Figures 3B–D**). As these nuclei numbers are all within a doubling sequence [2, 4, (8), 16] this data suggests co-ordinated nuclear division, however, further analysis is required to assess this hypothesis.

Differential Expression of Proteins Related to Invasion and Endogenous Development Processes Can Be Detected in the MDBK *in vitro* System

Over 200 proteins were identified by MS as differentially expressed at four different time points after *E. tenella* sporozoites infection of cell monolayers (4, 24, 36, and 48 hpi). From these identified proteins, we selected those described as being related to invasion and endogenous development and clustered them according to level of expression at the different time points (**Figure 4**). They grouped into three main distinct clusters: proteins expressed in freshly-released sporozoites (ready for invasion) which are downregulated after invasion and during development (**Figure 4B**); proteins overexpressed early after invasion (**Figure 4A**); proteins overexpressed during schizont

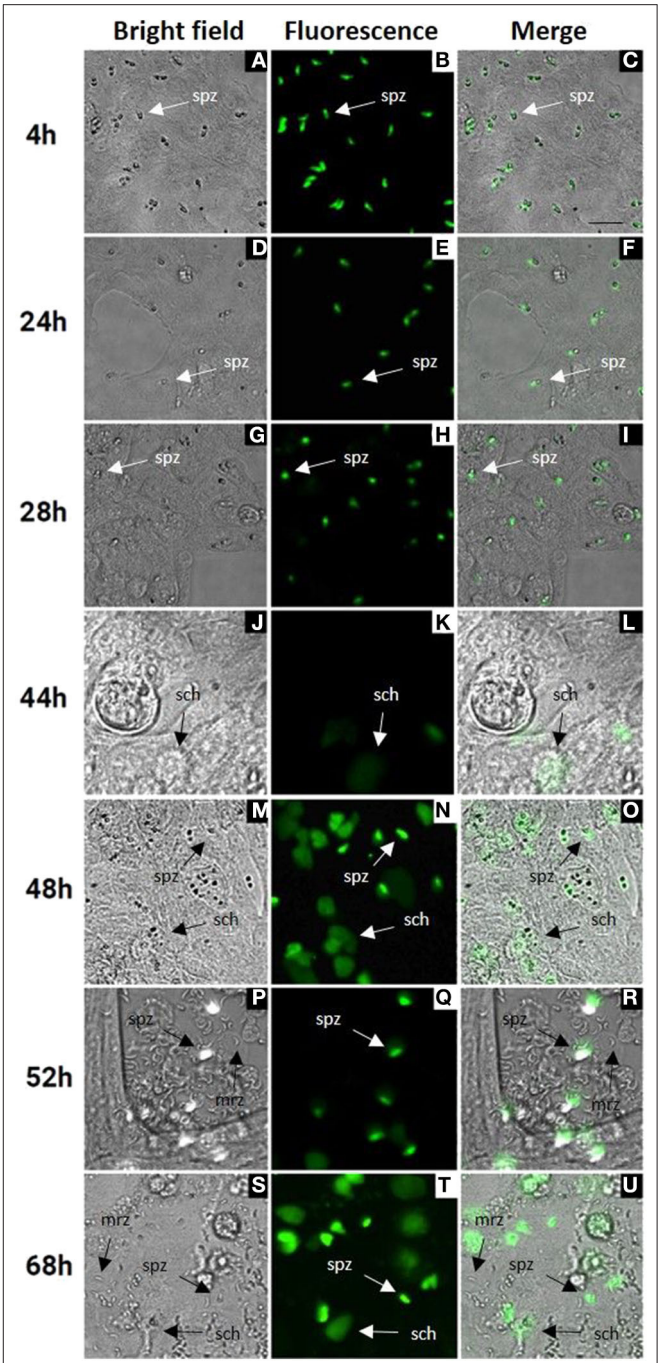

FIGURE 1 | MDBK cell monolayers after infection with *E. tenella* YFPmYFP sporozoites. Time points after infection are indicated in the left side (4–68 h). **(A–C)** Sporozoites (spz) after invasion of MDBK cells. **(D–I)** Rounded sporozoites (spz) preparing to undergo schizogony. **(J–L)** Appearance of early schizonts (sch). **(M–O)** Development of late schizonts (sch) with presence of undeveloped sporozoites (spz). **(P–U)** Release of first-generation merozoites (mrz) with presence of late schizonts (sch) and undeveloped sporozoites (spz), cell monolayer destruction is observed. Scale ∼25 μm.

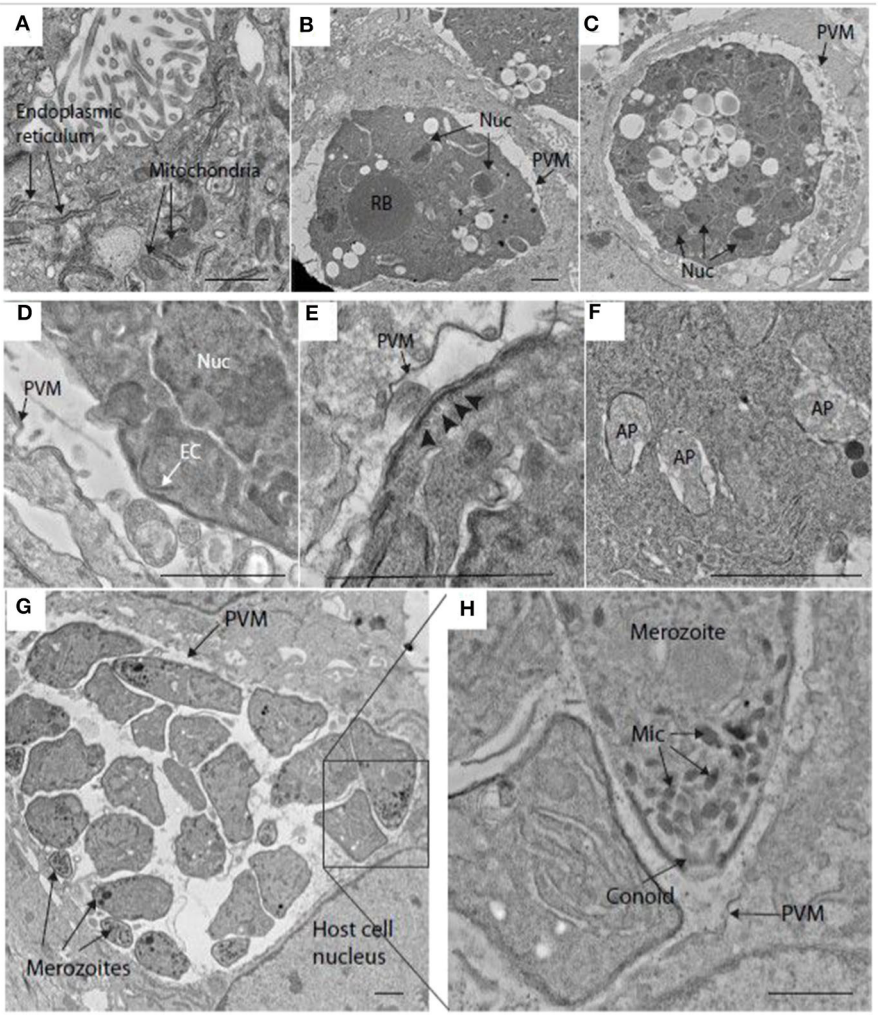

FIGURE 2 | Transmission electron microscopy (TEM) image of schizonts in MDBK cells. **(A)** MDBK cell at 48 hpi showing mitochondria and endoplasmic reticulum. **(B,C)** Parasite at 48 hpi containing multiple nuclei (Nuc) within a specialized compartment bound by the parasitophorous vacuole membrane (PVM). **(D)** Early merozoite formation at the surface of a schizont at 48 hpi. A structure resembling an early conoid (EC) is near one of the schizont nuclei (Nuc). **(E)** Surface of a schizont close to the PVM, microtubules can be seen running below the multi-laminar schizont surface (arrowheads, 48 hpi). **(F)** Multiple apicoplasts (AP) within the cytoplasm of a schizont at 48 hpi. **(G)** Mature schizont encased within a PVM containing several well-developed merozoites at 68 hpi (some indicated by arrows). **(H)** This image is a magnification form the squared area in image **(G)**. showing some merozoite organelles such as the micronemes (Mic) and conoid. Scale ∼1 μm.

development and/or in fully-formed fist-generation merozoites (**Figure 4C**).

There was very good correlation between the identified proteins expression along the time course and what has been described in the literature. Sporozoites ready to invade show overexpression of five different surface antigens (SAGs) which are important proteins in the recognition and attachment of the host cell (Tabares et al., 2004), as well overexpression of apical membrane antigen-1 (AMA1) and three rhoptry neck proteins (RONs) which are components of the moving junction, an essential structure for the invasion of the host cell in many Apicomplexa parasites (Besteiro et al., 2011). Three rhoptry kinases (ROPK), essential for intracellular survival through interaction with host proteins (Diallo et al., 2019), are also overexpressed by these pre-invading sporozoites. Once sporozoites have invaded the host cell (4 hpi), a switch in repertoire of SAG protein expression was observed, with four different SAGs found overexpressed here. All the detected microneme proteins (MICs), which are secreted and re-distributed onto the sporozoite surface to establish physical contact with the host cell during invasion (Carruthers and Tomley, 2008) are overexpressed in this cluster, indicative of recent and active invasion that is still taking place at this point (see **Figure 1A**). A rhomboid proteinase, involved in the cleavage of MICs from the parasite surface during invasion (Zheng et al., 2014), was also found. Sporozoite antigen SO7 and Eimepsin, proteins stored in refractile bodies—the largest sporozoite organelles that are of unknown function (de Venevelles et al.,

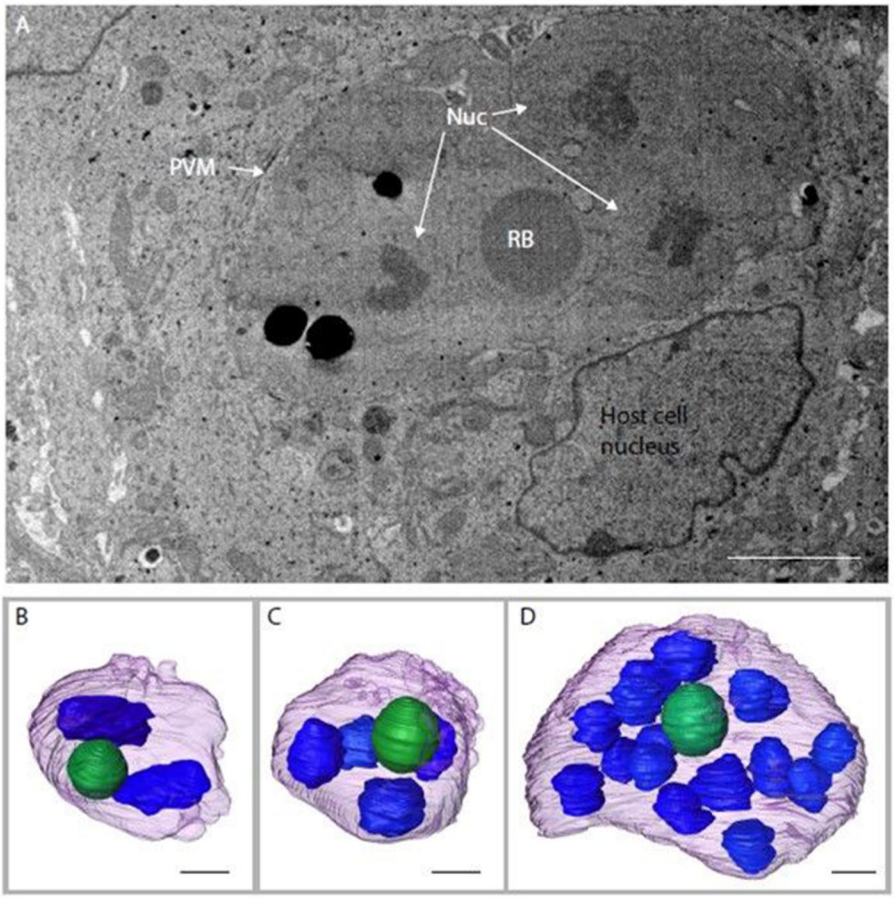

FIGURE 3 | Schizonts imaged by SBF-SEM. **(A)** Single slice from SBF-SEM data showing a multi-nuclear schizont developing within a host cell at 48 hpi (Nuc, nuclei; RB, refractile body; PVM, parasitophorous vacuole membrane). **(B-D)** Surface-rendered models of three schizonts found by SBF-SEM imaging at 48 hpi: schizont with a volume of 311.4 μm^3 containing two nuclei (blue) and a single refractile body (green) **(B)**; schizont with a volume of 308.7 μm^3 containing four nuclei and a single refractile body **(C)**; schizont with a volume of 359.8 μm^3 containing 16 nuclei and a single refractile body **(D)**. Schizont outer surface is shown in purple. Scale ~2 μm.

2006), were also overexpressed at this point. Another different set of SAG proteins were overexpressed in the third cluster (corresponding to late development and/or fully-formed first-generation merozoites), together with two proteins homologous to dense granule proteins (GRAs) of other coccidians but not studied in *Eimeria* parasites; with functions are related to the formation of the parasitophorous vacuole membrane for intracellular survival (Mercier and Cesbron-Delauw, 2015).

Parasite Replication and Stage-Specific Gene Transcription Evaluated by qPCR and RT-qPCR Evidenced the Endogenous Development Previously Observed by Microscopy

Parasite development was analyzed in a time course experiment by qPCR (**Figure 5**). Increasing amounts of parasite DNA were detected from 28 hpi onwards (indicative of nuclear replication; **Figure 5A**) with levels increasing in a linear fashion thereafter (with a doubling time of 13.2 h). To determine if we could detect changes in parasite endogenous gene expression earlier in the process of schizogony (before the onset of nuclear replication detected by qPCR) we targeted two abundant stage-specific genes (by RT-qPCR). Transcripts of the sporozoite specific gene product SP25 showed a linear decrease in abundance immediately after infection (**Figure 5B**), before nuclear division started, and were almost undetectable from 44 hpi onwards. In contrast, transcripts of the merozoite specific gene product MZ80 increased slowly during the initial 28 hpi and thereafter increased rapidly until around 52 hpi (**Figure 5C**). These later time points show high variability due to the asynchronous nature of development in addition to the schizont rupture and merozoite release observed at these time points (see **Figures 1P–R**). The transcription of EtActin remained at a low and constant level throughout schizogony, as reported previously (Marugan-Hernandez et al., 2017a). We conclude that measuring the transcription of these two stage-specific gene products provides a useful assay for detecting changes to parasite metabolism that can be measured prior to DNA replication or schizont visualization. SP25 and MZ80 normalized RT-qPCR datasets showed a strong

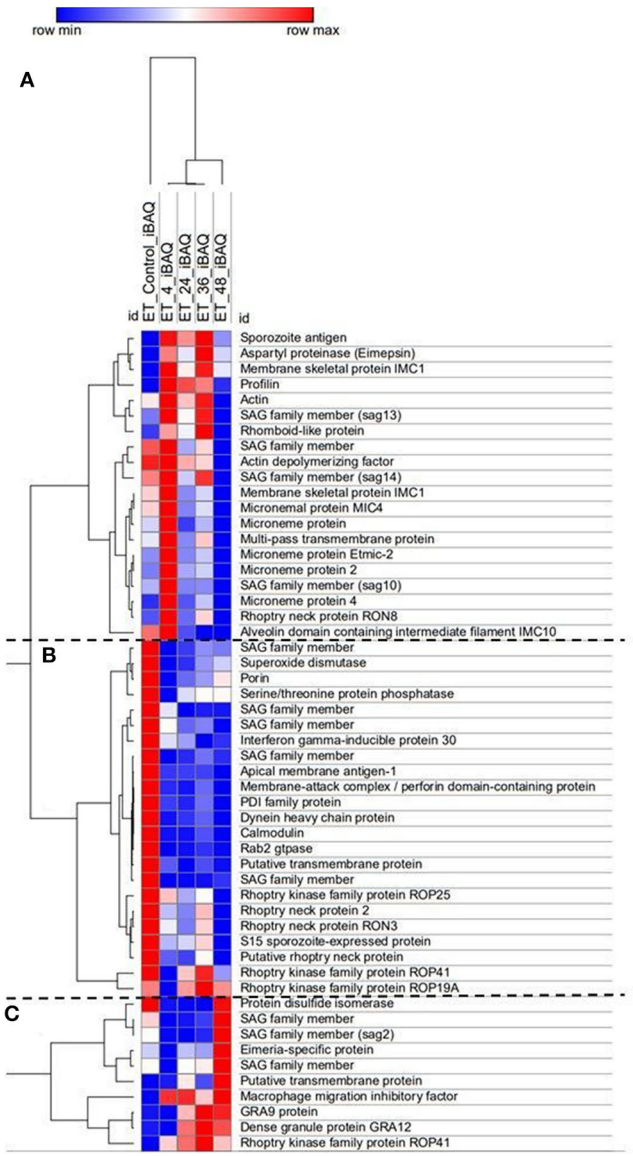

FIGURE 4 | Heat map of *E. tenella* proteins differentially expressed during the *in vitro* development with samples taken at 4, 24, 36, and 48 hpi and freshly-purified sporozoites (control). Cluster **(A)** Proteins highly expressed early after invasion (4 hpi). Cluster **(B)** Proteins expressed in sporozoites whose expression decreased right after invasion and development. Cluster **(C)** Proteins highly expressed during late schizont development (36–48 hpi) and fully-formed first-generation merozoites (48 hpi). iBAQ = Protein abundance. Red/Blue = high/low expression of an individual protein in one specific time point in relation with the rest of time course point and control. Shades of Red/Blue = intermediate values of expression in relation to the extreme values (Red/Blue).

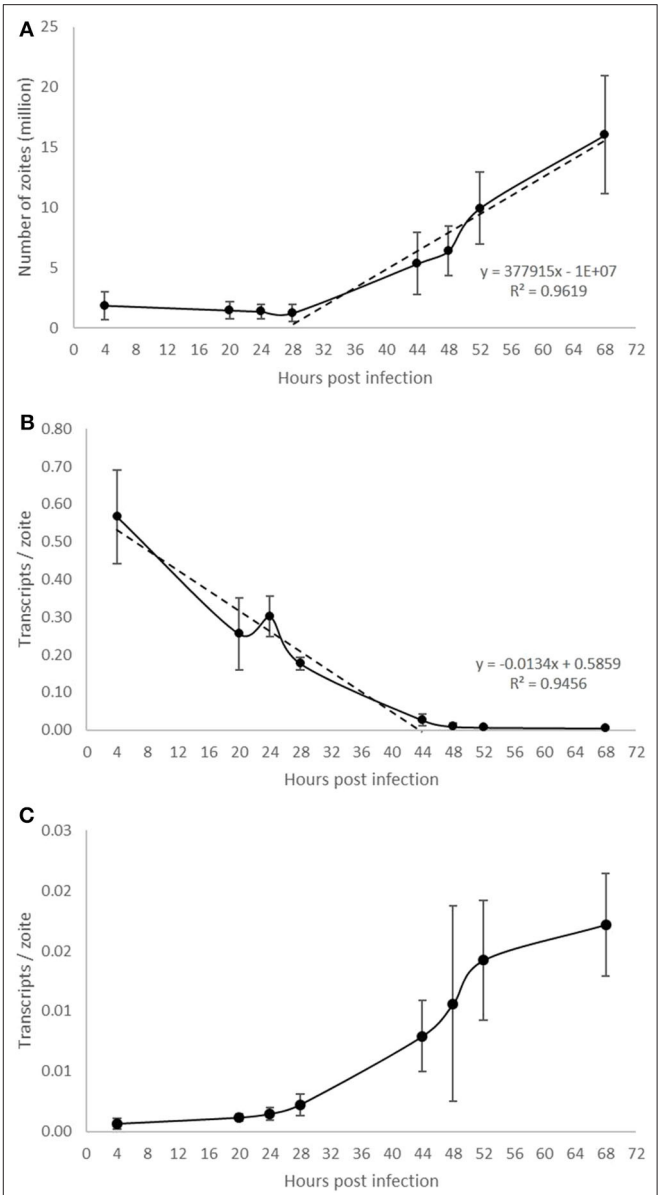

FIGURE 5 | Evaluation of *E. tenella* endogenous development *in vitro* by qPCR and RT-qPCR. **(A)** DNA replication of the parasite commences around 28 hpi and increases in a linear fashion throughout the whole sampling time-course. **(B)** The number of transcripts per zoite corresponding to sporozoite-specific target SP25 decreases during first generation schizogony and is barely detectable after 44 hpi. **(C)** The number of transcripts per zoite corresponding to merozoite-specific target MZ25 increases during schizogony, starting before the onset of DNA replication at 28 hpi and continuing in a linear fashion until around 52 hpi when the first released merozoites were seen in cultures (see **Figures 1P–R**). Bars = SD.

negative correlation ($r = -0.929$) which fits perfectly with the decreased numbers of sporozoites in the cultures at 28 hpi and the appearance of immature then maturing schizonts. Wild type parasites of *E. tenella* and transgenic *E. tenella* YFPmYFP displayed equivalent replication rates and levels of transcription (data not shown).

ImageJ Semi-Automated Analysis Simulated the Endogenous Development

Computational analysis of photographs taken via microscopy strongly supported the visual observations (**Figure 1**). Normalized datasets for sporozoite and schizont numbers

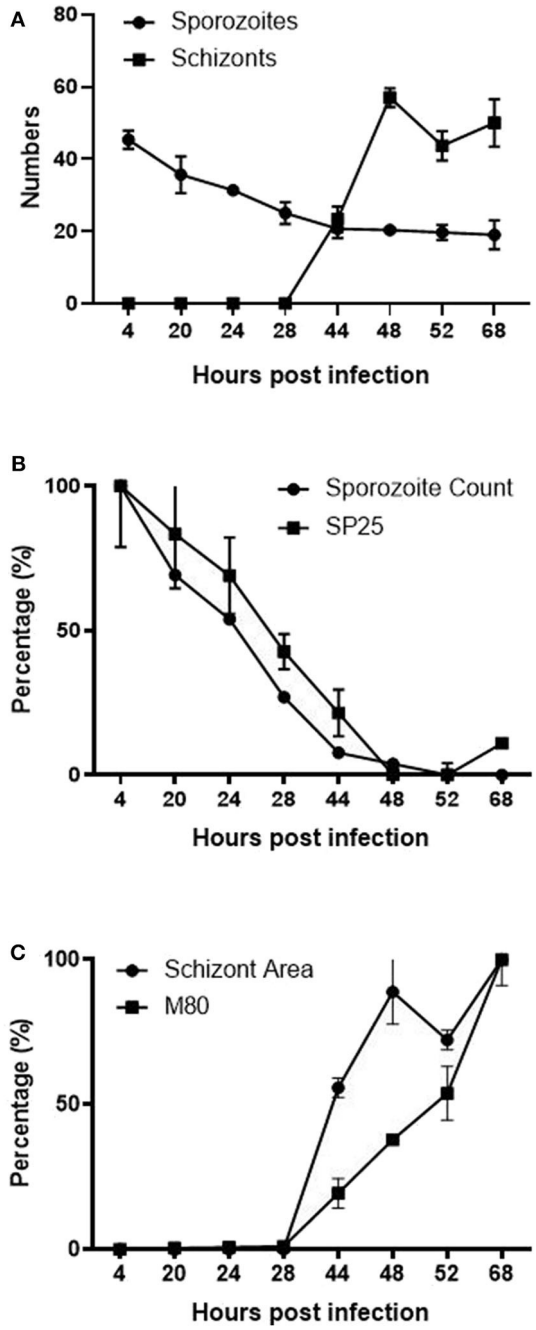

FIGURE 6 | Correlation between ImageJ semi-automated analysis and qPCR data. **(A)** Graph showing the normalized number of fluorescent (YFP expression) sporozoites and schizonts detected by semi-automated image analysis over time. **(B)** Normalized data showing the number of sporozoites and SP25 gene transcription over time. **(C)** Normalized data comparing the average size of schizonts and MZ80 gene transcription over time.

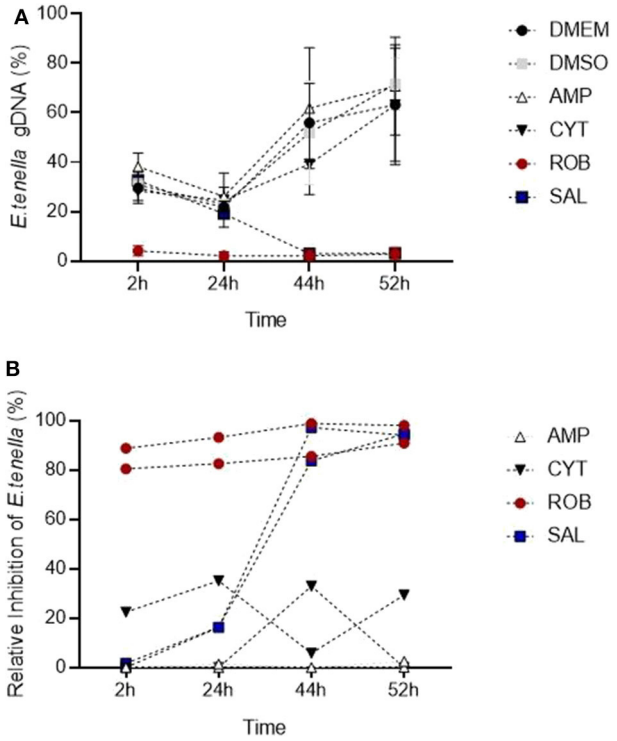

FIGURE 7 | Detection of changes in invasion and endogenous development of *E. tenella* by qPCR when sporozoites are pre-incubated with anticoccidial drugs (5 μg/ml). **(A)** Time course showing the impact of drugs: robenidine (ROB) affected sporozoite invasion; salinomycin (SAL) allowed invasion but not development (parasite could have potentially died after invasion); amprolium (AMP) and cytochalasin D (CIT) did not have any effect at the tested concentrations (potentially caused by a reversible effect after the drug was removed). Bars = SD. **(B)** Relative inhibition of each drug (in percentage) in invasion and development for each time point when normalized to DMSO controls. Each line correspond to an individual experiment.

taken from semi-automated image analysis were shown to have a strongly negative correlation ($r = -0.855$). In the first 28 hpi, the number of sporozoites gradually decreases as schizont development begins, reaching a plateau at 44 hpi (**Figure 6A**). Conversely, the numbers of schizonts sharply rises between 28 and 48 hpi contributing to this correlation pattern. A drop in schizont numbers is seen at 52 hpi, which correlates with a decrease in the overall measured schizont area at this time, which is attributed to the rupture of fully mature schizonts releasing merozoites (**Figures 1P–U**) and the decrease of YFP expression caused by the EtMIC1 promoter. A remaining base level of sporozoites can be seen until the end of the experiment which can be attributed to intracellular sporozoites that fail to develop.

Normalized transcript levels by RT-qPCR for SP25 gene and sporozoite numbers from semi-automated analysis were shown to have a very strong positive correlation ($r = 0.979$). SP25 transcription values fell between 4 and 44 hpi (**Figure 5B**) as sporozoites invaded the host cells and began schizogony (**Figures 1J–L**). These values were supported by the numbers of sporozoites documented during image analysis, which mirrored these changes (**Figure 6B**). Normalized MZ80 transcripts and schizont area data were shown to have a strong positive correlation ($r = 0.913$) (**Figure 6C**). The steady increase in MZ80 transcription beginning from 28 hpi onwards is shortly followed

by the appearance of small schizonts at 44 hpi. Schizont growth and MZ80 gene transcription continued in a linear fashion until 52 hpi, when a drop in mean schizont area size can be seen with no comparative effect on MZ80 transcription. These findings can be attributed to the presence of newly-released first-generation merozoites emerging at 52 hpi from ruptured schizonts (**Figures 1P–R**), allowing MZ80 levels to be detected but not ruptured schizonts.

The Effects of Anticoccidial Drugs on Invasion and Endogenous Development Can Be Assessed by qPCR *in vitro*

The *in vitro* system for *E. tenella* followed by qPCR analysis was suitable to detect the effect of different anticoccidial drugs on sporozoite invasion and development in a time course experiment (**Figure 7A**). Early after sporozoites were added to MDBK monolayers (2 hpi), sporozoites pre-incubated with robenidine showed a significant reduction of invasion compared to the control (**Figure 7A**; ROB vs. DMSO, Dunnett's multiple comparisons test) but no effect was seen with any of the other treatments. At later points of *Eimeria* endogenous development (44–52 hpi), a significant reduction in schizont area was seen in samples incubated with salinomycin (**Figure 7A**; SAL vs. DMSO, Dunnett's multiple comparisons test). No significant effects were seen in samples treated with amprolium (AMP) or cytochalasin D (CYT).

To assess the level of inhibition caused by pre-incubation with each drug, the proportion of parasites for each time point was also evaluated normalizing values of treated samples to their DMSO control (**Figure 7B**; Thabet et al., 2017). Proportions showed that amprolium caused the lowest effect against the invasion and development with a maximum inhibition of 1.3%. In contrast, a high effect (> 80%) was seen for robenidine from 2 hpi to the end of the time course. There was also an inhibition after exposition of parasites to salinomycin and cytochalasin D until 44 hpi, however the proportion of parasites increased again for this last group until 52 hpi.

In summary, pre-incubation with 5 μg/ml with amprolium or cytochalasin did not affect the invasion and development, probably due to a reversible effect after the removal of these drugs. Pre-incubation with salinomycicn did not affect invasion but inhibited further development, potentially caused by sporozoites dying early after invasion. Finally, pre-incubation with robenidine strongly affected invasion and therefore no further development was possible. The significant interaction between the specific anticoccidial drug and the time point supported that the development of *E. tenella* is dependent of both factors (drug and time) (Two-way RM ANOVA test, $p < 0.001$).

DISCUSSION

The use of *in vitro* models has been paramount for the study of protozoan parasites. The ability to replicate behaviors in a controlled environment has allowed the study of specific mechanisms and/or treatments in isolation of other factors, validating hypotheses and/or formulation of new ones to be verified later by *in vivo* models. The availability of *in vitro* models for apicomplexan parasites is limited and usually restricted to only one or a few stages of their complex life cycles (Muller and Hemphill, 2013). In heteroxenous Sarcocystidae coccidia (e.g., *Toxoplasma gondii*, *Neospora caninum*, or *Besnoitia besnoiti*) the tachyzoite stage responsible for the organic dissemination of the parasite in intermediate hosts can be continuously grown *in vitro* and this has advanced our understanding of many cellular mechanisms in apicomplexan parasites (Boothroyd, 2020). For monoxenous Eimeriidae coccidia (e.g., *Eimeria* species) there is no efficient *in vitro* system supporting continuous replication of a single stage or the completion of the lifecycle and much research in these species relies on the use of animals. This significantly limits studies especially for understanding the whole endogenous lifecycle including both asexual and sexual phases. A recent study revealed that successful endogenous development and production of small numbers of sexual stages can be achieved in the immortalized CLEC-213 chicken lung epithelial cell line; however, no oocysts were observed (Bussiere et al., 2018).

There are several immortalized cell lines that can support *Eimeria* sporozoite infection and first generation schizogony. In a comparative analysis Tierney and Mulcahy (2003) concluded that MDBK cells were most suitable, and this has been the line of choice for research in *E. tenella* for many years (Crane et al., 1984). Using this *in vitro* MDBK system we observed fully formed first-generation merozoites that exhibit the same structures as those described previously for first-generation merozoites generated in chick kidney cells (Pacheco et al., 1975). Nonetheless, as has been reported previously, these merozoites did not reinvade MDBK cells, for reasons that are not clear but which seem to represent a bottleneck to completing the full lifecycle *in vitro*, since second-generation merozoites obtained from chickens are capable to continue development when added to a monolayer of cultured cells (Xie et al., 1990). Another interesting observation is the apparent co-ordinated nuclear division seen in the three schizonts imaged by SBF-SEB; nonetheless further data would be necessary for the verification of this hypothesis.

Additionally, the MS identified a series of proteins directly related to invasion and development which are differentially expressed at specific time points in an *in vitro* time course. Results correlated with previous findings for some of these proteins: (i) presence of alternative types of surface antigen proteins (SAGs) between sporozoites and merozoites (Tabares et al., 2004); (ii) high abundance of microneme (MIC) proteins during invasion (Bumstead and Tomley, 2000); and (iii) overexpression of rhoptry (ROP) and dense granule (GRA) proteins during endogenous development (Oakes et al., 2013; Xue et al., 2020). These data further corroborate the suitability of the *in vitro* system to mimic endogenous development (Burrell et al., 2020) and are an important source of information to design specific interventions for the study of these relevant proteins. The detection by MS of these proteins indicated that they are present at significantly abundant levels to be targeted (e.g., antibody binding, enzymatic cleavage) and evaluated by this *in vitro* system.

Eimeria parasites undergo asexual replication by the process of schizogony (Pacheco et al., 1975). The beginning and end products of each round of multiplication are host cell invasion-competent "zoites" (sporozoite or merozoite). Between ∼30 and ∼48 h post-invasion intracellular parasites undergo multiple rounds of DNA replication and mitosis, followed by cytoplasmic expansion and budding of new zoites at the plasma membrane of the enlarged schizont from ∼ 48 and ∼72 h (Pacheco et al., 1975; Ferguson et al., 2008). This complex process can be monitored in cell culture by counting numbers of intracellular sporozoites, immature/mature schizonts, and released merozoites. Since early schizonts are not easily visualized by bright field, monolayers require fixation and staining (Brown et al., 2000) to perform counts. This is labor-intensive and may be subjective, especially at later times where there is asynchronous growth. Higher throughput quantification of parasite DNA replication can be achieved by measuring [3H] uracil incorporation into acid-insoluble material (Pfefferkorn and Pfefferkorn, 1977). Use of qPCR to count parasite genomes in newly invaded or developing cell cultures has been also reported recently (Jenkins et al., 2014; Thabet et al., 2015). Since the use of qPCR is as reliable as traditional methodologies to quantify parasites in chickens (Nolan et al., 2015) we evaluated its suitability to reflect the changes observed by microscopy in this *in vitro* system. To avoid time-consuming staining of samples, we used a fluorescent population of *E. tenella* previously generated by transgenesis (Clark et al., 2008), which allowed the direct visualization of schizonts and a reduced number of samples (micrographs can be taken at different time points from the same sample). Furthermore, to avoid subjectivity, we used semi-automated image analysis by the generation of an ImageJ plugin to provide quantitative data from the images. A perfect correlation was found between visual observations, qPCR data and image analysis whereby there were no significant changes before the 28 hpi sampling point and thereafter both DNA content and total schizont area increased in a linear fashion until 54 hpi. Therefore, both ways of quantification are valid to predict endogenous development of *E. tenella* in MDBK cells.

Neither of the two methods for quantification detected changes before the 28 hpi time-point. We hypothesized that quantifying stage-specific gene transcription from cDNA could provide strong markers and a more robust method to monitor parasite progression through the early and late stages of schizogony through to release of merozoites, which cannot be done using qPCR alone. Although there are no published reports on the timing of merozoite-specific gene transcription during first generation schizogony in cell culture, from analysis of the *E. tenella* genome by Reid et al. (2014) and consideration of the accompanying RNAseq database (ToxoDB) we selected genes that were suitable for monitoring endogenous development based on previous experiments performed in our group (unpublished). SP25 is expressed only in sporozoites whereas MZ80 is merozoite specific. Both are members of a novel gene family that is found only in the *Eimeria* genus and for which there is currently no ascribed biological function (*esf2* family; Reid et al., 2014). During first generation schizogony the number of SP25 transcripts decreased rapidly between 4 and 44 hpi reaching a level that was close to undetectable. In contrast, transcripts for MZ80 were detected at a low level until 20–24 hpi and thereafter increased rapidly until 52 hpi, which coincides with the start of merozoite release. We consider therefore that the reduction of SP25 transcription could be a marker to predict changes at early time points (without the need of performing a longer time course) whereas MZ80 a marker for late schizogony and merozoite formation.

Once the *in vitro* system was well-characterized by quantitative methods, we used compounds with known effects as anticoccidials to test how sensitive these methods were in detecting changes in sporozoite invasion and schizont development. We used a protocol in which sporozoites were pre-treated for 1 h and then drugs were removed before adding them to the cell monolayer. This was to simplify the assay and avoiding having to perform cytotoxicity tests for each drug. In addition, unpublished results showed that DMSO, the usual solvent for drugs, affected *Eimeria* development when added to the monolayer at 0.05% compared to the untreated control (data not shown). Therefore, pre-treatment was considered a better way to test the *in vitro* model to detect changes in invasion/development if drugs are prepared in DMSO; an alternative solvent would be recommended for a direct treatment onto the cell monolayer.

Amprolium, a thiamine antagonist with recorded peak activity against maturing first generation schizonts (McDougald and Galloway, 1976), did not show any effect on sporozoite invasion and schizont development, which is likely to be because of the early removal of the treatment, several hours before this peak of action. We did not detect a reduction of invasion when pre-treating with cytochalasin D, an inhibitor of actin polymerization that blocks movement and in consequence reduced sporozoite invasion (Bumstead and Tomley, 2000). Since the action of this drug is reversible, we assume that removal of the treatment allowed parasites to infect cells normally. By contrast robenidine, a guanidine derivative which inhibits oxidative phosphorylation, had a strong effect on sporozoite invasion which was clearly reflected by the qPCR data. McDougald and Galloway (1976) did not find these same effects, but in their study treatment was added at the time of invasion and at a lower dose (0.01 μg/ml) to what was used here. Microscopic observations of lack of movements and changes in the morphology of sporozoites pre-exposed to robenidine suggests that the low amount of gDNA we found throughout the time course was due to early death of the parasites. Finally, the progressive reduction from 24 hpi in parasite gDNA and transcripts following salinomycin treatment indicates that sporozoites were able to invade cells, being affected only during further development. We hypothesize that treatment with this ionophore damaged sporozoite membranes allowing parasite invasion to occur but inducing death thereafter since there is no previous evidence that ionophores can affect intracellular stages (Mehlhorn et al., 1983; Thabet et al., 2015). The latter authors used a similar method to calculate inhibition/development based on qPCR and showed that treating sporozoites for 2 h with 1 μg/ml of salinomycin did not affect invasion of MDBK cells whereas significant inhibition was found if sporozoites were treated for 4 h. In this same study,

inhibition assays using the same concentration of salinomycin reduced sporozoite replication to 50% after 24 hpi and by 95% after 48, 72, or 96 hpi. Our results agree with those of Thabet et al. (2015) showing a time-dependant and a progressive effect of salinimycin in the later stages of development.

In conclusion, in this study we have validated the suitability of the MDBK cell culture *in vitro* system to mimic the *in vivo* behavior of sporozoite invasion and first generation schizogony of the endogenous *E. tenella* lifecycle. We have described quantitative methods for use in assessing the effects of anticoccidial drugs and novel compounds against parasite invasion and asexual development that can support a guiding principle for the ethical use of animals in sciences, reducing their use in *Eimeria* research.

DATA AVAILABILITY STATEMENT

The raw data supporting the conclusions of this article will be made available by the authors, without undue reservation.

ETHICS STATEMENT

The animal study was reviewed and approved by Royal Veterinary College Ethical Review Committees and the United Kingdom Government Home Office.

AUTHOR CONTRIBUTIONS

VM-H and FT conceived and designed the project. AB and SV performed the TEM and SBF-SEM. VM-H, DX, and NR generated the samples and MS data. VM-H standardized the qPCR and RT-Qpcr and wrote the manuscript. GJ run qPCR and RT-qPCR and developed the ImageJ plugin for semi-automated image analysis. KA-M performed the anticoccidial drug assays and analyzed the data. FT and SV critically reviewed and edited the paper. All authors read and approved the final version of the manuscript.

FUNDING

This work was funded by the Houghton Trust Small Grants, Biotechnology and Biological Sciences Research Council (BBSRC) grant reference BB/L002477/1 and the RVC Ph.D. Studentship programme.

ACKNOWLEDGMENTS

The authors wish to thank Dr. Louise Hughes (Oxford Brookes University) for operation of the SBF-SEM system. This manuscript has been assigned the reference PPS_2200 by the Royal Veterinary College.

REFERENCES

Allen, P. C. (2007). Anticoccidial effects of xanthohumol. *Avian Dis.* 51, 21–26. doi: 10.1637/0005-2086(2007)051[0021:AEOX]2.0.CO;2

Alnassan, A. A., Thabet, A., Daugschies, A., and Bangoura, B. (2015). *In vitro* efficacy of allicin on chicken *Eimeria tenella* sporozoites. *Parasitol. Res.* 114, 3913–3915. doi: 10.1007/s00436-015-4637-2

Besteiro, S., Dubremetz, J. F., and Lebrun, M. (2011). The moving junction of apicomplexan parasites: a key structure for invasion. *Cell. Microbiol.* 13, 797–805. doi: 10.1111/j.1462-5822.2011.01597.x

Boothroyd, J. C. (2020). What a difference 30 years makes! *a perspective on changes in research methodologies used to study Toxoplasma gondii. Methods Mol. Biol.* 2071, 1–25. doi: 10.1007/978-1-4939-9857-9_1

Brown, P. J., Billington, K. J., Bumstead, J. M., Clark, J. D., and Tomley, F. M. (2000). A microneme protein from *Eimeria tenella* with homology to the apple domains of coagulation factor XI and plasma pre-kallikrein. *Mol. Biochem. Parasitol.* 15, 1–102. doi: 10.1016/S0166-6851(00)00179-1

Bumstead, J., and Tomley, F. (2000). Induction of secretion and surface capping of microneme proteins in *Eimeria tenella*. *Mol. Biochem. Parasitol.* 110, 311–21. doi: 10.1016/S0166-6851(00)00280-2

Burrell, A., Tomley, F. M., Vaughan, S., and Marugan-Hernandez, V. (2020). Life cycle stages, specific organelles and invasion mechanisms of *Eimeria* species. *Parasitology* 147, 263–278. doi: 10.1017/S0031182019001562

Bussiere, F. I., Niepceron, A., Sausset, A., Esnault, E., Silvestre, A., Walker, R. A., et al. (2018). Establishment of an *in vitro* chicken epithelial cell line model to investigate *Eimeria tenella* gamete development. *Parasit. Vectors* 11:44. doi: 10.1186/s13071-018-2622-1

Carruthers, V. B., and Tomley, F. M. (2008). Microneme proteins in apicomplexans. *Subcell. Biochem.* 47, 33–45. doi: 10.1007/978-0-387-78267-6_2

Clark, J. D., Billington, K., Bumstead, J. M., Oakes, R. D., Soon, P. E., Sopp, P., et al. (2008). A toolbox facilitating stable transfection of *Eimeria* species. *Mol. Biochem. Parasitol.* 162, 77–86. doi: 10.1016/j.molbiopara.2008.07.006

Crane, M. S., Schmatz, D. M., Stevens, S., Habbersett, M. C., and Murray, P. K. (1984). *Eimeria tenella*: *in vitro* development in irradiated bovine kidney cells. *Parasitology 88(Pt.* 3), 521–530. doi: 10.1017/S0031182000054780

de Venevelles, P., Francois Chich, J., Faigle, W., Lombard, B., Loew, D., Pery, P., et al. (2006). Study of proteins associated with the *Eimeria tenella* refractile body by a proteomic approach. *Int. J. Parasitol.* 36, 1399–1407. doi: 10.1016/j.ijpara.2006.06.018

Diallo, M. A., Sausset, A., Gnahoui-David, A., Silva, A. R. E., Brionne, A., Le Vern, Y., et al. (2019). Eimeria tenella ROP kinase EtROP1 induces G0/G1 cell cycle arrest and inhibits host cell apoptosis. *Cell. Microbiol.* 21:e13027. doi: 10.1111/cmi.13027

Doran, D. J. (1971). Increasing the yield of *Eimeria tenella* oocysts in cell culture. *J. Parasitol.* 57, 891–900. doi: 10.2307/3277823

Doran, D. J., and Augustine, P. C. (1973). Comparative development of *Eimeria tenella* from sporozoites to oocysts in primary kidney cell cultures from gallinaceous birds. *J. Protozool.* 20, 658–661. doi: 10.1111/j.1550-7408.1973.tb03593.x

Doran, D. J., and Vetterling, J. M. (1967). Comparative cultivation of poultry coccidia in mammalian kidney cell cultures. *J. Protozool.* 14, 657–662. doi: 10.1111/j.1550-7408.1967.tb02058.x

Ferguson, D. J., Sahoo, N., Pinches, R. A., Bumstead, J. M., Tomley, F. M., and Gubbels, M. J. (2008). MORN1 has a conserved role in asexual and sexual development across the apicomplexa. *Eukaryotic Cell.* 7, 698–711. doi: 10.1128/EC.00021-08

Hofmann, J., and Raether, W. (1990). Improved techniques for the *in vitro* cultivation of *Eimeria tenella* in primary chick kidney cells. *Parasitol. Res.*76, 479–486. doi: 10.1007/BF00931053

Horcajo, P., Xia, D., Randle, N., Collantes-Fernandez, E., Wastling, J., Ortega-Mora, L. M., et al. (2018). Integrative transcriptome and proteome analyses define marked differences between neospora caninum isolates throughout the tachyzoite lytic cycle. *J. Proteomics* 180, 108–119. doi: 10.1016/j.jprot.2017.11.007

Jenkins, M. C., O'Brien, C. N., Fuller, L., Mathis, G. F., and Fetterer, R. (2014). A rapid method for determining salinomycin and monensin sensitivity in *Eimeria tenella*. *Vet. Parasitol.* 206, 153–158. doi: 10.1016/j.vetpar.2014.09.017

Kogut, M. H., and Lange, C. (1989). Interferon-gamma-mediated inhibition of the development of *Eimeria tenella* in cultured cells. *J. Parasitol.* 75, 313–317. doi: 10.2307/3282782

Marugan-Hernandez, V., Cockle, C., Macdonald, S., Pegg, E., Crouch, C., Blake, D. P., et al. (2016). Viral proteins expressed in the protozoan parasite *Eimeria tenella* are detected by the chicken immune system. *Parasit. Vectors* 9:463. doi: 10.1186/s13071-016-1756-2

Marugan-Hernandez, V., Fiddy, R., Nurse-Francis, J., Smith, O., Pritchard, L., and Tomley, F. M. (2017a). Characterization of novel microneme adhesive repeats (MAR) in *Eimeria tenella*. *Parasit. Vectors* 10:491. doi: 10.1186/s13071-017-2454-4

Marugan-Hernandez, V., Long, E., Blake, D., Crouch, C., and Tomley, F. (2017b). *Eimeria tenella* protein trafficking: differential regulation of secretion versus surface tethering during the life cycle. *Sci. Rep.* 7:4557. doi: 10.1038/s41598-017-04049-1

McDougald, L. R., and Galloway, R. B. (1976). Anticoccidial drugs: effects on infectivity and survival intracellularly of *Eimeria tenella* sporozoites. *Exp. Parasitol.* 40, 314–319. doi: 10.1016/0014-4894(76)90098-9

McDougald, L. R., and Jeffers, T. K. (1976). Comparative *in vitro* development of precocious and normal strains of *Eimeria tenella* (Coccidia). *J. Protozool.* 23, 530–534. doi: 10.1111/j.1550-7408.1976.tb03834.x

Mehlhorn, H., Pooch, H., and Raether, W. (1983). The action of polyether ionophorous antibiotics (monensin, salinomycin, lasalocid) on developmental stages of *Eimeria tenella* (Coccidia, Sporozoa) *in vivo* and *in vitro*: study by light and electron microscopy. *Z Parasitenkd.* 69, 457–471. doi: 10.1007/BF00927702

Mercier, C., and Cesbron-Delauw, M. F. (2015). Toxoplasma secretory granules: one population or more? *Trends Parasitol.* 31, 60–71. doi: 10.1016/j.pt.2014.12.002

Muller, J., and Hemphill, A. (2013). *In vitro* culture systems for the study of apicomplexan parasites in farm animals. *Int. J. Parasitol.* 43, 115–124. doi: 10.1016/j.ijpara.2012.08.004

Nolan, M. J., Tomley, F. M., Kaiser, P., and Blake, D. P. (2015). Quantitative real-time PCR (qPCR) for *Eimeria tenella* replication–implications for experimental refinement and animal welfare. *Parasitol. Int.* 64, 464–470. doi: 10.1016/j.parint.2015.06.010

Oakes, R. D., Kurian, D., Bromley, E., Ward, C., Lal, K., Blake, D. P., et al. (2013). The rhoptry proteome of *Eimeria tenella* sporozoites. *Int. J. Parasitol.* 43, 181–188. doi: 10.1016/j.ijpara.2012.10.024

Pacheco, N. D., Vetterling, J. M., and Doran, D. J. (1975). Ultrastructure of cytoplasmic and nuclear changes in *Eimeria tenella* during first-generation schizogony in cell culture. *J. Parasitol.* 61, 31–42. doi: 10.2307/3279101

Pastor-Fernandez, I., Pegg, E., Macdonald, S. E., Tomley, F. M., Blake, D. P., and Marugan-Hernandez, V. (2019). Laboratory growth and genetic manipulation of *Eimeria tenella*. *Curr. Protoc. Microbiol.* 27:e81. doi: 10.1002/cpmc.81

Patton, W. H. (1965). Eimeria tenella: cultivation of the asexual stages in cultured animal cells. *Science* 150, 767–769. doi: 10.1126/science.150.3697.767

Pfefferkorn, E. R., and Pfefferkorn, L. C. (1977). Specific labeling of intracellular *Toxoplasma gondii* with uracil. *J. Protozool.* 24, 449–453. doi: 10.1111/j.1550-7408.1977.tb04774.x

Reid, A. J., Blake, D. P., Ansari, H. R., Billington, K., Browne, H. P., Bryant, J., et al. (2014). Genomic analysis of the causative agents of coccidiosis in domestic chickens. *Genome Res.* 24, 1676–1685. doi: 10.1101/gr.168955.113

Shirley, M. (1995). "Eimeria species and strains of chickens," in *Guidelines on Techniques in Coccidiosis Research,* eds J. Eckert, R. Braun, M. Shirley, and P. Coudert (Luxembourg: European Commission), 4–10.

Strout, R. G., and Ouellette, C. A. (1969). Gametogony of *Eimeria tenella* (coccidia) in cell cultures. *Science* 163, 695–696. doi: 10.1126/science.163.3868.695

Tabares, E., Ferguson, D., Clark, J., Soon, P. E., Wan, K. L., and Tomley, F. (2004). Eimeria tenella sporozoites and merozoites differentially express glycosylphosphatidylinositol-anchored variant surface proteins. *Mol. Biochem. Parasitol.* 135, 123–132. doi: 10.1016/j.molbiopara.2004.01.013

Thabet, A., Alnassan, A. A., Daugschies, A., and Bangoura, B. (2015). Combination of cell culture and qPCR to assess the efficacy of different anticoccidials on *Eimeria tenella* sporozoites. *Parasitol. Res.* 114, 2155–2163. doi: 10.1007/s00436-015-4404-4

Thabet, A., Zhang, R., Alnassan, A. A., Daugschies, A., and Bangoura, B. (2017). Anticoccidial efficacy testing: *in vitro Eimeria tenella* assays as replacement for animal experiments. *Vet. Parasitol.* 233, 86–96. doi: 10.1016/j.vetpar.2016.12.005

Tierney, J., Gowing, H., Van Sinderen, D., Flynn, S., Stanley, L., McHardy, N., et al. (2004). *In vitro* inhibition of *Eimeria tenella* invasion by indigenous chicken lactobacillus species. *Vet. Parasitol.* 122, 171–182. doi: 10.1016/j.vetpar.2004.05.001

Tierney, J., and Mulcahy, G. (2003). Comparative development of *Eimeria tenella* (Apicomplexa) in host cells *in vitro*. *Parasitol. Res.* 90, 301–304. doi: 10.1007/s00436-003-0846-1

Whitmire, W. M., Kyle, J. E., Speer, C. A., and Burgess, D. E. (1988). Inhibition of penetration of cultured cells by *Eimeria bovis* sporozoites by monoclonal immunoglobulin G antibodies against the parasite surface protein P20. *Infect. Immun.* 56, 2538–2543. doi: 10.1128/IAI.56.10.2538-2543.1988

Xie, M. Q., Gilbert, J. M., Fuller, A. L., and McDougald, L. R. (1990). A new method for purification of *Eimeria tenella* merozoites. *Parasitol. Res.*76, 566–569. doi: 10.1007/BF00932562

Xue, Y., Theisen, T. C., Rastogi, S., Ferrel, A., Quake, S. R., and Boothroyd, J. C. (2020). A single-parasite transcriptional atlas of *Toxoplasma gondii* reveals novel control of antigen expression. *Elife* 9:e54129. doi: 10.7554/eLife.54129.sa2

Zheng, J., Gong, P., Jia, H., Li, M., Zhang, G., Zhang, X., et al. (2014). Eimeria tenella rhomboid 3 has a potential role in microneme protein cleavage. *Vet. Parasitol.* 201, 146–149. doi: 10.1016/j.vetpar.2014.01.010

Zhu, G., Johnson, J., and McDougald, L. R. (1994). Amplification of ionophore resistance in a field strain of *Eimeria tenella* by treating free sporozoites with monensin *in vitro*. *Vet. Parasitol.* 51, 211–217. doi: 10.1016/0304-4017(94)90158-9

Conflict of Interest: The authors declare that the research was conducted in the absence of any commercial or financial relationships that could be construed as a potential conflict of interest.

frontiers in Cellular and Infection Microbiology

MINI REVIEW
published: 18 November 2020
doi: 10.3389/fcimb.2020.587296

Crypto-Currency: Investing in New Models to Advance the Study of *Cryptosporidium* Infection and Immunity

N. Bishara Marzook and Adam Sateriale *

Cryptosporidiosis Laboratory, The Francis Crick Institute, London, United Kingdom

Cryptosporidiosis is a leading cause of diarrheal disease and an important contributor to global morbidity and mortality. Although the brunt of disease burden is felt by children in developing countries, *Cryptosporidium* is a ubiquitous intestinal parasite with frequent outbreaks around the world. There are no consistently effective treatments for cryptosporidiosis and the research to drive new developments has stagnated, largely due to a lack of efficient *in vivo* and *in vitro* models. Fortunately, these research barriers have started to fall. In this review, we highlight two recent advances aiding this process: A tractable mouse model for *Cryptosporidium* infection and stem cell-based *in vitro* culture systems that mimic the complexity of the host intestine. These models are paving the way for researchers to investigate *Cryptosporidium* infection and host immunity down to a molecular level. We believe that wise investments made to adopt and develop these new models will reap benefits not only for the *Cryptosporidium* community but also for the intestinal immunology field at large.

Keywords: Parasites (Apicomplexa), host-pathogen, intestinal epithelial barrier, *Cryptosporidium*, intestinal immunity, organoid culture, mouse model

OPEN ACCESS

Edited by:
Chandra Ramakrishnan, University of Zurich, Switzerland

Reviewed by:
Chiranjib Pal, West Bengal State University, India
Nicholas Charles Smith, University of Technology Sydney, Australia

***Correspondence:**
Adam Sateriale
adam.sateriale@crick.ac.uk

Specialty section:
This article was submitted to Parasite and Host, a section of the journal Frontiers in Cellular and Infection Microbiology

Received: *25 July 2020*
Accepted: *20 October 2020*
Published: *18 November 2020*

Citation:
Marzook NB and Sateriale A (2020) Crypto-Currency: Investing in New Models to Advance the Study of Cryptosporidium Infection and Immunity. Front. Cell. Infect. Microbiol. 10:587296. doi: 10.3389/fcimb.2020.587296

INTRODUCTION

Cryptosporidium is a member of the apicomplexan phylum of parasites and a distant relative of *Plasmodium*, the causative agent of malaria. Unlike *Plasmodium*, *Cryptosporidium* is monoxenous—completing its entire life cycle within a single host—and infection is specifically localized to the gastrointestinal tract. The infectious form of the parasite, known as the oocyst, is resistant to a variety of standard disinfectants, including chlorination. Each *Cryptosporidium* oocyst harbors four sporozoites, which are released when oocysts are ingested by a host and invade the apical side of polarized intestinal epithelial cells. Parasitophorous vacuoles can be readily seen lining the intestine of an infected host (**Figure 1A**). *Cryptosporidium* then undergo asexual and sexual cycles of replication, leading to the production of new oocysts that are shed by the infected host (**Figure 1B**).

Human cryptosporidiosis is mainly caused by two species: the anthroponotic *Cryptosporidium hominis* and the zoonotic *Cryptosporidium parvum*. The pathology of a *Cryptosporidium* infection manifests as diarrhoeal disease, particularly in children in low-income countries during the first 2 years

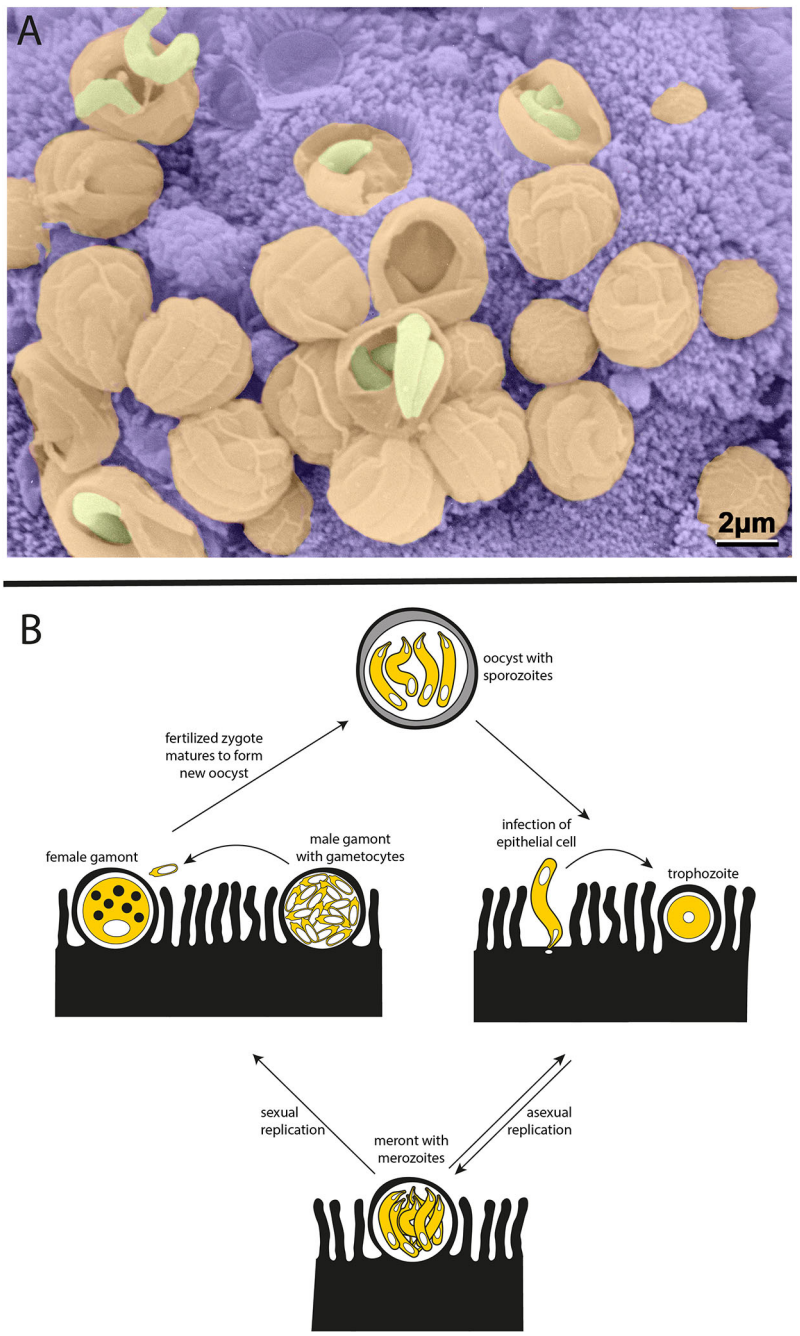

FIGURE 1 | *Cryptosporidium* parasites. **(A)** Parasitophorous vacuoles line the wall of the small intestine in an infected mouse. Scanning electron microscopy with parasites in yellow, parasitophorous vacuoles in orange, and host intestinal villi in purple (image courtesy of Prof. David Ferguson, Oxford University, copyright retained). **(B)** Life cycle of the *Cryptosporidium* parasite. Each oocyst contains four sporozoites that can infect the epithelium lining the host intestinal tract. Sporozoites mature to trophozoites and then meronts. Meronts release merozoites which go on to reinvade nearby epithelial cells. The switch from asexual to sexual replication during the *Cryptosporidium* life cycle is poorly understood and remains an area of great interest. During sexual replication, male and female gametes are produced, and fertilization leads to the formation of new infectious oocysts.

of life (Kotloff et al., 2013). While severe cases can be fatal, the majority of *Cryptosporidium* infections resolve within a few weeks. Because of this self-limiting nature, it is tempting to focus solely on acute symptoms and short-term consequences. However, infection in young children is closely associated with bouts of prolonged malnutrition that lead to important long-term consequences, such as impaired growth and cognitive development (Korpe et al., 2016). A recent re-evaluation of the *Cryptosporidium* disease burden

estimates an annual global loss of nearly 13 million disability adjusted life years; a figure largely driven by malnutrition associated morbidity (Khalil et al., 2018). Despite this substantial disease burden, there are no consistently effective treatments for cryptosporidiosis. Nitazoxanide, the only FDA-approved drug to treat infection, has limited efficacy in the immunocompetent and performs on par with placebo in immunocompromised or malnourished patients (Amadi et al., 2002). Development of new therapeutics has been severely hindered by a lack of effective *in vitro* and *in vivo* models for *Cryptosporidium* infection. However, recent advances in these fields are very promising, with novel platforms for *Cryptosporidium* research that allow for infection and immunity to be studied in more physiologically-relevant settings.

IN VIVO: A GENETICALLY TRACTABLE NATURAL MOUSE MODEL

The genus *Cryptosporidium* infects a broad range of vertebrate hosts from humans to fish. Despite this wide range of hosts, animal models that recapitulate human infection are historically lacking. Calves, gnotobiotic piglets, and immunocompromised mice have all been used to model infection with varying degrees of success. These *in vivo* models are still the gold standard of *Cryptosporidium* infection studies, since they provide the unique dynamic environment of the host intestine, its complex tissue architecture, diversity of cell types, and host immune responses (**Figure 2A**). However, due to the inability to adequately further manipulate the genetics of these host organisms, and the high costs associated with their upkeep, researchers have been unable to explore mechanisms of the immune response to *Cryptosporidium*. In an effort to overcome these restrictions, *Cryptosporidium tyzzeri*, a species of the parasite that naturally infects mice, has recently been developed as a genetically tractable model of human infection (Sateriale et al., 2019).

C. tyzzeri derives its name from EE Tyzzer, the researcher who first discovered *Cryptosporidium* as a natural parasite infection of laboratory mice at the turn of the 20th century. Tyzzer named the parasites that he found in the mouse small intestine *Cryptosporidium parvum*, a Latin reference to its morphology (cryptosporidium, 'hidden spore') and size (parvum, 'small'). Over the next century, '*Cryptosporidium parvum*' was continually rediscovered in the intestines of many species, including cows (Slapeta, 2011). With the

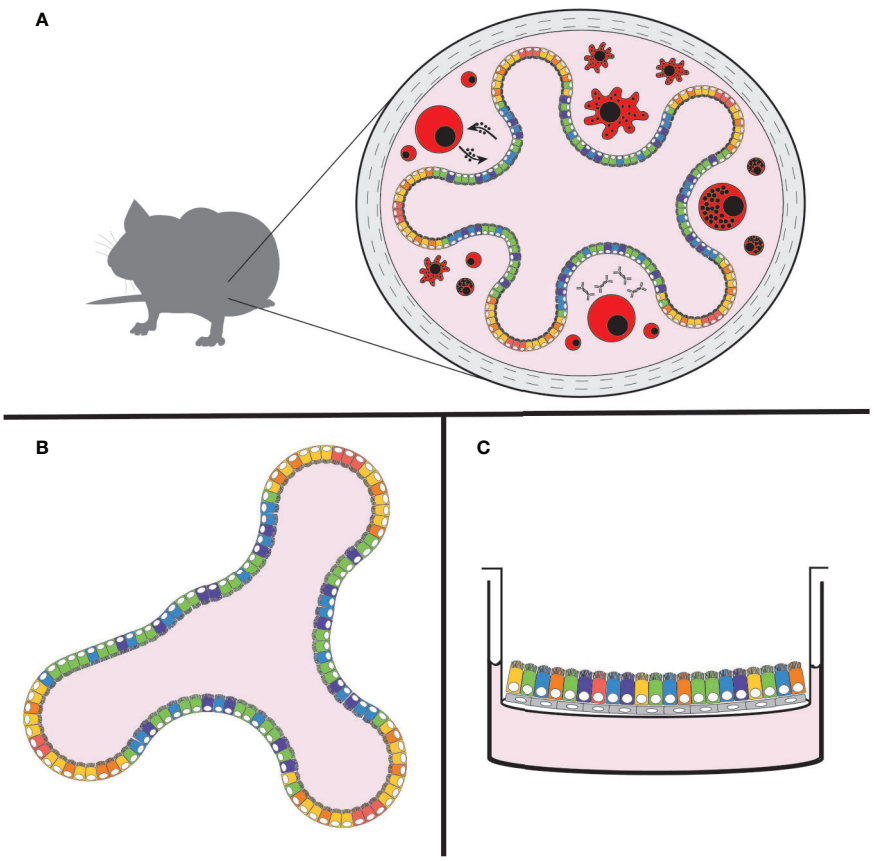

FIGURE 2 | New models of *Cryptosporidium* infection. **(A)** Natural mouse model of cryptosporidiosis, **(B)** intestinal organoid model, and **(C)** air-liquid interface (ALI) model. The use of colours is meant to demonstrate the complexity and diversity of cell types that are present in these models, with the natural mouse model including the host immune response (in red).

help of improved genetic analyses, it was later determined that these new isolates of '*Cryptosporidium parvum*' are, in fact, many separate species of the parasite. Despite efforts to rescue the original nomenclature, the taxonomic name *Cryptosporidium parvum* currently refers to the parasite species that is a natural infection of cows, and *Cryptosporidium tyzzeri* refers to the natural mouse pathogen that Tyzzer likely discovered (Ren et al., 2012). Now recognized as a ubiquitous infection of the common house mouse, *Mus musculus*, the *C. tyzzeri* parasite appears to be co-evolving with the various subspecies of its murine host (Kváč et al., 2013).

C. tyzzeri is a very close relative of the human-infecting parasite species; genetically 95-96% identical at the nucleotide level to *C. hominis* and *C. parvum*. Most importantly, *C. tyzzeri* infection in mice mimics human disease in pathology and immune response. Cryptosporidiosis is a common infection among patients with HIV/AIDS, and the disease can be protracted and severe. Because there are no effective drug treatments, resolution of infection is closely tied to the recovery of normal CD4 T-cell counts (Wang et al., 2018). In the murine model, mice lacking T-cells suffer from protracted and severe infections with *C. tyzzeri*. Mice lacking B-cells, however, show no protracted illness and clear the parasite just as well as wild-type mice (Sateriale et al., 2019). In humans, patients that produce insufficient amounts of the cytokine interferon gamma (IFNγ) are documented to be highly susceptible to cryptosporidiosis (Morales et al., 1996). In mice, IFNγ deficiency also leads to a much higher parasite burden that is controlled but never cleared (Griffiths et al., 1998; Sateriale et al., 2019).

Genetic modification of the *C. tyzzeri* genome is possible through adaptation of CRISPR/Cas9-driven homologous recombination. Originally pioneered in *C. parvum* (Vinayak et al., 2015), this technique can be used to derive stable transgenic *Cryptosporidium* strains expressing luminescent and fluorescent reporters for quantitative studies of mouse infections, and mutant strains for the study of particular parasite genes. For those genes that are found to be essential, or for the temporal control of protein expression, the newly developed technique of conditional protein degradation in *Cryptosporidium* should prove very useful (Choudhary et al., 2020). With *C. tyzzeri*, this ability to genetically manipulate the parasite can be leveraged with the variety of mouse species and strains available to researchers to allow for host-pathogen interactions to be rigorously interrogated at a new level.

IN VITRO: STEM CELL-BASED CELL CULTURE MODELS

The most widely used cell culture model for *Cryptosporidium* infection is the ileocecal adenocarcinoma cell line HCT-8 (Upton et al., 1994). This cell line has served as the primary infection model for anti-cryptosporidial drug screening and has provided many important insights into the biology of infection (Love et al., 2017; Jumani et al., 2019; Pawlowic et al., 2019). However, HCT-8s and the standard 2-D model of infection is restrictive in two crucial aspects: 1) Cell monolayers lack the cell diversity and architecture of the host intestine that is important for investigating pathogenesis, and 2) parasite growth is short-lived in this system as they are unable to complete the sexual stage of their life cycle. Recent research has implicated this sexual cycle, specifically the inability of male parasite gametes to fertilize female gametes, as the restrictive stage in the 2-D cell monolayer infection model (Tandel et al., 2019). This breakdown of fertilization is hypothesized to cause the arrested parasite growth that occurs around 72 hours after infection of HCT-8s (and other 2-D epithelial cell models). However, several *in vitro* systems have been able to sustain long-lived *Cryptosporidium* infections by recapitulating conditions that more closely mimic the host intestine.

Intestinal Organoid Model

The developing organoid model system of *in vitro* cell culture has been a game-changer for stem cell and cancer biologists, with infectious disease studies following closely behind [for a comprehensive review see Rossi et al. (2018)]. In brief, organoids are three-dimensional growths arising from embryonic, induced pluripotent, or adult stem cells. When given proper differentiation signals and an extracellular matrix (ECM)-derived scaffold, stem cells can develop into avatars of the desired organ. Organoids from adult stem cells recapitulate most of the architecture and cell types characteristic of the tissue from which they were derived and hence can be used to study a range of aspects including basic cell and tumor biology, organ regeneration, and increasingly host-pathogen interactions in a more physiologically relevant setting. Organoids of many different systems including the brain, liver, and lung have been successfully created; however, arguably the most well-established and studied platform is that of the intestinal organoid, which has been well-characterized from both mice and men (Sato et al., 2009). In a mixture of ECM proteins, small intestinal crypt-derived stem cells self-organize into mini-organs consisting of differentiated enterocytes and secretory cells, while still maintaining intestinal stem cells, a strict apical-basal polarity, and basic crypt-villus architecture (**Figure 2B**) (Sato et al., 2009).

Recently, Heo *et al.* were able to deploy human small intestinal (SI) and lung organoid systems to model a *C. parvum* infection (Heo et al., 2018). Transmission electron microscopy (TEM) showed the presence of asexual parasite stages 1 day post-infection, as well as the presence of sexual stages and oocysts after 5 days. TEM of infected organoids was also able to indicate that enterocytes in SI organoids, but both secretory and non-secretory cells in lung organoids, were predominantly infected by *Cryptosporidium*. New oocysts produced in organoids were capable of maintaining productive infections over three rounds of serial passage in SI organoids, however the authors noted a reduction in parasite numbers over 4 weeks of passaging. High-throughput RNAseq analysis of infected organoids revealed the activation of an enterocyte-based interferon response. Analysis of parasite RNA expression also demonstrated the upregulation of oocyst wall genes (especially COWP1) at 72 hours in both SI and lung organoids, a finding that supports the observation of new oocyst generation in this system. It should be noted, however, that female gametes produce oocyst wall proteins even in the absence of fertilization from male gametes (Tandel et al., 2019). Male or microgamete specific genes such as HAP2 were not identified as being upregulated in this study. One of the features of SI organoids is the possibility of maintaining them in either

'expanding' (more undifferentiated stem cells and highly proliferative progenitor cells) or 'differentiating' (more terminally differentiated cells) states, depending on which growth factors are provided. Interestingly, *C. parvum* propagation was on average almost ten times higher in differentiated organoids compared to expanding ones.

Air-Liquid Interface (ALI) Model

Originally devised for the culture of primary nasal epithelial cells, another recently-developed system to create differentiated intestinal cells from stem cells is the air-liquid interface (ALI) culture (**Figure 2C**) (Wang et al., 2015). Here, stem cells (either from primary sources or previously maintained as spheroids) can be plated onto 2-D membrane-supported cell culture inserts with or without an ECM-derived gel base. A layer of irradiated fibroblasts can also be used as feeder cells. Removal of liquid media from the top of the inserts results in the differentiation of stem cells into enterocyte and secretory cells. This technique was recently adapted by Wilke *et al.* to successfully infect differentiated mouse intestinal epithelial cells with *C. parvum* (Wilke et al., 2019). Parasite growth monitored by quantitative PCR showed amplification by nearly 100-fold over 20 days. Similar to the organoid model, ALI cultures were capable of producing new infectious oocysts 3 days post-infection; oocysts were capable of infecting both mice and new membrane-supported cell monolayers, albeit with diminishing returns. Also similar to the organoid model, TEM showed the preferential infection of enterocytes, however some infected secretory cells were also reported. Interestingly again, *C. parvum* grew significantly better in differentiated ALI cells.

Using CRISPR/Cas9-based genetic manipulation, Wilke *et al.* were also able to demonstrate meiotic recombination within the ALI system with fluorescently labelled parasite lines (Wilke et al., 2019). This meiotic recombination event, which naturally occurs in the final stages of the *Cryptosporidium* life cycle, appears in their ALI model after the third day of infection and coincides with the production of new infectious oocysts. The ability to perform controlled genetic crosses of *Cryptosporidium* parasites using a cell culture platform is a major advancement for the field. Exploring the nature and frequency of recombination events and how they contribute to pathogenicity and ongoing evolution of *Cryptosporidium* will greatly further the study of this deadly parasite.

DISCUSSION

Children living in endemic regions are particularly vulnerable to *Cryptosporidium* infection and this is well evidenced in large scale studies of diarrheal aetiology. In the Global Enteric Multicenter (GEM) study, with a cohort of over 20,000 children across Africa and southeast Asia, *Cryptosporidium* was identified as one of the primary causes of severe diarrheal events (Kotloff et al., 2013). However, from the third year onward, cryptosporidiosis becomes a negligible infection with very few attributable cases of severe disease reported in the GEM study. This apparent resistance in older children and adults in endemic regions is likely to be a matter of acquired immunity rather than age; *Cryptosporidium* is a common cause of travellers' diarrhoea in adults traveling from non-endemic regions. Early results using *C. tyzzeri* to model human infection support these observations. Mice that recover from a natural *C. tyzzeri* infection show resistance to subsequent infections (Sateriale et al., 2019). Vaccination using irradiated parasites had the same effect of protecting against subsequent infection and disease. Unlike its relative *Plasmodium*, *Cryptosporidium* appears to lack the large gene families required for antigenic switching (Abrahamsen et al., 2004). This may be a great advantage for development of a vaccine, yet researchers first need to understand the mechanism and markers of *Cryptosporidium* immunity.

The true power of this newly developed mouse model of cryptosporidiosis lies in the ability to genetically manipulate both the host and parasite. With *C. tyzzeri*, researchers can branch out from the few immunocompromised mouse strains that are traditionally used for *Cryptosporidium* infection studies. There is a vast range of mouse species, strains, congenics and transgenics to explore pathogenesis. Next generation panels of recombinant inbred lines, such as the Collaborative Cross, can be leveraged for genome-wide interrogation of the host response to *Cryptosporidium* infections (Aylor et al., 2011). This new mouse model of infection holds the potential to study both innate and adaptive mechanisms of immunity and, coupled with stem cell-based *in vitro* culture, microscopic observations can be studied in controlled environments.

Both the organoid and ALI culture systems raise the possibility of conducting *in vitro* studies of immune cell interaction with *Cryptosporidium*-infected epithelial cells. Co-culture studies of infected epithelial cells with immune cells have already proven successful for other host-pathogen studies [for a comprehensive review see Bar-Ephraim et al. (2019)], and therefore could enhance our understanding of how the immune system detects and responds to a *Cryptosporidium* infection. There are also many areas of molecular immunology that are poorly recapitulated in the 2-D cell culture systems. Although it has been known for nearly 30 years that IFN$\gamma$is a crucial cytokine for resistance to *Cryptosporidium*, the particular mechanism of this cytokine's effect on *Cryptosporidium* infection remains largely a mystery. It is likely that stem cell-based models will allow for the study of these immune mechanisms in a finely tuneable system that closely resembles the infected intestine.

Another key feature of stem cell-based parasite propagation systems is that they allow the presence of all cell types normally present in the gut (often arising from a single stem cell), and hence they provide us with the opportunity to better understand the particular intestinal niche of this obligate parasite, as well as observe any effects it might exert on existing host cell dynamics and populations over time. One of the open questions in the field is why infections of traditional 2-D cell culture systems don't lend themselves to the generation of new oocysts. Recent work in standard HCT-8 culture has elegantly shown that this process is likely stalled at the stage of male gametocyte penetration into the female macrogamont (Tandel et al., 2019). However, this block is overcome in the ALI cultures which are still technically 2-D but involve more polarised and differentiated epithelial cells (Wilke et al., 2019). Changes in host cell metabolism, such as an upregulation of genes involved in oxidative phosphorylation, with

a concomitant downregulation of the glycolytic pathway, was also associated with ALI cultures that supported parasite development. Further work to pinpoint specific conditions necessary to allow the completion of the parasite life cycle and expand them is required here. Stage-specific protein tagging either by CRISPR/Cas9-based methods (Tandel et al., 2019) or using newly-developed monoclonal antibodies (Wilke et al., 2018) can now assist in monitoring the life cycle progression of parasites in these *in vitro* models. Although both stem cell-based systems were able to demonstrate production of new oocysts, each suffered from diminishing returns that bar long-term cultivation. The inability to easily maintain transgenic parasite lines *in vitro* still poses a challenge to the *Cryptosporidium* field. With improvements that sustain higher oocyst yields, these new *in vitro* systems could possibly be adapted for the maintenance of transgenic parasite stocks, as well as other traditionally host-restricted *Cryptosporidium* species such as the anthroponotic *C. hominis*, which remains regrettably understudied.

Cryptosporidium research has been restricted by the lack of suitable model systems that accurately model infection and this has led to significant gaps in our understanding of infection and immunity. A major gap in our understanding is how immunity to *Cryptosporidium* infection is acquired and sustained. Further, the mechanisms behind growth stunting exhibited by afflicted infants are yet to be elucidated, as is the role of gut microbiota during and after infection. Parasite entry, replication, sexual reproduction, and oocyst release are yet to be truly visualized and studied at a molecular level. We believe these new *in vivo* and *in vitro* models can provide the basis for concerted explorations to expand our understanding of *Cryptosporidium* pathogenesis. By investing wisely in these new methods and pushing them to their maximal potentials, the *Cryptosporidium* and intestinal immunity research communities have much to gain.

AUTHOR CONTRIBUTIONS

NBM and AS wrote this manuscript together. All authors contributed to the article and approved the submitted version.

FUNDING

This work was supported by funding from The Francis Crick Institute (https://www.crick.ac.uk/), which receives its core funding from Cancer Research UK, the UK Medical Research Council and the Wellcome Trust.

REFERENCES

Abrahamsen, M. S., Templeton, T. J., Enomoto, S., Abrahante, J. E., Zhu, G., Lancto, C. A., et al. (2004). Complete Genome Sequence of the Apicomplexan, Cryptosporidium parvum. *Science* 304, 441–445. doi: 10.1126/science.1094786

Amadi, B., Mwiya, M., Musuku, J., Watuka, A., Sianongo, S., Ayoub, A., et al. (2002). Effect of nitazoxanide on morbidity and mortality in Zambian children with cryptosporidiosis: a randomised controlled trial. *Lancet* 360, 1375–1380. doi: 10.1016/s0140-6736(02)11401-2

Aylor, D. L., Valdar, W., Foulds-Mathes, W., Buus, R. J., Verdugo, R. A., Baric, R. S., et al. (2011). Genetic analysis of complex traits in the emerging Collaborative Cross. *Genome Res.* 21, 1213–1222. doi: 10.1101/gr.111310.110

Bar-Ephraim, Y. E., Kretzschmar, K., and Clevers, H. (2019). Organoids in immunological research. *Nat. Rev. Immunol.* 20, 279–293. doi: 10.1038/s41577-019-0248-y

Choudhary, H. H., Nava, M. G., Gartlan, B. E., Rose, S., and Vinayak, S. (2020). A Conditional Protein Degradation System To Study Essential Gene Function in Cryptosporidium parvum. *Mbio* 11, e01231–e01220. doi: 10.1128/mbio.01231-20

Griffiths, J. K., Theodos, C., Paris, M., and Tzipori, S. (1998). The Gamma Interferon Gene Knockout Mouse: a Highly Sensitive Model for Evaluation of Therapeutic Agents againstCryptosporidium parvum. *J. Clin. Microbiol.* 36, 2503–2508. doi: 10.1128/jcm.36.9.2503-2508.1998

Heo, I., Dutta, D., Schaefer, D. A., Iakobachvili, N., Artegiani, B., Sachs, N., et al. (2018). Modelling Cryptosporidium infection in human small intestinal and lung organoids. *Nat. Microbiol.* 3, 814–823. doi: 10.1038/s41564-018-0177-8

Jumani, R. S., Hasan, M. M., Stebbins, E. E., Donnelly, L., Miller, P., Klopfer, C., et al. (2019). A suite of phenotypic assays to ensure pipeline diversity when prioritizing drug-like Cryptosporidium growth inhibitors. *Nat. Commun.* 10, 1862. doi: 10.1038/s41467-019-09880-w

Khalil, I. A., Troeger, C., Rao, P. C., Blacker, B. F., Brown, A., Brewer, T. G., et al. (2018). Morbidity, mortality, and long-term consequences associated with diarrhoea from Cryptosporidium infection in children younger than 5 years: a meta-analyses study. *Lancet Global Heal.* 6, e758–e768. doi: 10.1016/s2214-109x(18)30283-3

Korpe, P. S., Haque, R., Gilchrist, C., Valencia, C., Niu, F., Lu, M., et al. (2016). Natural History of Cryptosporidiosis in a Longitudinal Study of Slum-Dwelling Bangladeshi Children: Association with Severe Malnutrition. *PloS Negl. Trop. D* 10, e0004564. doi: 10.1371/journal.pntd.0004564

Kotloff, K. L., Nataro, J. P., Blackwelder, W. C., Nasrin, D., Farag, T. H., Panchalingam, S., et al. (2013). Burden and aetiology of diarrhoeal disease in infants and young children in developing countries (the Global Enteric Multicenter Study, GEMS): a prospective, case-control study. *Lancet* 382, 209–222. doi: 10.1016/s0140-6736(13)60844-2

Kváč, M., McEvoy, J., Loudová, M., Stenger, B., Sak, B., Květoňová, D., et al. (2013). Coevolution of Cryptosporidium tyzzeri and the house mouse (Mus musculus). *Int. J. Parasitol.* 43, 805–817. doi: 10.1016/j.ijpara.2013.04.007

Love, M. S., Beasley, F. C., Jumani, R. S., Wright, T. M., Chatterjee, A. K., Huston, C. D., et al. (2017). A high-throughput phenotypic screen identifies clofazimine as a potential treatment for cryptosporidiosis. *PloS Negl. Trop. D* 11, e0005373. doi: 10.1371/journal.pntd.0005373

Morales, M. A. G., Ausiello, C. M., Guarino, A., Urbani, F., Spagnuolo, M.II, Pignata, C., et al. (1996). Severe, Protracted Intestinal Cryptosporidiosis Associated with Interferon Deficiency: Pediatric Case Report. *Clin. Infect. Dis.* 22, 848–850. doi: 10.1093/clinids/22.5.848

Pawlowic, M. C., Somepalli, M., Sateriale, A., Herbert, G. T., Gibson, A. R., Cuny, G. D., et al. (2019). Genetic ablation of purine salvage in Cryptosporidium parvum reveals nucleotide uptake from the host cell. *P Natl. Acad. Sci. U.S.A.* 116, 21160–21165. doi: 10.1073/pnas.1908239116

Ren, X., Zhao, J., Zhang, L., Ning, C., Jian, F., Wang, R., et al. (2012). Cryptosporidium tyzzeri n. sp. (Apicomplexa: Cryptosporidiidae) in domestic mice (Mus musculus). *Exp. Parasitol.* 130, 274–281. doi: 10.1016/j.exppara.2011.07.012

Rossi, G., Manfrin, A., and Lutolf, M. P. (2018). Progress and potential in organoid research. *Nat. Rev. Genet.* 19, 671–687. doi: 10.1038/s41576-018-0051-9

Sateriale, A., Šlapeta, J., Baptista, R., Engiles, J. B., Gullicksrud, J. A., Herbert, G. T., et al. (2019). A Genetically Tractable, Natural Mouse Model of Cryptosporidiosis Offers Insights into Host Protective Immunity. *Cell Host Microbe* 26, 135–146.e5. doi: 10.1016/j.chom.2019.05.006

Sato, T., Vries, R. G., Snippert, H. J., van de Wetering, M., Barker, N., Stange, D. E., et al. (2009). Single Lgr5 stem cells build crypt-villus structures in vitro without a mesenchymal niche. *Nature* 459, 262–265. doi: 10.1038/nature07935

Slapeta, J. (2011). Naming of Cryptosporidium pestis is in accordance with the ICZN Code and the name is available for this taxon previously recognized as C. parvum "bovine genotype". *Vet. Parasitol.* 177, 1–5. doi: 10.1016/j.vetpar.2011.01.049

Tandel, J., English, E. D., Sateriale, A., Gullicksrud, J. A., Beiting, D. P., Sullivan, M. C., et al. (2019). Life cycle progression and sexual development of the

apicomplexan parasite Cryptosporidium parvum. *Nat. Microbiol.* 4, 2226–2236. doi: 10.1038/s41564-019-0539-x

Upton, S. J., Tilley, M., and Brillhart, D. B. (1994). Comparative development of Cryptosporidium parvum (Apicomplexa) in 11 continuous host cell lines. *FEMS Microbiol. Lett.* 118 (3), 233–236. doi: 10.1111/j.1574-6968.1994.tb06833.x

Vinayak, S., Pawlowic, M. C., Sateriale, A., Brooks, C. F., Studstill, C. J., Bar-Peled, Y., et al. (2015). Genetic modification of the diarrhoeal pathogen Cryptosporidium parvum. *Nature* 523, 477–480. doi: 10.1038/nature14651

Wang, X., Yamamoto, Y., Wilson, L. H., Zhang, T., Howitt, B. E., Farrow, M. A., et al. (2015). Cloning and variation of ground state intestinal stem cells. *Nature* 522, 173–178. doi: 10.1038/nature14484

Wang, R.-J., Li, J.-Q., Chen, Y.-C., Zhang, L.-X., and Xiao, L.-H. (2018). Widespread occurrence of Cryptosporidium infections in patients with HIV/AIDS: Epidemiology, clinical feature, diagnosis, and therapy. *Acta Trop.* 187, 257–263. doi: 10.1016/j.actatropica.2018.08.018

Wilke, G., Ravindran, S., Funkhouser-Jones, L., Barks, J., Wang, Q., VanDussen, K. L., et al. (2018). Monoclonal Antibodies to Intracellular Stages of Cryptosporidium parvum Define Life Cycle Progression In Vitro. *Msphere* 3, e00124–e00118. doi: 10.1128/msphere.00124-18

Wilke, G., Funkhouser-Jones, L. J., Wang, Y., Ravindran, S., Wang, Q., Beatty, W. L., et al. (2019). A Stem-Cell-Derived Platform Enables Complete Cryptosporidium Development In Vitro and Genetic Tractability. *Cell Host Microbe* 26, 123–134.e8. doi: 10.1016/j.chom.2019.05.007

Conflict of Interest: The authors declare that the research was conducted in the absence of any commercial or financial relationships that could be construed as a potential conflict of interest.

frontiers in Cellular and Infection Microbiology

MINI REVIEW
published: 11 December 2020
doi: 10.3389/fcimb.2020.593159

Midgut Mitochondrial Function as a Gatekeeper for Malaria Parasite Infection and Development in the Mosquito Host

Shirley Luckhart[1,2*] *and Michael A. Riehle*[3]

[1] Department of Entomology, Plant Pathology and Nematology, University of Idaho, Moscow, ID, United States, [2] Department of Biological Sciences, University of Idaho, Moscow, ID, United States, [3] Department of Entomology, University of Arizona, Tucson, AZ, United States

Across diverse organisms, various physiologies are profoundly regulated by mitochondrial function, which is defined by mitochondrial fusion, biogenesis, oxidative phosphorylation (OXPHOS), and mitophagy. Based on our data and significant published studies from *Caenorhabditis elegans*, *Drosophila melanogaster* and mammals, we propose that midgut mitochondria control midgut health and the health of other tissues in vector mosquitoes. Specifically, we argue that trade-offs among resistance to infection, metabolism, lifespan, and reproduction in vector mosquitoes are fundamentally controlled both locally and systemically by midgut mitochondrial function.

Keywords: mosquito, malaria, *Anopheles*, *Plasmodium*, mitochondria, midgut, resistance, immunity

OPEN ACCESS

Edited by:
Robert Sinden,
Imperial College London,
United Kingdom

Reviewed by:
Jingwen Wang,
Yale University, United States
Gabriele Pradel,
RWTH Aachen University, Germany

****Correspondence:***
Shirley Luckhart
sluckhart@uidaho.edu

Specialty section:
This article was submitted to Parasite and Host, a section of the journal Frontiers in Cellular and Infection Microbiology

Received: *09 August 2020*
Accepted: *13 November 2020*
Published: *11 December 2020*

Citation:
Luckhart S and Riehle MA (2020) Midgut Mitochondrial Function as a Gatekeeper for Malaria Parasite Infection and Development in the Mosquito Host. Front. Cell. Infect. Microbiol. 10:593159. doi: 10.3389/fcimb.2020.593159

INTRODUCTION

Across diverse organisms, physiology is profoundly regulated by mitochondrial function, which is defined by the sum of mitochondrial fusion, biogenesis, oxidative phosphorylation (OXPHOS) and mitophagy (Zhu et al., 2013; Yu et al., 2020). Based on significant work from *Caenorhabditis elegans* (Chikka et al., 2016; Kwon et al., 2018) and *Drosophila melanogaster* (Miguel-Aliaga et al., 2018), it is likely that mitochondrial control of tissue health—and gut health in particular—is conserved across the Ecdysozoa. Importantly, the balance of mitochondrial function and dysfunction, particularly in the midgut, is highly relevant to mosquito vectors of human pathogens (Luckhart and Riehle, 2017). We hypothesize that mitochondrial activity in the midgut, the initial interface between the mosquito and *Plasmodium* parasites, dictates the balance of pathogen susceptibility and the life history traits essential

Abbreviations: 20E, 20-hydroxyecdysone; Akt, IIS kinase, also known as protein kinase B; AMPK, 5' adenosine monophosphate-activated protein kinase; Atg, autophagy; ERK, extracellular signal-regulated kinase; ETC, electron transport chain; FOXO, class O forkhead box transcription factors; IGF1, insulin-like growth factor 1; IIS, insulin/insulin-like growth factor signaling; ILP, insulin-like peptide; IRS, insulin receptor substrate; MEK, mitogen-activated protein kinase kinase; MSC, midgut stem cells; mTOR, mechanistic target of rapamycin; NADH, reduced form of nicotinamide adenine dinucleotide; NF-κB, nuclear factor-kappa B; NO, nitric oxide; NTG, non-transgenic; OEH, ovarian ecdysteroidogenic hormone; OXPHOS, oxidative phosphorylation; p38 MAPK, p38 mitogen-activated protein kinase; p70S6K, p70 S6 kinase; PGC-1, peroxisome proliferator-activated receptor gamma coactivator-1; PI-3K, phosphatidylinositol-3-kinase; PINK1, PTEN-induced kinase 1; PTEN, IIS protein, also known as phosphatase and tensin homolog; ROS, reactive oxygen species; TG, transgenic.

for ensuring pathogen transmission. Further, the regulation of midgut mitochondrial activity is regulated in a large part through the insulin/insulin-like growth factor signaling (IIS) cascade. In this review, we will discuss data that support the inference that trade-offs among resistance to infection, lifespan and reproduction in mosquito vectors of malaria parasites are fundamentally controlled both locally and systemically by midgut mitochondrial function *via* IIS. While this mini-review will focus on mitochondrial activity in the mosquito gut, due to the central regulatory role of the gut and its unique interaction with pathogens in the bloodmeal, it is likely that mitochondrial activity in diverse tissues also has important roles in regulating the physiologies described below.

INSULIN/INSULIN-LIKE GROWTH FACTOR SIGNALING CONTROLS MITOCHONDRIAL FUNCTION TO ALTER DIVERSE PHYSIOLOGIES IMPACTING VECTORIAL CAPACITY

IIS regulates mitochondrial function across a wide range of organisms and, in this capacity, contributes to control of longevity, host immunity, cellular metabolism and the response to stress in mammals and in the model organisms *D. melanogaster* and *C. elegans*. We and others have demonstrated that IIS in adult female mosquitoes regulates egg production, longevity, defenses against infection, metabolism and the host stress response (Graf et al., 1997; Riehle and Brown, 1999; Riehle and Brown, 2002; Riehle and Brown, 2003; Lim et al., 2005; Kang et al., 2007; Roy et al., 2007; Brown et al., 2008; Sim and Denlinger, 2008; Arik et al., 2009; Corby-Harris et al., 2010; Horton et al., 2010; Gulia-Nuss et al., 2011; Marquez et al., 2011; Surachetpong et al., 2011; Pakpour et al., 2012; Hauck et al., 2013; Luckhart et al., 2013; Drexler et al., 2014; Arik et al., 2015; Pietri et al., 2016; Nuss and Brown, 2018). Further, substantial data indicate that IIS-dependent phenotypes are mediated through changes in mitochondrial function (**Figure 1**) in model invertebrates, mosquitoes and in mammals (Tóth et al., 2008; Cheng et al., 2010; Tiefenbock et al., 2010; Luckhart et al., 2013; Sadagurski and White, 2013; Drexler et al., 2014; Mukherjee et al., 2014; Pietri et al., 2016; Chaudhari and Kipreos, 2017; Ruegsegger et al., 2018; Wang et al., 2019; Wardelmann et al., 2019; Charmpilas and Tavernarakis, 2020; Sheard et al., 2020). Specifically, perturbations of both the IIS activator Akt and the inhibitor PTEN in the midgut of *Anopheles stephensi* led to profound changes in midgut mitochondrial number, quality and function as discussed below (Luckhart et al., 2013; Hauck et al., 2013).

MITOCHONDRIAL FUNCTION IS EVOLUTIONARILY CONSERVED AND REGULATED BY MITOCHONDRIAL QUALITY CONTROL

Mitochondrial biogenesis or the generation of new mitochondria and elimination of damaged mitochondria *via* mitophagy, a form of organelle-specific autophagy, control mitochondrial function and have profound effects on health and disease in diverse organisms (Palikaras et al., 2018). In particular, the balance between mitochondrial biogenesis and mitophagy is highly responsive to the host environment, including changes in cellular metabolism and energy status and activation of immunity to infection, to ensure tissue and organismal homeostasis (Youle and van der Bliek, 2012; Ma et al., 2020).

In general, mitochondrial damage from oxidative stress, stress-induced changes in energy status and xenobiotic insults can initiate mitochondrial fission or the separation of compromised mitochondria for removal by mitophagy (Elgass et al., 2012). The genomes of *A. stephensi* and *Anopheles gambiae* encode autophagy machinery orthologs for Parkin, PINK1, more than a dozen autophagy-related (Atg) genes and two vacuolar protein sorting genes. In brief, damaged mitochondria are targeted for the aggregation of PINK1, which recruits the E3 ubiquitin ligase Parkin to activate Atg proteins to form the autophagosome. Activators of autophagy include mitochondrial reactive oxygen species (ROS) as well as signaling through ERK-dependent and p38 MAPK and AMP-activated protein kinase (AMPK; Huang et al., 2011; Levine et al., 2011; Corona Velazquez and Jackson, 2018). Autophagy is inhibited by signaling through the PI-3K/Akt branch of the IIS cascade, signaling that also controls mitochondrial biogenesis (Huang et al., 2011; Levine et al., 2011; Denton et al., 2012; Manning and Toker, 2017). Specifically, when FOXO is excluded from the nucleus by PI-3K/Akt signaling, PPAR gamma coactivator-1 alpha (PGC-1), a key mediator of mitochondrial biogenesis, is not activated (Cheng et al., 2009). Conversely, overexpression of the IIS inhibitor PTEN, which results in FOXO translocation into the nucleus, induces PGC-1 activity (Garcia-Cao et al., 2012). In *D. melanogaster*, FOXO-induced PGC-1 increased levels and activity of electron transport chain (ETC) complexes I, II, and IV, indicating that enhanced functioning of the ETC is positively associated with biogenesis (Rera et al., 2011). Increased midgut mitochondrial biogenesis in *D. melanogaster* resulted in improved midgut epithelial integrity, and we have associated this biological dynamic in *A. stephensi* with reduced development of the human malaria parasite *Plasmodium falciparum* in the absence of enhanced NF-κB-dependent immune gene expression (Rera et al., 2011; Pakpour et al., 2012; Hauck et al., 2013; Pakpour et al., 2013). Mitochondrial biogenesis, which is activated by NO-dependent guanylate cyclase as well as by AMPK signaling, was hyperactivated and out of balance with mitophagy in *A. stephensi* engineered to overexpress activated Akt in the midgut epithelium (Nisoli et al., 2003; Nisoli et al., 2004; Nisoli et al., 2005; Fernandez-Marcos and Auwerx, 2011; Luckhart et al., 2013). While Akt-dependent mitochondrial dysfunction was deleterious to *A. stephensi*, it also conferred extreme resistance to *P. falciparum* infection (Corby-Harris et al., 2010; Luckhart et al., 2013).

MITOCHONDRIAL FUNCTION CONTROLS EPITHELIAL BARRIER INTEGRITY AND STEM CELL ACTIVITY IN THE GUT

An analysis of mitochondrially controlled phenotypes is informative for the idea that mitochondria are master regulators

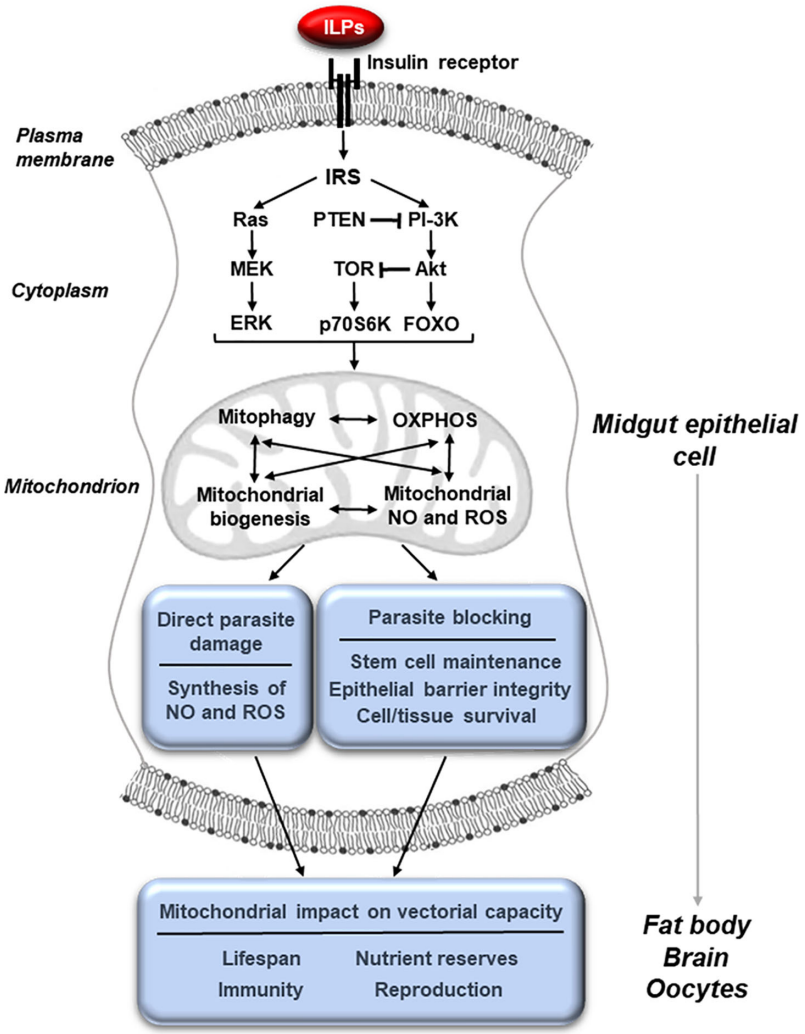

FIGURE 1 | Midgut mitochondrial function, activated through IIS, controls physiologies that govern vectorial capacity. The binding of insulin-like peptides (ILPs) to the insulin receptor at the membrane of midgut epithelial cells activates the insulin/insulin-like growth factor signaling (IIS) cascade leading to changes in mitochondrial activity. These can include changes in mitophagy, biogenesis, oxidative phosphorylation (OXPHOS) and the synthesis of nitric oxide (NO) and reactive oxygen species (ROS). These mitochondrial changes can in turn directly result in parasite killing and improve the integrity of the epithelial barrier, making it difficult for the parasite to escape from the midgut cell. In addition, mitochondrial changes in the midgut epithelium can influence other tissues, altering key physiologies such as reproduction, lifespan, metabolism and immunity that affect vectorial capacity.

of key physiologies in mosquitoes (**Figure 1**). When AMPK was overexpressed in the midgut of *D. melanogaster*, the age-related decline in epithelial barrier integrity was reduced, indicating that both autophagy and mitochondrial biogenesis protected the integrity of the midgut barrier (Rera et al., 2011; Ulgherait et al., 2014). In more recent work, treatment with rapamycin, which inhibits Akt-dependent mechanistic Target of Rapamycin (mTOR) signaling, maintained epithelial barrier integrity and extended lifespan in *D. melanogaster* independently of any changes in the gut microbiota (Schinaman et al., 2019). In mammals, AMPK is required for regulation of polarity of hepatocytes and other epithelial cell types as well as tight junction and barrier integrity through increased mitochondrial fusion and biogenesis (Treyer and Müsch, 2013; Kang et al., 2016; Ghosh, 2017). Successful *P. falciparum* infection of hepatocytes has been associated with reduced AMPK activity in these cells, whereas pharmacological induction of hepatocyte AMPK reduced intracellular parasite growth (Ruivo et al., 2016). In our work, we observed increased midgut barrier integrity in transgenic (TG) *A. stephensi* with increased PTEN expression in the midgut, which limited *P. falciparum* infection without changes to NF-κB-dependent anti-parasite gene expression (Hauck et al., 2013). Since the IIS activator Akt can suppress both mitochondrial biogenesis and autophagy, it is likely that overexpression of the IIS inhibitor PTEN in *A. stephensi* increased autophagy, mitochondrial fusion and mitochondrial biogenesis to enhance midgut barrier integrity, in turn increasing mosquito resistance to *P. falciparum* infection (Huang et al., 2011; Levine et al., 2011; Denton et al., 2012; Hauck et al., 2013).

Supporting this idea, biomarker expression for both midgut stem cells (MSC) and autophagy were increased in TG *A. stephensi* overexpressing PTEN relative to non-transgenic (NTG) controls (Hauck et al., 2013). Collectively, our data and these observations suggest that manipulation of pathways leading to increased midgut mitochondrial fusion and biogenesis have the potential to improve midgut epithelial integrity and in turn resistance to *P. falciparum* infection in *A. stephensi*.

A proper balance between mitophagy and mitochondrial biogenesis is essential for optimal stem cell differentiation and maintenance. Previous studies have demonstrated the important roles stem cells play in the midgut of insects, including mosquitoes (Brown et al., 1985; Baton and Ranford-Cartwright, 2007). Intriguingly, Janeh et al. (2019) reported that, in contrast to *Aedes albopictus* and *Culex pipiens*, midgut tissue in *A. gambiae* does not contain cells that undergo mitosis to repair gut damage. The authors speculated that this difference could underlie permissiveness to malaria parasite infection and rightly suggested that additional mechanistic studies are necessary to fully understand the biological importance of these differences across mosquito genera. In *D. melanogaster*, upregulation of mitochondrial biogenesis in the midgut prevented MSC over-proliferation and the accumulation of improperly differentiated cells (Rera et al., 2012a). Coupled with an enhanced epithelial barrier, this phenotype confirmed that reduced MSC dysplasia could extend lifespan. When *A. stephensi* were provisioned with human IGF1 in the bloodmeal at concentrations consistent with titers found during malaria, midgut cytoprotection was enhanced through the homeostatic regulation of ROS and patterns of gene expression consistent with both MSC activity and autophagy, resulting in improved mitochondrial function and a more robust midgut epithelium (Drexler et al., 2014). These data suggested that enhancing mitochondrial function to increase midgut health could improve both parasite resistance and lifespan in *A. stephensi* (Drexler et al., 2014). In addition to these processes, the Hippo pathway regulates mitochondrial function in both human and *D. melanogaster* cells (Nagaraj et al., 2012). In *D. melanogaster*, knockdown of Hippo or overexpression of Yorkie, the transcriptional effector of the pathway, enhanced MSC proliferation and prevented apoptosis, providing additional support for the role of mitochondrial function in epithelial homeostasis (Huang et al., 2005; Ren et al., 2010).

MITOCHONDRIAL FUNCTION CONTROLS DIVERSE PHYSIOLOGIES THAT ARE KEY TO VECTORIAL CAPACITY

Host immunity to infection is regulated by mitochondrial function. Increased biogenesis of mitochondria during infection, possibly in response to cell injury, can alter the production of pro- and anti-inflammatory cytokines to improve mammalian host convalescence and survival (Sweeney et al., 2010; Carré et al., 2010; Sweeney et al., 2011; Tran et al., 2011; Dada and Sznajder, 2011; Piantadosi et al., 2011). ETC Complex I- and III-generated ROS can also activate Toll-like receptor signaling and NF-kB-dependent gene expression for the targeted elimination of pathogens (Arnoult et al., 2011). In *A. stephensi*, activation of IIS induced high levels of mitochondrial anti-parasite ROS and NO, responses that also resulted in significant damage to the midgut epithelium (Luckhart et al., 2013). This damage, however, can be mitigated by parasite-induced p38 MAPK signaling and associated increases in mitochondrial biogenesis, oxidative phosphorylation (OXPHOS) and antioxidant biosynthesis for mosquito survival during infection (Wang et al., 2015). In an effort to establish cause-and-effect of these metabolic changes with infection outcome, we provisioned small molecule inhibitors to *A. stephensi* to demonstrate that midgut intermediary metabolism, in fact, regulates *P. falciparum* infection (Pietri et al., 2016). Notably, these small molecule inhibitors had no effect on NF-kB-dependent immune gene expression, thereby linking anti-parasite resistance to shifts in glycolysis and mitochondrial function (Pietri et al., 2016). To our knowledge, this was the first evidence in anopheline mosquitoes that direct manipulation of metabolism and mitochondrial function could alter anti-parasite immunity.

Longevity is one of the most complex phenotypes regulated by mitochondrial physiology and is a life history trait intimately connected to resistance to infection across a wide range of organisms. Specifically, modest reductions in mitochondrial ETC activity and OXPHOS can enhance survival in organisms ranging from yeast to mice (reviewed in Rera et al., 2012a). A modest *increase* in ETC activity, however, can be effective as well. When ETC Complex I activity was increased in *D. melanogaster* through the overexpression of yeast NADH-ubiquinone oxidoreductase the integrity of the midgut barrier was improved and lifespan extended, without a reduction in fecundity (Hur et al., 2013). The fact that both activation and inhibition of ETC Complex I can lead to increased longevity is an example of hormesis, where modest positive and negative changes can both drive an organism to improved mitochondrial function (Hur et al., 2014). Increased autophagy has also been found to extend lifespan of *D. melanogaster*. In this context, overexpression of Parkin, a key mediator of mitophagy, significantly extended lifespan *and* increased fruit fly fecundity (Rana et al., 2013). In contrast, mutations in PINK1, which binds to damaged mitochondria and recruits Parkin, were associated with a reduction in lifespan (Clark et al., 2006). In our work, PTEN overexpression in the *A. stephensi* midgut increased longevity, enhanced the midgut barrier, improved *P. falciparum* resistance and had no negative impact on fecundity (Hauck et al., 2013). This work suggested that PTEN overexpression in *A. stephensi* and the anticipated downstream effects on both PINK1 and Parkin improved mitochondrial quality control, which led to increased longevity and parasite resistance (Unoki and Nakamura, 2001). Extensive studies on AMPK in diverse organisms, including *D. melanogaster* and *A. aegypti*, demonstrated a key role for this protein in the regulation of senescence as well. In *D. melanogaster*, upregulation of AMPK in the midgut significantly extended lifespan (Ulgherait et al., 2014). In *A. aegypti*, a diet supplemented with polyphenols increased lifespan, in part through AMPK activation (Nunes et al., 2016). Our studies, however, did not replicate polyphenol-dependent life extension in *A. stephensi*, suggesting that these two mosquito species may have

intriguing differences in longevity regulation (Johnson and Riehle, 2015).

Reproduction in mosquitoes, unlike most other Diptera including *D. melanogaster*, is intermittent and dependent on nutrient-rich bloodmeals, which initiate a reproductive cycle. This reproductive cycle, including oogenesis and vitellogenesis, is tightly regulated through a combination of hormonal signals, signaling cascades and nutrient sensors. In response to the blood-filled midgut, signals from the brain including insulin-like peptides (ILPs) and ovarian ecdysteroidogenic hormone (OEH) induce ovarian synthesis of 20-hydroxyecdysone (20E), which triggers fat body biosynthesis of lipids and other nutrients for egg development. The impact of 20E on malaria parasite infection is complex, with two studies reporting that 20E increases resistance of *A. gambiae* to *P. falciparum* and *Plasmodium berghei* (Upton et al., 2015; Reynolds et al., 2020). In contrast, Dahalan et al. (2019) showed that male-derived 20E, delivered to the female mosquito during mating, dramatically altered the midgut transcriptome in patterns distinct from those of systemic effects of 20E and decreased resistance of *Anopheles coluzzii* to *P. falciparum*. In addition to IIS regulation of 20E, IIS regulation of mitochondrial dynamics governs reproductive success in *D. melanogaster* while mitochondrial variation-dependent outcomes in innate immunity of fruit flies likely also drives immunity-fecundity tradeoffs. Notably, ubiquitous and neuron-specific overexpression of Parkin in adult fruit flies led to a significant increase in fecundity, in addition to lifespan extension (Rana et al., 2013). In a recent review, Salminen and Vale (2020) elegantly argue that variation in mitochondrial function of *D. melanogaster*, which has many hallmarks of the same biology in mammals, likely drives variation in fruit fly innate immune function. By extrapolation, this variation, which ranges from optimal mitochondrial dynamics to extreme dysfunction, would be predicted to underlie observed tradeoffs between immunity and fecundity observed in fruit flies with abnormal mitochondrial energy metabolism (Buchanan et al., 2018). Our own work in *A. stephensi* demonstrated that Akt signaling directly influences mitochondrial activity in the midgut (Luckhart et al., 2013). Further, increased Akt signaling in the fat body of *A. stephensi*, which most likely influences mitochondrial activity in this tissue as well, led to a significant increase in lifetime fecundity (Hun et al., 2019). In light of these observations, it is likely that IIS/TOR-dependent mitochondrial activity controls reproduction in *Anopheles* spp., but we would add that underlying IIS-dependent mitochondrial variation likely also drives the somewhat puzzling range of tradeoffs that are evident during infection.

CONCLUSION

The *C. elegans* and *D. melanogaster* guts are among the most stress sensitive tissues and function as critical "signaling centers" for communicating changes in mitochondrial function (Alic et al., 2014; Owusu-Ansah and Perrimon, 2015; Liu and Jin, 2017). For example, aging in *D. melanogaster* has been associated with a general decline in tissue mitochondrial biogenesis, but manipulations to *systemically* increase mitochondrial biogenesis had no effect on fruit fly longevity. However, targeted enhancements in *gut-specific* mitochondrial biogenesis enhanced *D. melanogaster* longevity *via* coordinated changes in tissue mitochondrial function (Vellai, 2009; Rera et al., 2012b; Ulgherait et al., 2014). Notably, gut mitochondrial biogenesis was associated with an improved midgut epithelial barrier, preventing lumenal microbes from initiating disseminated infections (Rera et al., 2012b). Accordingly, manipulation of *gut* mitochondrial function in *D. melanogaster* can enhance immunity locally and fitness systemically. Importantly, mitochondrial changes in fat body and muscle can contribute independently to these phenotypes as well, indicating that local mitochondrial changes induce *functional* systemic changes to extend local effects (Owusu-Ansah and Perrimon, 2015). Based on these observations, our data and the work of others, we hypothesize that changes in midgut mitochondrial dynamics function both *locally* and *systemically* to coordinate pathogen resistance, metabolism, lifespan and reproduction in *Anopheles* mosquitoes (**Figure 1**).

Is the *Anopheles* midgut a signaling center for mitochondrial physiology and the coordination of changes in host biology during infection? Published data and our data argue that this is case, but considerable work remains to be done in understanding this biology and its influence on mosquito resistance to infection, networking of life history traits critical to vectorial capacity and the dependency of this network on the coordination of mitochondrial function among the midgut and other tissues. Will this biology simply be a carbon copy of what is known from model invertebrates and mammals? If viewed *only* from the perspective of gene conservation, the answer is likely to be yes. However, the relevance of this biology to mosquitoes is uniquely elevated, defined and dictated by bloodfeeding and the consequences to human health that are vastly different from other organisms. Accordingly, this biology has both translational importance to "getting over the gut" and critical relevance to our basic scientific knowledge, with likely twists and turns that will provide a fascinating and substantive extension of our general knowledge of mitochondrial control of animal physiology.

AUTHOR CONTRIBUTIONS

SL and MR wrote and revised this mini-review. All authors contributed to the article and approved the submitted version.

FUNDING

The authors' work cited here has been supported by the National Institutes of Health, National Institute of Allergy and Infectious Diseases awards R01AI060664, R01AI080799, R56AI107263, R56AI118926, R56AI129420, R01AI073745, and R21AI125823.

ACKNOWLEDGMENT

We also acknowledge and appreciate many critical discussions of mosquito physiology over the course of our collective work with Dr. Mark R. Brown (University of Georgia).

REFERENCES

Alic, N., Tullet, J. M., Niccoli, T., Broughton, S., Hoddinott, M. P., Slack, C., et al. (2014). Cell-nonautonomous effects of dFOXO/DAF-16 in aging. *Cell Rep.* 6, 608–616. doi: 10.1016/j.celrep.2014.01.015

Arik, A. J., Rasgon, J. L., Quicke, K. M., and Riehle, M. A. (2009). Manipulating insulin signaling to enhance mosquito reproduction. *BMC Physiol.* 9, 15. doi: 10.1186/1472-6793-9-15

Arik, A. J., Hun, L. V., Quicke, K., Piatt, M., Ziegler, R., Scaraffia, P. Y., et al. (2015). Increased Akt signaling in the mosquito fat body increases adult survivorship. *FASEB J.* 29, 1404–1413. doi: 10.1096/fj.14-261479

Arnoult, D., Soares, F., Tattoli, I., and Girardin, S. E. (2011). Mitochondria in innate immunity. *EMBO Rep.* 12, 901–910. doi: 10.1038/embor.2011.157

Baton, L., and Ranford-Cartwright, L. (2007). Morphological evidence for proliferative regeneration of the *Anopheles stephensi* midgut epithelium following *Plasmodium falciparum* ookinete invasion. *J. Invertebr. Pathol.* 96, 244–254. doi: 10.1016/j.jip.2007.05.005

Brown, M. R., Raikhel, A. S., and Lea, A. O. (1985). Ultrastructure of midgut endocrine cells in the adult mosquito, *Aedes aegypti*. *Tissue Cell.* 17, 709–721. doi: 10.1016/0040-8166(85)90006-0

Brown, M. R., Clark, K. D., Gulia, M., Zhao, Z., Garczynski, S. F., Crim, J. W., et al. (2008). An insulin-like peptide regulates egg maturation and metabolism in the mosquito *Aedes aegypti*. *Proc. Natl. Acad. Sci. U. S. A.* 105, 5716–5721. doi: 10.1073/pnas.0800478105

Buchanan, J. L., Meiklejohn, C. D., and Montooth, K. L. (2018). Mitochondrial dysfunction and infection generate immunity–fecundity tradeoffs in *Drosophila*. *Integr. Comp. Biol.* 58, 591–603. doi: 10.1093/icb/icy078

Carré, J. E., Orban, J. C., Re, L., Felsmann, K., Iffert, W., Bauer, M., et al. (2010). Survival in critical illness is associated with early activation of mitochondrial biogenesis. *Am. J. Respir. Crit. Care Med.* 182, 745–751. doi: 10.1164/rccm.201003-0326OC

Charmpilas, N., and Tavernarakis, N. (2020). Mitochondrial maturation drives germline stem cell differentiation in *Caenorhabditis elegans*. *Cell Death Differ.* 27, 601–617. doi: 10.1038/s41418-019-0375-9

Chaudhari, S. N., and Kipreos, E. T. (2017). Increased mitochondrial fusion allows the survival of older animals in diverse *C. elegans* longevity pathways. *Nat. Commun.* 8, 1–16. doi: 10.1038/s41467-017-00274-4

Cheng, Z., Guo, S., Copps, K., Dong, X., Kollipara, R., Rodgers, J. T., et al. (2009). Foxo1 integrates insulin signaling with mitochondrial function in the liver. *Nat. Med.* 15, 1307–1311. doi: 10.1038/nm.2049

Cheng, Z., Tseng, Y., and White, M. F. (2010). Insulin signaling meets mitochondria in metabolism. *Trends Endrocrinol. Metab.* 21, 589–598. doi: 10.1016/j.tem.2010.06.005

Chikka, M. R., Anbalagan, C., Dvorak, K., Dombeck, K., and Prahlad, V. (2016). The mitochondria-regulated immune pathway activated in the *C. elegans* intestine is neuroprotective. *Cell Rep.* 16, 2399–2414. doi: 10.1016/j.celrep.2016.07.077

Clark, I. E., Dodson, M. W., Jiang, C., Cao, J. H., Huh, J. R., Seol, J. H., et al. (2006). *Drosophila* pink1 is required for mitochondrial function and interacts genetically with parkin. *Nature* 441, 1162–1166. doi: 10.1038/nature04779

Corby-Harris, V., Drexler, A., Watkins de Jong, L., Antonova, Y., Pakpour, N., Ziegler, R., et al. (2010). Activation of Akt signaling reduces the prevalence and intensity of malaria parasite infection and lifespan in *Anopheles stephensi* mosquitoes. *PLoS Pathog.* 6, e1001003. doi: 10.1371/journal.ppat.1001003

Corona Velazquez, A. F., and Jackson, W. T. (2018). So many roads: The multifaceted regulation of autophagy induction. *Mol. Cell. Biol.* 38, e00303–e00318. doi: 10.1128/MCB.00303-18

Dada, L. A., and Sznajder, J. II (2011). Mitochondrial Ca2 and ROS take center stage to orchestrate TNF-α–mediated inflammatory responses. *J. Clin. Invest.* 121, 1683–1685. doi: 10.1172/JCI57748

Dahalan, F. A., Churcher, T. S., Windbichler, N., and Lawniczak, M. K. (2019). The male mosquito contribution towards malaria transmission: Mating influences the *Anopheles* female midgut transcriptome and increases female susceptibility to human malaria parasites. *PLoS Pathog.* 15, e1008063. doi: 10.1371/journal.ppat.1008063

Denton, D., Chang, T., Nicolson, S., Shravage, B., Simin, R., Baehrecke, E., et al. (2012). Relationship between growth arrest and autophagy in midgut programmed cell death in *Drosophila*. *Cell Death Differ.* 19, 1299–1307. doi: 10.1038/cdd.2012.43

Drexler, A. L., Pietri, J. E., Pakpour, N., Hauck, E., Wang, B., Glennon, E. K., et al. (2014). Human IGF1 regulates midgut oxidative stress and epithelial homeostasis to balance lifespan and *Plasmodium falciparum* resistance in *Anopheles stephensi*. *PLoS Pathog.* 10, e1004231. doi: 10.1371/journal.ppat.1004231

Elgass, K., Pakay, J., Ryan, M. T., and Palmer, C. S. (2012). Recent advances into the understanding of mitochondrial fission. *BBA-Mol. Cell. Res.* 1833, 150–161. doi: 10.1016/j.bbamcr.2012.05.002

Fernandez-Marcos, P. J., and Auwerx, J. (2011). Regulation of PGC-1α, a nodal regulator of mitochondrial biogenesis. *Am. J. Clin. Nutr.* 93, 884S–890S. doi: 10.3945/ajcn.110.001917

Garcia-Cao, I., Song, M. S., Hobbs, R. M., Laurent, G., Giorgi, C., de Boer, V. C. J., et al. (2012). Systemic elevation of PTEN induces a tumor-suppressive metabolic state. *Cell* 149, 49–62. doi: 10.1016/j.cell.2012.02.030

Ghosh, P. (2017). The stress polarity pathway: AMPK 'GIV'-es protection against metabolic insults. *Aging* 9, 303–314. doi: 10.18632/aging.101179

Graf, R., Neuenschwander, S., Brown, M. R., and Ackermann, U. (1997). Insulin-mediated secretion of ecdysteroids from mosquito ovaries and molecular cloning of the insulin receptor homologue from ovaries of bloodfed *Aedes aegypti*. *Insect Mol. Biol.* 6, 151–163. doi: 10.1111/j.1365-2583.1997.tb00083.x

Gulia-Nuss, M., Robertson, A. E., Brown, M. R., and Strand, M. R. (2011). Insulin-like peptides and the target of rapamycin pathway coordinately regulate blood digestion and egg maturation in the mosquito *Aedes aegypti*. *PLoS One* 6, e20401. doi: 10.1371/journal.pone.0020401

Hauck, E. S., Antonova-Koch, Y., Drexler, A., Pietri, J., Pakpour, N., Liu, D., et al. (2013). Overexpression of phosphatase and tensin homolog improves fitness and decreases *Plasmodium falciparum* development in *Anopheles stephensi*. *Microbes Infect.* 15, 775–787. doi: 10.1016/j.micinf.2013.05.006

Horton, A. A., Lee, Y., Coulibaly, C. A., Rashbrook, V. K., Cornel, A. J., Lanzaro, G. C., et al. (2010). Identification of three single nucleotide polymorphisms in *Anopheles gambiae* immune signaling genes that are associated with natural *Plasmodium falciparum* infection. *Malar. J.* 9, 160. doi: 10.1186/1475-2875-9-160

Huang, J., Wu, S., Barrera, J., Matthews, K., and Pan, D. (2005). The Hippo signaling pathway coordinately regulates cell proliferation and apoptosis by inactivating yorkie, the *Drosophila* homolog of YAP. *Cell* 122, 421–434. doi: 10.1016/j.cell.2005.06.007

Huang, J., Lam, G. Y., and Brumell, J. H. (2011). Autophagy signaling through reactive oxygen species. *Antioxid. Redox Signal.* 14, 2215–2231. doi: 10.1089/ars.2010.3554

Hun, L. V., Luckhart, S., and Riehle, M. A. (2019). Increased Akt signaling in the fat body of *Anopheles stephensi* extends lifespan and increases lifetime fecundity through modulation of insulin-like peptides. *J. Insect Physiol.* 118, 103932. doi: 10.1016/j.jinsphys.2019.103932

Hur, J. H., Bahadorani, S., Graniel, J., Koehler, C. L., Ulgherait, M., Rera, M., et al. (2013). Increased longevity mediated by yeast NDI1 expression in *Drosophila* intestinal stem and progenitor cells. *Aging (Albany NY)* 5, 662–681. doi: 10.18632/aging.100595

Hur, J. H., Stork, D. A., and Walker, D. W. (2014). Complex-I-ty in aging. *J. Bioenerg. Biomembr.* 46, 329–335. doi: 10.1007/s10863-014-9553-0

Hur, L. V., Luckhart, S., and Riehle, M. A. (2019). Increased Akt signaling in the fat body of *Anopheles stephensi* extends lifespan and increases lifetime fecundity through modulation of insulin-like peptides. *J. Insect Physiol.* 118, 103932. doi: 10.1016/j.jinsphys.2019.103932

Janeh, M., Osman, D., and Kambris, Z. (2019). Comparative analysis of midgut regeneration capacity and resistance to oral infection in three disease-vector mosquitoes. *Sci. Rep.* 9, 1–10. doi: 10.1038/s41598-019-50994-4

Johnson, A. A., and Riehle, M. A. (2015). Resveratrol fails to extend life span in the mosquito *Anopheles stephensi*. *Rejuvenation Res.* 18, 473–478. doi: 10.1089/rej.2015.1670

Kang, C., You, Y. J., and Avery, L. (2007). Dual roles of autophagy in the survival of *Caenorhabditis elegans* during starvation. *Genes Dev.* 21, 2161–2171. doi: 10.1101/gad.1573107

Kang, S. W. S., Haydar, G., Taniane, C., Farrell, G., Arias, I. M., Lippincott-Schwartz, J., et al. (2016). AMPK activation prevents and reverses drug-induced mitochondrial and hepatocyte injury by promoting mitochondrial fusion and function. *PloS One* 11, e0165638. doi: 10.1371/journal.pone.0165638

Kwon, S., Kim, E. J. E., and Lee, S. V. (2018). Mitochondria-mediated defense mechanisms against pathogens in *Caenorhabditis elegans*. *BMB Rep.* 51, 274–279. doi: 10.5483/BMBRep.2018.51.6.111

Levine, B., Mizushima, N., and Virgin, H. W. (2011). Autophagy in immunity and inflammation. *Nature* 469, 323–335. doi: 10.1038/nature09782

Lim, J., Gowda, D. C., Krishnegowda, G., and Luckhart, S. (2005). Induction of nitric oxide synthase in *Anopheles stephensi* by *Plasmodium falciparum*: mechanism of signaling and the role of parasite glycosylphosphatidylinositols. *Infect. Immun.* 73, 2778–2789. doi: 10.1128/IAI.73.5.2778-2789.2005

Liu, Q., and Jin, L. H. (2017). Organ-to-organ communication: a *Drosophila* gastrointestinal tract perspective. *Front. Cell Dev. Biol.* 5, 29. doi: 10.3389/fcell.2017.00029

Luckhart, S., Giulivi, C., Drexler, A. L., Antonova-Koch, Y., Sakaguchi, D., Napoli, E., et al. (2013). Sustained activation of Akt elicits mitochondrial dysfunction to block *Plasmodium falciparum* infection in the mosquito host. *PLoS Pathog.* 9, e1003180. doi: 10.1371/journal.ppat.1003180

Luckhart, S., and Riehle, M. A. (2017). "Conservation and convergence of immune signaling pathways with mitochondrial regulation in vector arthropod physiology," in *Arthropod Vector: Controller of Disease Transmission, Volume 1* (London, United Kingdom: Elsevier), 15–33. doi: 10.1016/B978-0-12-805350-8.00002-7

Ma, K., Chen, G., Li, W., Kepp, O., Zhu, Y., and Chen, Q. (2020). Mitophagy, mitochondrial homeostasis, and cell fate. *Front. Cell Dev. Biol.* 8, 467. doi: 10.3389/fcell.2020.00467

Manning, B. D., and Toker, A. (2017). AKT/PKB signaling: navigating the network. *Cell* 169, 381–405. doi: 10.1016/j.cell.2017.04.001

Marquez, A. G., Pietri, J. E., Smithers, H. M., Nuss, A., Antonova, Y., Drexler, A. L., et al. (2011). Insulin-like peptides in the mosquito *Anopheles stephensi*: identification and expression in response to diet and infection with *Plasmodium falciparum*. *Gen. Comp. Endocrinol.* 173, 303–312. doi: 10.1016/j.ygcen.2011.06.005

Miguel-Aliaga, I., Jasper, H., and Lemaitre, B. (2018). Anatomy and physiology of the digestive tract of *Drosophila melanogaster*. *Genetics* 210, 357–396. doi: 10.1534/genetics.118.300224

Mukherjee, S., Basar, M. A., Davis, C., and Duttaroy, A. (2014). Emerging functional similarities and divergences between *Drosophila* Spargel/dPGC-1 and mammalian PGC-1 protein. *Front. Genet.* 5, 216. doi: 10.3389/fgene.2014.00216

Nagaraj, R., Gururaja-Rao, S., Jones, K. T., Slattery, M., Negre, N., Braas, D., et al. (2012). Control of mitochondrial structure and function by the Yorkie/YAP oncogenic pathway. *Genes Dev.* 26, 2027–2037. doi: 10.1101/gad.183061.111

Nisoli, E., Clementi, E., Paolucci, C., Cozzi, V., Tonello, C., Sciorati, C., et al. (2003). Mitochondrial biogenesis in mammals: the role of endogenous nitric oxide. *Sci. Signal.* 299, 896–899. doi: 10.1126/science.1079368

Nisoli, E., Falcone, S., Tonello, C., Cozzi, V., Palomba, L., Fiorani, M., et al. (2004). Mitochondrial biogenesis by NO yields functionally active mitochondria in mammals. *Proc. Natl. Acad. Sci. U. S. A.* 101, 16507–16512. doi: 10.1073/pnas.0405432101

Nisoli, E., Tonello, C., Cardile, A., Cozzi, V., Bracale, R., Tedesco, L., et al. (2005). Calorie restriction promotes mitochondrial biogenesis by inducing the expression of eNOS. *Sci. Signal.* 310, 314–317. doi: 10.1126/science.1117728

Nunes, R. D., Ventura-Martins, G., Moretti, D. M., Medeiros-Castro, P., Rocha-Santos, C., de Oliveira, D.-F., et al. (2016). Polyphenol-rich diets exacerbate ampk-mediated autophagy, decreasing proliferation of mosquito midgut microbiota, and extending vector lifespan. *PLoS Negl. Trop. Dis.* 10, e0005034. doi: 10.1371/journal.pntd.0005034

Nuss, A. B., and Brown, M. R. (2018). Isolation of an insulin-like peptide from the Asian malaria mosquito, *Anopheles stephensi*, that acts as a steroidogenic gonadotropin across diverse mosquito taxa. *Gen. Comp. Endocrinol.* 258, 140–148. doi: 10.1016/j.ygcen.2017.05.007

Owusu-Ansah, E., and Perrimon, N. (2015). Stress signaling between organs in Metazoa. *Annu. Rev. Cell Dev. Biol.* 31, 497–522. doi: 10.1146/annurev-cellbio-100814-125523

Pakpour, N., Corby-Harris, V., Green, G. P., Smithers, H. M., Cheung, K. W., Riehle, M. A., et al. (2012). Ingested human insulin inhibits the mosquito NF-kappaB-dependent immune response to *Plasmodium falciparum*. *Infect. Immun.* 80, 2141–2149. doi: 10.1128/IAI.00024-12

Pakpour, N., Camp, L., Smithers, H. M., Wang, B., Tu, Z., Nadler, S. A., et al. (2013). Protein Kinase C-dependent signaling controls the midgut epithelial barrier to malaria parasite infection in Anopheline mosquitoes. *PLoS One* 8, e76535. doi: 10.1371/journal.pone.0076535

Palikaras, K., Lionaki, E., and Tavernarakis, N. (2018). Mechanisms of mitophagy in cellular homeostasis, physiology and pathology. *Nat. Cell Biol.* 20, 1013–1022. doi: 10.1038/s41556-018-0176-2

Piantadosi, C. A., Withers, C. M., Bartz, R. R., MacGarvey, N. C., Fu, P., Sweeney, T. E., et al. (2011). Heme oxygenase-1 couples activation of mitochondrial biogenesis to anti-inflammatory cytokine expression. *J. Biol. Chem.* 286, 16374–16385. doi: 10.1074/jbc.M110.207738

Pietri, J. E., Pakpour, N., Napoli, E., Song, G., Pietri, E., Potts, R., et al. (2016). Two insulin-like peptides differentially regulate malaria parasite infection in the mosquito through effects on intermediary metabolism. *Biochem. J.* 437, 3487–3503. doi: 10.1042/BCJ20160271

Rana, A., Rera, M., and Walker, D. W. (2013). Parkin overexpression during aging reduces proteotoxicity, alters mitochondrial dynamics, and extends lifespan. *Proc. Natl. Acad. Sci. U. S. A.* 110, 8638–8643. doi: 10.1073/pnas.1216197110

Ren, F., Wang, B., Yue, T., Yun, E. Y., Ip, Y. T., and Jiang, J. (2010). Hippo signaling regulates *Drosophila* intestine stem cell proliferation through multiple pathways. *Proc. Natl. Acad. Sci. U. S. A.* 107, 21064–21069. doi: 10.1073/pnas.1012759107

Rera, M., Bahadorani, S., Cho, J., Koehler, C. L., Ulgherait, M., Hur, J. H., et al. (2011). Modulation of longevity and tissue homeostasis by the *Drosophila* PGC-1 homolog. *Cell Metab.* 14, 623–634. doi: 10.1016/j.cmet.2011.09.013

Rera, M., Azizi, M. J., and Walker, D. W. (2012a). Organ-specific mediation of lifespan extension: More than a gut feeling? *Ageing Res. Rev.* 12, 436–444. doi: 10.1016/j.arr.2012.05.003

Rera, M., Clark, R.II, and Walker, D. W. (2012b). Intestinal barrier dysfunction links metabolic and inflammatory markers of aging to death in *Drosophila*. *Proc. Natl. Acad. Sci. U. S. A.* 109, 21528–21533. doi: 10.1073/pnas.1215849110

Reynolds, R. A., Kwon, H., and Smith, R. C. (2020). 20-Hydroxyecdysone primes innate immune responses that limit bacterial and malarial parasite survival in *Anopheles* gambiae. *Msphere* 5, 10.1128/mSphere.00983–19. doi: 10.1128/mSphere.00983-19

Riehle, M. A., and Brown, M. R. (1999). Insulin stimulates ecdysteroid production through a conserved signaling cascade in the mosquito *Aedes aegypti*. *Insect Biochem. Mol. Biol.* 29, 855–860. doi: 10.1016/S0965-1748(99)00084-3

Riehle, M. A., and Brown, M. R. (2002). Insulin receptor expression during development and a reproductive cycle in the ovary of the mosquito *Aedes aegypti*. *Cell Tissue Res.* 308, 409–420. doi: 10.1007/s00441-002-0561-8

Riehle, M. A., and Brown, M. R. (2003). Molecular analysis of the serine/threonine kinase Akt and its expression in the mosquito *Aedes aegypti*. *Insect Mol. Biol.* 12, 225–232. doi: 10.1046/j.1365-2583.2003.00405.x

Roy, S. G., Hansen, I. A., and Raikhel, A. S. (2007). Effect of insulin and 20-hydroxyecdysone in the fat body of the yellow fever mosquito, *Aedes aegypti*. *Insect Biochem. Mol. Biol.* 37, 1317–1326. doi: 10.1016/j.ibmb.2007.08.004

Ruegsegger, G. N., Creo, A. L., Cortes, T. M., Dasari, S., and Nair, K. S. (2018). Altered mitochondrial function in insulin-deficient and insulin-resistant states. *J. Clin. Invest.* 128, 3671–3681. doi: 10.1172/JCI120843

Ruivo, M. T. G., Vera, I. M., Sales-Dias, J., Meireles, P., Gural, N., Bhatia, S. N., et al. (2016). Host AMPK is a modulator of *Plasmodium* liver infection. *Cell Rep.* 16, 2539–2545. doi: 10.1016/j.celrep.2016.08.001

Sadagurski, M., and White, M. F. (2013). Integrating metabolism and longevity through insulin and IGF1 signaling. *Endocrinol. Metab. Clin. North Am.* 42, 127–148. doi: 10.1016/j.ecl.2012.11.008

Salminen, T. S., and Vale, P. F. (2020). *Drosophila* as a model system to investigate the effects of mitochondrial variation on innate immunity. *Front. Immunol.* 11:521. doi: 10.3389/fimmu.2020.00521

Schinaman, J. M., Rana, A., William, W. J., Clark, R.II, and Walker, D. W. (2019). Rapamycin modulates tissue aging and lifespan independently of the gut microbiota in *Drosophila*. *Sci. Rep.* 9, 1–10. doi: 10.1038/s41598-019-44106-5

Sheard, K. M., Thibault-Sennett, S. A., Sen, A., Shewmaker, F., and Cox, R. T. (2020). Clueless forms dynamic, insulin-responsive bliss particles sensitive to stress. *Dev. Biol.* 459, 149–160. doi: 10.1016/j.ydbio.2019.12.004

Sim, C., and Denlinger, D. L. (2008). Insulin signaling and FOXO regulate the overwintering diapause of the mosquito *Culex pipiens*. *Proc. Natl. Acad. Sci. U. S. A.* 105, 6777–6781. doi: 10.1073/pnas.0802067105

Surachetpong, W., Pakpour, N., Cheung, K. W., and Luckhart, S. (2011). Reactive oxygen species-dependent cell signaling regulates the mosquito immune

response to *Plasmodium falciparum*. *Antioxid. Redox Signal.* 14, 943–955. doi: 10.1089/ars.2010.3401

Sweeney, T. E., Suliman, H. B., Hollingsworth, J. W., and Piantadosi, C. A. (2010). Differential regulation of the PGC family of genes in a mouse model of *Staphylococcus aureus* sepsis. *PLoS One* 5, e11606. doi: 10.1371/journal.pone.0011606

Sweeney, T. E., Suliman, H. B., Hollingsworth, J. W., Welty-Wolf, K. E., and Piantadosi, C. A. (2011). A Toll-like receptor 2 pathway regulates the Ppargc1a/b metabolic co-activators in mice with *Staphylococcal aureus* sepsis. *PLoS One* 6, e25249. doi: 10.1371/journal.pone.0025249

Tiefenbock, S. K., Baltzer, C., Egli, N. A., and Frei, C. (2010). The *Drosophila* PGC-1 homologue Spargel coordinates mitochondrial activity to insulin signalling. *EMBO J.* 29, 171–183. doi: 10.1038/emboj.2009.330

Tóth, M. L., Sigmond, T., Borsos, É, Barna, J., Erdélyi, P., Takács-Vellai, K., et al. (2008). Longevity pathways converge on autophagy genes to regulate life span in *Caenorhabditis elegans*. *Autophagy* 4, 330–338. doi: 10.4161/auto.5618

Tran, M., Tam, D., Bardia, A., Bhasin, M., Rowe, G. C., Kher, A., et al. (2011). PGC-1α promotes recovery after acute kidney injury during systemic inflammation in mice. *J. Clin. Invest.* 121, 4003–4014. doi: 10.1172/JCI58662

Treyer, A., and Müsch, A. (2013). Hepatocyte Polarity. *Compr. Physiol.* 3, 243–287 doi: 10.1002/cphy.c120009

Ulgherait, M., Rana, A., Rera, M., Graniel, J., and Walker, D. W. (2014). AMPK modulates tissue and organismal aging in a non-cell-autonomous manner. *Cell Rep.* 8, 1767–1780. doi: 10.1016/j.celrep.2014.08.006

Unoki, M., and Nakamura, Y. (2001). Growth-suppressive effects of BPOZ and EGR2, two genes involved in the PTEN signaling pathway. *Oncogene* 20, 4457–4465. doi: 10.1038/sj.onc.1204608

Upton, L. M., Povelones, M., and Christophides, G. K. (2015). *Anopheles gambiae* blood feeding initiates an anticipatory defense response to *Plasmodium berghei*. *J. Innate. Immun.* 7, 74–86. doi: 10.1159/000365331

Vellai, T. (2009). Autophagy genes and ageing. *Cell Death Differ.* 16, 94–102. doi: 10.1038/cdd.2008.126

Wang, B., Pakpour, N., Napoli, E., Drexler, A., Glennon, E., Surachetpong, W., et al. (2015). *Anopheles stephensi* p38 MAPK signaling induces tolerance during *Plasmodium falciparum* infection. *Parasit. Vectors* 8, 424. doi: 10.1186/s13071-015-1016-x

Wang, Z., Liu, Y., Chaitankar, V., Pirooznia, M., and Xu, H. (2019). Electron transport chain biogenesis activated by a JNK-insulin-Myc relay primes mitochondrial inheritance in *Drosophila*. *Elife* 8, e49309. doi: 10.7554/eLife.49309.043

Wardelmann, K., Blümel, S., Rath, M., Alfine, E., Chudoba, C., Schell, M., et al. (2019). Insulin action in the brain regulates mitochondrial stress responses and reduces diet-induced weight gain. *Parasit. Vectors* 21, 68–81. doi: 10.1016/j.molmet.2019.01.001

Youle, R. J., and van der Bliek, A. M. (2012). Mitochondrial fission, fusion, and stress. *Science* 337, 1062–1065. doi: 10.1126/science.1219855

Yu, R., Lendahl, U., Nistér, M., and Zhao, J. (2020). Regulation of mammalian mitochondrial dynamics: Opportunities and challenges. *Front. Endocrinol.* 11, 374. doi: 10.3389/fendo.2020.00374

Zhu, J., Wang, K. Z., and Chu, C. T. (2013). After the banquet: mitochondrial biogenesis, mitophagy, and cell survival. *Autophagy* 9, 1663–1676. doi: 10.4161/auto.24135

Conflict of Interest: The authors declare that the research was conducted in the absence of any commercial or financial relationships that could be construed as a potential conflict of interest.

frontiers in Cellular and Infection Microbiology

ORIGINAL RESEARCH
published: 08 January 2021
doi: 10.3389/fcimb.2020.615343

A Hetero-Multimeric Chitinase-Containing *Plasmodium falciparum* and *Plasmodium gallinaceum* Ookinete-Secreted Protein Complex Involved in Mosquito Midgut Invasion

Kailash P. Patra[1†], Hargobinder Kaur[1†], Surendra Kumar Kolli[2†], Jacob M. Wozniak[3], Judith Helena Prieto[4,5], John R. Yates III[4], David J. Gonzalez[3], Chris J. Janse[2] and Joseph M. Vinetz[1]*

[1] Section of Infectious Diseases, Department of Internal Medicine, Yale School of Medicine, New Haven, CT, United States, [2] Department of Parasitology, Leiden University Medical Center, Leiden, Netherlands, [3] Department of Pharmacology and the Skaggs School of Pharmacy and Pharmaceutical Sciences, University of California San Diego, La Jolla, CA, United States, [4] Department of Molecular Medicine, The Scripps Research Institute, La Jolla, CA, United States, [5] Department of Chemistry, Western Connecticut State University, Danbury, CT, United States

OPEN ACCESS

Edited by:
Robert Sinden,
Imperial College London,
United Kingdom

Reviewed by:
Takafumi Tsuboi,
Ehime University, Japan
Arthur Talman,
Institut de Recherche Pour le Développement (IRD), France
Andrew Michael Blagborough,
University of Cambridge,
United Kingdom

***Correspondence:**
Joseph M. Vinetz
joseph.vinetz@yale.edu

[†]These authors have contributed equally to this work

Specialty section:
This article was submitted to Parasite and Host, a section of the journal Frontiers in Cellular and Infection Microbiology

Received: 08 October 2020
Accepted: 30 November 2020
Published: 08 January 2021

Citation:
Patra KP, Kaur H, Kolli SK, Wozniak JM, Prieto JH, Yates JR III, Gonzalez DJ, Janse CJ and Vinetz JM (2021) A Hetero-Multimeric Chitinase-Containing Plasmodium falciparum and Plasmodium gallinaceum Ookinete-Secreted Protein Complex Involved in Mosquito Midgut Invasion. Front. Cell. Infect. Microbiol. 10:615343. doi: 10.3389/fcimb.2020.615343

Malaria parasites are transmitted by *Anopheles* mosquitoes. During its life cycle in the mosquito vector the *Plasmodium* ookinete escapes the proteolytic milieu of the post-blood meal midgut by traversing the midgut wall. This process requires penetration of the chitin-containing peritrophic matrix lining the midgut epithelium, which depends in part on ookinete-secreted chitinases. *Plasmodium falciparum* ookinetes have one chitinase (PfCHT1), whereas ookinetes of the avian-infecting parasite, *P. gallinaceum*, have two, a long and a short form, PgCHT1 and PgCHT2, respectively. Published data indicates that PgCHT2 forms a high molecular weight (HMW) reduction-sensitive complex; and one binding partner is the ookinete-produced von Willebrand A-domain-containing protein, WARP. Size exclusion chromatography data reported here show that *P. gallinaceum* PgCHT2 and its ortholog, *P. falciparum* PfCHT1 are covalently-linked components of a HMW chitinase-containing complex (> 1,300 kDa). Mass spectrometry of ookinete-secreted proteins isolated using a new chitin bead pull-down method identified chitinase-associated proteins in *P. falciparum* and *P. gallinaceum* ookinete-conditioned culture media. Mass spectrometry of this complex showed the presence of several micronemal proteins including von Willebrand factor A domain-related protein (WARP), ookinete surface enolase, and secreted ookinete adhesive protein (SOAP). To test the hypothesis that ookinete-produced PfCHT1 can form a high molecular homo-multimer or, alternatively, interacts with *P. berghei* ookinete-produced proteins to produce an HMW hetero-multimer, we created chimeric *P. berghei* parasites expressing *PfCHT1* to replace *PbCHT*1, enabling the production of large numbers of PfCHT1-expressing ookinetes. We show that chimeric *P. berghei* ookinetes express monomeric PfCHT1, but a HMW

complex containing *PfCHT1* is not present. A better understanding of the chitinase-containing HMW complex may enhance development of next-generation vaccines or drugs that target malaria transmission stages.

Keywords: *Plasmodium*, chitinase, complex, invasion, malaria-transmission

INTRODUCTION

Plasmodium parasites cause human malaria, one of the deadliest vector-borne diseases, which has medical and economic impacts affecting nearly half of the world's populations (Delves et al., 2019). **Human-infecting** *Plasmodium* parasites complete a complex life cycle that alternates between definitive female *Anopheline* mosquito and the intermediate human hosts. Despite continuous control measures to reduce transmission, malaria remains a significant public health threat in most tropical and sub-tropical countries (Mlambo et al., 2008). This parasitic human-mosquito-human journey results in more than 400,000 thousand deaths annually; mostly young children under five years of age living in sub-Saharan Africa (Murray et al., 2012; Viebig et al., 2015; Greenwood, 2017). The effectiveness of malaria control programs is deteriorating due to the emergence of drug resistance to artemisinin-based combination therapies (ACTs) - the only available regimen in malaria-endemic countries (Cui et al., 2015) - and the lack of an effective malaria vaccine. The World Health Organization's Millennium Goals for malaria elimination are not likely to be met in the foreseeable future through existing approaches and technology (Mahmoudi and Keshavarz, 2017). The mosquito midgut gamete, zygote, and ookinete parasite stages are vulnerable developmental bottlenecks in the parasite life cycle and offer opportunities for the elimination of malaria parasites as targets for novel transmission-blocking vaccines, drugs, or transgenic mosquitoes expressing anti-parasite effector molecules (Sinden, 2015; Delves et al., 2018).

The malaria transmission cycle starts when a mosquito ingests a human host blood meal containing the sexual stages of the parasite. Gametogenesis and fertilization of male and female gametes occur within the mosquito midgut and result in zygote formation. Motile, crescent-shaped ookinetes transform from zygotes within hours, which then traverse the peritrophic matrix (Giersing et al., 2019) and midgut epithelium to continue the transmission cycle by developing into sporozoite-producing oocysts (Mlambo et al., 2008). Midgut gametocytes, gametes, zygotes, and ookinetes are targeted by transmission-blocking vaccines (TBVs) that are currently under clinical development (Duffy and Patrick Gorres, 2020). Malaria TBVs are a community-wide approach akin to seeking herd immunity and target developmentally-regulated antigens expressed during the mosquito midgut parasite stages, to interrupt the sporogonic cycle and prevent transmission from humans to mosquitoes (Langer and Vinetz, 2001). TBVs can synergize with other control and elimination strategies, such as insecticide-treated bednets, with the potential for global malaria eradication.

The key role of *Plasmodium* chitinases in enabling the sporogonic cycle has been described (Shahabuddin et al., 1993; Dessens et al., 2001; Langer et al., 2002a). The *Plasmodium* ookinete-secreted chitinase(s) are endochitinases in family 18 glycohydrolases that facilitate the parasite to dissolve the chitin (N-acetylglucosamine polymer)-containing peritrophic matrix (Giersing et al., 2019) within the mosquito midgut, *en route* to crossing the midgut epithelium (Shahabuddin et al., 1993; Shen and Jacobs-Lorena, 1998; Langer and Vinetz, 2001; Sinden, 2017a). An electron microscopy study of *P. gallinaceum* showed the ookinete focally disrupting and traversing the PM (Sieber et al., 1991). *Plasmodium* ookinete-secreted chitinases are of two types: short forms (*PfCHT1, PgCHT2*, and *PrCHT1*) which possess an N-terminal proenzyme and a C-terminal chitin-binding domain (CBD), and long-forms (*PgCHT1, PvCHT1*, and *PbCHT1*) which lack both domains (Li et al., 2005). The chitinase inhibitor, allosamidin, and anti-chitinase antibodies are known to block or reduce parasite transmission from the vertebrate host to mosquito, suggesting that the PM is a critical barrier to *Plasmodium* invasion of the midgut (Vinetz et al., 1999; Vinetz et al., 2000; Dessens et al., 2001; Takeo et al., 2009). However, details of the molecular mechanisms and macromolecular interactions that ookinetes use to invade the mosquito midgut remain unknown.

Here we demonstrate that *P. falciparum* and *P. gallinaceum* ookinetes secrete a short chitinase as a component of a hetero-multimeric, high molecular weight (HMW) chitinase-containing protein complex that includes WARP, SOAP, and ookinete-surface enolase. To investigate interactions within the complex we used the rodent malaria parasite, *P. berghei*, which is an important model system for understanding mosquito stage biology of *Plasmodium* because of its ability to be transgenically manipulated (Espinosa et al., 2017). *P. berghei* has only the long form of chitinase (*PbCHT1*), which is not part of an HMW complex. Therefore, we used a gene insertion/marker out (GIMO) system to replace *PbCHT1* with *P. falciparum* chitinase (*PfCHT1*; short form) to test the hypothesis that *PfCHT1* expressed within *P. berghei* ookinetes would use the endogenous machinery of *P. berghei* to heterologously express *PfCHT1* in a HMW complex. Using three *Plasmodium* species that infect human, avian, and rodent vertebrate hosts, respectively, we hypothesize that *Plasmodium* species-specific ookinete-secreted micronemal partner proteins play a vital role in the formation of a chitinase-containing hetero-multimeric HMW complex. The chitinase-containing HMW complex secreted by ookinetes binds to chitin with high affinity and might mediate recognition, attachment, and invasion of the mosquito midgut. Disruption of the complex could represent a novel Achilles heel for interrupting malaria transmission. These cross-species approaches to studying the ookinete invasion of the mosquito midgut may provide a new dimension to our understanding of the biology of malaria transmission biology and underpin future experimental approaches to delineate mechanisms by which the *Plasmodium* ookinete invades the mosquito midgut.

MATERIALS AND METHODS

Animal Studies, Malaria Parasites, and Mosquitoes

All animal experiments of this study were granted with a license by Competent Authority after ethical evaluation by the Animal Experiments Committee Leiden (AVD1160020171625) and Institutional Review Board and the Institutional Animal Care and Use Committee (IACUC) of Yale University (Protocol ID: 2019-20243). All experiments were performed in accordance with the Experiments on Animals Act (Wod, 2014), which is the applicable legislation in Netherlands in accordance with the European guidelines (EU directive no. 2010/63/EU) regarding the protection of animals used for scientific purposes. Female OF1 and male Swiss Webster mice (6–7 weeks; Charles River, NL and MA, USA) were used for *P. berghei* infection. The Institutional Animal Care and Use Committee (IACUC), University of California San Diego, approved the animal protocol used for the production of *P. gallinaceum* ookinetes in 4 to 6 weeks-old White Leghorn chickens (Charles River, MA, USA).

A reference *P. berghei* ANKA parasite line (1868cl1) (www.pberghei.edu, line RMgm-1320) was used to generate the chimeric *P. berghei* lines. This reporter line does not contain a drug-selectable marker and expresses *mCherry* under the control of the constitutive *hsp70* promoter (*PBANKA*_0711900) and luciferase under the control of the constitutive *eef1α* promoter (*PBANKA*_1133400). These reporter gene expression cassettes are integrated into the neutral *p230p* gene locus (*PBANKA*_0306000). The detailed methodology for the generation of transgenic *P. berghei* parasite cell lines is given at the end of the methods section. The avian malaria parasite, *P. gallinaceum* 8A strain, was obtained from MR4 (BEI Resources, Manassas, VA, USA) to infect chickens following the approved protocol. The gametocyte producing *P. falciparum NF54* strain was obtained from MR4 and *in vitro* cultured following a standard method (Bounkeua et al., 2010).

A. stephensi mosquitoes were housed and maintained at 27°C and 75% relative humidity under a 12-h light/dark cycle at Leiden University Medical Center. For *P. berghei* infections, mosquitoes were fed one time (day 0) on anesthetized *P. berghei* infected mice and kept within a 21°C and 80% humidity incubator and dissected 10-12 days after blood feeding for midgut and oocyst counts.

In Vitro Production of *Plasmodium gallinaceum, Plasmodium falciparum*, and *Plasmodium berghei* Ookinetes

The avian malaria parasite, *P. gallinaceum* 8A strain passage 1 (blood from the chicken that was infected through the bites of infective mosquitoes), was used to infect 4 to 6 weeks-old White Leghorn chickens. At 5%–10% parasitemia, heparinized blood was collected by cardiac puncture and used immediately for *in vitro* production of ookinetes following a published method (Patra and Vinetz, 2012). Purified zygotes stages were incubated in serum-free medium (M199 containing 0.2% glucose, 2 mM L-glutamine, 50 units of penicillin, and 50 μg of streptomycin/ml) at 26°C for 36 h to allow transformation into mature ookinetes. Cultures with above 50% ookinete transformation were centrifuged (4,000 rpm, 10 min), and supernatants were collected for further use.

The *P. falciparum* NF54 strain was used for *in vitro* gametocyte and ookinete production per a published method with slight modifications (Bounkeua et al., 2010). After the fertilization step, the zygote pellets were washed three times with serum-free ookinete medium (M199 medium containing 0.2% glucose, 2 mM L-glutamine, 50 units of penicillin, and 50 μg of streptomycin/ml) and incubated in 20 ml of serum-free M199 medium at 28°C for 48 h in a slow-shaking incubator. Cultures with >30% ookinete transformation were used for biochemical studies. Human serum and other animal serum-containing media show high chitinase activity, and we therefore developed a serum free *P. falciparum* ookinete culture method for these studies, which needs improvement to achieve higher ookinete transformation.

P. berghei ookinetes were obtained as described (Janse et al., 1985; Janse and Waters, 1995). The gametocyte conversion rate is defined as the percentage of ring-forms that develop into gametocytes in standard synchronized *in vivo* infections in mice (done in triplicate). *In vitro* ookinete formation assays were performed following published methods using gametocyte-enriched blood collected from mice (Janse et al., 1985). Briefly, infected blood from ~3 to 5 mice containing gametocytes was mixed in standard ookinete culture medium and cultures were incubated for 18–24 h at 21°C –22°C. Between 12 and 20 min after the activation of gametocytes the number of exflagellating male gametocytes was determined by counting exflagellating males (in triplicate) in a Bürker cell chamber. The fertilization rate (ookinete conversion rate), defined as the percentage of female gametes that develop into zygotes or ookinetes, was determined (in triplicate) by counting female gametes and zygotes/ookinetes in Giemsa-stained blood smears at 18–24 h after *in vitro* induction of gamete formation. The ookinete cultures were further centrifuged as mentioned above and passed through 0.22 μm filters (50 ml Steriflip, EMD Millipore, MT). In the case of *P. berghei* infection of *A. stephensi* mosquitoes, collection and counting of oocyst (at day 12–14 post feeding) were performed as described (Sinden, 1997; Janse et al., 2006; Othman et al., 2018).

Size Exclusion HPLC Fractionation of Ookinete Culture Supernatants and Analysis of Chitinase Activity

Approximately 50 ml of *P. gallinaceum* ookinete culture supernatant was concentrated using a 10 kDa cut off Centricon device, EMD Millipore, MT to 1 ml final volume. Chitinase activity of the concentrated sample was tested before loading onto a silica-based SEC column (TSKgel G2000SW, Tosoh Biosciences LLC, King of Prussia, PA), and HPLC was performed using a Beckman Gold 500 instrument and autoclaved PBS (pH 7.4). Approximately 100 μl of each fraction (total 0.5 ml volume/1 min) was analyzed in duplicate for the presence of chitinase activity that showed two distinct activity peaks. Gel filtration standards (Bio-rad, Hercules, CA) were analyzed in similar conditions and the retention times of the protein sizes were determined. Similarly, concentrated serum-free ookinete culture supernatant of *P. falciparum* was subjected to HPLC following the condition for *P. gallinaceum*; however, it showed low activity in the fractions due to the sample dilutions, but showed two distinct peaks when fractions were coated on ELISA plated and probed with 1C3, anti-PfCHT1 monoclonal antibodies

(data not shown). To further resolve the HMW complex and determine the approximate mass, subjected samples were used for high-resolution chromatography, immunodetection, and estimation of the chitinase complex in both *P. falciparum* and *P. gallinaceum.*

Size Exclusion Chromatography for Estimation of the Native Chitinase Complex Molecular Weight

Ookinete culture supernatants (*P. gallinaceum* and *P. falciparum*) were passed through 0.22 μm spin columns and loaded separately onto gel filtration columns (Superose-6, 10/300, MW separation range 5–5,000 kDa of globular proteins) in PBS, pH 7.4, and fractions (0.5 ml/min) were collected on ice. Each fraction was coated onto duplicate wells of an ELISA plate and probed with anti-chitinase mAb (1C3) followed by goat-anti-mouse IgG-HRPO conjugate and BCIP/NBT substrate addition to detect the chitinase in the fraction coated wells. The absorbance optical density (OD) values were plotted to determine the peak vs. retention time of both *P. falciparum* and *P. gallinaceum* ookinete culture supernatants. Blue Dextran was used to estimate the void (V_o, 2 min retention time) volume of the column and commercially available gel filtration standards (17–670 kDa) were run under the same conditions and retention times were noted. We used a standard method to calculate the molecular weight based on the retention time of the known standards used to estimate the partition coefficient ($K_{av} = V_e - V_0/V_t - V_0$) and a standard calibration curve (Panel C) was plotted; where V_0 is the void volume, V_e is the elution volume of the sample, and V_t is total column volume. The molecular weights of the fractions containing the peak chitinase were estimated from the equation and are presented in the **Supplementary Data Sheet 1**.

Chitinase Activity and Chitin Affinity Pull-Down of the Chitinase Complex From Ookinete Culture Supernatants, SDS-PAGE, and Western Immunoblot Analysis

Chitinase activity of the ookinete supernatants from the three *Plasmodium* species was tested by adding chitinase substrate (4-methylumbelliferyl-N, N′, N″-β-D-triacetylchitotrioside; Sigma), and the linear increase in the enzymatic activity was determined by kinetic fluorescence detection (Gemini EM, Molecular Devices LLC, CA; excitation, 365 nm; emission, 450 nm) as described (Li et al., 2005). Chitin beads (Catalog, S6651S, New England Biolabs, MA) were washed three times with PBS (pH 7.4) and made into a 50% slurry with PBS. To 10 ml of 0.22 μm filtered ookinete culture supernatant, 200 μl of 50% chitin bead slurry was added and incubated at 4°C overnight on a slow rocker. The tubes were centrifuged (2,300 rpm, 5 min) and protein bound chitin beads were washed three times with PBS or PBST (0.1% Tween 20) and SDS-sample buffer was added directly to the beads. The samples were then heated for 3 min at 70°C and subjected to SDS/PAGE under reducing (β-mercaptoethanol) and non-reducing conditions. Primary antibody incubation was done with 5% nonfat dry milk in PBS containing (0.1% Tween 20) (PBST) overnight at 4°C. Secondary antibody controls were run with each blot, under non-reducing and reducing conditions. For the detection of bound primary antibodies, the membrane was washed three times with PBST and incubated with alkaline phosphatase-conjugated goat anti-mouse IgG (H+L) antibody (1:2500) (KPL, USA) in 5% nonfat dry milk in PBS containing (0.1% Tween 20) (PBST) at RT for 1 h. The blot was then developed with a 5-bromo-4-chloro-3-indolyl phosphate (BCIP)/nitro blue tetrazolium (NBT) solution (KPL, MD, USA). For *P. gallinaceum*, one SDS-PAGE gel was stained with silver nitrate (Silver Quest kit, Thermo Fisher Scientific) and the other was subjected to Western immunoblot analysis. Membranes containing the *P. gallinaceum* and *P. falciparum* pull-down samples were probed with the anti-chitinase active site peptide mouse polyclonal antibody, B993 (Langer et al., 2002a), and anti-*PfCHT1* (1C3) monoclonal antibodies, as reported (Langer et al., 2002b). For the three *P. berghei* parasite lines (*Pb-PfCHT1(r)*, *PbCHT1 (WT)*, and *PbΔCHT1*), membranes run under both conditions were probed using anti-*PfCHT1* monoclonal (1C3, 25 μg/ml) and anti-*PbCHT1* polyclonal antibodies (1:2000 dilutions) as described in the figure legends.

Mass Spectrometry Analysis of the Ookinete Secreted Chitinase Complex

To identify proteins associated with *P. gallinaceum* chitinases (*PgCHT1* and *PgCHT2*), washed protein-bound beads were subjected directly to enzymatic digestions, and MudPIT analysis and the collected MS/MS spectra were analyzed as described (Patra et al., 2008). The MS/MS spectra were verified against chicken (*Gallus gallus*) protein entries, and manually compared with a list of common contaminants (e.g., human keratin and trypsin). The final list of peptides sequences was used for BLAST searches against the PlasmoDB databases (PlasmoDB.org) to identify proteins and their function. For *P. falciparum*, the chitinase complex bound chitin beads were washed three times with PBS and submitted for mass spectrometry analysis. The chitinase complex-bound chitin beads were suspended in 8M urea to denature and detach the bound proteins. Following resuspension, proteins were reduced, alkylated, and digested with LysC and trypsin. Tryptic peptides were desalted *via* Sep-Pak (Waters, MA, USA) and dried in a speed vacuum overnight. The digested peptides were quantified using the Pierce quantitative fluorometric peptide assay (Thermo Fisher Scientific, Carlsbad, CA). The digested peptides were analyzed on an Orbitrap Fusion Mass Spectrometer with an in-line Easy-nLC 1000. Samples were loaded onto the column (pressure 500 bar and eluted over 85 min with a linear gradient of 11%–30% acetonitrile in 0.125% formic acid). Nanospray ionization was achieved by applying 2000V through the stainless-steel T and the inlet of the column. MS1 was performed to select precursors for identification, peptides were fragmented to identify their amino acid sequence at the MS2 level, and the acquired spectra was analyzed against the *P. falciparum* (strain 3D7) reference proteome (UniProt) using the SEQUEST search algorithm (Eng et al., 1994). Search parameters included the dynamic oxidation of methionine and the static carbamidomethylation of cysteine (modifications that arise from sample preparation). The data was filtered to a 1% false discovery rate at both the peptide and protein levels using a reverse database search.

For *P. berghei*, mass spectrometry analysis of the chitin bound chitinase and other proteins were performed at the W.M. Keck Biotechnology Resource Laboratory, Yale University. Briefly, the sample was washed four times; first with 60% acetonitrile containing 0.1%TFA and then with 5% acetic acid, then with 50% H_2O/50% acetonitrile, followed by 50% CH_3CN/50 mM NH_4HCO_3. A final wash with 50% CH_3CN/10 mM NH_4HCO_3 was given and gel pieces were completely dried prior to removal of the wash solution. Trypsin digestion was carried out by incubating the sample at 37°C for 18 h and the samples were stored at -20°C until analysis (Ghosh et al., 2019). The trypsin digested proteins products were fractionated using LC-MS/MS. The Mascot algorithm was used for all MS/MS spectra searches (Hirosawa et al., 1993) (Matrix Science, London, UK; version Mascot in Proteome Discoverer 2.2.0.388) and Mascot was set up to search the *PbergANKA*_PDB11 and Plasmo_*Pfal3D7* databases. Protein identification criteria were the match of 2 or more peptides with 90% peptide threshold, a Decoy FDR of 0.5%, and a mascot ion score of >30.

Site-Directed Mutagenesis of Conserved Cysteines of Plasmodium gallinaceum Chitinase (PgCHT1) and Chitin Binding Affinity Analysis of rPgCHT1 and rPfCHT1

PgCHT1 putative chitinase binding domain mutants were constructed using a QuickChange Multi Site-Directed Mutagenesis Kit (Agilent Technology, CA). The expression construct *PgCHT1*-pET32b plasmid DNA (Langer et al., 2000) was used as a template to amplify the long form of *P. gallinaceum* chitinase (*PgCHT1*) which was already synthesized in *E. coli*-preferred codons. The primers were designed to modify bases at positions 1,355 bp (TGC to TCC), 1,502 bp (TGC to TCC), and 1,670 bp (TGT to TCT) of the plasmid construct to mutate three cysteine (C) residues to serine (S). These three cysteines are conserved across the long form of *Plasmodium* chitinases of different *Plasmodium* species and are located in the putative chitin-binding domain at the C-terminal end of the *P. gallinaceum* chitinase, *PgCHT1* (Li et al., 2005). The mutant *PgCHT1*- pET32b plasmid constructs (1 and 2, **Figure 6**) were confirmed by Sanger sequencing before expressing as recombinant protein. We also synthesized *PfCHT1*- pET-32b expression plasmid (Gene Universal, Newark,DE) in *E. coli* preferred codons to express rPfCHT1 in *E.coli*.

The mutant plasmids (1 and 2 mutant-*PgCHT1*-PET32b) and wild type (*PgCHT2*-pET32 and *PfCHT1*-pET32b) were transformed into SHuffle T7 Express Competent *E. coli* cells (New England Biolabs, MA). Small scale protein expression was carried out as described (Li et al., 2005). Bacterial pellets from 1 ml of IPTG (isopropyl-ß-D-1-thiogalactopyranoside) induced cultures were suspended in 500 µl of PBS and sonicated (Sonicator 3000, Misonix, CT) using a microprobe for 3 min (10 s on and 10 s off mode) on ice. Similarly, recombinant *E. coli* expressing *PfCHT1* were lysed using mild detergent at room temperature and a fraction (1 ml) of the lysate was used for the chitin pull-down assays and the rest of the soluble fraction used for the Ni-NTA purification using HisTrap HP columns (Cytiva, Marlborough, MA).

For chitin binding assays, lysates from rPgCHT, rPgCHT1 mutants and r*PfCHT1* were centrifuged and supernatants were incubated in a rotor shaker for 30 min with washed chitin beads. Further centrifugation was performed to wash the chitin bead pellet three times with PBS with or without 1% Triton X-100 for *PgCHT1* and 0.2%–1% Triton X-100 for *PfCHT1*. After the final washing sample buffer was added directly to the protein-bound chitin beads, boiled for 5 min, and analyzed by SDS-PAGE and western immunoblot. The membrane was probed with anti-thioredoxin monoclonal antibodies (Abcam, MA) to detect bound recombinant *PgCHT1* proteins in the wild types and mutants (1 and 2) in which all the three conserved cysteines were modified in the chitin binding domain. For *PfCHT1*, the membranes were incubated with 1C3 monoclonal antibody to detect *PfCHT1* in the ookinete culture supernatant pull-downs.

Generation of DNA Constructs and Genotyping of Chimeric *Plasmodium berghei* Expressing *PfCHT1*

The detailed sequence and names of the primers used for PCR and genotyping are listed (**Supplementary Table 1**). A two-step gene insertion/marker out (GIMO) transfection protocol was used to generate chimeric parasites in which the *PbCHT1* coding sequence (CDS; PBANKA_0800500) was replaced by the CDS of *PfCHT1* (PF3D7_1252200). In the first step we deleted the *PbCHT1* CDS by replacing it with the positive-negative selectable marker (SM) to create a *P. berghei CHT1* deletion GIMO line, *PbΔCHT1*. To do this, we generated DNA construct pL2321, which is based on the standard GIMO DNA construct pL0034. This construct contains the positive-negative human dihydrofolate reductase: yeast cytosine deaminase, and a uridyl phosphoribosyl transferase (h*dhfr: yfcu*) selection marker (SM) cassette. The 5' and 3' targeting regions of *PbCHT1* were amplified from *P. berghei* ANKA genomic DNA using the primers 9450/9451 and 9452/9453. Fragments were digested with ApaI/SacII and KpnI/NotI, respectively, and ligated into vector pL0034 to obtain pL2321. For transfection, pL2321 was linearized with ApaI/NotI and the linear construct was introduced into parasites of the *P. berghei* ANKA reference line 1868cl1 using standard transfection methods (Janse et al., 2006). Transfected parasites (exp. 3152) were positively selected in mice by providing pyrimethamine in the drinking water. Transfected parasites were cloned by limiting dilution, resulting in cloned line ***PbΔCHT1*** (line 3152cl1). The correct deletion of *PbCHT1* was confirmed by diagnostic PCR analysis of genomic DNA (gDNA) and Southern analysis of pulsed-field gel (PFG)-separated chromosomes. In the second step, we replaced the positive-negative SM cassette in *PbΔCHT1* with the *PfCHT1* CDS by GIMO transfection to create the *P. berghei* chimeric *Pb-PfCHT1*(r) replacement line. This was achieved by modifying the construct used in the first step (pL2321); specifically, the h*dfhr*: yfcu SM cassette was removed and replaced with the *Pfcht1* CDS sequence, generating plasmid pL2322. The *PfCHT1* CDS was amplified from the DNA of *P. falciparum* NF54 (PF3D7_1252200) using the primers 9454/9455. *PfCHT1* CDS fragment was digested with SacII/KpnI and ligated into vector pL2321 to obtain pL2322. The pL2322 construct was sequenced to ensure that there were no mutations in the *PfCHT1* CDS. The construct was linearized using ApaI and NotI restriction enzymes outside the 5' and 3' targeting regions before transfection. The construct was used to transfect parasites of *PbΔCHT1* (line 3152cl1)

using standard methods of GIMO transfection (Lin et al., 2011; Salman et al., 2015). Transfected parasites (exp 3165) were negatively selected in mice by providing 5-fluorocytosine (5-FC) in the drinking water. Negative selection results in the selection of chimeric parasites where the h*dhfr*::y*fcu* SM in the *cht1* locus of *PbΔCHT1* is replaced by the CDS of *PfCHT1*. Selected chimeric parasites were cloned by limiting dilution resulting in the cloned line 3165cl1 (*Pb-PfCHT1*(r)). Correct integration of the constructs into the genome of *Pb-PfCHT1*(r) was analyzed by diagnostic PCR analysis of gDNA and Southern analysis of PFG-separated chromosomes as described (Janse et al., 2006). The PFG-separated chromosomes were hybridized with a mixture of two probes: a probe recognizing the h*dhfr* gene and an ~800 bp fragment of the 5′UTR of PBANKA_0508000 located on chromosome 5. This method creates chimeric gene replacement *P. berghei* parasites that lack the *Pbcht1* CDS but possess the *PfCHT1* CDS under the control of the *PbCHT1* 3'- and 5'-UTR regulatory sequences.

RESULTS

In Vitro Production of *Plasmodium gallinaceum*, *Plasmodium falciparum*, and *Plasmodium berghei* Ookinetes in Serum-Free and 5% Serum-Containing Media

Ookinetes were transformed from zygotes using serum free M199 medium for the *P. gallinaceum* 8A and *P. falciparum* NF54 lines (**Figures 1A, B**) and RPMI 1640 with 5% serum for *P. berghei* parasite lines (*Pb-PfCHT1 (r)*, *PbCHT1* (WT), and *PbΔCHT1*) (**Figure 1C**). *P. gallinaceum* preparations routinely resulted in > 50% ookinete transformation in serum-free medium. Mature ookinetes were accurately distinguished from gametocytes using light microscopy (**Figure 2**); specifically, ookinetes were identified as extracellular and with banana-shaped morphologies clearly distinguishable from gametocytes. As confirmation anti-chitinase mouse monoclonal antibodies (1C3) showed apical fluorescence on the *P. gallinaceum* ookinete stages as described [7].

Published methods describe the use of 10%–20% human serum or Albumax in culture medium for the *in vitro* production of *P. falciparum* ookinetes [10-13]. Serum- or Albumax-containing media have variable levels of chitinase activity (**Supplementary Figure 1**) that remains partially active after heat inactivation (58°C for 30–60 min), which introduced potential analytical limitations into our system. Batch adsorbing with chitin beads depletes human serum chitinase activity from human serum-containing ookinete culture media, as determined using the 4-methylumbelliferone chitotrioside substrate-based enzymatic assay (**Supplementary Figure 1**). Despite the absence of observable enzymatic activity in the culture medium, a faint band representing the human serum chitinase (approximately a band at 60 kDa reacting with anti-chitinase active site peptide antibodies) was observed by western immunoblot (data not shown). Nonetheless, *in vitro* production of mature *P. falciparum* ookinetes was improved in terms of the ability to identify parasite-specific chitinase activity. Further, a modified method for the *in vitro* culture of *P. falciparum* ookinetes in serum-free medium was developed (**Figure 1**). Enumeration of ookinetes was done using Giemsa-stained slides examined by light microscopy (**Figure 2**). The ookinete transformation efficiency was estimated at 20%–30% using serum-free M199 medium and specific modifications including incubation in a shaker incubator (60 rpm) at 28°C temperature for 48 h. The concentrated *P. falciparum* ookinete culture supernatants demonstrated detectable enzymatic activity by standard chitinase assay and were used for further studies.

In vitro production of *P. berghei* ookinetes for the three parasitic cell lines *Pb-PfCHT1*(r), *PbCHT1* (WT) and *PbΔCHT1* was carried out using an established protocol. The parasites showed normal asexual blood stage multiplication in mice (data not shown). In addition, *PbΔCHT1* and *Pb-PfCHT1*(r) parasites produced gametocytes and mature ookinetes *in vitro* comparable to wild type *P. berghei* (**Table 1**) with greater than 50% of the ookinete transformation rate. The fully mature Giemsa-stained *P. berghei* ookinetes are further viewed under the microscope, where the blunt apical and tapered posterior end with the presence of the nucleus can be visualized (**Figure 2**). *PbCHT1 (WT)*, *PbΔCHT1*, and *Pb-PfCHT1*(r) lines were passed through *A. stephensi* mosquitoes; and all lines produced oocysts with numbers in the expected range for *A. stephensi* mosquitoes directly fed on wild type *P. berghei* ANKA parasites infected mice (**Table 1**). This result shows that the *PbΔCHT1* formed oocysts normally in the mosquito midgut; head-to-head comparisons of WT vs. *PbΔCHT1* were not done. Earlier, membrane feeding of *PbCHT1 KO* resulted in a 30%–90% reduction of oocysts, with mean oocyst ranges from 25 to 63 oocysts/gut in PbCHT1-KO line (Dessens et al., 2001), suggesting that *P. berghei* ookinetes escape the midgut early, before the peritrophic matrix fully forms in *An. stephensi*.

P. gallinaceum, P. falciparum, and *P. berghei* (*Pb-PfCHT1*(r) and *PbCHT1* (WT)) ookinete culture supernatants demonstrated detectable chitinase enzymatic activity (data not shown), as measured by a fluorometric assay using 4-methyl-umbelliferyl-N, N′, N″-β-D-triacetyl-chitotrioside (4MU) as substrate. This result suggests that the ookinete-secreted chitinases are enzymatically active and thus these preparations were used for further studies. We did not observed chitinase activity in the ookinete supernatants of PbΔCHT1 parasite lines, despite the observation of mature ookinetes.

Identification of a *Plasmodium gallinaceum* and *Plasmodium falciparum* Ookinete-Secreted High Molecular Weight Chitinase-Containing Complex

Published data have shown that *P. gallinaceum* produces two forms of chitinase that are distinguished by SDS-PAGE and immunoblot analyses and physical characteristics as determined *via* strong anion exchange chromatography; specifically, a long form, with proenzyme and chitin binding domains, and a short form that contains the core TIM-barrel catalytic domain, but which lacks proenzyme and chitin-binding domains (Vinetz et al., 2000; Li et al., 2005). Western immuno-blot analysis following anion exchange chromatography of *P. gallinaceum* ookinete culture supernatant had shown a reduction-sensitive, high molecular mass (>200 kDa) chitinase-containing band, which was subsequently found to

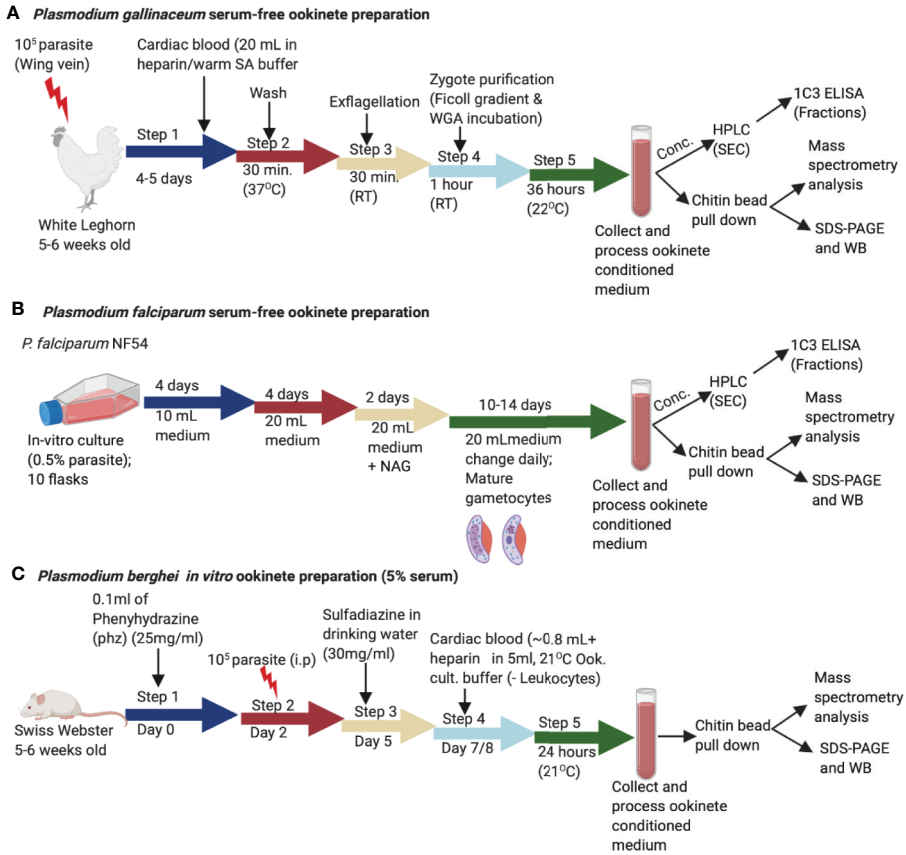

FIGURE 1 | Schematic representation of the *in vitro* production of *Plasmodium gallinaceum* and *Plasmodium falciparum* ookinetes in serum free media and *Plasmodium berghei* lines (*Pb-PfCHT1* (r), *PbCHT1* (WT), and *PbΔCHT1*). **(A)** Blood samples were collected into suspended animation buffer from *P. gallinaceum* infected White Leghorn chickens, centrifuged, and process as described in the methods section. For transformation to mature ookinete stages, purified zygote pellets were washed twice with ookinete culture serum free medium and incubated in the same media at 26°C for 36 h. The culture supernatants were characterized with a chitin bead pull-down assay, mass spectrometry, size exclusion fractionation, and immunological detections of a high molecular weight complex. **(B)** Synchronized *P. falciparum* NF54 cultures were seeded at 0.5% parasitemia with 5% hematocrit in 10 ml complete growth medium and cultured for gametocyte production as described in the methods section. The gametocyte cultures were pelleted, added to exflagellation media, and incubated for 30 min followed by centrifugation. The pellet was washed three times with serum free ookinete media and incubated in 20 ml of serum free ookinete media at 28°C for 48 h in a shaker incubator. The ookinete transformations were determined by examining Giemsa-stained thin smear slides. The culture supernatant was passed through a 0.22 µm filter, incubated with chitin beads to pull down the chitinase complex, and characterized as described above for *P. gallinaceum*. **(C)** The sulfadiazine method was used for the preparation of gametocyte-enriched blood from asynchronous infections in mice. Briefly, mice were treated with 0.1 ml phenylhydrazine (phz) to induce reticulocytosis and infected with 10^7 erythrocytes (*Pb-PfCHT1* (r), *PbCHT1* (WT), and *PbΔCHT1* lines). After the sulfadiazine treatment (30 mg/ml) on day 5, the mice were sacrificed and diluted in ookinete culture medium and leukocytes were removed through a Plasmodipur leukocyte filter. The *in vitro* cultures were further incubated at 21°C for 24 h. The culture supernatants were stored at –20°C for further biochemical and qualitative assays.

contain covalently bound WARP (Vinetz et al., 2000; Vinetz, 2005), but otherwise was not further characterized.

We further characterized the *P. gallinaceum* chitinase-containing high molecular mass complex by subjecting concentrated ookinete culture supernatants to HPLC size exclusion chromatography (TSKgel G2000SW), and fractions (0.5 ml/min) were collected and analyzed for chitinase activity (**Supplementary Figure 2**). We observed two peaks of *P. gallinaceum* chitinase activity, one just before the retention time of 11.5 min and the other at 14.0 min (**Supplementary Figure 2**). To determine whether the sole chitinase of *P. falciparum* (PfCHT1), the ortholog of the second, short form *P. gallinaceum* chitinase, PgCHT2, binds to chitin, concentrated *P. falciparum* ookinete culture medium was analyzed by HPLC as was done for *P. gallinaceum*. Because the protein yields of *P. falciparum* ookinete cultures are lower than those of *P. gallinaceum* ookinete cultures, we could not detect chitinase activity in the fractionated samples. Therefore, we used high resolution size exclusion chromatography and ELISA to detect chitinase-containing fractions, using the anti-chitinase monoclonal antibody, 1C3, for detection (Langer et al., 2002a).

Size Exclusion Chromatography of *Plasmodium gallinaceum* and *Plasmodium falciparum* Ookinete Culture Supernatants

To estimate the mass of the ookinete-secreted, short chitinase-containing high molecular complex, we followed standard

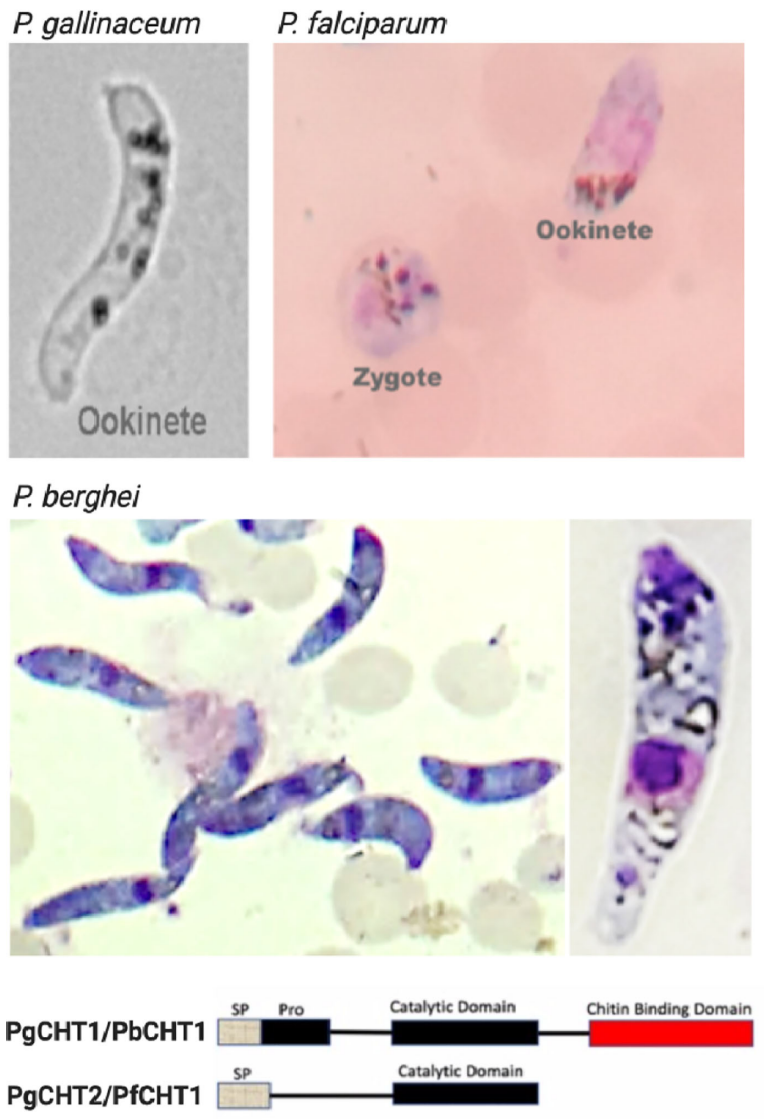

FIGURE 2 | Light microscopy images of *Plasmodium gallinaceum* and *Plasmodium falciparum* ookinetes produced *in vitro* using serum-free media, and *P. berghei* ookinetes in serum-containing medium. The lower panel shows the structural feature of the two types (long and short forms) of chitinases seen in *Plasmodium*. The characteristic banana shaped *P. gallinaceum* ookinete under bright field microscopy. This species possesses long and short form chitinases (*PgCHT1*, long form with chitin binding domain and *PgCHT2*, short form without CBD). Giemsa-stained smear of *P. falciparum* ookinete culture shows ookinete and zygote stages which are difficult to differentiate under bright field. The *P. falciparum* genome has only the short form (*PfCHT1*) of chitinase which lacks a chitin binding domain and is the ortholog of *PgCHT1*. *P. bergehi* ookinete production required serum and has only the long form chitinase, *PbCHT1*. The images were taken at 1000x magnification with a cell phone camera.

methods of high-resolution gel filtration chromatography (Superose-6, 10/300, MW separation range 5–5,000 kDa of globular proteins) and fractions (0.5 ml/min) were collected on ice. Each fraction was coated onto duplicate wells of an ELISA plate, and the presence of the short-form chitinase was detected by anti-chitinase mAb (1C3) [which reacts with *PfCHT1* and *PgCHT2* but not *PgCHT1*; (Langer et al., 2002a)] and absorbance/optical density (OD) values were plotted to determine the peak vs. retention times of both *P. falciparum* (**Figure 3A**) and *P. gallinaceum* (**Figure 3B**) ookinete culture supernatants. Blue Dextran was used to estimate the void (Vo) volume of the column, and commercially available gel-filtration standards were run in the same conditions (retention times and chromatograms are shown in **Supplementary Data File 1**). The approximate size of the peak was estimated by calculating the partition coefficient (K_{av}) and a standard calibration curve was plotted to estimate the molecular weight (Ohno et al., 1986) following the manufacturer's instructions (https://cdn.

TABLE 1 | Gametocyte, ookinete, and oocyst production of *PbΔCHT1* (3152cl1) and *Pb-PfCHT1(r)* (3165cl1) transgenic lines in comparison to wild type strains (WT).

Mutant	Gametocyte production (%) [a]mean (s.d.)	Male exflagellation rate (%) [b]mean (s.d.)	Ookinete production (%) [c]mean (s.d.)	Number of oocysts per mosquito [d]mean (s.d.)
***PbΔCHT1* (3152cl1)**	18.3 (2.0), n=3	79 (2.4), n=3	80.3 (3.7), n=3	174.6 (104.0), n=21
***Pb-PfCHT1(r)* (3165cl1)**	20.7 (1.7), n=3	89.6 (2.5), n=3	62.5 (6.6), n=3	164.3 (91.9), n=16
WT[e]	15-25, n>10	65-95, n>10	50-90, n>10	75-249, n>10

[a]*The mean percentage of blood stage parasites developing into gametocytes in vivo.*
[b]*The mean percentage of males that exflagellate in vitro 12–15 min after activation.*
[c]*The mean percentage of female gametes developing into mature ookinetes in vitro 16–18 h after activation of gametocytes.*
[d]*The mean number of oocysts per mosquito (days 12–13).*
[e]*Wild type: reference P. berghei ANKA reporter line 1868cl1.*
s.d., standard deviation.

cytivalifesciences.com). The molecular weight of the fraction containing the peak chitinase was estimated from the equation presented (**Supplementary Data File 1**). Blue dextran was used as a void volume determination and had a 2 min retention time, whereas chitinase containing *P. gallinaceum* and *P. falciparum* ookinete culture supernatants showed early peaks at 8 min, which correspondence to an estimated MW of 1,300 kDa, approximately the predicted size of the chitinase complex in native forms. These observations indicate that the first 1C3-positive peak represents the chitinase complex and the second peak represents free monomeric chitinase present in the ookinete culture supernatants.

Identification of Chitinase-Binding Partners by Chitin Bead Affinity Pull-Down of *Plasmodium gallinaceum*, *Plasmodium falciparum*, and *Plasmodium berghei* Chitinases From the Ookinete Secretome

P. gallinaceum, *P. falciparum*, and *P. berghei* ookinete culture supernatants were centrifuged, concentrated, and passed through 0.22 μm filters prior to chitin bead affinity pull-down experiments. Immuno-precipitation (IP) using anti-chitinase antibodies (mAb-1C3, rabbit anti-*PgCHT1* polyclonal antibodies, and anti-active site peptide antibodies) had failed to pull down chitinase(s) or chitinase complexes from ookinete culture supernatants. Therefore, an alternative approach was used in which chitin beads were added directly to the 0.22 μm filtered ookinete culture supernatant to allow the parasite chitinase(s) to interact directly with the chitin. The chitin bound proteins were then pelleted and washed to remove non-specific binding. SDS sample buffer was then added directly to the pelleted chitin beads, which were subjected to SDS-PAGE and western immunoblots performed under both non-reducing and reducing conditions.

Western immunoblot analysis performed on chitin bead pull-down of *P. gallinaceum* ookinete conditioned medium showed two chitinases recognized by the mouse anti-chitinase active site peptide antibody (**Figure 4**) (anti-chitinase active site-derived peptide antibody, B993), as shown (Vinetz and Kaslow, 1998; Vinetz et al., 2000). Bands were present at >200 and >75 kDa, and a duplex band at approximately 50 kDa. A silver-stained SDS-PAGE gel for the same sample showed an enriched duplex band at the corresponding 50 kDa immuno-reactive band (**Supplementary Figure 3**). An additional band at 37 kDa enriched by the chitin bead pull-down was not recognized by the anti-chitinase active site antibodies [B993, (Vinetz and Kaslow, 1998; Vinetz et al., 2000)] and is predicted to be *PgCHT2* (**Supplementary Figure 3**), consistent with our hypothesis that the high molecular weight chitinase complex represents specific protein-protein interactions, which are reduction sensitive (Langer and Vinetz, 2001), as previously observed. The duplex bands are consistent with previous data that indicate the presence of *PgCHT1* with a pro-domain and mature form of the enzyme (Vinetz et al., 2000). The higher molecular bands are consistent with the gel filtration chromatography data (see above) that indicate chitinase to be part of a high molecular weight complex. The high molecular bands are consistent with the gel filtration chromatography results and indicate that chitinase is a major protein in the hetero-multimeric complex secreted from ookinetes.

With *P. falciparum*, the chitin affinity pull-down complex from both serum-free (**Figure 5**) and serum-containing (**Supplementary Figure 4**) ookinete culture supernatants were resolved using SDS-PAGE under reduced and non-reduced conditions, followed by western immunoblot probed with the anti-chitinase monoclonal antibody, 1C3. Reduction with DTT eliminated the high molecular mass *P. falciparum* chitinase-containing complex, indicating dependency on disulfide linkages for forming a HMW complex. However, the monomeric form of *PfCHT1* (37 kDa) was also observed under non-reduced conditions, suggesting that the monomeric/free form of *PfCHT1* is also secreted by mature ookinetes. The mass spectrometry analyses of the chitinase complex formation were similar with and without human serum in the ookinete transformation media, indicating that the high molecular weight complex is of parasite origin.

Mass Spectrometry Identified Key Micronemal Proteins in the Short Chitinase-Containing Chitin Affinity Pull-Downs of *Plasmodium gallinaceum* and *Plasmodium falciparum* Ookinete-Conditioned Media

Mass spectrometry analysis was carried out directly on the affinity pull-down chitin beads to identify the proteins present in the high molecular weight chitinase complex in both *P. gallinaceum* (**Table 2**) and *P. falciparum* (**Table 3**). *PgCHT1* and *PgCHT2* were

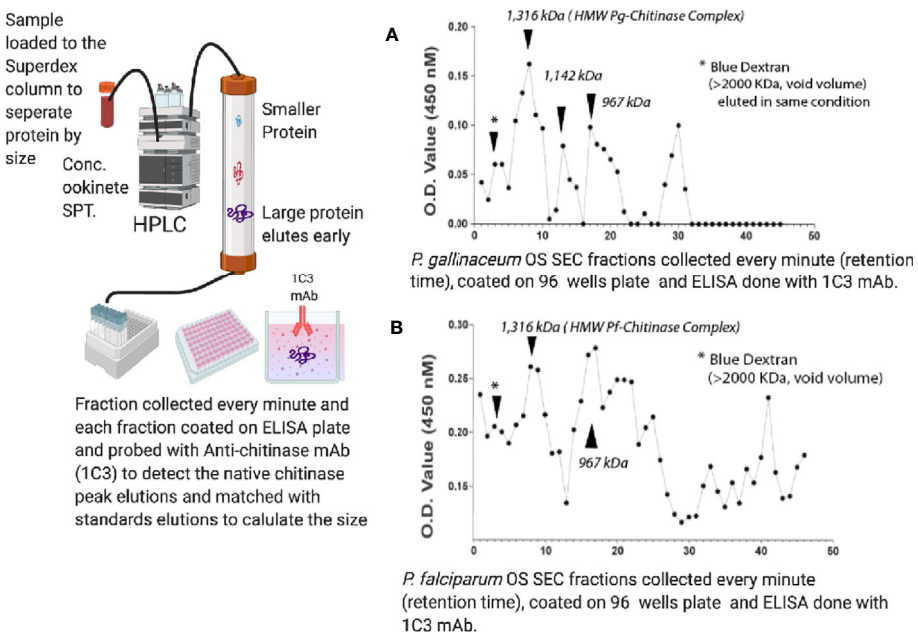

FIGURE 3 | Size exclusion chromatography estimation of the molecular mass of the ookinete-secreted native chitinase complex in ookinete culture supernatants of *P. falciparum* **(A)** and *P. gallinaceum* **(B)**. Concentrated ookinete culture supernatants from *P. gallinaceum* and *P. falciparum* were loaded separately onto a gel filtration column (Superose-6, 10/300, MW separation range 5–5,000 kDa of globular proteins) in PBS, pH 7.4, and fractions (0.5 ml/min) were collected on ice. Each fraction was coated onto duplicate wells of an ELISA plate, probed with anti-chitinase mAb (1C3), followed by goat-anti-mouse IgG-horse radish peroxidase-conjugate and 5-bromo-4-chloro-3-indolyl phosphate (BCIP)/nitro blue tetrazolium (NBT) substrate. Absorbance/optical density (OD) values were plotted to determine the peak versus retention times of both *P. falciparum* ookinete **(A)** and *P. gallinaceum* ookinete culture supernatants **(B)**. Dextran Blue was used to estimate the void (V_o) volume of the column and commercially available gel-filtration standards (17–670 kDa) were run in the same conditions, with retention times and chromatogram shown in **Supplementary Figure 3**. The retention time of the standards were used to estimate the partition coefficient ($K_{av} = V_e - V_0/V_t - V_0$) and a standard calibration curve (**Supplementary Figure 3**) was plotted. V_0 is void volume, V_e is the elution volume of the sample, and V_t is the total column volume. The molecular weight of the fraction containing the peak chitinase was estimated from the equation, and details are presented in the table below and calculation in **Supplementary Table 3**. Blue dextran (void volume) had a 2 min retention time, whereas chitinase-containing fractions of *P. gallinaceum* and *P. falciparum* ookinete culture supernatants showed an early peak at 8 min, which corresponds to a protein MW of roughly 1,300 MDa, yielding the estimated size of the chitinase complex in native forms.

identified (spectra counts of 32 and 53 respectively) along with equally enriched ookinete micronemal proteins known to play roles in mosquito midgut invasion (Dessens et al., 2003; Li et al., 2004; Ramakrishnan et al., 2011), including WARP (spectra count 36) and ookinete-surface enolase (Ghosh et al., 2011) (spectra count 30). A plasmepsin [an aspartic protease (Li et al., 2010)] was detected in the chitin bead pull-down material, but the spectra count was too low to conclude an association with the complex (**Supplementary Data File 2**). Taken together, these results show that *P. gallinaceum* chitinases are present in a complex along with key proteins that are essential for mosquito midgut invasion. The reduction sensitivity suggests that the integrity of the complex depends either on intermolecular disulfide bonds or intramolecular bonds within essential protein globular domains.

For *P. falciparum* chitin bead pull-down samples *PfCHT1* was found as an abundant protein along with WARP, fructose-bisphosphate aldolase, gamete antigen 27/25, and SOAP. The mass spectrometry analysis of SDS-PAGE gel slices including the *PfCHT1* HMW complex and the 37 kDa *PfCHT1* (**Figure 5**, **Supplementary Data File 3**) further confirmed that WARP is a key, covalently-linked or otherwise reduction-sensitive PfCHT1 partner involved in the high molecular weight chitinase complex, and is also found in the chitin bead affinity pull-down mass spectrometry samples (**Supplementary Data File 4**).

PgCHT1 Conserved Cysteines Involved in Chitin Binding *Via* Analysis of Site-Directed Mutagenesis and *rPfCHT1* Binds to Chitin Beads That Is Resistant to High Detergent Wash

The long form chitinase (*PgCHT1*) gene encodes a protein possessing a putative chitin binding domain (CBD) (Vinetz et al., 2000), in contrast to the short form chitinases (PgCHT2 and PfCHT1). Earlier experiments showed that both the long and short form chitinases binds to chitin. Here we examined the putative role of the three conserved cysteines in the PgCHT1 CBD by site directed mutagenesis to individually replace each cysteine to serine. Mutated rPgCHT1 proteins were expressed in

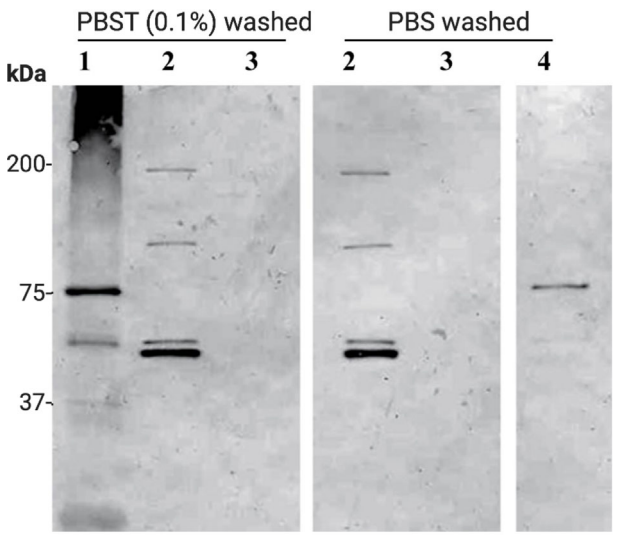

FIGURE 4 | Affinity pull-down of *Plasmodium gallinaceum* chitinase complex from serum free ookinete culture supernatant. Chitin beads were added to serum free *P. gallinaceum* ookinete culture supernatants to affinity pull down the chitinase and chitinase-associated protein complex. The protein-bound beads were washed three times with PBS containing (0.1% Tween 20) (PBST) or PBS (2) to remove non-specific proteins. For control, chitin beads were incubated in M199 media alone (3), *rPgCHT1* spiked media (4), and *E. coli* lysate culture supernatant expressing soluble *rPgCHT1* (1) and processed as above. Then SDS sample buffer was added to the beads, boiled, and subjected to 4%–12% Tris-Glycine gradient SDS-PAGE. The protein was transferred to a membrane and probed with mouse anti-chitinase active site peptide (B993) antibodies. Lane 2 shows that the chitin beads successfully pulled down the chitinases and interacting high molecular chitinase and protein complex band. Washing with PBST did not detach the complex from the chitin beads. The duplex band (lane 2, around 50 kDa, bottom panel) shows the pro-enzyme and mature forms of *PgCHT1*; and two other higher immuno-reactive bands (100 kDa and just below 200 kDa) are homo or hetero-multimeric forms of a complex. The soluble *E. coli*-produced rPgCHT1 (1) was specifically pulled down by the chitin beads and did not show a higher molecular weight band.

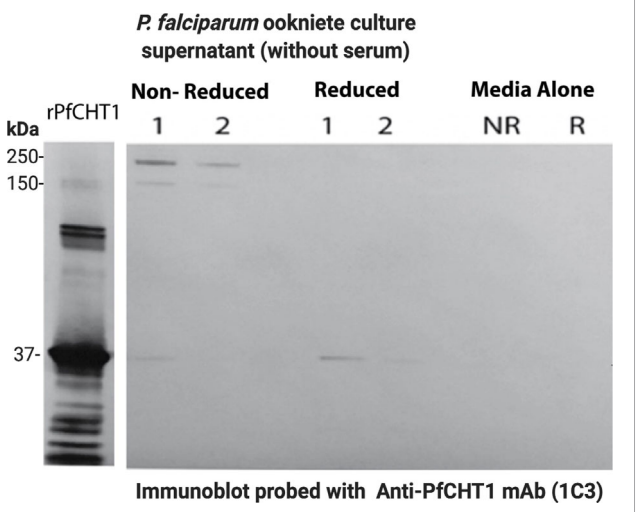

FIGURE 5 | Western immunoblot of affinity pull-down of *Plasmodium falciparum* chitinase complex from ookinete culture supernatants. Washed chitin beads were added to the serum-free *P. falciparum* ookinete culture supernatants in replicate preparations (1, 2) to affinity pull down the chitinase and chitinase-associated protein complex. The protein bound beads were washed three times, SDS sample buffer (non-reduced, NR and reduced or R) was added to the beads, boiled, subjected to SDS-PAGE, and Western immunoblot analysis using anti-chitinase mAb (1C3). The samples were run under reduced (Red or R) and non-reduced conditions (Non-Red or NR) along with chitin beads incubated in ookinete media alone (NR and R) as controls. *rPfCHT1* protein was used as a positive control that is known to be recognized by mAb 1C3. Both serum-free media showed a high molecular chitinase complex in non-reduced samples and the same sample showed a smaller band of 37 kDa. The results were similar to observations of serum-containing ookinete medium (**Supplementary Figure 3**).

E. coli and their binding to chitin beads compared to wild type protein (**Figure 6**). Mutated rPgCHT1 protein with three conserved cysteines replaced with serine in the CBD (clone 1) bound to the chitin beads was removed by the detergent wash (PBS with 1% Triton-X 100), whereas wild type bound protein resisted the detergent wash. This result demonstrates that a chitin binding domain is involved in PgCHT1 high-affinity interactions with chitin.

To assess the specificity of the chitin bead pull-down assay, rPfCHT1 (**Figures 6D, E**) was pulled down purely from gross rPfCHT1 *E. coli* lysate and PBS spiked with purified rPfCHT1; specifically, it was observed as a single band without non-specific contamination in Coomassie stained SDS-PAGE gels. PfCHT1 lacking a putative chitin binding domain showed high affinity binding for the chitin beads and resisted washing with high concentrations of detergent (1% Triton X-100 in PBS). It will be of interest to delineate which regions of PfCHT1 specifically bind to the solid phase chitin substrate.

Generation and Characterization of a *Plasmodium berghei* Transgenic Gene Insertion/Marker Out Parasite Line

A chimeric *P. berghei* parasite line was produced in which the coding sequence (CDS) of the *P. berghei* chitinase gene (*PbCHT1*; PBANKA_0800500) was replaced with the CDS of *P. falciparum* chitinase (*PfCHT1*; PF3D7_1252200), amplified from genomic DNA of *P. falciparum* NF54 (**Figure 1**). This chimeric line, *Pb-PfCHT1*(r), constitutively expressed mCherry and luciferase as reporter proteins throughout the life cycle. We confirmed the correct replacement of the *PbCHT1* CDS by the *PfCHT1* CDS in the chimeric line by Southern analysis of chromosomes separated by pulsed-field gel electrophoresis and by diagnostic PCR on genomic DNA (**Figure 7**). These parasites were then characterized as described below.

P. berghei ookinetes were equally well produced *in vitro* by all parasite lines. *P. berghei in vitro* ookinete culture supernatants from all three parasite lines (*Pb-PfCHT1(r)*, *PbCHT1 (WT)*, and *PbΔCHT1*) were used for the evaluation of the HMW multimeric complex using the chitin bead affinity pull-down assay. Washed chitin beads were subjected to SDS-PAGE and western immunoblots under both non-reducing and reducing conditions and probed with 1C3 and anti-*PbCHT1*-polyclonal

TABLE 2 | List of proteins identified by mass spectrometry in the *P. gallinaceum* chitinase complex.

Locus *P. gallinaceum* (Mol. wt/length aa)	Protein name	Spectracount (seq count)	Known function in ookinete stages
PGAL8A_00473200 (42 kDa, 733 aa)	Chitinase, *PgCHT2* (short form chitinase)	53 (37)	Invasion
PGAL8A_00321200 (68 kDa, 587 aa)	Chitinase, *PgCHT1* (long form chitinase)	32 (18)	Invasion
PGAL8A_00077400/ (33 kDa, 292 aa)	von Willebrand factor A domain-related protein (WARP)[a]	38 (18)	Cell adhesion
PGAL8A_00392100/ (48 kDa, 446 aa)	Enolase	30 (16)	Interact with mosquito gut protein (EBP)
PGAL8A_00471000/ (301 kDa, 2257 aa)	G377	26 (18)	Not known
PGAL8A_00185600 (24 kDa, 207 aa)	Gamete antigen[a]	18 (8)	Not known
PGAL8A_00016000/ (328 KDa, 2847 aa)	P230[a] 6-Cys protein	16 (8)	Gamete-gamete interaction
PGAL8A_00344300 24 kDa, 214 aa	GTP binding Ran TC4	7 (5)	Unknown signal pathway

Mass-spectrometry identification of proteins that are associated with P. gallinaceum chitinase complex purified via affinity pull-down by chitin beads. Multidimensional Protein Identification Technology (MudPIT) was carried out directly on the beads that were incubated in the P. gallinaceum ookinete culture supernatant to affinity pull down the chitinase complex. Chitin beads were washed with PBS three times before subjected to MudPIT and the presence of chitinase complex confirmed by western immunoblot. MS/MS spectra verified against chicken (Gallus gallus) protein entries and a manually added list of common contaminants (e.g. human keratin and trypsin). The final list of peptides sequences was used for BLAST of the PlasmoDB databases (PlasmoDB.org) to identify the updated list of proteins. Only the spectra which had more than five spectra counts are presented here.
[a]These proteins were also seen in the gel slice representing the high molecular complex that was positive by western blot with anti-chitinase (1C3) mAb.

TABLE 3 | Mass spectrometry analysis of the *Plasmodium falciparum* chitinase complex.

Locus *P. falciparum* orthologs (Mol. wt/length aa)	Protein name	Spectra count	Known function in ookinete stages
PF3D7_1252200 (42 kDa, 733 aa)	Chitinase, *PfCHT1*	17	Invasion
PF3D7_0801300 (32 kDa, 290 aa)	von Willebrand factor A domain-related protein (WARP)	12	Cell adhesion
PF3D7_1404300 (23 kDa, 202 aa)	Secreted ookinete adhesive protein (SOAP)	3	Interaction with mosquito gut protein (EBP)

Mass-spectrometry identification of proteins that are associated with P. falciparum chitinase complex purified by chitin bead affinity pull-down. Multidimensional Protein Identification Technology (MudPIT) was carried out directly on the beads that were incubated in the P. falciparum ookinete culture supernatant to affinity pull down the chitinase complex. Before subjected to MudPIT the chitin beads were washed with PBS three times and confirmed for the presence of chitinase complex by western-immunoblot. MS/MS spectra verified against protein entries manually added to a list of common contaminants (e.g. human keratin and trypsin) and normalized against zygote culture supernatant-chitin bead pull-down samples. The final list of peptides sequences was analyzed by BLAST against PlasmoDB (PlasmoDB.org) to identify the proteins. Out of 17 total identified proteins in the sample beads (affinity pull-down chitinase complex- chitin pull-down), only three proteins showed more than two peptides in normalized samples. In the zygote pull-down samples, chitinase, WARP, and SOAP showed low spectral counts 1, 0, and 0, respectively, indicating that they are present only in an ookinete-secreted complex.

antibody (**Figures 8A–F**). The successful expression of the native, monomeric form of *PfCHT1* (37 kDa) and *PbCHT1* (73 kDa) proteins were observed in the ookinete culture supernatants from the respective *Pb-PfCHT1(r)* and *PbCHT1 (WT)* parasite lines with the complete absence of *PbCHT1* in the *PbΔCHT1* parasite cell line ookinete culture supernatant. However, the chitin affinity pull-down was able to pull down monomeric *PfCHT1* (37 kDa) efficiently. The presence of a high molecular mass protein complex in the *Pb-PfCHT1*(r) (**Figure 8A**) *in vitro* ookinete culture supernatants was not observed when probed with 1C3 under non-reducing conditions.

Mass spectrometry analysis was carried out on the chitin affinity pulled down proteins from the *Pb-PfCHT1(r)* ookinete culture supernatant (**Figure 8G**). A high spectrum count of 16 was found for the native *PfCHT1* followed by low spectra counts for other microneme proteins that play important roles in mosquito midgut invasion (Dessens et al., 2003; Li et al., 2004). Other than the *P. berghei* von Willebrand Factor A domain-related protein (*PbWARP*; spectral count 6) and *P. berghei* secreted ookinete adhesive protein (*PbSOAP*; spectral count 3) proteins, an aspartic protease *P. berghei*. Plasmepsin IV (*PbPM4*) with low spectra count (**Figure 8G**) was also detected *via* mass spectrometry (**Supplementary Data File 5**). The mass spectrometry proteomics data have been deposited to the ProteomeXchange Consortium *via* the PRIDE partner repository with the dataset identifier PXD021970 (Perez-Riverol et al., 2019). To explore a possible reason for the absence of the HMW hetero-multimeric complex in the *Pb-PfCHT1(r)* ookinete culture supernatant, we examined differences in the primary structure of the chitinase binding protein partner WARP. The *Plasmodium* species with short form of the chitinases (*PfCHT1* and *PgCHT2*) have a conserved

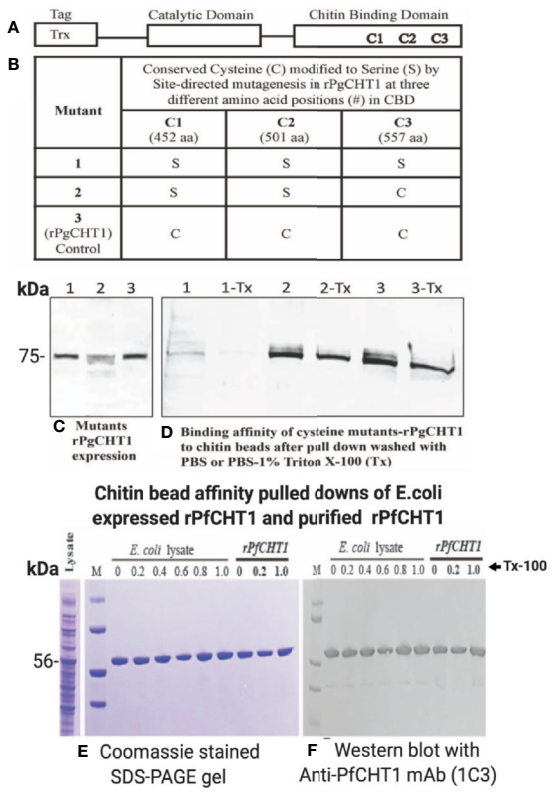

FIGURE 6 | Site-directed mutagenesis of conserved cysteines located in the chitin binding domain of *P. gallinaceum* chitinase (*rPgCHT1*) and evaluation of chitin binding affinity of mutant *rPgCHT1* and *rPfCHT1*. Three conserved three cysteines **(A)** that were selected for mutation using the QuickChange Multi Site-Directed Mutagenesis Kit (Stratagene) with the known template (*PgCHT1*- PET32b plasmid DNA expression construct) containing a thioredoxin epitope tag (TRX-Tag). The changes of single base pairs were achieved within codons 452 aa (1,355 bp, TGC to TCC), 501 aa (1,502 bp, TGC to TCC) and 557 aa (1,670 bp, TGT to TCT) of the plasmid constructs to mutate cysteine **(C)** residues to serine (S) as shown in **(B)**. The *PfCHT1*-pET-32b expression plasmid was obtained from Gene Universal (Newark DE). The #1 mutant plasmid (in which all three C were modified), #2 plasmid (only two C modified), and wild type (3, *rPgCHT2*-PET32) and *rPfCHT1* were transformed into SHuffle T7 Express Competent *E. coli* cells for protein expression. The *rPgCHT1* lysates were incubated with chitin beads, washed three times either with either PBS (1, 2, 3) or PBS with 1% Triton X-100 (1-Tx, 2-Tx, and 3-Tx) to remove non-specific or loosely bound chitinase, and evaluated for binding affinity of the mutant rPgCHT1. Similarly, primary *E. coli* lysate containing rPfCHT1 in soluble form Ni-NTA purified rPfCHT1 was incubated with chitin beads and washed with PBS and PBST (0.2%–1% Triton-X 100). The bound chitin beads were mixed with sample buffer and subjected to SDS-PAGE followed by Western immunoblot analysis with anti-thioredoxin monoclonal antibody (Abcam) to detect rPgCHT1, and 1C3 antibody to detect rPfCHT1 **(E, F)**. Panel **(C)** shows the expression of rPgCHT1 (75 kDa) protein in all clones. The binding affinity to chitin beads of mutant #58 (all three cysteines modified) was lower and largely eliminated with the Triton-X 100 wash **(D)**, indicating that the chitin binding domain is essential for the interaction of the long form chitinase (*PgCHT1*) to chitin. Panels **(E, F)** show the strong binding of rPfCHT1 to chitin beads in both **(E)** *coli* culture lysates and purified rPfCHT1. In **(E, F)**, chitin beads were washed with PBS with different concentrations of Triton X 100 (0%–1%). rPfCHT1 strongly binds to chitin beads despite lacking a chitin binding domain.

cysteine residue in the N-terminal region of the WARP protein, in contrast to a serine residue at this position in species possessing the long form of the chitinases (*PbCHT1* and *PvCHT1*). The conserved cysteine is possibly unpaired intramolecularly, and instead might participate in cross-linkages and stabilize partner proteins secreted as a HMW complex in *in vitro P. falciparum* ookinete culture supernatants (**Figure 9**).

DISCUSSION

Here we demonstrate that *Plasmodium falciparum* and *P. gallinaceum* ookinete secrete a short-form chitinase as a covalently-linked, reduction-sensitive, high molecular weight hetero-multimeric protein complex with highest approximate mass of 1,300 kDa. Proteomic analysis of material pulled down using chitin beads shows that this complex contains both reduction-sensitive, i.e. cysteine-disulfide bonded components (short chitinase-WARP) and SDS-sensitive components (non-covalently associated proteins such as SOAP and enolase). This complex potentially enables the *Plasmodium* ookinete to invade the mosquito midgut, and characterization of this pathway might reveal targets for malaria transmission blocking strategies. The complex appears to contain WARP, consistent with previous data (Li et al., 2004), and possibly other ookinete-expressed proteins, as suggested by mass spectrometry analysis of proteins pulled down using a chitin affinity assay as well as a gel slice that represents the anti-chitinase (1C3) positive HMW chitinase complex.

To determine whether the presence of this secreted, chitinase-containing invasion complex is generalizable to other *Plasmodium* species, we studied *P. gallinaceum*, an avian-infecting *Plasmodium* species which is a well-established model for studying ookinete biology, and *P. falciparum*, the major human pathogen for which ookinetes have only relatively recently been able to be produced *in vitro* (Dinglasan et al., 2007a; Dinglasan et al., 2007b; Bounkeua et al., 2010; Ghosh et al., 2010). There are two types of active chitinases in *P. gallinaceum* (PgCHT1 and PgCHT2, long and short form respectively) and only one short form of active chitinase present in *P. falciparum* (PfCHT1). *P. vivax* and other human-infecting malaria parasites encode only the long form chitinase (PvCHT1), homologous to PgCHT1 (Tsuboi et al., 2003). Published data showed the presence of a high molecular weight chitinase in *P. gallinaceum*, by anion-exchange chromatography of ookinete supernatants (Vinetz et al., 2000) and by western immunoblot using an anti-chitinase monoclonal antibody (1C3, a monoclonal developed against the active site of PfCHT1 chitinase that also recognizes an identical epitope in the short form of chitinase in *P. gallinaceum*, PgCHT2) (Langer et al., 2002a). However, we were unable to use antibodies to pull down the chitinase complex, possible due to steric hindrance or low affinity binding of antibodies to native enzymes or sequestered epitopes within the high molecular weight complex. We were able to overcome this technical problem by using chitin beads, which enabled us to identify the components of the high molecular mass chitinase-containing complexes in two phylogenetically distant *Plasmodium*

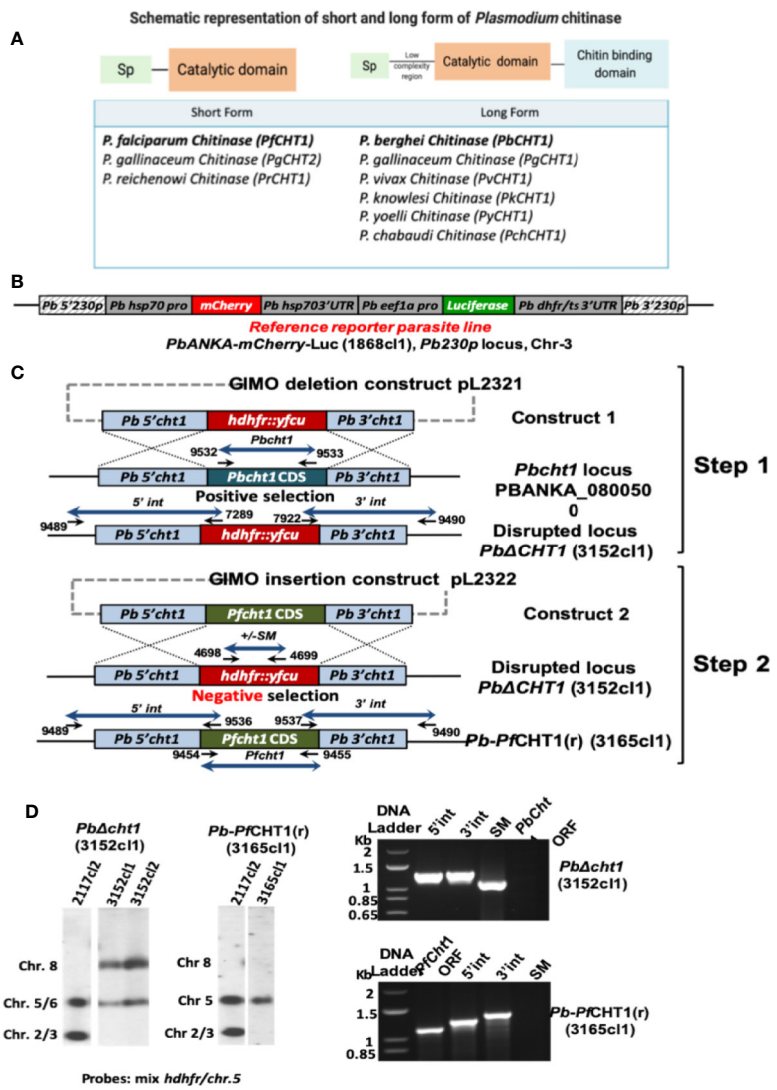

FIGURE 7 | Generation of the chimeric *P. berghei* parasite line, *Pb-PfCHT1*(r), expressing the short form of *P. falciparum* chitinase (*PfCHT1*). **(A)** Schematic representation of the short and long forms of chitinase found in different *Plasmodium* species. The short form chitinases lack the proenzyme and chitin-binding domains, compared with the long forms of chitinases which have proenzyme and chitin-binding domain in addition to substrate-binding and catalytic domains. **(B)** Schematic representation of the *Pb230p* locus of the reference reporter *P. berghei* ANKA parasite 1868cl1 which was used to generate the chimeric *Pb-PfCHT1* (r) parasite line (see C). This reporter line is selectable marker (SM)-free and expresses mCherry protein under the strong constitutive *Pbhsp70* promoter and firefly luciferase (LUC-IAV) under the constitutive *Pbeef1a* promoter. The reporter-cassette is integrated into the neutral *230p* locus in chromosome 3. **(C)** Schematic representation of the generation of the chimeric line *Pb-PfCHT1*(r) (line 3152cl1). First step: the GIMO deletion-construct (construct 1; pL2321) was used to replace the *Pbcht1* coding sequence (CDS) with the positive/negative selectable marker (SM; h*dhfr::yfcu*) cassette, resulting in the generation of the *PbΔcht1* (line 3152cl1) after positive selection with pyrimethamine. Construct 1 targets the *Pbcht1* gene by double cross-over homologous recombination. After genotyping and confirmation of correct construct integration, this line was cloned by limiting dilution. Second step: The GIMO insertion construct (construct 2) was used to replace the SM in the *PbΔCHT1* GIMO line with the *Pfcht1* CDS, resulting in the generation of line *Pb-PfCHT1*(r) (line 3165cl1) after negative (5-FC) selection. Construct 2 integrates by double cross-over homologous recombination using the same targeting regions employed in construct 1, resulting in the introduction of the *Pfcht1* CDS under the control of *Pbcht1* regulatory sequences. Black arrows: locations and primer numbers used for diagnostic PCR. **(D)** Genotype analysis of *PbΔcht1* and *Pb-PfCHT1*(r) parasites by Southern analysis of chromosomes (chr) separated by pulsed-field gel electrophoresis (PFGE) (left) and diagnostic PCR analysis (right). Hybridisation of PFG-separated chr of *PbΔcht1* with a mixture of *hdhfr* and a probe specific for chr 5 confirms integration of construct 1 into the *Pbcht1* gene on chr 8. The correct integration of construct 2 in *Pb-PfCHT1*(r) was confirmed by showing the removal of the *hdhfr::yfcu* selectable marker (SM) cassette by hybridisation of chr with the *hdhfr* and chr 5 probe. As an additional control (ctrl), parasite line 2117cl1 was used with the *hdhfr::yfcu* SM integrated into chr 3. Diagnostic PCR analysis confirms the deletion of *Pbcht1* in *PbΔcht1* and the correct integration of the *Pfcht1* expression cassette in *Pb-PfCHT1*(r). Correct integration is shown by the absence of the *hdhfr::yfcu* SM and the *Pbcht1* CDS, the presence of the *Pfcht1* CDS, and correct integration of the construct into the genome at both the 5' and 3' regions (5'int and 3'int; see B for primer numbers and locations). Primer sequences and expected PCR product sizes are shown in **Supplementary Table 1**.

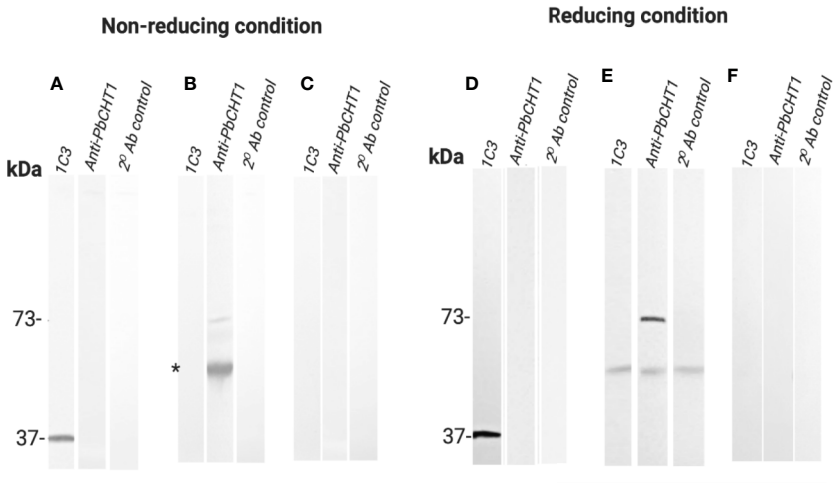

G **Mass Spectrometry analysis of proteins identified in Pb-PfCHT1 (3165cl1) ookinete chitin pull downs**

Accession number; Molecular Weight	Protein Names	Total Spectrum Count	Exclusive Unique peptide count	Protein identification Probability
PF3D7_1252200; 43kDa	PfCHT1	16	11	100%
PBANKA_103780; 18kDa	PbSOAP	3	3	100%
PBANKA_122890; 34kDa	PbWARP	6	6	100%
PBANKA_103440; 50kDa	PbPM4	2	2	100%

(Criteria used for Mass spectrometry analysis-Protein threshold-99%; Minimum peptides-2; Peptide threshold- 90%)

FIGURE 8 | Western Immunoblotting of chitin affinity pull-downs of *Pb-PfCHT1 (r)*, *PbCHT1 (WT)*, and *PbCHT1-KO* from *in vitro* ookinete culture supernatants: Figures show under non-reducing conditions **(A–C)** and under reducing conditions **(D–F)**. To pull down the chitinase (mainly PfCHT1)-associated microneme protein partners from the ookinete culture supernatants, washed chitin beads were added and incubated at 4°C for 4 h on a rotary shaker. Chitin beads were washed three times with PBST (0.5% Tween 20) followed by three washes with PBS (pH 7.4) and suspended in SDS sample buffer (+/– 2-mercaptoethanol). SDS-PAGE and western immunoblots were performed and probed with anti-PfCHT1 monoclonal antibody (1C3) and anti-PbCHT1 polyclonal antibody. A secondary antibody control was run with each blot under both conditions. **(A, D)** Pb-PfCHT1, under non-reducing and reducing conditions. Reactivity of native PfCHT1 (37 kDa) was seen exclusively with 1C3 monoclonal antibody and not with polyclonal anti-PbCHT1 under both conditions. No specific HMW band was detected with 1C3. **(B, E)** PbCHT1, under non-reducing and reducing conditions. Presence of native PbCHT1 (73 kDa) was observed specifically with polyclonal anti-PbCHT1 antibody and not with 1C3 in both NR and R conditions. Some non-specific reactivity (*) was observed when probed with 1C3 and anti-PbCHT1 and also in a secondary antibody control blot. **(E, F)** PbCHT1-KO, under non-reducing and reducing conditions. Native PbCHT1 was not observed either with 1C3 or polyclonal anti-PbCHT1 antibody. Secondary antibody controls were run with each blot, where no non-specific reactivity was observed. **(G)** Table represents the mass spectrometry analysis of proteins identified in Pb-PfCHT1 (3165cl1) ookinete culture supernatants chitin pull-downs. The presence of microneme proteins secreted ookinete adhesive protein (SOAP), von Willebrand factor A domain-related protein (WARP), and PM4 were observed. The data shows the absence of the high molecular weight (HMW) complex in the Pb-PfCHT1 parasite lines despite the presence of the partner proteins (*P. berghei* specific). This might suggest the importance of the species specific chitinase binding partner proteins to be present in order to form the HMW complex in a *P. berghei* mouse model.

species. The chitin bead pull-down method was successfully used to purify native parasite secreted chitinases as well as the recombinant chitinases rPfCHT1 and rPgCHT1. The data shows that rPfCHT1 (**Figures 6D, E**) was purified neatly from *E. coli* lysate without non-specific bands in Coomassie stained gels and resisted a high detergent wash. Unpublished data (Kaur and Vinetz, 2020) show that modification of conserved cysteines in the rPfCHT1 almost eliminates binding to chitin beads, versus its high affinity binding in native forms.

Ookinete-secreted chitinases are essential for the malaria parasite to establish mosquito infection, and hence continuation of the *Plasmodium* life cycle and malaria transmission (Huber et al., 1991; Sieber et al., 1991; Shahabuddin et al., 1993; Shahabuddin and Vinetz, 1999; Vinetz et al., 1999; Vinetz et al., 2000; Langer and Vinetz, 2001; Li et al., 2005). The ookinete-secreted native high molecular weight native chitinase complex, identified by size exclusion chromatography for both *P. gallinaceum* and *P. falciparum*, is reduction-sensitive suggesting that this complex is either produced in the ookinete secretory pathway as a cysteine-dependent hetero-multimer or that disulfide bond-stabilized protein globular domains are involved in the complex formation. Mass spectrometry analysis demonstrated that interacting partners of chitinase are other known ookinete proteins, including WARP, enolase and SOAP, which are known to play a role in midgut invasion (Dessens et al., 2003; Abraham et al., 2004; Li et al., 2004). In *P. gallinaceum*, both *PgCHT1* and *PgCHT2* are part of the complex, along with the micronemal proteins WARP and SOAP that were also identified in *P. falciparum*.

P. falciparum ookinetes were produced *in vitro* using serum-containing medium [16, 17] and these methods were not suitable for

FIGURE 9 | Identification of a putative cysteine (C) residue involved in the formation of the multimeric high molecular chitinase complex of *Plasmodium gallinaceum* and *Plasmodium falciparum*. Multiple sequence alignment (MSA) of full-length von Willebrand factor A domain-related protein (WARP) proteins of *Plasmodium berghei*, *P. falciparum*, *P. gallinaceum* and *P. vivax*. Fully conserved amino acid residues are shown by an asterisk (*), amino acids showing strongly similar properties are represented by a colon (:) and weakly conserved by a period (.). The *Plasmodium* species with a short form chitinase (*P. falciparum, PfCHT1*; *P. gallinaceum*, *PgCHT2*) have one conserved cysteine residue in the N-terminal structure of the WARP protein compared to all long form chitinases (*PbCHT1* and *PvCHT1*) which instead have a serine (shown in red rectangles). The conservation of the cysteine residue in *P. falciparum* and *P. gallinaceum* suggests a species-specific WARP - short chitinase covalent interaction responsible for the formation of the reduction-sensitive multimeric high molecular weight chitinase complex. The lack of a HMW complex formation in transgenic *P. berghei* heterologously-expressing *PfCHT1* supports this hypothesis. The other cysteine residues are highly conserved in the other *Plasmodium* WARP proteins depicted.

our studies due to chitinase activity of the serum. Therefore, we successfully produced ookinetes of *P. falciparum in vitro* using serum free conditional medium and the supernatant was used to affinity pull-down the chitinase using chitin beads. A *PfCHT1* high molecular mass complex was pulled down from ookinete culture supernatant by chitin beads, recognized by anti-PfCHT1 mAb (1C3), and confirmed by mass spectrometry analysis. The mass spectrometry analysis of a gel band corresponding to the high molecular weight *P. falciparum* identified WARP protein, similar to its presence in the *P. gallinaceum*-secreted chitinase complex.

To our knowledge this report is the first to demonstrate the presence of P. falciparum ookinete-produced native chitinase, which necessitates further explorations of its biological functions. While we recognize the limitation of the chitin bead affinity pull-down of native chitinase for mass spectrometry analysis, which might have non-specifically pulled down 'sticky' micronemal proteins, our size exclusion chromatography analysis of *P. falciparum* and *P. gallinaceum* ookinete-secreted chitinases showed both reduction-sensitive (WARP) and SDS-sensitive components (SOAP, enolase) of the high molecular complex. The high degree of purity of chitin bead pulldown of rPfCHT1 from recombinant *E. coli* lysate (**Figure 6**) supports the specificity of this method for detecting chitin-binding activity along with proteins that bind to the chitinase and therefore are indirectly bound by chitin beads. Therefore, mass spectrometry analysis of an anti-chitinase immunoreactive gel slice representing the HMW, and comparing with mass spectrometry analysis of chitin pull-down samples confirms that WARP and other proteins are consistently present in the chitinase complex of both species.

Previous experimental work was not able to directly observe the *P. falciparum* ookinete-produced chitinase because of technical limitations, which were overcome in the present study. Moreover, while the *P. gallinaceum* ookinete-secreted long form of the chitinase has a predicted chitin-binding domain, *P. falciparum* chitinase, *PfCHT1*, does not (Vinetz et al., 1999). Mutation of three conserved cysteines within in the putative chitin-binding domain of *PgCHT1* using site directed mutagenesis showed, for the first time, that this domain is involved in chitin binding. Hence a key conclusion of the present work is that two *Plasmodium* ookinete-secreted chitinases with unrelated primary structures bind to chitin, as demonstrated by mass spectrometry analysis of a chitin bead pull-down assay as well as by size exclusion chromatography.

To further characterize the HMW complex using a genetic approach, the *P. berghei* model was developed by using a novel GIMO method to successfully replace the *PbCHT1* (long form) with *PfCHT1* (short form). The *in vitro* ookinetes culture supernatants revealed the absence of a reduction sensitive HMW chitinase-containing complex, confirming the importance of the species-specific binding protein partners in the complex formation. However, mass spectrometry analysis performed on the *Pb-PfCHT1(r)* pull-downs confirms the presence of other important micronemal proteins including PbWARP and PbSOAP that play a role in mosquito midgut invasion (Hirosawa et al., 1993; Dessens et al., 2003).The inability of heterologously-expressed PfCHT1 to form the high molecular weight complex in the *P. berghei* system could be attributed to a number of possibilities, one of which might be the absence of a suitable WARP protein with the necessary cysteine and other structural features that would enable covalent linkage to PfCHT1 and other micronemal proteins to form the short chitinase-containing high molecular weight complex (Li et al., 2004). This possibility is of fundamental interest and is the focus of ongoing experiments.

Plasmodium actively invades host cells without depending on host uptake pathways (Paing and Tolia, 2014), and parasites are known to have evolved diverse methods to form high avidity complexes for invasion (Wright and Rayner, 2014). There is growing evidence that multimeric assemblies of parasitic ligands and host surface molecules strengthen the host-parasite interactions necessary for invasion (Paing and Tolia, 2014). Sporozoites invade hepatocytes and the invasion complex of CSP and TRAP mediate the invasion process (Wengelnik et al., 1999). Merozoites invade red blood cells facilitated through a series of merozoite surface proteins (MSPs), including MSP complexes (Lin et al., 2016) and the AMA1-RON complex. It was recently shown that vaccination with the AMA1-RON2L protein complex produced protective antibodies providing a novel path for next-generation vaccine candidates against malaria (Srinivasan et al., 2014). Because the only known secretory organelles of ookinetes are micronemes, the microneme-secreted chitinase and its high molecular, chitinase-containing complex are a useful model system for understanding protein secretion mechanisms in *Plasmodium*. Given the recent successes in using the CRISPR/Cas9 system to modify genes in *Plasmodium* (Bansal et al., 2017; Knuepfer et al., 2017; Singer and Frischknecht, 2017; Vanaerschot et al., 2017; Zhang et al., 2017), the present work reveals future experiments to identify the mechanisms involved in protein secretion and secretory organelle formation, particularly in exploring the roles of the invariant cysteines in chitinase complex formation in the ookinete.

The mosquito midgut stages of the parasite are a critical bottleneck in the life cycle of *Plasmodium* (Bennink et al., 2016; Sinden, 2017b). The protein complexes formed at the mosquito malaria parasite stages are largely undetermined compared to the asexual stage protein complexes. Antibodies against zygote and ookinete surface proteins effectively block parasite development within the mosquito midgut (Patra et al., 2015); and these antigens are candidates of transmission blocking vaccine development (Dinglasan and Jacobs-Lorena, 2008; Atkinson et al., 2015; Delrieu et al., 2015; Patra et al., 2015; Brickley et al., 2016; Theisen et al., 2017). The protein complexes that are involved during ookinete invasion of the mosquito midgut are not understood either in terms of structure or precise function. The identification and functional assessment of these protein comprising the high molecular weight complex is important to understand their role played in mosquito midgut invasion. Therefore, novel interventions to interfere with high molecular weight complex formation in *Plasmodium* may arise from understanding the cell biology and biochemistry of novel malaria parasite development within the vector mosquito.

DATA AVAILABILITY STATEMENT

The mass spectrometry proteomics data have been deposited to the ProteomeXchange Consortium via the PRIDE [1] partner repository with the dataset identifier PXD021970; ProteomeXchange: PXD021911; and MassIVE: MSV000086264.

ETHICS STATEMENTS

The animal study was reviewed and approved by Yale University, Leiden University Medical Center, University of California San Diego.

AUTHOR CONTRIBUTIONS

KP, HK, SK designed and carried out experimental work and drafted the manuscript. JG carried out the chitin bead pull-down assays. JW and DG carried out the mass spectrometry of *P. falciparum* chitin pull-down proteins and analysis. HP and JY were responsible for the mass spectrometry of *P. gallinaceum* proteins, and CJ planned the chimeric *P. berghei* experiments and supervised the work. JV designed the experiments, originated and supervised the project, and finalized the manuscript. All authors contributed to the article and approved the submitted version.

FUNDING

This work was supported by grants from the United States Public Health Service, National Institute of Health grants U19AI089681 (JV), AI45999 (JV), and P41 GM103533 (JY). The funders had no role in deciding to publish this work. JW was supported by the UCSD Graduate Training Program in Cellular and Molecular Pharmacology through the National Institute of General Medical Sciences (T32 GM007752) and the UCSD Training Program in Rheumatic Diseases Research through the National Institute of Arthritis and Musculoskeletal and Skin Diseases (T32 AR064194).

ACKNOWLEDGMENTS

We thank Andrew Li for supporting the *P. gallinaceum* and *P. falciparum* ookinete culture and chitin bead pull-down assay and

to Alan Marroquin for help with the *P. berghei* mouse work. We also acknowledge the NIH Shared Instrumentation Grant 1S10OD018034-01 and Yale School of Medicine for the purchase of the Orbitrap Fusion and Q-Exactive Plus mass spectrometer systems. We also thank Florine Collin, Jean Kanyo, and TuKiet Lam from the Yale MS and Proteomics Resource for their help in the mass spectrometry work. Some of the figures were created with BioRender.

SUPPLEMENTARY MATERIAL

The Supplementary Material for this article can be found online at: https://www.frontiersin.org/articles/10.3389/fcimb.2020.615343/full#supplementary-material

SUPPLEMENTARY FIGURE 1 | Chitinase activity of human serum, ookinete media, and method to deplete chitinase activity from media.

SUPPLEMENTARY FIGURE 2 | Size exclusion HPLC fractionation of *Plasmodium gallinaceum* ookinete culture supernatant and analysis of chitinase activity.

SUPPLEMENTARY FIGURE 3 | Silver staining of chitin bead affinity pull-down of *Plasmodium gallinaceum* chitinase complex.

SUPPLEMENTARY FIGURE 4 | Serum containing media used for *P. falciparum* ookinete culture to affinity pull-down the *P. falciparum* chitinase complex.

SUPPLEMENTARY TABLE 1 | List of primers used for generating transgenic *P. berghei* chimeric parasite lines expressing *PfCHT1* and their product sizes.

SUPPLEMENTARY DATA SHEET 1 | Estimation of HMW complex size by using high resolution chromatography and gel filtration standards and Blue Dextran.

SUPPLEMENTARY DATA SHEET 2 | Mass spec data of *P. gallinaceum* chitinase complex chitin bead pull-down from the serum free samples ookinete culture supernatant.

SUPPLEMENTARY DATA SHEET 3 | Mass spec data of *P. falciparum* chitinase complex chitin bead pull-down from the serum free samples ookinete culture supernatant.

SUPPLEMENTARY DATA SHEET 4 | Mass spec data of 1C3 (anti-*PfCHT1* mAb) positive gel bands under reduced and non-reduced conditions.

SUPPLEMENTARY DATA SHEET 5 | Mass spec data of Pb-PfCH1 (r) chitin bead pull-down samples from the samples from ookinete culture supernatant.

REFERENCES

Abraham, E. G., Islam, S., Srinivasan, P., Ghosh, A. K., Valenzuela, J. G., Ribeiro, J. M., et al. (2004). Analysis of the Plasmodium and Anopheles transcriptional repertoire during ookinete development and midgut invasion. *J. Biol. Chem.* 279, 5573–5580. doi: 10.1074/jbc.M307582200

Atkinson, S. C., Armistead, J. S., Mathias, D. K., Sandeu, M. M., Tao, D., Borhani-Dizaji, N., et al. (2015). The Anopheles-midgut APN1 structure reveals a new malaria transmission-blocking vaccine epitope. *Nat. Struct. Mol. Biol.* 22, 532–539. doi: 10.1038/nsmb.3048

Bansal, A., Molina-Cruz, A., Brzostowski, J., Mu, J., and Miller, L. H. (2017). Plasmodium falciparum Calcium-Dependent Protein Kinase 2 Is Critical for Male Gametocyte Exflagellation but Not Essential for Asexual Proliferation. *MBio* 8, 1–17. doi: 10.1128/mBio.01656-17

Bennink, S., Kiesow, M. J., and Pradel, G. (2016). The development of malaria parasites in the mosquito midgut. *Cell Microbiol.* 18, 905–918. doi: 10.1111/cmi.12604

Bounkeua, V., Li, F., and Vinetz, J. M. (2010). In vitro generation of Plasmodium falciparum ookinetes. *Am. J. Trop. Med. Hyg.* 83, 1187–1194. doi: 10.4269/ajtmh.2010.10-0433

Brickley, E. B., Coulibaly, M., Gabriel, E. E., Healy, S. A., Hume, J. C., Sagara, I., et al. (2016). Utilizing direct skin feeding assays for development of vaccines that interrupt malaria transmission: A systematic review of methods and case study. *Vaccine* 34, 5863–5870. doi: 10.1016/j.vaccine.2016.10.027

Cui, L., Mharakurwa, S., Ndiaye, D., Rathod, P. K., and Rosenthal, P. J. (2015). Antimalarial Drug Resistance: Literature Review and Activities and Findings of the ICEMR Network. *Am. J. Trop. Med. Hyg.* 93, 57–68. doi: 10.4269/ajtmh.15-0007

Delrieu, I., Leboulleux, D., Ivinson, K., Gessner, B. D., and Malaria Transmission Blocking Vaccine Technical Consultation, G. (2015). Design of a Phase III cluster randomized trial to assess the efficacy and safety of a malaria transmission blocking vaccine. *Vaccine* 33, 1518–1526. doi: 10.1016/j.vaccine.2015.01.050

Delves, M. J., Angrisano, F., and Blagborough, A. M. (2018). Antimalarial Transmission-Blocking Interventions: Past, Present, and Future. *Trends Parasitol.* 34, 735–746. doi: 10.1016/j.pt.2018.07.001

Delves, M., Lafuente-Monasterio, M. J., Upton, L., Ruecker, A., Leroy, D., Gamo, F. J., et al. (2019). Fueling Open Innovation for Malaria Transmission-Blocking Drugs: Hundreds of Molecules Targeting Early Parasite Mosquito Stages. *Front. Microbiol.* 10, 1–10. doi: 10.3389/fmicb.2019.02134

Dessens, J. T., Mendoza, J., Claudianos, C., Vinetz, J. M., Khater, E., Hassard, S., et al. (2001). Knockout of the rodent malaria parasite chitinase pbCHT1 reduces infectivity to mosquitoes. *Infect. Immun.* 69, 4041–4047. doi: 10.1128/IAI.69.6.4041-4047.2001

Dessens, J. T., Siden-Kiamos, I., Mendoza, J., Mahairaki, V., Khater, E., Vlachou, D., et al. (2003). SOAP, a novel malaria ookinete protein involved in mosquito midgut invasion and oocyst development. *Mol. Microbiol.* 49, 319–329. doi: 10.1046/j.1365-2958.2003.03566.x

Dinglasan, R. R., and Jacobs-Lorena, M. (2008). Flipping the paradigm on malaria transmission-blocking vaccines. *Trends Parasitol.* 24, 364–370. doi: 10.1016/j.pt.2008.05.002

Dinglasan, R. R., Alaganan, A., Ghosh, A. K., Saito, A., Van Kuppevelt, T. H., and Jacobs-Lorena, M. (2007a). Plasmodium falciparum ookinetes require mosquito midgut chondroitin sulfate proteoglycans for cell invasion. *Proc. Natl. Acad. Sci. U.S.A.* 104, 15882–15887. doi: 10.1073/pnas.0706340104

Dinglasan, R. R., Kalume, D. E., Kanzok, S. M., Ghosh, A. K., Muratova, O., Pandey, A., et al. (2007b). Disruption of Plasmodium falciparum development by antibodies against a conserved mosquito midgut antigen. *Proc. Natl. Acad. Sci. U.S.A.* 104, 13461–13466. doi: 10.1073/pnas.0702239104

Duffy, P. E., and Patrick Gorres, J. (2020). Malaria vaccines since 2000: progress, priorities, products. *NPJ Vaccines* 5, 48. doi: 10.1038/s41541-020-0196-3

Eng, J. K., Mccormack, A. L., and Yates, J. R. (1994). An approach to correlate tandem mass spectral data of peptides with amino acid sequences in a protein database. *J. Am. Soc. Mass Spectrom.* 5, 976–989. doi: 10.1016/1044-0305(94)80016-2

Espinosa, D. A., Vega-Rodriguez, J., Flores-Garcia, Y., Noe, A. R., Munoz, C., Coleman, R., et al. (2017). The Plasmodium falciparum Cell-Traversal Protein for Ookinetes and Sporozoites as a Candidate for Preerythrocytic and Transmission-Blocking Vaccines. *Infect. Immun.* 85, 1–10. doi: 10.1128/IAI.00498-16

Ghosh, A. K., Dinglasan, R. R., Ikadai, H., and Jacobs-Lorena, M. (2010). An improved method for the in vitro differentiation of Plasmodium falciparum gametocytes into ookinetes. *Malar. J.* 9, 194. doi: 10.1186/1475-2875-9-194

Ghosh, A. K., Coppens, I., Gardsvoll, H., Ploug, M., and Jacobs-Lorena, M. (2011). Plasmodium ookinetes coopt mammalian plasminogen to invade the mosquito midgut. *Proc. Natl. Acad. Sci. U.S.A.* 108, 17153–17158. doi: 10.1073/pnas.1103657108

Ghosh, D., Egbuta, C., Kanyo, J. E., and Lam, T. T. (2019). Phosphorylation of human placental aromatase CYP19A1. *Biochem. J.* 476, 3313–3331. doi: 10.1042/BCJ20190633

Giersing, B. K., Vekemans, J., Nava, S., Kaslow, D. C., Moorthy, V., and Committee, W. H. O. P. D. F. V. A. (2019). Report from the World Health Organization's third Product Development for Vaccines Advisory Committee (PDVAC) meeting, Geneva, 8-10th June 2016. *Vaccine* 37, 7315–7327. doi: 10.1016/j.vaccine.2016.10.090

Greenwood, B. (2017). New tools for malaria control - using them wisely. *J. Infect.* 74 Suppl 1, S23–S26. doi: 10.1016/S0163-4453(17)30187-1

Hirosawa, M., Hoshida, M., Ishikawa, M., and Toya, T. (1993). MASCOT: multiple alignment system for protein sequences based on three-way dynamic programming. *Comput. Appl. Biosci.* 9, 161–167. doi: 10.1093/bioinformatics/9.2.161

Huber, M., Cabib, E., and Miller, L. H. (1991). Malaria parasite chitinase and penetration of the mosquito peritrophic membrane. *Proc. Natl. Acad. Sci. U.S.A.* 88, 2807–2810. doi: 10.1073/pnas.88.7.2807

Janse, C. J., and Waters, A. P. (1995). Plasmodium berghei: the application of cultivation and purification techniques to molecular studies of malaria parasites. *Parasitol. Today* 11, 138–143. doi: 10.1016/0169-4758(95)80133-2

Janse, C. J., Mons, B., Rouwenhorst, R. J., Van Der Klooster, P. F., Overdulve, J. P., and Van Der Kaay, H. J. (1985). In vitro formation of ookinetes and functional maturity of Plasmodium berghei gametocytes. *Parasitology* 91 (Pt 1), 19–29. doi: 10.1017/S0031182000056481

Janse, C. J., Ramesar, J., and Waters, A. P. (2006). High-efficiency transfection and drug selection of genetically transformed blood stages of the rodent malaria parasite Plasmodium berghei. *Nat. Protoc.* 1, 346–356. doi: 10.1038/nprot.2006.53

Knuepfer, E., Napiorkowska, M., Van Ooij, C., and Holder, A. A. (2017). Generating conditional gene knockouts in Plasmodium - a toolkit to produce stable DiCre recombinase-expressing parasite lines using CRISPR/Cas9. *Sci. Rep.* 7, 1–12. doi: 10.1038/s41598-017-03984-3

Langer, R. C., and Vinetz, J. M. (2001). Plasmodium ookinete-secreted chitinase and parasite penetration of the mosquito peritrophic matrix. *Trends Parasitol.* 17, 269–272. doi: 10.1016/S1471-4922(01)01918-3

Langer, R. C., Hayward, R. E., Tsuboi, T., Tachibana, M., Torii, M., and Vinetz, J. M. (2000). Micronemal transport of Plasmodium ookinete chitinases to the electron-dense area of the apical complex for extracellular secretion. *Infect. Immun.* 68, 6461–6465. doi: 10.1128/IAI.68.11.6461-6465.2000

Langer, R. C., Li, F., Popov, V., Kurosky, A., and Vinetz, J. M. (2002a). Monoclonal antibody against the Plasmodium falciparum chitinase, PfCHT1, recognizes a malaria transmission-blocking epitope in Plasmodium gallinaceum ookinetes unrelated to the chitinase PgCHT1. *Infect. Immun.* 70, 1581–1590. doi: 10.1128/IAI.70.3.1581-1590.2002

Langer, R. C., Li, F., and Vinetz, J. M. (2002b). Identification of novel Plasmodium gallinaceum zygote- and ookinete-expressed proteins as targets for blocking malaria transmission. *Infect. Immun.* 70, 102–106. doi: 10.1128/IAI.70.1.102-106.2002

Li, F., Templeton, T. J., Popov, V., Comer, J. E., Tsuboi, T., Torii, M., et al. (2004). Plasmodium ookinete-secreted proteins secreted through a common micronemal pathway are targets of blocking malaria transmission. *J. Biol. Chem.* 279, 26635–26644. doi: 10.1074/jbc.M401385200

Li, F., Patra, K. P., and Vinetz, J. M. (2005). An anti-Chitinase malaria transmission-blocking single-chain antibody as an effector molecule for creating a Plasmodium falciparum-refractory mosquito. *J. Infect. Dis.* 192, 878–887. doi: 10.1086/432552

Li, F., Patra, K. P., Yowell, C. A., Dame, J. B., Chin, K., and Vinetz, J. M. (2010). Apical Surface Expression of Aspartic Protease Plasmepsin 4, a Potential Transmission-blocking Target of the *Plasmodium* Ookinete. *J. Biol. Chem.* 285, 8076–8083. doi: 10.1074/jbc.M109.063388

Lin, J. W., Annoura, T., Sajid, M., Chevalley-Maurel, S., Ramesar, J., Klop, O., et al. (2011). A novel 'gene insertion/marker out' (GIMO) method for transgene expression and gene complementation in rodent malaria parasites. *PLoS One* 6, e29289. doi: 10.1371/journal.pone.0029289

Lin, C. S., Uboldi, A. D., Epp, C., Bujard, H., Tsuboi, T., Czabotar, P. E., et al. (2016). Multiple Plasmodium falciparum Merozoite Surface Protein 1 Complexes Mediate Merozoite Binding to Human Erythrocytes. *J. Biol. Chem.* 291, 7703–7715. doi: 10.1074/jbc.M115.698282

Mahmoudi, S., and Keshavarz, H. (2017). Efficacy of phase 3 trial of RTS, S/AS01 malaria vaccine: The need for an alternative development plan. *Hum. Vaccin. Immunother.* 13 (9), 2098–2101. doi: 10.1080/21645515.2017.1295906

Mlambo, G., Maciel, J., and Kumar, N. (2008). Murine model for assessment of Plasmodium falciparum transmission-blocking vaccine using transgenic Plasmodium berghei parasites expressing the target antigen Pfs25. *Infect. Immun.* 76, 2018–2024. doi: 10.1128/IAI.01409-07

Murray, C. J., Rosenfeld, L. C., Lim, S. S., Andrews, K. G., Foreman, K. J., Haring, D., et al. (2012). Global malaria mortality between 1980 and 2010: a systematic analysis. *Lancet* 379, 413–431. doi: 10.1016/S0140-6736(12)60034-8

Ohno, H., Blackwell, J., Jamieson, A. M., Carrino, D. A., and Caplan, A. I. (1986). Calibration of the relative molecular mass of proteoglycan subunit by column chromatography on Sepharose CL-2B. *Biochem. J.* 235, 553–557. doi: 10.1042/bj2350553

Othman, A. S., Franke-Fayard, B. M., Imai, T., Van Der Gracht, E. T. I., Redeker, A., Salman, A. M., et al. (2018). OX40 Stimulation Enhances Protective Immune Responses Induced After Vaccination With Attenuated Malaria Parasites. *Front. Cell Infect. Microbiol.* 8, 247. doi: 10.3389/fcimb.2018.00247

Paing, M. M., and Tolia, N. H. (2014). Multimeric assembly of host-pathogen adhesion complexes involved in apicomplexan invasion. *PLoS Pathog.* 10, e1004120. doi: 10.1371/journal.ppat.1004120

Patra, K. P., and Vinetz, J. M. (2012). New ultrastructural analysis of the invasive apparatus of the Plasmodium ookinete. *Am. J. Trop. Med. Hyg.* 87, 412–417. doi: 10.4269/ajtmh.2012.11-0609

Patra, K. P., Johnson, J. R., Cantin, G. T., Yates, J. R.,. 3., and Vinetz, J. M. (2008). Proteomic analysis of zygote and ookinete stages of the avian malaria parasite Plasmodium gallinaceum delineates the homologous proteomes of the lethal human malaria parasite Plasmodium falciparum. *Proteomics* 8, 2492–2499. doi: 10.1002/pmic.200700727

Patra, K. P., Li, F., Carter, D., Gregory, J. A., Baga, S., Reed, S. G., et al. (2015). Alga-produced malaria transmission-blocking vaccine candidate Pfs25 formulated with a human use-compatible potent adjuvant induces high-affinity antibodies that block Plasmodium falciparum infection of mosquitoes. *Infect. Immun.* 83, 1799–1808. doi: 10.1128/IAI.02980-14

Perez-Riverol, Y., Csordas, A., Bai, J., Bernal-Llinares, M., Hewapathirana, S., Kundu, D. J., et al. (2019). The PRIDE database and related tools and resources in 2019: improving support for quantification data. *Nucleic Acids Res.* 47, D442–D450. doi: 10.1093/nar/gky1106

Ramakrishnan, C., Dessens, J. T., Armson, R., Pinto, S. B., Talman, A. M., Blagborough, A. M., et al. (2011). Vital functions of the malarial ookinete protein, CTRP, reside in the A domains. *Int. J. Parasitol.* 41, 1029–1039. doi: 10.1016/j.ijpara.2011.05.007

Salman, A. M., Mogollon, C. M., Lin, J. W., Van Pul, F. J., Janse, C. J., and Khan, S. M. (2015). Generation of Transgenic Rodent Malaria Parasites Expressing Human Malaria Parasite Proteins. *Methods Mol. Biol.* 1325, 257–286. doi: 10.1007/978-1-4939-2815-6_21

Shahabuddin, M., and Vinetz, J. M. (1999). Chitinases of human parasites and their implications as antiparasitic targets. *EXS* 87, 223–234. doi: 10.1007/978-3-0348-8757-1_16

Shahabuddin, M., Toyoshima, T., Aikawa, M., and Kaslow, D. C. (1993). Transmission-blocking activity of a chitinase inhibitor and activation of malarial parasite chitinase by mosquito protease. *Proc. Natl. Acad. Sci. U.S.A.* 90, 4266–4270. doi: 10.1073/pnas.90.9.4266

Shen, Z., and Jacobs-Lorena, M. (1998). A type I peritrophic matrix protein from the malaria vector Anopheles gambiae binds to chitin. Cloning, expression, and characterization. *J. Biol. Chem.* 273, 17665–17670. doi: 10.1074/jbc.273.28.17665

Sieber, K. P., Huber, M., Kaslow, D., Banks, S. M., Torii, M., Aikawa, M., et al. (1991). The peritrophic membrane as a barrier: its penetration by Plasmodium gallinaceum and the effect of a monoclonal antibody to ookinetes. *Exp. Parasitol.* 72, 145–156. doi: 10.1016/0014-4894(91)90132-G

Sinden, R. (1997). "Infection of mosquitoes with rodent malaria," in *The molecular biology of insect disease vectors*. Eds. J. M. B.C.B. Crampton and C. Louis (Dordrecht: Springer), 67–91. doi: 10.1007/978-94-009-1535-0_7

Sinden, R. E. (2015). The cell biology of malaria infection of mosquito: advances and opportunities. *Cell Microbiol.* 17, 451–466. doi: 10.1111/cmi.12413

Sinden, R. E. (2017a). Developing transmission-blocking strategies for malaria control. *PLoS Pathog.* 13, e1006336. doi: 10.1371/journal.ppat.1006336

Sinden, R. E. (2017b). Targeting the Parasite to Suppress Malaria Transmission. *Adv. Parasitol.* 97, 147–185. doi: 10.1016/bs.apar.2016.09.004

Singer, M., and Frischknecht, F. (2017). Time for Genome Editing: Next-Generation Attenuated Malaria Parasites. *Trends Parasitol.* 33, 202–213. doi: 10.1016/j.pt.2016.09.012

Srinivasan, P., Ekanem, E., Diouf, A., Tonkin, M. L., Miura, K., Boulanger, M. J., et al. (2014). Immunization with a functional protein complex required for erythrocyte invasion protects against lethal malaria. *Proc. Natl. Acad. Sci. U.S.A.* 111, 10311–10316. doi: 10.1073/pnas.1409928111

Takeo, S., Hisamori, D., Matsuda, S., Vinetz, J., Sattabongkot, J., and Tsuboi, T. (2009). Enzymatic characterization of the Plasmodium vivax chitinase, a

potential malaria transmission-blocking target. *Parasitol. Int.* 58, 243–248. doi: 10.1016/j.parint.2009.05.002

Theisen, M., Jore, M. M., and Sauerwein, R. (2017). Towards clinical development of a Pfs48/45-based transmission blocking malaria vaccine. *Expert Rev. Vaccines* 16, 329–336. doi: 10.1080/14760584.2017.1276833

Tsuboi, T., Kaneko, O., Eitoku, C., Suwanabun, N., Sattabongkot, J., Vinetz, J. M., et al. (2003). Gene structure and ookinete expression of the chitinase genes of Plasmodium vivax and Plasmodium yoelii. *Mol. Biochem. Parasitol.* 130, 51–54. doi: 10.1016/S0166-6851(03)00140-3

Vanaerschot, M., Lucantoni, L., Li, T., Combrinck, J. M., Ruecker, A., Kumar, T. R. S., et al. (2017). Hexahydroquinolines are antimalarial candidates with potent blood-stage and transmission-blocking activity. *Nat. Microbiol.* 2, 1403–1414. doi: 10.1038/s41564-017-0007-4

Viebig, N. K., D'alessio, F., Draper, S. J., Sim, B. K., Mordmuller, B., Bowyer, P. W., et al. (2015). Workshop report: Malaria vaccine development in Europe-preparing for the future. *Vaccine* 33 (2015), 6137–44. doi: 10.1016/j.vaccine.2015.09.074

Vinetz, J. M., and Kaslow, D. C. (1998). Plasmodium gallinaceum: use of antisera to degenerate synthetic peptides derived from the active site of protozoal chitinases to characterize an ookinete-specific chitinase. *Exp. Parasitol.* 90, 199–202. doi: 10.1006/expr.1998.4322

Vinetz, J. M., Dave, S. K., Specht, C. A., Brameld, K. A., Xu, B., Hayward, R., et al. (1999). The chitinase PfCHT1 from the human malaria parasite Plasmodium falciparum lacks proenzyme and chitin-binding domains and displays unique substrate preferences. *Proc. Natl. Acad. Sci. U.S.A.* 96, 14061–14066. doi: 10.1073/pnas.96.24.14061

Vinetz, J. M., Valenzuela, J. G., Specht, C. A., Aravind, L., Langer, R. C., Ribeiro, J. M., et al. (2000). Chitinases of the avian malaria parasite Plasmodium gallinaceum, a class of enzymes necessary for parasite invasion of the mosquito midgut. *J. Biol. Chem.* 275, 10331–10341. doi: 10.1074/jbc.275.14.10331

Vinetz, J. M. (2005). Plasmodium ookinete invasion of the mosquito midgut. *Curr. Top. Microbiol. Immunol.* 295, 357–382. doi: 10.1007/3-540-29088-5_14

Wengelnik, K., Spaccapelo, R., Naitza, S., Robson, K. J., Janse, C. J., Bistoni, F., et al. (1999). The A-domain and the thrombospondin-related motif of Plasmodium falciparum TRAP are implicated in the invasion process of mosquito salivary glands. *EMBO J.* 18, 5195–5204. doi: 10.1093/emboj/18.19.5195

Wright, G. J., and Rayner, J. C. (2014). Plasmodium falciparum erythrocyte invasion: combining function with immune evasion. *PLoS Pathog.* 10, e1003943. doi: 10.1371/journal.ppat.1003943

Zhang, C., Gao, H., Yang, Z., Jiang, Y., Li, Z., Wang, X., et al. (2017). CRISPR/Cas9 mediated sequential editing of genes critical for ookinete motility in Plasmodium yoelii. *Mol. Biochem. Parasitol.* 212, 1–8. doi: 10.1016/j.molbiopara.2016.12.010

Conflict of Interest: The authors declare that the research was conducted in the absence of any commercial or financial relationships that could be construed as a potential conflict of interest.

frontiers in Cellular and Infection Microbiology

REVIEW
published: 11 January 2021
doi: 10.3389/fcimb.2020.614701

From Initiators to Effectors: Roadmap Through the Intestine During Encounter of *Toxoplasma gondii* With the Mucosal Immune System

Lindsay M. Snyder * *and Eric Y. Denkers* *

Center for Evolutionary and Theoretical Immunology and Department of Biology, University of New Mexico, Albuquerque, NM, United States

OPEN ACCESS

Edited by:
Nicholas Charles Smith, University of Technology Sydney, Australia

Reviewed by:
Carsten Lüder, Universitätsmedizin Göttingen, Germany
Glenn McConkey, University of Leeds, United Kingdom
Sarah Ewald, University of Virginia, United States

***Correspondence:**
Lindsay M. Snyder
lmsnyder@unm.edu
Eric Y. Denkers
edenkers@unm.edu

Specialty section:
This article was submitted to Parasite and Host, a section of the journal Frontiers in Cellular and Infection Microbiology

Received: *06 October 2020*
Accepted: *24 November 2020*
Published: *11 January 2021*

Citation:
Snyder LM and Denkers EY (2021) From Initiators to Effectors: Roadmap Through the Intestine During Encounter of Toxoplasma gondii With the Mucosal Immune System. Front. Cell. Infect. Microbiol. 10:614701. doi: 10.3389/fcimb.2020.614701

The gastrointestinal tract is a major portal of entry for many pathogens, including the protozoan parasite *Toxoplasma gondii*. Billions of people worldwide have acquired *T. gondii* at some point in their life, and for the vast majority this has led to latent infection in the central nervous system. The first line of host defense against *Toxoplasma* is located within the intestinal mucosa. Appropriate coordination of responses by the intestinal epithelium, intraepithelial lymphocytes, and lamina propria cells results in an inflammatory response that controls acute infection. Under some conditions, infection elicits bacterial dysbiosis and immune-mediated tissue damage in the intestine. Here, we discuss the complex interactions between the microbiota, the epithelium, as well as innate and adaptive immune cells in the intestinal mucosa that induce protective immunity, and that sometimes switch to inflammatory pathology as *T. gondii* encounters tissues of the gut.

Keywords: *Toxoplasma gondii*, mucosal immunity, protective immunity, immunopathology, adaptive immunity, innate immunity

TOXOPLASMA GONDII LIFE CYCLE

Toxoplasma gondii is a globally distributed microorganism whose host range includes humans, domestic animals, and wildlife. The parasite is a life-threatening risk in immunocompromised individuals and a potential cause of abortion and birth defects following congenital transmission (Pfaff et al., 2007; McLeod et al., 2013). Infection is initiated in the small intestine. The parasites disseminate through the host as tachyzoites, infecting and proliferating in numerous cell types. This is followed by chronic, or latent infection, which is associated with formation of cysts containing the bradyzoite parasite form in muscle tissue and the central nervous system. *Toxoplasma* undergoes sexual reproduction in the gastrointestinal tract, but only in felines. The reason for this selectivity was a mystery until recently. Now it appears that unique aspects of lipid metabolism in cats results in unusually high systemic levels of linoleic acid that somehow signals parasite gametogenesis (Martorelli Di Genova et al., 2019). This is due to lack of intestinal delta-6-desaturase activity that is required for linoleic acid metabolism. Ingestion of oocysts (the environmentally resistant products of *Toxoplasma* sexual reproduction) shed in cat feces, as well as direct carnivorism of cysts within muscle tissue helps account for the widespread distribution of *T. gondii*.

THE MILLENIAL PARASITE

Discovered in 1908, *Toxoplasma* remained a relatively obscure parasite for most of the 20th century. In large part, this was due to the asymptomatic nature of chronic infection (Dubey, 2013). With the emergence of the AIDS pandemic in the 1980s, the parasite gained widespread recognition as an opportunistic pathogen, and modern day research on *Toxoplasma* was born (McCabe and Remington, 1988). The ease of maintaining the *Toxoplasma* life cycle in the laboratory, the ability to do classical and molecular genetics on the parasite, and the rise in mouse gene knockout technology all came together to ignite an explosion in our understanding of the *Toxoplasma*–host interaction that continues to this day (Weiss and Kim, 2014).

Toxoplasma was one of the first microbial pathogens recognized for its ability to induce a highly polarized Th1 response that is essential for immune protection (Sher and Coffman, 1992; Denkers and Gazzinelli, 1998; Dupont et al., 2012). The parasite also played a prominent role in revealing the significance of IL-12 in triggering Th1 immunity, and conversely the key role of IL-10 in preventing these proinflammatory responses from becoming pathological (Gazzinelli et al., 1994; Gazzinelli et al., 1996). *T. gondii* was the first eukaryotic pathogen for which the importance of TLR-MyD88 signaling in immune initiation was recognized (Scanga et al., 2002; Gazzinelli and Denkers, 2006). The parasite is also a prime and possibly sole example of how an intracellular protozoan pathogen manipulates immunity through injection of host-directed effector proteins contained within parasite secretory organelles (Denkers et al., 2012; Hunter and Sibley, 2012).

The focus of this review is to assess our current state of knowledge with regard to interactions of *Toxoplasma* and the host intestinal mucosa. As the site of entry, this tissue is where the parasite establishes a foothold within the host and where it first encounters the immune system. The initial interactions occurring here are likely to determine the course of infection as the parasite spreads through the body and eventually establishes latency in the central nervous system.

OVERVIEW OF *TOXOPLASMA* IN THE INTESTINE

Establishing a Foothold: Entry, Dissemination

The earliest events in establishment of *Toxoplasma* infection in the intestine are among the most crucial in determining the outcome of this host–parasite interaction, yet they are at the same time among the most difficult to study and consequently the least well understood. Use of low dose inocula that likely represent typical natural infection pushes the limits of detection, while employing artificially high infectious doses may yield results prone to artifact. Nevertheless, with current highly sensitive imaging techniques such as two-photon microscopy of living tissues, we are gaining insight into how *Toxoplasma* establishes an early foothold in its host (Luu and Coombes, 2015).

As *T. gondii* excysts from tissue cysts or oocysts in the lumen of the gut, parasites are faced with the challenge of crossing the intestinal epithelium, a barrier specialized to keep microbes out of the underlying lamina propria. The current view is that this is achieved through multiple pathways. *Toxoplasma* carries its own toolbox for cell invasion, including proteins contained within secretory granules called rhoptries and micronemes. Mechanical force for cell invasion is supplied by a parasite actin-myosin based motor. Thus, the parasite is equipped to directly enter virtually any cell type, including epithelial cells. Indeed, replicating parasites can be observed in the intestinal epithelium during early infection (Speer and Dubey, 1998). Epithelial monolayer cultures are also readily infected by tachyzoites (Briceno et al., 2016). In the intestine, rupture of these cells during the parasite lytic cycle can be expected to release tachyzoites into the underlying lamina propria. It is likely that under high infectious parasite inocula, lytic epithelial tissue destruction also enables luminal bacterial translocation triggering inflammatory gut pathology that may emerge during *Toxoplasma* infection (Heimesaat et al., 2006; Craven et al., 2012; Molloy et al., 2013).

Tachyzoites can also breach the intestinal barrier using a mechanism of transepithelial migration involving passage of the parasite between adjacent epithelial cells (**Figure 1**). Movement of *Toxoplasma* in this manner does not compromise the integrity of the epithelial barrier. Paracellular migration is linked to parasite genotype, with virulent Type I strains possessing greater ability to transmigrate than less virulent Type II and III strains (Barragan and Sibley, 2002; Barragan and Sibley, 2003). Binding between intercellular adhesion molecule (ICAM)-1 and the *Toxoplasma* microneme protein MIC2 appears to mediate this process. It has also been observed that tachyzoites co-localize with the tight junction protein occludin, which appears to facilitate paracellular transmigration of the parasite (Barragan et al., 2005; Weight and Carding, 2012). Recent data suggest that paracellular migration is facilitated by parasite secretory proteases that target tight junction proteins ZO-1, occludin, and claudin-1 (Ramirez-Flores et al., 2020).

Use of 2-photon laser scanning microscopy has more recently revealed a novel and unexpected form of *Toxoplasma* entry and spread through the intestinal mucosa. Thus, infection elicits a retrograde migration response in which large numbers of neutrophils move into the intestinal lumen. Here, or possibly in the lamina propria prior to migration, neutrophils are infected by *Toxoplasma* and they appear to subsequently establish new foci of infection throughout the intestine (Coombes et al., 2013). This may contribute to the patchiness of infection centers that are observed in the gut following oral inoculation of *Toxoplasma* (**Figure 1**).

Within a few days of infection, *T. gondii* has breached the epithelial layer and is present within the lamina propria where interactions with cells of the immune system commence in earnest. IL-12-producing mucosal dendritic cells can serve as hosts for replicating parasites (Cohen and Denkers, 2015).

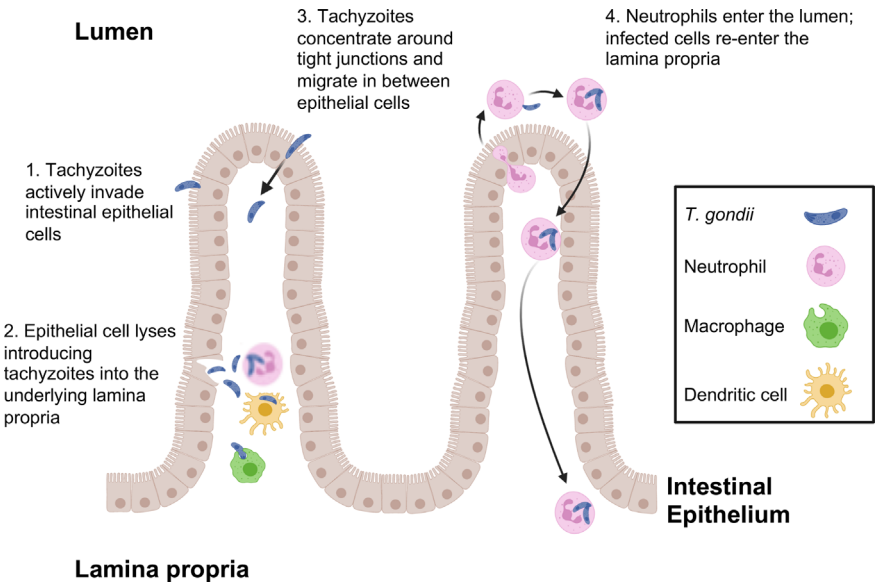

FIGURE 1 | *T. gondii* pathways for crossing the intestinal epithelial barrier and early encounters with the immune system during infection. Tachyzoites cross the intestinal barrier through (1) direct invasion of intestinal epithelial cells followed by (2) cell lysis and release of parasites into the lamina propria where macrophages, dendritic cells and neutrophils are the predominant infected cell types. (3) Parasites also display the property of paracellular migration from the intestinal lumen into the lamina propria. Infection also triggers transepithelial migration of neutrophils into the intestinal lumen (4). Neutrophils in the intestine are infected, then re-enter the lamina propria at a different location. This phenomenon may account for the patchy foci of parasites that often characterize infection in the intestine.

However, the major host cells at this location appear to be neutrophils, macrophages, and inflammatory monocytes (Gregg et al., 2013). Using the cells as Trojan horses, or possibly moving as extracellular tachyzoites, parasites begin to leave the lamina propria and disseminate throughout host tissues concurrent with the rise in adaptive immunity (Courret et al., 2006).

Parasite Molecules That Trigger Innate Immunity: View From the Intestine

The well-known ability of *Toxoplasma* to supply a strong signal for Th1 immunity early on started a search for parasite molecules that trigger IL-12—a pursuit that continues to this day. The parasite invasion-associated protein profilin fulfills the criteria for a bona fide pathogen-associated molecular pattern (PAMP) and is recognized by Toll-like receptors (TLR) 11 and 12 (Yarovinsky et al., 2005; Kucera et al., 2010; Koblansky et al., 2012; Raetz et al., 2013a). While most studies on the influence of these TLR during *Toxoplasma* infection have been carried out in intraperitoneal inoculation models, it is also clear that profilin-TLR11 interactions are important in innate immune responses within the intestinal mucosa. Thus, there is a partial defect in generation of lamina propria Th1 cells and a partial increase in susceptibility in the absence of TLR11 (Benson et al., 2009). Parasite-induced disappearance of Paneth cells triggered by Th1 cells is also dependent upon signaling through TLR11 (Raetz et al., 2013b). Nevertheless, because humans and many other hosts of *Toxoplasma* express neither TLR11 nor TLR12, it is unlikely that profilin functions as a universal PAMP for all species the parasite infects (Gazzinelli et al., 2014). Other TLR could also be involved, although distinguishing microbiota versus parasite-driven TLR activation is a complex matter.

The dense granule protein GRA15 is a polymorphic parasite effector molecule involved in activation of NFκB from within the infected cell (Rosowski et al., 2011). In host macrophages this leads to acquisition of an M1 phenotype, including production of IL-12 (Jensen et al., 2011). Of the three major parasite strains that predominate in Europe and North America (Types I, II and III), only the Type II strain expresses active GRA15 (Rosowski et al., 2011). During oral infection, deletion of GRA15 alone does not influence mouse susceptibility or parasite replication. However, in the context of Type I ROP16, a secretory parasite kinase that activates STAT3, 5 and 6 and promotes an anti-inflammatory M2 macrophage phenotype, deletion of $GRA15_{II}$ increases parasite number and inflammation in the intestine (Jensen et al., 2013). Thus, active GRA15 most likely exerts effects on innate immune effectors in the intestine through its ability to commandeer NFκB signaling in infected cells.

Another dense granule protein that can induce IL-12 is GRA24. This molecule is inserted into the host cytoplasm where it triggers autoactivation of mitogen activated protein kinase p38 leading to increased IL-12 gene transcription (Kim et al., 2005; Braun et al., 2013; Mercer et al., 2020; Mukhopadhyay et al., 2020). While GRA24 can drive a protective immune response in an intraperitoneal vaccination model, its role in infection of the intestinal mucosa is not yet known.

Inflammasomes have recently attracted a great deal of attention as cytoplasmic sensors of infection. This is particularly true for

intracellular protozoan parasites (Zamboni and Lima-Junior, 2015; de Carvalho and Zamboni, 2020). For the case of *Toxoplasma*, inflammasome components NLRP1 and NLRP3 respond to infection resulting in IL-1β and IL-18 release, in turn promoting resistance to infection (Witola et al., 2011; Ewald et al., 2014; Gorfu et al., 2014). As yet unresolved are findings of others indicating that inflammasome activation only emerges as a significant factor in the absence of TLR11 signaling (Lopez-Yglesias et al., 2019). The parasite secretory molecule $GRA15_{II}$ has been implicated in IL-1β and IL-18 production, although whether this is due to inflammasome assembly or NFκB-dependent induction of pro-IL-1β and pro-IL-18 is not clear (Gov et al., 2013). Rat macrophage pyroptosis, diagnostic of inflammasome activation, was recently found to be dependent upon GRA35, 42 and 43 (Wang Y. et al., 2019). Along parallel lines, *T. gondii*-triggered potassium efflux can act as a signal for IL-1β release, suggesting that it may drive inflammasome assembly as is known to occur in other situations (Gov et al., 2017). An increase in susceptibility was reported during oral infection of caspase1/11 knockout mice suggesting inflammasome involvement (Ewald et al., 2014). In human intestinal epithelial cells, *Toxoplasma* infection resulted in NLRP3-dependent IL-1β release that was mediated through the ATP receptor P2X7 (Quan et al., 2018). Finally, it was reported that IL-1R knockout mice display increased Paneth cell depletion associated with *T. gondii* infection, further implicating inflammasome activation (Villeret et al., 2013). The role of inflammasome activation in detecting infection in the intestinal mucosa, as well as downstream inflammation and immunity requires further attention.

Recently, the alarmin S100A11 was identified as a host molecule that triggers early immune responses in human monocytes (Safronova et al., 2019). It was also found to promote monocyte recruitment during oral infection in mice, likely through the chemokine CCL2. The S100A1 protein may function as a damage associated molecular pattern molecule released by infected cells with an important function in initiation of immunity. Rather than directly triggering IL-12 production and Th1 response initiation, this alarmin is more likely to be involved in immune recruitment during early infection. The PAMPs and DAMPs currently believed to be involved in the response to *Toxoplasma* in the gut mucosa are shown in **Table 1**.

Intestinal Microbiota Influences Progression of Infection

Infection with *T. gondii* can result in an effective protective Th1 immune response or in fulminant and ultimately lethal inflammatory tissue destruction in the small intestine. Genetics and infectious dose play important roles in determining these polar outcomes (Liesenfeld et al., 1996; Liesenfeld et al., 1999). We now also understand that the gut microflora strongly influences each of these divergent responses.

Typically, the intestine is regarded as a location of continual, low intensity skirmishes between the immune system and normal microbiota, while overall the immune system remains tolerant to gut microbes (Sansonetti, 2011; Kayama and Takeda, 2012; Nutsch and Hsieh, 2012). *Toxoplasma* breaks this tolerance, insofar as oral infection stimulates a Th1 response to bacterial flagellin (Hand et al., 2012). Remarkably, the microbiota-specific T cells emerging during *T. gondii* infection are comparable in number to parasite-specific T cells in the intestinal mucosa. While the trigger for the breach in tolerance is not known, it may be a downstream effect of loss of Paneth cells, a rich source of antimicrobial peptides, that is driven by *Toxoplasma* infection (Raetz et al., 2013b; Burger et al., 2018).

Other studies have revealed that the intestinal microbiota exerts an important adjuvant-like effect on development of *Toxoplasma*-specific immunity. Thus, in the absence of TLR11, IL-12 and parasite-specific Th1 responses are retained—unlike the immune response following intraperitoneal parasite inoculation which is highly TLR11-dependent (Benson et al., 2009). Importantly, depletion of microflora with antibiotics abrogates this TLR11-independent response in the gut and there is a concomitant increase in susceptibility to *Toxoplasma*. The mucosal response occurring in the absence of TLR11 appears to involve the combination of TLR2, 4 and 9, receptors well known to recognize bacterial ligands. While each of these TLRs signals through the MyD88 molecule, it is known that in the absence of this signaling adaptor, Th1 responses while diminished are still retained

TABLE 1 | Pathogen-associated molecular pattern molecules and host danger-associated molecular pattern molecules that play a role in anti-*Toxoplasma* immunity in the gut.

PAMP/DAMP	Receptor	Downstream Function	References
Profilin	TLR11/12	Activation of DC, macrophages, and neutrophils triggering IL-12 production	(Yarovinsky and Sher, 2006; Kucera et al., 2010; Koblansky et al., 2012; Raetz et al., 2013a)
Commensal-derived molecules	TLR2	IL-12 production and enhanced type I immunity	(Benson et al., 2009)
Bacterial flagellin	TLR5	Flagellin specific CD4+ T cells that contribute to anti-*Toxoplasma* type I immunity	(Hand et al., 2012)
Commensal-derived molecules (LPS)	TLR4	Enhanced IL-12 and IFN-γ production	(Benson et al., 2009)
CpG	TLR9	Enhanced type I immunity and reduced systemic parasite burdens	(Minns et al., 2006; Benson et al., 2009)
ATP	P2X7	NLRP1, NLRP3, NLRC4 and AIM2 inflammasome activation and IFN-β production	(Quan et al., 2018)
S100A11	RAGE	Induction of CCL2 and recruitment of inflammatory monocytes	(Safronova et al., 2019)

(Sukhumavasi et al., 2008). Clearly there are other MyD88-independent pathways in the mucosal immune system that await discovery.

We also understand that perturbations in intestinal microflora play a key role in inflammatory tissue damage associated with high dose *T. gondii* infection. Similar trends in microbial dysbiosis have been observed in Crohn's disease patients (Egan et al., 2011a; Vester-Andersen et al., 2019). After peroral infection with *Toxoplasma*, mice exhibit decreased microbial diversity, outgrowth of γ-Proteobacteria (including *Enterobacteriaceae*) and increased epithelial adhesion and invasion by *Escherichia coli* (Heimesaat et al., 2006; Craven et al., 2012). This culminates in extensive epithelial tissue damage and bacterial translocation into the underlying lamina propria. A direct role for gut microbes in this process is demonstrated by the fact that *Toxoplasma*-induced intestinal pathology is prevented by antibiotic administration prior to infection. There is evidence that bacterial TLR4 ligands are involved in this uncontrolled proinflammatory response (Heimesaat et al., 2007). It has also been reported that *Toxoplasma* infection elicits neutrophil migration into the intestinal lumen, generating structures that encapsulate microbiota which limits contact with damaged epithelium (Molloy et al., 2013). In addition, transfer of lamina propria $CD4^+$ T cells along with intraepithelial lymphocytes from infected mice into non-infected mice drives intestinal damage that is dependent upon recipient gut flora (Egan et al., 2011b). This indicates that at least part of the inflammatory pathology is due to bacteria-specific T cells in the mucosal immune compartment. The effects of the intestinal microbiome on acute infection are well established. However, it is also possible that the microbiome influences later events in infection, for example parasite reactivation in the brain and emergence of toxoplasmic encephalitis. While corresponding effects have been characterized elsewhere (Zhu et al., 2020), this is an unexplored area in *Toxoplasma* research.

MUCOSAL IMMUNE RESPONSE DURING *TOXOPLASMA* INFECTION: CAST OF CHARACTERS

When *Toxoplasma* enters the gut, cells of the mucosal immune system and associated tissues are rapidly alerted to infection. Some of the key cells are resident in the intestinal mucosa, others are recruited. Regardless, there is a coordinated response involving cells of innate and adaptive immunity. As outlined above, the outcome may be protective immunity and survival, or tissue pathology and death. The following summarizes the activities of cells most relevant to the course of infection in the gut.

Epithelial Cells

The intestinal epithelium is the initial line of defense between the host and intestinal pathogens. As such, cells in this compartment are the first to encounter *Toxoplasma* in the gut. Epithelial cells include enterocytes, goblet cells, Paneth cells, M cells, and enteroendocrine cells (van der Flier and Clevers, 2009; Allaire et al., 2018). Paneth cells, a rich source of antimicrobial peptides in the intestine, decrease in number during *Toxoplasma* infection. Loss of Paneth cells has been implicated in *T. gondii*-driven intestinal dysbiosis and immunopathology. Raetz et al. showed that Paneth cells are destroyed by IFN-γ producing $CD4^+$ T cells triggered by *T. gondii* infection (Raetz et al., 2013b). Destruction of Paneth cells is dependent upon presence of the intestinal microbiota and T cell intrinsic MyD88 signaling. Loss of Paneth cells results in impaired intestinal barrier function, *Enterobacteriaceae* outgrowth, and intestinal pathology (Raetz et al., 2013b; Burger et al., 2018). In addition to antimicrobial peptide production, Paneth cell intrinsic autophagy is important for regulating immunopathology in response to *T. gondii* infection. Loss of the autophagy protein Atg5 in Paneth cells results in severe immunopathology, loss of crypt structures, and increased host mortality, all of which are dependent upon presence of the intestinal microbiota (Burger et al., 2018). Together, these studies describe new, important roles for Paneth cell autophagy and antimicrobial peptide production in limiting immunopathology and microbiota dysbiosis driven by *T. gondii* infection.

Intraepithelial Lymphocytes

Intraepithelial lymphocytes (IELs) are interspersed throughout the intestinal epithelium and evidence indicates they play an important role in anti-*Toxoplasma* immunity. The IEL compartment is comprised primarily of $\gamma\delta^+$ T cells and $CD8^+$ T cells, most of which express the CD8α homodimer (Guy-Grand et al., 1991; Cheroutre et al., 2011). A homeostatic function in the intestine is often ascribed to this compartment. Nevertheless, the complexity of the IEL population suggests their role extends beyond homeostasis. When primed IEL isolated from infected mice are adoptively transferred into naïve mice, recipients experience reduced mortality rates after lethal parasite challenge (Lepage et al., 1998; Buzoni-Gatel et al., 1999). The protective effects are recapitulated when CD8$\alpha\beta$ expressing IEL are adoptively transferred, although $\gamma\delta^+$ T cells also contribute to protection (Lepage et al., 1998). Primed CD8$\alpha\beta^+$ IEL were also described as possessing antigen specific cytotoxic activity and producing IFN-γ. Thus, it is likely that $CD8^+$ IEL kill *T. gondii* infected epithelial cells and contribute to type I immunity. Further studies using $CCR2^{-/-}$ mice showed that although they succumb to oral challenge with *T. gondii*, knockout animals exhibit significantly less intestinal pathology compared to WT mice (Egan et al., 2009). The decrease in immunopathology was attributed to lack of retention of $CD103^+$ IEL, and adoptive transfer of wildtype IEL resulted in both improved survival and more severe intestinal pathology (Egan et al., 2009). Thus, although the IEL compartment contributes to protective *Toxoplasma* immunity, it can also play a role in initiating damage and inflammation in the small intestine.

Innate Lymphoid Cells

Innate lymphoid cells (ILCs) are a newly described family of immune cells comprised of three subsets (ILC1, 2, and 3). They are prominent at mucosal interfaces including the small intestine

(Spits and Cupedo, 2012; Bennett et al., 2015). ILC1 produce IFN-γ, ILC2 are associated with Th2-like cytokines, and ILC3 produce IL17 and IL-22 (Spits et al., 2013; Artis and Spits, 2015; Eberl et al., 2015). It remains unclear how each contribute to mucosal anti-*Toxoplasma* immunity. There is evidence that T-bet$^+$ ILC1 secrete IFN-γ in response to oral inoculation with *T. gondii*; however, the contribution appears minor compared to CD4$^+$ T cells. Tbx21$^{-/-}$ mice, which lack ILC1, generate a strong IFN-γ response driven by T-bet independent CD4$^+$ T cells (Lopez-Yglesias et al., 2018). Nevertheless, other studies found that ILC-like cells are protective against *T. gondii* infection (Klose et al., 2014). It was found that RORγt$^+$ ILC3 frequencies decrease during *T. gondii* infection, and it was suggested that these cells play a role in limiting T cell responses and pathology during *T. gondii* infection (Wagage et al., 2015). Further studies are necessary to discern the role the ILC compartment plays during intestinal *T. gondii* infection.

Dendritic Cells and Inflammatory Monocytes

Dendritic cells (DCs) are widely regarded as being pivotal in activation of T cell immunity, as well as playing a crucial role in maintenance of tolerance in the intestinal environment (Stagg, 2018; Sun et al., 2020). In the gut, discrete DC subsets can be identified based upon expression of CD11b and CD103 (Persson et al., 2013). Because of a requirement for transcription factor IRF8, the CD11b$^-$CD103$^+$ subset of lamina propria DC are likely related to splenic CD8α$^+$ DC that produce IL-12 and mediate protection in i. p. models of *T. gondii* infection (Edelson et al., 2010; Cohen et al., 2014). Essentially all of the IL-12 produced by CD11b$^-$CD103$^+$ lamina propria DC comes from non-infected cells (Cohen and Denkers, 2015). This suggests that these cells respond to parasite molecules present in the extracellular environment, or that the cells have been injected with parasite effector proteins as is known to occur for *Toxoplasma* rhoptry proteins (Koshy et al., 2012; Chen et al., 2020). Alternatively, it is possible DC responses are initiated by host-derived alarm signals triggered by infection.

Oral infection with *Toxoplasma* elicits a large influx of inflammatory monocytes into the lamina propria (Cohen and Denkers, 2015). Recruitment of these cells, whose presence is dependent upon chemokine receptor CCR2, mediates resistance to *Toxoplasma* as the parasite enters the intestinal mucosa (Dunay et al., 2008). Inflammatory monocytes in the lamina propria express IL-12, and it is possible that they play a role in promoting induction of protective Th1 cells (Cohen et al., 2013). Nevertheless, inflammatory monocytes are recruited into the intestine concomitant with appearance of Th1 effectors. Therefore, these cells may be more important as executioners of IFN-γ-dependent control of *T. gondii* using mechanisms such as iNOS/NOS2 and the IRG effector family that destroy the parasitophorous vacuole membrane (Khan et al., 1997; Hunn et al., 2011; Wang S. et al., 2019).

Neutrophils

Neutrophils are among the first immune cells to infiltrate the site of infection. Within three days of oral inoculation with *T. gondii*, a rapid influx into the small intestine lamina propria is observed (Sukhumavasi et al., 2008; Gregg et al., 2013). Additionally, it has been reported that *T. gondii* preferentially infects infiltrating neutrophils to disseminate into other host tissues (Coombes et al., 2013). Activated neutrophils can secrete cytokines important for type I immunity including IL-12 and TNF-α, and they deploy neutrophil extracellular traps that ensnare and kill extracellular tachyzoites (Bliss et al., 1999; Bliss et al., 2000; Bliss et al., 2001; Sukhumavasi et al., 2008; Abi Abdallah et al., 2012). Whether these mechanisms operate within the intestinal mucosa during *T. gondii* infection is not known. The role neutrophils play in inducing intestinal immunity and pathology also remains unclear. In one study wildtype mice depleted of neutrophils with monoclonal antibody treatment survived the infection and displayed similar intestinal pathology compared to untreated mice. In the same study, CCR2$^{-/-}$ mice depleted of neutrophils exhibited less intestinal tissue damage compared to untreated CCR2$^{-/-}$ mice (Dunay et al., 2010). In an intraperitoneal infection model, depletion of neutrophils within the first four days of infection resulted in mortality associated with severe lesions and increased systemic parasite burdens, and a similar result was seen with CXCR2 knockout mice that are defective in neutrophil recruitment (Bliss et al., 2001; Del Rio et al., 2001). These disparate results might be explained by different routes of infection or different effectiveness of antibody depletion protocols. Further studies are required to discern the role neutrophils play in intestinal anti-*Toxoplasma* immunity.

T Cells

T. gondii is a well-known inducer of type I immunity that during oral infection includes an expansion of parasite and microbiota-specific Th1 cells (Hand et al., 2012). Myeloid cell derived IL-12 is the primary driver of type I immunity (Gazzinelli et al., 1994; Yap et al., 2000). Although Th1 immunity generated in response to *Toxoplasma* is required to survive infection, it also underlies the severe intestinal immunopathology that can occur during infection (Liesenfeld et al., 1996; Raetz et al., 2013b; Burger et al., 2018). Interestingly, a robust IFN-γ$^+$ CD4$^+$ T cell response was observed in Tbx21$^{-/-}$ mice that lack expression of T-bet, regarded as the master regulator of Th1 differentiation. This clearly indicates that the anti-*Toxoplasma* Th1 response and Th1-mediated intestinal damage can be elicited without T-bet (Lopez-Yglesias et al., 2018).

Although the Th1 CD4$^+$ T cell response dominates during *T. gondii* infection, Th17 cells have also been shown to play a role in *T. gondii* immunity. Mice lacking class I-restricted T cell-associated molecule (CRTAM) expression on T cells have fewer IL-17a and IL-22-secreting Th17 cells. This is associated with decreased antimicrobial peptide production, and increased pathology and microbial translocation into systemic tissues after oral inoculation with *T. gondii* (Cortez et al., 2014; Cervantes-Barragan et al., 2019). These data highlight emerging roles for Th17 T cells in controlling *T. gondii* induced intestinal dysbiosis, systemic dissemination of intestinal microbes, and immunopathology.

Regulatory T cells (T_{reg}) are well-known to possess an important function in controlling proinflammatory tissue damage in the intestinal mucosa, in large part through production of IL-10 (Neumann et al., 2019). During *Toxoplasma* infection, the T_{reg} population rapidly disappears which likely plays a role in inflammatory pathology induced by the parasite (Oldenhove et al., 2009). In part, this is due to conversion of Treg cells into T-bet$^+$ IFN-γ producing cells. Nevertheless, the collapse in the intestinal T_{reg} population appears to have a multifactorial root cause insofar as deprivation of IL-2 associated with massive Th1 expansion also underlies this phenomenon (Benson et al., 2012).

B Cells

B cells are present in large number in both the lamina propria and Peyer's patches of the small intestine (Gregg et al., 2013; Reboldi and Cyster, 2016). Following oral infection with type II strain cysts, μMT mice (which lack B cells) survive acute infection, but eventually succumb during the chronic stage 3–4 weeks later (Kang et al., 2000). In an oral inoculation model following i. p. vaccination with an attenuated *T. gondii* strain, μMT animals survive lethal challenge in a manner indistinguishable from wildtype vaccinated controls (Johnson et al., 2004). However, during i. p. infection with highly virulent type I parasites, vaccinated μMT mice succumb to lethal challenge (Sayles et al., 2000). Taken together, while B cells may have a role in i. p. vaccination-induced immunity, they appear less important in the context of protection in the intestinal mucosa.

CONCLUSIONS AND FUTURE DIRECTIONS

While our understanding of pathogenesis of *Toxoplasma* infection in the intestinal mucosa has expanded significantly in recent decades, there are still areas requiring exploration. The precise events in early innate immune triggering remain shrouded in mystery. The exact relationship between parasite-derived signals, host-derived signals and possibly host damage-associated danger signals remains to be clarified. Along similar lines, the precise sequence of events that lead to immunopathology in the intestine remains obscure. Also largely unexplored is how the mucosal immune system remembers and responds to secondary infection with *Toxoplasma*, an area that has significant relevance to issues of vaccine development not only to *T. gondii*, but to orally acquired microbial pathogens as a whole.

AUTHOR CONTRIBUTIONS

ED and LS conceived and wrote the manuscript. All authors contributed to the article and approved the submitted version.

REFERENCES

Abi Abdallah, D. S., Lin, C., Ball, C. J., King, M. R., Duhamel, G. E., and Denkers, E. Y. (2012). Toxoplasma gondii triggers release of human and mouse neutrophil extracellular traps. *Infect. Immun.* 80 (2), 768–777. doi: 10.1128/IAI.05730-11

Allaire, J. M., Crowley, S. M., Law, H. T., Chang, S. Y., Ko, H. J., and Vallance, B. A. (2018). The Intestinal Epithelium: Central Coordinator of Mucosal Immunity. *Trends Immunol.* 39 (9), 677–696. doi: 10.1016/j.it.2018.04.002

Artis, D., and Spits, H. (2015). The biology of innate lymphoid cells. *Nature* 517 (7534), 293–301. doi: 10.1038/nature14189

Barragan, A., and Sibley, L. D. (2002). Transepithelial migration of *Toxoplasma gondii* is linked to parasite migration and virulence. *J. Exp. Med.* 195, 1625–1633. doi: 10.1084/jem.20020258

Barragan, A., and Sibley, L. D. (2003). Migration of *Toxoplasma gondii* across biological barriers. *Trends Microbiol.* 11 (9), 426–430. doi: 10.1016/s0966-842x(03)00205-1

Barragan, A., Brossier, F., and Sibley, L. D. (2005). Transepithelial migration of *Toxoplasma gondii* involves an interaction of intercellular adhesion molecule 1 (ICAM-1) with parasite adhesin MIC2. *Cell Microbiol.* 7, 561–568. doi: 10.1111/j.1462-5822.2005.00486.x

Bennett, M. S., Round, J. L., and Leung, D. T. (2015). Innate-like lymphocytes in intestinal infections. *Curr. Opin. Infect. Dis.* 28 (5), 457–463. doi: 10.1097/QCO.0000000000000189

Benson, A., Pifer, R., Behrendt, C. L., Hooper, L. V., and Yarovinsky, F. (2009). Gut commensal bacteria direct a protective immune response against Toxoplasma gondii. *Cell Host Microbe* 6 (2), 187–196. doi: 10.1016/j.chom.2009.06.005

Benson, A., Murray, S., Divakar, P., Burnaevskiy, N., Pifer, R., Forman, J., et al. (2012). Microbial Infection-Induced Expansion of Effector T Cells Overcomes the Suppressive Effects of Regulatory T Cells via an IL-2 Deprivation Mechanism. *J. Immunol.* 188, 800–810. doi: 10.4049/jimmunol.1100769

Bliss, S. K., Marshall, A. J., Zhang, Y., and Denkers, E. Y. (1999). Human polymorphonuclear leukocytes produce IL-12, TNF-a, and the chemokines macrophage-inflammatory protein-1a and -1b in response to *Toxoplasma gondii* antigens. *J. Immunol.* 162, 7369–7375.

Bliss, S. K., Butcher, B. A., and Denkers, E. Y. (2000). Rapid recruitment of neutrophils with prestored IL-12 during microbial infection. *J. Immunol.* 165, 4515–4521. doi: 10.4049/jimmunol.165.8.4515

Bliss, S. K., Gavrilescu, L. C., Alcaraz, A., and Denkers, E. Y. (2001). Neutrophil depletion during Toxoplasma gondii infection leads to impaired immunity and lethal systemic pathology. *Infect. Immun.* 69 (8), 4898–4905. doi: 10.1128/IAI.69.8.4898-4905.2001

Braun, L., Brenier-Pinchart, M. P., Yogavel, M., Curt-Varesano, A., Curt-Bertini, R. L., Hussain, T., et al. (2013). A Toxoplasma dense granule protein, GRA24, modulates the early immune response to infection by promoting a direct and sustained host p38 MAPK activation. *J. Exp. Med.* 210 (10), 2071–2086. doi: 10.1084/jem.20130103

Briceno, M. P., Nascimento, L. A., Nogueira, N. P., Barenco, P. V., Ferro, E. A., Rezende-Oliveira, K., et al. (2016). Toxoplasma gondii Infection Promotes Epithelial Barrier Dysfunction of Caco-2 Cells. *J. Histochem. Cytochem.* 64 (8), 459–469. doi: 10.1369/0022155416656349

Burger, E., Araujo, A., Lopez-Yglesias, A., Rajala, M. W., Geng, L., Levine, B., et al. (2018). Loss of Paneth Cell Autophagy Causes Acute Susceptibility to Toxoplasma gondii-Mediated Inflammation. *Cell Host Microbe* 23 (2), 177–90.e4. doi: 10.1016/j.chom.2018.01.001

Buzoni-Gatel, D., Debbabi, H., Moretto, M., Dimier-Poisson, I. H., Lepage, A. C., Bout, D. T., et al. (1999). Intraepithelial lymphocytes traffic to the intestine and enhance resistance to Toxoplasma gondii oral infection. *J. Immunol.* 162 (10), 5846–5852.

Cervantes-Barragan, L., Cortez, V. S., Wang, Q., McDonald, K. G., Chai, J. N., Di Luccia, B., et al. (2019). CRTAM Protects Against Intestinal Dysbiosis During Pathogenic Parasitic Infection by Enabling Th17 Maturation. *Front. Immunol.* 10, 1423. doi: 10.3389/fimmu.2019.01423

Chen, L., Christian, D. A., Kochanowsky, J. A., Phan, A. T., Clark, J. T., Wang, S., et al. (2020). The Toxoplasma gondii virulence factor ROP16 acts in cis and trans, and suppresses T cell responses. *J. Exp. Med.* 217 (3), e20181757. doi: 10.1084/jem.20181757

Cheroutre, H., Lambolez, F., and Mucida, D. (2011). The light and dark sides of intestinal intraepithelial lymphocytes. *Nat. Rev. Immunol.* 11 (7), 445–456. doi: 10.1038/nri3007

Cohen, S. B., and Denkers, E. Y. (2015). Impact of Toxoplasma gondii on Dendritic Cell Subset Function in the Intestinal Mucosa. *J. Immunol.* 195 (6), 2754–2762. doi: 10.4049/jimmunol.1501137

Cohen, S. B., Maurer, K. J., Egan, C. E., Oghumu, S., Satoskar, A. R., and Denkers, E. Y. (2013). CXCR3-dependent CD4(+) T cells are required to activate inflammatory monocytes for defense against intestinal infection. *PLoS Pathog.* 9 (10), e1003706. doi: 10.1371/journal.ppat.1003706

Cohen, S. B., Smith, N. L., McDougal, C., Pepper, M., Shah, S., Yap, G. S., et al. (2014). beta-Catenin Signaling Drives Differentiation and Proinflammatory Function of IRF8-Dependent Dendritic Cells. *J. Immunol.* 194, 210–222. doi: 10.4049/jimmunol.1402453

Coombes, J. L., Charsar, B. A., Han, S. J., Halkias, J., Chan, S. W., Koshy, A. A., et al. (2013). Motile invaded neutrophils in the small intestine of Toxoplasma gondii-infected mice reveal a potential mechanism for parasite spread. *Proc. Natl. Acad. Sci. U. S. A.* 110 (21), E1913–E1922. doi: 10.1073/pnas.1220272110

Cortez, V. S., Cervantes-Barragan, L., Song, C., Gilfillan, S., McDonald, K. G., Tussiwand, R., et al. (2014). CRTAM controls residency of gut CD4+CD8+ T cells in the steady state and maintenance of gut CD4+ Th17 during parasitic infection. *J. Exp. Med.* 211 (4), 623–633. doi: 10.1084/jem.20130904

Courret, N., Darche, S., Sonigo, P., Milon, G., Buzoni-Gatel, D., and Tardieux, I. (2006). CD11c and CD11b expressing mouse leukocytes transport single *Toxoplasma gondii* tachyzoites to the brain. *Blood* 107, 309–316. doi: 10.1182/blood-2005-02-0666

Craven, M., Egan, C. E., Dowd, S. E., McDonough, S. P., Dogan, B., Denkers, E. Y., et al. (2012). Inflammation drives dysbiosis and bacterial invasion in murine models of ileal Crohn's disease. *PLoS One* 7 (7), e41594. doi: 10.1371/journal.pone.0041594

de Carvalho, R. V. H., and Zamboni, D. S. (2020). Inflammasome Activation in Response to Intracellular Protozoan Parasites. *Trends Parasitol.* 36 (5), 459–472. doi: 10.1016/j.pt.2020.02.006

Del Rio, L., Bennouna, S., Salinas, J., and Denkers, E. Y. (2001). CXCR2 deficiency confers impaired neutrophil recruitment and increased susceptibility during Toxoplasma gondii infection. *J. Immunol.* 167 (11), 6503–6509. doi: 10.4049/jimmunol.167.11.6503

Denkers, E. Y., and Gazzinelli, R. T. (1998). Regulation and function of T-cell-mediated immunity during Toxoplasma gondii infection. *Clin. Microbiol. Rev.* 11 (4), 569–588. doi: 10.1128/CMR.11.4.569

Denkers, E. Y., Bzik, D. J., Fox, B. A., and Butcher, B. A. (2012). An inside job: hacking into Janus kinase/signal transducer and activator of transcription signaling cascades by the intracellular protozoan Toxoplasma gondii. *Infect. Immun.* 80 (2), 476–482. doi: 10.1128/IAI.05974-11

Dubey, J. P. (2013). "The history and life-cycle of Toxoplasma gondii," in *Toxoplasma gondii the model apicomplexan: perspective and methods, 2nd ed.* Eds. L. M. Weiss and K. Kim (San Diego: Academic Press), 1–17.

Dunay, I. R., Damatta, R. A., Fux, B., Presti, R., Greco, S., Colonna, M., et al. (2008). Gr1(+) Inflammatory Monocytes Are Required for Mucosal Resistance to the Pathogen Toxoplasma gondii. *Immunity* 29 (2), 306–317. doi: 10.1016/j.immuni.2008.05.019

Dunay, I. R., Fuchs, A., and Sibley, L. D. (2010). Inflammatory monocytes but not neutrophils are necessary to control infection with Toxoplasma gondii in mice. *Infect. Immun.* 78 (4), 1564–1570. doi: 10.1128/IAI.00472-09

Dupont, C. D., Christian, D. A., and Hunter, C. A. (2012). Immune response and immunopathology during toxoplasmosis. *Semin. Immunopathol.* 34 (6), 793–813. doi: 10.1007/s00281-012-0339-3

Eberl, G., Colonna, M., Di Santo, J. P., and McKenzie, A. N. (2015). Innate lymphoid cells. Innate lymphoid cells: a new paradigm in immunology. *Science* 348 (6237), aaa6566. doi: 10.1126/science.aaa6566

Edelson, B. T., Kc, W., Juang, R., Kohyama, M., Benoit, L. A., Klekotka, P. A., et al. (2010). Peripheral CD103+ dendritic cells form a unified subset developmentally related to CD8alpha+ conventional dendritic cells. *J. Exp. Med.* 207 (4), 823–836. doi: 10.1084/jem.20091627

Egan, C. E., Craven, M. D., Leng, J., Mack, M., Simpson, K. W., and Denkers, E. Y. (2009). CCR2-dependent intraepithelial lymphocytes mediate inflammatory gut pathology during Toxoplasma gondii infection. *Mucosal Immunol.* 2 (6), 527–535. doi: 10.1038/mi.2009.105

Egan, C. E., Cohen, S. B., and Denkers, E. Y. (2011a). Insights into inflammatory bowel disease using Toxoplasma gondii as an infectious trigger. *Immunol. Cell Biol.* 90, 668–675. doi: 10.1038/icb.2011.93

Egan, C. E., Maurer, K. J., Cohen, S. B., Mack, M., Simpson, K. W., and Denkers, E. Y. (2011b). Synergy between intraepithelial lymphocytes and lamina propria T cells drives intestinal inflammation during infection. *Mucosal Immunol.* 4, 658–670. doi: 10.1038/mi.2011.31

Ewald, S. E., Chavarria-Smith, J., and Boothroyd, J. C. (2014). NLRP1 is an inflammasome sensor for Toxoplasma gondii. *Infect. Immun.* 82 (1), 460–468. doi: 10.1128/IAI.01170-13

Gazzinelli, R. T., and Denkers, E. Y. (2006). Protozoan encounters with Toll-like receptor signalling pathways: implications for host parasitism. *Nat. Rev. Immunol.* 6 (12), 895–906. doi: 10.1038/nri1978

Gazzinelli, R. T., Wysocka, M., Hayashi, S., Denkers, E. Y., Hieny, S., Caspar, P., et al. (1994). Parasite-induced IL-12 stimulates early IFN-gamma synthesis and resistance during acute infection with Toxoplasma gondii. *J. Immunol.* 153 (6), 2533–2543.

Gazzinelli, R. T., Wysocka, M., Hieny, S., Scharton-Kersten, T., Cheever, A., Kuhn, R., et al. (1996). In the absence of endogenous IL-10, mice acutely infected with Toxoplasma gondii succumb to a lethal immune response dependent on CD4+ T cells and accompanied by overproduction of IL-12, IFN-gamma and TNF-alpha. *J. Immunol.* 157 (2), 798–805.

Gazzinelli, R. T., Mendonca-Neto, R., Lilue, J., Howard, J., and Sher, A. (2014). Innate resistance against Toxoplasma gondii: an evolutionary tale of mice, cats, and men. *Cell Host Microbe* 15 (2), 132–138. doi: 10.1016/j.chom.2014.01.004

Gorfu, G., Cirelli, K. M., Melo, M. B., Mayer-Barber, K., Crown, D., Koller, B. H., et al. (2014). Dual role for inflammasome sensors NLRP1 and NLRP3 in murine resistance to Toxoplasma gondii. *MBio* 5 (1), e01117–13. doi: 10.1128/mBio.01117-13

Gov, L., Karimzadeh, A., Ueno, N., and Lodoen, M. B. (2013). Human innate immunity to Toxoplasma gondii is mediated by host caspase-1 and ASC and parasite GRA15. *MBio* 4 (4), e00255–13. doi: 10.1128/mBio.00255-13

Gov, L., Schneider, C. A., Lima, T. S., Pandori, W., and Lodoen, M. B. (2017). NLRP3 and Potassium Efflux Drive Rapid IL-1beta Release from Primary Human Monocytes during Toxoplasma gondii Infection. *J. Immunol.* 199 (8), 2855–2864. doi: 10.4049/jimmunol.1700245

Gregg, B., Taylor, B. C., John, B., Tait-Wojno, E. D., Girgis, N. M., Miller, N., et al. (2013). Replication and distribution of Toxoplasma gondii in the small intestine after oral infection with tissue cysts. *Infect. Immun.* 81 (5), 1635–1643. doi: 10.1128/IAI.01126-12

Guy-Grand, D., Cerf-Bensussan, N., Malissen, B., Malassis-Seris, M., Briottet, C., and Vassalli, P. (1991). Two gut intraepithelial CD8+ lymphocyte populations with different T cell receptors: a role for the gut epithelium in T cell differentiation. *J. Exp. Med.* 173 (2), 471–481. doi: 10.1084/jem.173.2.471

Hand, T. W., Dos Santos, L. M., Bouladoux, N., Molloy, M. J., Pagan, A. J., Pepper, M., et al. (2012). Acute Gastrointestinal Infection Induces Long-Lived Microbiota-Specific T Cell Responses. *Science* 337, 1553–1556. doi: 10.1126/science.1220961

Heimesaat, M. M., Bereswill, S., Fischer, A., Fuchs, D., Struck, D., Niebergall, J., et al. (2006). Gram-Negative Bacteria Aggravate Murine Small Intestinal Th1-Type Immunopathology following Oral Infection with Toxoplasma gondii. *J. Immunol.* 177 (12), 8785–8795. doi: 10.4049/jimmunol.177.12.8785

Heimesaat, M. M., Fischer, A., Jahn, H. K., Niebergall, J., Freudenberg, M., Blaut, M., et al. (2007). Exacerbation of Murine Ileitis By Toll-Like Receptor 4 Meditated Sensing of Lipopolysaccharide From Commensal Escherichia coli. *Gut* 56, 941–948. doi: 10.1136/gut.2006.104497

Hunn, J. P., Feng, C. G., Sher, A., and Howard, J. C. (2011). The immunity-related GTPases in mammals: a fast-evolving cell-autonomous resistance system against intracellular pathogens. *Mamm. Genome* 22 (1-2), 43–54. doi: 10.1007/s00335-010-9293-3

Hunter, C. A., and Sibley, L. D. (2012). Modulation of innate immunity by Toxoplasma gondii virulence effectors. *Nat. Rev. Microbiol.* 10 (11), 766–778. doi: 10.1038/nrmicro2858

Jensen, K. D., Wang, Y., Wojno, E. D., Shastri, A. J., Hu, K., Cornel, L., et al. (2011). Toxoplasma polymorphic effectors determine macrophage polarization and intestinal inflammation. *Cell Host Microbe* 9 (6), 472–483. doi: 10.1016/j.chom.2011.04.015

Jensen, K. D., Hu, K., Whitmarsh, R. J., Hassan, M. A., Julien, L., Lu, D., et al. (2013). Toxoplasma rhoptry kinase ROP16 promotes host resistance to oral infection and intestinal inflammation only in the context of the dense granule protein GRA15. *Infect. Immun.* 81, 2156–2167. doi: 10.1128/iai.01185-12

Johnson, L. L., Lanthier, P., Hoffman, J., and Chen, W. (2004). Vaccination protects B cell-deficient mice against an oral challenge with mildly virulent Toxoplasma gondii. *Vaccine* 22 (29-30), 4054–4061. doi: 10.1016/j.vaccine.2004.03.056

Kang, H., Remington, J. S., and Suzuki, Y. (2000). Decreased resistance of B cell-deficient mice to infection with Toxoplasma gondii despite unimpaired expression of IFN-gamma, TNF-alpha, and inducible nitric oxide synthase. *J. Immunol.* 164 (5), 2629–2634. doi: 10.4049/jimmunol.164.5.2629

Kayama, H., and Takeda, K. (2012). Regulation of intestinal homeostasis by innate and adaptive immunity. *Int. Immunol.* 24 (11), 673–680. doi: 10.1093/intimm/dxs094

Khan, I. A., Schwartzman, J. D., Matsuura, T., and Kasper, L. H. (1997). A dichotomous role for nitric oxide during acute *Toxoplasma gondii* infection in mice. *Proc. Natl. Acad. Sci. U. S. A.* 94, 13955–13960. doi: 10.1073/pnas.94.25.13955

Kim, L., Del Rio, L., Butcher, B. A., Mogensen, T. H., Paludan, S., Flavell, R. A., et al. (2005). p38 MAPK autophosphorylation drives macrophage IL-12 production during intracellular infection. *J. Immunol.* 174, 4178–4184. doi: 10.4049/jimmunol.174.7.4178

Klose, C. S., Flach, M., Mohle, L., Rogell, L., Hoyler, T., Ebert, K., et al. (2014). Differentiation of type 1 ILCs from a common progenitor to all helper-like innate lymphoid cell lineages. *Cell* 157 (2), 340–356. doi: 10.1016/j.cell.2014.03.030

Koblansky, A. A., Jankovic, D., Oh, H., Hieny, S., Sungnak, W., Mathur, R., et al. (2012). Recognition of Profilin by Toll-like Receptor 12 Is Critical for Host Resistance to Toxoplasma gondii. *Immunity* 38, 119–130. doi: 10.1016/j.immuni.2012.09.016

Koshy, A. A., Dietrich, H. K., Christian, D. A., Melehani, J. H., Shastri, A. J., Hunter, C. A., et al. (2012). Toxoplasma Co-opts Host Cells It Does Not Invade. *PLoS Pathog.* 8 (7), e1002825. doi: 10.1371/journal.ppat.1002825

Kucera, K., Koblansky, A. A., Saunders, L. P., Frederick, K. B., De La Cruz, E. M., Ghosh, S., et al. (2010). Structure-based analysis of Toxoplasma gondii profilin: a parasite-specific motif is required for recognition by Toll-like receptor 11. *J. Mol. Biol.* 403 (4), 616–629. doi: 10.1016/j.jmb.2010.09.022

Lepage, A. C., Buzoni-Gatel, D., Bout, D. T., and Kasper, L. H. (1998). Gut-derived intraepithelial lymphocytes induce long term immunity against Toxoplasma gondii. *J. Immunol.* 161 (9), 4902–4908.

Liesenfeld, O., Kosek, J., Remington, J. S., and Suzuki, Y. (1996). Association of $CD4^+$ T cell-dependent, IFN-g-mediated necrosis of the small intestine with genetic susceptibility of mice to peroral infection with *Toxoplasma gondii*. *J. Exp. Med.* 184, 597–607. doi: 10.1084/jem.184.2.597

Liesenfeld, O., Kang, H., Park, D., Nguyen, T. A., Parkhe, C. V., Watanabe, H., et al. (1999). TNF-a, nitric oxide and IFN-g are all critical for development of necrosis in the small intestine and early mortality in genetically susceptible mice infected perorally with *Toxoplasma gondii*. *Parasite Immunol.* 21, 365–376. doi: 10.1046/j.1365-3024.1999.00237.x

Lopez-Yglesias, A. H., Burger, E., Araujo, A., Martin, A. T., and Yarovinsky, F. (2018). T-bet-independent Th1 response induces intestinal immunopathology during Toxoplasma gondii infection. *Mucosal Immunol.* 11 (3), 921–931. doi: 10.1038/mi.2017.102

Lopez-Yglesias, A. H., Camanzo, E., Martin, A. T., Araujo, A. M., and Yarovinsky, F. (2019). TLR11-independent inflammasome activation is critical for CD4+ T cell-derived IFN-gamma production and host resistance to Toxoplasma gondii. *PLoS Pathog.* 15 (6), e1007872. doi: 10.1371/journal.ppat.1007872

Luu, L., and Coombes, J. L. (2015). Dynamic two-photon imaging of the immune response to Toxoplasma gondii infection. *Parasite Immunol.* 37 (3), 118–126. doi: 10.1111/pim.12161

Martorelli Di Genova, B., Wilson, S. K., Dubey, J. P., and Knoll, L. J. (2019). Intestinal delta-6-desaturase activity determines host range for Toxoplasma sexual reproduction. *PLoS Biol.* 17 (8), e3000364. doi: 10.1371/journal.pbio.3000364

McCabe, R., and Remington, J. S. (1988). Toxoplasmosis: The time has come. *N. Eng. J. Med.* 380, 313–315. doi: 10.1056/NEJM198802043180509

McLeod, R. M., van Tubbergen, C., Montoya, J. G., and Petersen, E. (2013). "Human Toxoplasma infection," in *Toxoplasma gondii The Model Apicomplexan: Perspectives and Methods*, *2nd ed.* Eds. L. M. Weiss and K. Kim (San Diego: Academic Press), 100–159.

Mercer, H. L., Snyder, L. M., Doherty, C. M., Fox, B. A., Bzik, D. J., and Denkers, E. Y. (2020). Toxoplasma gondii dense granule protein GRA24 drives MyD88-independent p38 MAPK activation, IL-12 production and induction of protective immunity. *PloS Pathog.* 16 (5), e1008572. doi: 10.1371/journal.ppat.1008572

Minns, L. A., Menard, L. C., Foureau, D. M., Darche, S., Ronet, C., Mielcarz, D. W., et al. (2006). TLR9 Is Required for the Gut-Associated Lymphoid Tissue Response following Oral Infection of Toxoplasma gondii. *J. Immunol.* 176 (12), 7589–7597. doi: 10.4049/jimmunol.176.12.7589

Molloy, M. J., Grainger, J. R., Bouladoux, N., Hand, T. W., Koo, L. Y., Naik, S., et al. (2013). Intraluminal containment of commensal outgrowth in the gut during infection-induced dysbiosis. *Cell Host Microbe* 14 (3), 318–328. doi: 10.1016/j.chom.2013.08.003

Mukhopadhyay, D., Arranz-Solis, D., and Saeij, J. P. J. (2020). Toxoplasma GRA15 and GRA24 are important activators of the host innate immune response in the absence of TLR11. *PLoS Pathog.* 16 (5), e1008586. doi: 10.1371/journal.ppat.1008586

Neumann, C., Scheffold, A., and Rutz, S. (2019). Functions and regulation of T cell-derived interleukin-10. *Semin. Immunol.* 44, 101344. doi: 10.1016/j.smim.2019.101344

Nutsch, K. M., and Hsieh, C. S. (2012). T cell tolerance and immunity to commensal bacteria. *Curr. Opin. Immunol.* 24 (4), 385–391. doi: 10.1016/j.coi.2012.04.009

Oldenhove, G., Bouladoux, N., Wohlfert, E. A., Hall, J. A., Chou, D., Dos Santos, L., et al. (2009). Decrease of Foxp3(+) Treg Cell Number and Acquisition of Effector Cell Phenotype during Lethal Infection. *Immunity* 31, 772–786. doi: 10.1016/j.immuni.2009.10.001

Persson, E. K., Scott, C. L., Mowat, A. M., and Agace, W. W. (2013). Dendritic cell subsets in the intestinal lamina propria: ontogeny and function. *Eur. J. Immunol.* 43 (12), 3098–3107. doi: 10.1002/eji.201343740

Pfaff, A. W., Liesenfeld, O., and Candolfi, E. (2007). "Congenital toxoplasmosis," in *Toxoplasma molecular and cellular biology*. Eds. J. W. Ajioka and D. Soldati (Norfolk: Horizon Bioscience), 93–110.

Quan, J. H., Huang, R., Wang, Z., Huang, S., Choi, I. W., Zhou, Y., et al. (2018). P2X7 receptor mediates NLRP3-dependent IL-1beta secretion and parasite proliferation in Toxoplasma gondii-infected human small intestinal epithelial cells. *Parasit. Vectors* 11 (1), 1. doi: 10.1186/s13071-017-2573-y

Raetz, M., Kibardin, A., Sturge, C. R., Pifer, R., Li, H., Burstein, E., et al. (2013a). Cooperation of TLR12 and TLR11 in the IRF8-dependent IL-12 response to Toxoplasma gondii profilin. *J. Immunol.* 191 (9), 4818–4827. doi: 10.4049/jimmunol.1301301

Raetz, M., Hwang, S. H., Wilhelm, C. L., Kirkland, D., Benson, A., Sturge, C. R., et al. (2013b). Parasite-induced TH1 cells and intestinal dysbiosis cooperate in IFN-gamma-dependent elimination of Paneth cells. *Nat. Immunol.* 14 (2), 136–142. doi: 10.1038/ni.2508

Ramirez-Flores, C. J., Cruz-Miron, R., Lagunas-Cortes, N., Mondragon-Castelan, M., Mondragon-Gonzalez, R., Gonzalez-Pozos, S., et al. (2020). Toxoplasma gondii excreted/secreted proteases disrupt intercellular junction proteins in epithelial cell monolayers to facilitate tachyzoites paracellular migration. *Cell Microbiol.* 1–9. doi: 10.1111/cmi.13283

Reboldi, A., and Cyster, J. G. (2016). Peyer's patches: organizing B-cell responses at the intestinal frontier. *Immunol. Rev.* 271 (1), 230–245. doi: 10.1111/imr.12400

Rosowski, E. E., Lu, D., Julien, L., Rodda, L., Gaiser, R. A., Jensen, K. D., et al. (2011). Strain-specific activation of the NF-kappaB pathway by GRA15, a novel Toxoplasma gondii dense granule protein. *J. Exp. Med.* 208 (1), 195–212. doi: 10.1084/jem.20100717

Safronova, A., Araujo, A., Camanzo, E. T., Moon, T. J., Elliott, M. R., Beiting, D. P., et al. (2019). Alarmin S100A11 initiates a chemokine response to the human pathogen Toxoplasma gondii. *Nat. Immunol.* 20 (1), 64–72. doi: 10.1038/s41590-018-0250-8

Sansonetti, P. J. (2011). To be or not to be a pathogen: that is the mucosally relevant question. *Mucosal Immunol.* 4 (1), 8–14. doi: 10.1038/mi.2010.77

Sayles, P. C., Gibson, G. W., and Johnson, L. L. (2000). B cells are essential for vaccination-induced resistance to virulent Toxoplasma gondii. *Infect. Immun.* 68 (3), 1026–1033. doi: 10.1128/iai.68.3.1026-1033.2000

Scanga, C. A., Aliberti, J., Jankovic, D., Tilloy, F., Bennouna, S., Denkers, E. Y., et al. (2002). Cutting edge: MyD88 is required for resistance to *Toxoplasma gondii* infection and regulates parasite-induced IL-12 production by dendritic cells. *J. Immunol.* 168, 5997–6001. doi: 10.4049/jimmunol.168.12.5997

Sher, A., and Coffman, R. L. (1992). Regulation of immunity to parasites by T cells and T cell-dependent cytokines. *Ann. Rev. Immunol.* 10, 385–410. doi: 10.1146/annurev.iy.10.040192.002125

Speer, C. A., and Dubey, J. P. (1998). Ultrastructure of early stages of infections in mice fed Toxoplasma gondii oocysts. *Parasitology* 116 (Pt 1), 35–42. doi: 10.1017/s0031182097001959

Spits, H., and Cupedo, T. (2012). Innate lymphoid cells: emerging insights in development, lineage relationships, and function. *Annu. Rev. Immunol.* 30, 647–675. doi: 10.1146/annurev-immunol-020711-075053

Spits, H., Artis, D., Colonna, M., Diefenbach, A., Di Santo, J. P., Eberl, G., et al. (2013). Innate lymphoid cells–a proposal for uniform nomenclature. *Nat. Rev. Immunol.* 13 (2), 145–149. doi: 10.1038/nri3365

Stagg, A. J. (2018). Intestinal Dendritic Cells in Health and Gut Inflammation. *Front. Immunol.* 9, 2883. doi: 10.3389/fimmu.2018.02883

Sukhumavasi, W., Egan, C. E., Warren, A. L., Taylor, G. A., Fox, B. A., Bzik, D. J., et al. (2008). TLR adaptor MyD88 is essential for pathogen control during oral toxoplasma gondii infection but not adaptive immunity induced by a vaccine strain of the parasite. *J. Immunol.* 181 (5), 3464–3473. doi: 10.4049/jimmunol.181.5.3464

Sun, T., Nguyen, A., and Gommerman, J. L. (2020). Dendritic Cell Subsets in Intestinal Immunity and Inflammation. *J. Immunol.* 204 (5), 1075–1083. doi: 10.4049/jimmunol.1900710

van der Flier, L. G., and Clevers, H. (2009). Stem cells, self-renewal, and differentiation in the intestinal epithelium. *Annu. Rev. Physiol.* 71, 241–260. doi: 10.1146/annurev.physiol.010908.163145

Vester-Andersen, M. K., Mirsepasi-Lauridsen, H. C., Prosberg, M. V., Mortensen, C. O., Trager, C., Skovsen, K., et al. (2019). Increased abundance of proteobacteria in aggressive Crohn's disease seven years after diagnosis. *Sci. Rep.* 9 (1), 13473. doi: 10.1038/s41598-019-49833-3

Villeret, B., Brault, L., Couturier-Maillard, A., Robinet, P., Vasseur, V., Secher, T., et al. (2013). Blockade of IL-1R signaling diminishes Paneth cell depletion and Toxoplasma gondii induced ileitis in mice. *Am. J. Clin. Exp. Immunol.* 2 (1), 107–116.

Wagage, S., Harms Pritchard, G., Dawson, L., Buza, E. L., Sonnenberg, G. F., and Hunter, C. A. (2015). The Group 3 Innate Lymphoid Cell Defect in Aryl Hydrocarbon Receptor Deficient Mice Is Associated with T Cell Hyperactivation during Intestinal Infection. *PLoS One* 10 (5), e0128335. doi: 10.1371/journal.pone.0128335

Wang, S., El-Fahmawi, A., Christian, D. A., Fang, Q., Radaelli, E., Chen, L., et al. (2019). Infection-Induced Intestinal Dysbiosis Is Mediated by Macrophage Activation and Nitrate Production. *MBio* 10 (3), e00935–19. doi: 10.1128/mBio.00935-19

Wang, Y., Cirelli, K. M., Barros, P. D. C., Sangare, L. O., Butty, V., Hassan, M. A., et al. (2019). Three Toxoplasma gondii Dense Granule Proteins Are Required for Induction of Lewis Rat Macrophage Pyroptosis. *mBio* 10 (1), e02388–18. doi: 10.1128/mBio.02388-18

Weight, C. M., and Carding, S. R. (2012). The protozoan pathogen Toxoplasma gondii targets the paracellular pathway to invade the intestinal epithelium. *Ann. N. Y. Acad. Sci.* 1258, 135–142. doi: 10.1111/j.1749-6632.2012.06534.x

Weiss, L. M., and Kim, K. (2014). *Toxoplasma gondii, the Model Apicomplexan: Perspectives and Methods. 2nd ed* (Amsterdam: Academic Press).

Witola, W. H., Mui, E., Hargrave, A., Liu, S., Hypolite, M., Montpetit, A., et al. (2011). NALP1 influences susceptibility to human congenital toxoplasmosis, proinflammatory cytokine response, and fate of Toxoplasma gondii-infected monocytic cells. *Infect. Immun.* 79 (2), 756–766. doi: 10.1128/IAI.00898-10

Yap, G., Pesin, M., and Sher, A. (2000). Cutting edge: IL-12 is required for the maintenance of IFN-gamma production in T cells mediating chronic resistance to the intracellular pathogen, Toxoplasma gondii. *J. Immunol.* 165 (2), 628–631. doi: 10.4049/jimmunol.165.2.628

Yarovinsky, F., and Sher, A. (2006). Toll-like receptor recognition of Toxoplasma gondii. *Int. J. Parasitol.* 36 (3), 255–259. doi: 10.1016/j.ijpara.2005.12.003

Yarovinsky, F., Zhang, D., Anderson, J. F., Bannenberg, G. L., Serhan, C. N., Hayden, M. S., et al. (2005). TLR11 activation of dendritic cells by a protozoan profilin-like protein. *Science* 308, 1626–1629. doi: 10.1126/science.1109893

Zamboni, D. S., and Lima-Junior, D. S. (2015). Inflammasomes in host response to protozoan parasites. *Immunol. Rev.* 265 (1), 156–171. doi: 10.1111/imr.12291

Zhu, F., Li, C., Chu, F., Tian, X., and Zhu, J. (2020). Target Dysbiosis of Gut Microbes as a Future Therapeutic Manipulation in Alzheimer's Disease. *Front. Aging Neurosci.* 12, 544235. doi: 10.3389/fnagi.2020.544235

Conflict of Interest: The authors declare that the research was conducted in the absence of any commercial or financial relationships that could be construed as a potential conflict of interest.

frontiers in Cellular and Infection Microbiology

ORIGINAL RESEARCH
published: 04 February 2021
doi: 10.3389/fcimb.2020.632556

The Absence of Gut Microbiota Alters the Development of the Apicomplexan Parasite *Eimeria tenella*

Pauline Gaboriaud[1†], Guillaume Sadrin[1†], Edouard Guitton[2], Geneviève Fort[1], Alisson Niepceron[1], Nathalie Lallier[1], Christelle Rossignol[1], Thibaut Larcher[3], Alix Sausset[1], Rodrigo Guabiraba[1], Anne Silvestre[1], Sonia Lacroix-Lamandé[1], Catherine Schouler[1], Fabrice Laurent[1] and Françoise I. Bussière[1]*

[1] INRAE, Université de Tours, UMR ISP, Nouzilly, France, [2] INRAE, UE PFIE, Nouzilly, France, [3] INRAE, Oniris, PAnTher, APEX, Nantes, France

OPEN ACCESS

Edited by:
Chandra Ramakrishnan, University of Zurich, Switzerland

Reviewed by:
Damer Blake, Royal Veterinary College (RVC), United Kingdom
Emanuel Heitlinger, Leibniz Institute for Zoo and Wildlife Research (LG), Germany

***Correspondence:**
Françoise I. Bussière
Francoise.Bussiere@inrae.fr

[†]These authors have contributed equally to this work

Specialty section:
This article was submitted to Parasite and Host, a section of the journal Frontiers in Cellular and Infection Microbiology

Received: *23 November 2020*
Accepted: *24 December 2020*
Published: *04 February 2021*

Citation:
Gaboriaud P, Sadrin G, Guitton E, Fort G, Niepceron A, Lallier N, Rossignol C, Larcher T, Sausset A, Guabiraba R, Silvestre A, Lacroix-Lamandé S, Schouler C, Laurent F and Bussière FI (2021) The Absence of Gut Microbiota Alters the Development of the Apicomplexan Parasite Eimeria tenella. Front. Cell. Infect. Microbiol. 10:632556. doi: 10.3389/fcimb.2020.632556

Coccidiosis is a widespread intestinal disease of poultry caused by a parasite of the genus *Eimeria*. *Eimeria tenella,* is one of the most virulent species that specifically colonizes the caeca, an organ which harbors a rich and complex microbiota. Our objective was to study the impact of the intestinal microbiota on parasite infection and development using an original model of germ-free broilers. We observed that germ-free chickens presented significantly much lower load of oocysts in caecal contents than conventional chickens. This decrease in parasite load was measurable in caecal tissue by RT-qPCR at early time points. Histological analysis revealed the presence of much less first (day 2pi) and second generation schizonts (day 3.5pi) in germ-free chickens than conventional chickens. Indeed, at day 3.5pi, second generation schizonts were respectively immature only in germ-free chickens suggesting a lengthening of the asexual phase of the parasite in the absence of microbiota. Accordingly to the consequence of this lengthening, a delay in specific gamete gene expressions, and a reduction of gamete detection by histological analysis in caeca of germ-free chickens were observed. These differences in parasite load might result from an initial reduction of the excystation efficiency of the parasite in the gut of germ-free chickens. However, as bile salts involved in the excystation step led to an even higher excystation efficiency in germ-free compared to conventional chickens, this result could not explain the difference in parasite load. Interestingly, when we shunted the excystation step *in vivo* by infecting chickens with sporozoites using the cloacal route of inoculation, parasite invasion was similar in germ-free and in conventional chickens but still resulted in significantly lower parasite load in germ-free chickens at day 7pi. Overall, these data highlighted that the absence of intestinal microbiota alters *E. tenella* replication. Strategies to modulate the microbiota and/or its metabolites could therefore be an alternative approach to limit the negative impact of coccidiosis in poultry.

Keywords: *Eimeria tenella*, microbiota, germ-free, chicken, parasite, parasite invasion and development

INTRODUCTION

Eimeria is an obligate intracellular parasite belonging to the phylum of Apicomplexa. In birds, various *Eimeria* species colonize the intestine with a localization that is specific to each species. *Eimeria tenella* (*E. tenella*) colonizes the caeca and is one of the most virulent species. It leads to haemorrhagic diarrhoea and high levels of morbidity and mortality in poultry flocks. Prevention and treatment of *Eimeria* infection are responsible for very high economic cost recently re-assessed to the level of about 13 billion dollars per year in the world (Blake et al., 2020). Current prophylaxis is based on anticoccidial drugs and vaccination, both with its advantages and limitations.

E. tenella invades and develops in intestinal epithelial cells. The *in vivo* parasite life cycle is divided in two parts: the endogenous asexual multiplication with three rounds of merogony and the sexual phase with the formation of macrogametes (female gametocytes) and microgametes (male gametocytes). Microgametes may fertilize a macrogamete resulting in the formation of a zygote (Ferguson et al., 2003). After maturation, it becomes an unsporulated oocyst released in the environment through the feces where it will develop into an infectious sporulated oocyst (exogenous phase or sporogony). Caeca are the richest part of the intestine in terms of bacteria abundance and diversity. Firmicutes, Bacteroidetes, and Proteobacteria are the main caecal bacterial phyla (Wei et al., 2013; Oakley et al., 2014; Qi et al., 2019). Importantly, *E. tenella* infection leads to alterations in the microbiota diversity and composition (Huang et al., 2018a). Taxa belonging to the order *Enterobacteriaceae* from the phylum Proteobacteria were increased in caecal contents from *E. tenella* infected chickens compared to those uninfected. Within the phylum Firmicutes, non-pathogenic bacteria *Lactobacillus* and *Faecalibacterium* were decreased while bacteria such as *Clostridium perfringens* are increased during the infection with *E. tenella* and are related to an increased occurrence of necrotic enteritis of chickens (Al-Sheikhly and Al-Saieg, 1980; Macdonald et al., 2017; Huang et al., 2018a; Huang et al., 2018b). The microbiota promotes the gut immune system maturation which in turn protect the host from enteric bacterial infections such as *Salmonella* infection (Crhanova et al., 2011). Studies have shown that the modulation of the chicken intestinal microbiota can limit *Salmonella* colonization (Stecher et al., 2010; Yang et al., 2014). In the case of an apicomplexan parasite such as *Plasmodium falciparum*, when *Enterobacter* is present in the gut, it confers a resistance to the parasite infection in *Anopheles* (Cirimotich et al., 2011a; Cirimotich et al., 2011b). However, other pathogens such as *Histomonas meleagridis* depend on bacteria for their growth *in vitro* (Ganas et al., 2012). Concerning *E. tenella*, most of the studies have focused on the effect of the microbiota on the clinical signs associated with infection (Visco and Burns, 1972a; Visco and Burns, 1972b; Bradley and Radhakrishnan, 1973; Lafont et al., 1975).

Abbreviations: GAM56, Macrogamete specific protein; FOA1, Flagellar Outer Arm protein 1.

In the present study, we investigated the influence of the absence of microbiota on *E. tenella* infection. For this purpose, we used a recently developed model of germ-free fast-growing broilers (Guitton et al., 2020). Our results highlight a critical role for the microbiota in sustaining the optimal development of the parasite in the chicken intestinal tract. Strategies to modulate the composition of the microbiota and/or derived metabolites might therefore represent a promising strategy to improve the prophylaxis of coccidiosis.

MATERIALS AND METHODS

Ethical Statement

Animal experimental protocols were performed in accordance with the French legislation (Décret: 2001-464 29/05/01) and the EEC regulation (86/609/CEE) about laboratory animals. All chicken experiments were approved by the local ethics committee for animal experimentation of Centre Val de Loire (CEEA VdL n°19): 2018-04-26 (APAFIS N°13904).

Parasite

The *E. tenella* INRAE PAPt36 strain (*Et*-INRAE) was used for all experiments except for studying the effect of the microbiota on parasite invasion. *E. tenella* strain was isolated from a poultry farming in France in 1974. Initially referenced as *E. tenella* strain PAPt38 is now renamed as *E. tenella*-INRAE strain. The strain was maintained by regular passages on chicken in the PFIE facility since then (Laurent et al., 2001). For parasite invasion studies, *Et*-INRAE was transfected with *nano luciferase* and *mcherry* genes under the *E. tenella actin* promoter [*Et*-INV; (Yan et al., 2009; Swale et al., 2019)]. The *mcherry* gene allows sorting by flow cytometry of sporulated oocysts after inoculation of transfected sporozoites to chickens and for parasite amplification. The nano luciferase activity (NanoLuc® Luciferase, Promega) facilitates the detection of low load of parasites and accurate parasite quantification in tissues. Purification of sporozoites was performed as described by (Shirley, 1995). Briefly, 0.5 mm sterilized glass beads (Carl Roth, Karlsruhe, Germany) were added to sporulated oocysts. The oocyst wall was broken by vortexing for 17 s. Released sporocysts were washed with PBS and incubated in standard excystation medium (trypsin 0.25% and biliary salts 0.5% in PBS; pH 7.4) at 41°C for 1 h. Sporozoites were then washed in PBS and ready for cloacal inoculation.

Animals

Conventional and germ-free Ross PM3 broilers were hatched in the Infectiology of Farm, Model and Wildlife Animals Facility (PFIE, Centre INRAE Val De Loire: https://doi.org/10.15454/1.5572352821559333E12; member of the National Infrastructure EMERG'IN) as described by (Guitton et al., 2020). Briefly, Ross PM3 eggs from two French farms were collected, decontaminated with a 1.5% peracetic acid solution (1.5% Divosan Plus VT53, Johnson Diversey, France). Eggs were then incubated, decontaminated a second time as described above and placed in a hatching incubator for production of conventional chicks or an

isolator for the production of germ-free animals. Bacteriological controls were performed as described by (Guitton et al., 2020); animals were confirmed to be bacteria-free while conventional chickens developed a microbiota.

Infection

Two-week-old chickens were orally infected with different doses of sporulated oocysts of the *Et*-INRAE strain. At day 6 to 9 post-infection, chickens were euthanized by electronarcosis and caeca were collected. On caecal contents, oocysts were counted on MacMaster counting chambers. At day 2, 3.5, 5.5, and 7 post-infection, caecal tissues were washed and fixed in 4% formaldehyde (Laurypath, Chaponost, France) for histological analysis or directly frozen in liquid nitrogen and stored at -80°C for gene expression analysis.

To study parasite invasion, the *Et*-INV strain was used. In order to shunt the natural excystation step *in vivo*, chickens were artificially infected by the cloacal route with 10^6 sporozoites. After 16 h of infection, chickens were euthanized; caeca were removed and washed for measurement of the nano-luciferase activity (Promega). To investigate the parasite development in these conditions, chickens were cloacally infected with a lower dose of *Et*-INRAE sporozoites (8×10^4). At day 7 post-infection, chickens were euthanized and caeca were removed. Oocyst numbers in caecal contents were determined and caecal tissues were fixed or frozen as described above.

Sporozoite Excystation Test

For *ex vivo* sporozoite excystation test, the bile from the gall bladder and intestinal contents from different segments of the intestine of non-infected germ-free and conventional non-infected chickens were collected. Only intestinal contents were centrifuged at 7,000 g for 15 min. Intestinal supernatants (dilution 1/10 in PBS) and bile (dilution 1/100 in PBS) were incubated at 41°C for 30 min to 1h30 with sporocysts obtained as described by (Shirley, 1995). As a control, the standard excystation medium described above was used. The number of sporocysts and excysted sporozoites were counted and the excystation efficiency was calculated as follows: (number of excysted sporozoites/2)/[(number of excysted sporozoites/2) + number of sporocysts)] x 100.

Histological Analysis

Caecal tissues were collected, fixed in 4% formaldehyde (Laurypath) and embedded in paraffin wax (Leica). Tissue sections were stained with kit Masson Trichrome, light green variation (RAL diagnostics) or Hemalun Eosin Saffron.

RT-qPCR

Total RNA was isolated from caeca using TRIzol extraction (Life Technologies, Carlsbad, CA, USA). cDNA was synthetized using M-MLV Reverse Transcriptase (Promega, Madison, WI, USA), with random hexamer primers and oligo(dT)15 primer (Promega). cDNAs were then amplified by qPCR (CFX96, Bio-Rad, Hercules, CA, USA) using iQ™ SYBR® Green Supermix (Bio-Rad). Parasite load into caecal tissues was determined using specific primers to the *E. tenella* housekeeping genes *Et18S*, *Etprofilin* and *Gallus gallus* housekeeping genes *g10* and *gapdh* (**Table 1**). *Et18S* is commonly used as a housekeeping gene during the parasite cycle (Walker et al., 2015); we added *Etprofilin* for which the expression was not modified in our experiment (data not shown). Microgamete and macrogamete gene expressions were determined using *Etfoa1*, (microgamete-specific gene; ETH_00025255) and *Etgam56*, (macrogamete-specific gene, ETH_00007320) both obtained from ToxoDB release 34 (**Table 1**; Eurogentec, Seraing, Belgium) and the previously cited *E. tenella* housekeeping genes. The protocol used for qPCR was: 95°C for 5 min and 40 cycles at 95°C for 10 s and 60°C for 15 s followed by 60°C for 5 s. Melting curves were performed at 60°C for 5 s followed by gradual heating (0.5°C/s) to 95°C. qPCR were performed in duplicate for each experiments. For parasite load, expression of *Et18S* and *Etprofilin* were normalized to Ct values obtained for *Gallus gallus g10 and gapdh* using the formula: $2^{-(\text{Ct mean of } Et \text{ housekeeping genes} - \text{Ct mean of } gallus\ gallus \text{ housekeeping genes})}$. For parasite microgamete and macrogamete gene expression, *Etgam56* and *Etfoa1* were normalized to Ct values obtained for *Et18S and Etprofilin*RNA using the formula: $2^{-(\text{Ct } Et \text{ gamete specific gene} - \text{Ct mean of } Et \text{ housekeeping genes})}$. Gene expression values are expressed as medians.

Nano Luciferase Activity

Caecal tissues were weighted, placed in lysis buffer (Tris 50 mM, EDTA 2 mM, Glycerol 10%, Triton X-100 1%) for 30 min at 4°C and then homogenized. After centrifugation (750 g, 5 min), 25 µl of supernatant were transferred to a 96-well plate and 25 µl of buffer with substrate (1/50) was added (Nano-Glo® Luciferase Assay System, Promega). Nano luciferase activity was measured using GloMax®-Multi Detection plate reader (Promega).

Statistical Analysis

Data were analyzed using GraphPad Prism® 6 (GraphPad Software Inc., La Jolla, CA, USA). For data with only two

TABLE 1 | Sequences of primers used for RT-qPCR.

Primer name	Accession number	Forward sequence (5' to 3')	Reverse sequence (5' to 3')
Et18S	18S rRNA gene in Supercontig190	CTGATGCATGCAACGAGTTT	GACCAGCCCCACAAAGTAAG
Etprofilin	ETH_00010645	GGAAGACGGAACCTCCATTT	CCAGAATCGCCACATCATAG
Etfoa1	ETH_00025255	TCTCGCATTCCTCACAGATG	ATTTCGCCTTGTGGATGAAC
Etgam56	ETH_00007320	AGTGGCTGGAGAACTTCGTG	ATGCGGTTCGTGATCATGTC
Gallus gallus g10	416492	TCAAGGAAGGGTACGCTACA	AACAGCCTCTGCATCCACAGT
Gallus gallus gapdh	374193	GTCCTCTCTGGCAAAGTCCAAG	CCACAACATACTCAGCACCTGC

groups of animals, a non-parametric Mann-Whitney test was performed. When more than two groups of chickens were compared, a non-parametric ANOVA followed by Dunn's multiple comparisons test was performed. When repeated measurements were performed, a non-parametric two-way ANOVA with multiple comparisons test was performed.

RESULTS

Effect of the Absence of Microbiota on Oocyst Load in Caecal Contents and on Parasite Developmental Stages in Caecal Tissue

To study the absence of microbiota on *E. tenella* infection, germ-free and conventional ROSS PM3 fast-growing broilers were infected with different doses of oocysts. The animals were euthanized and oocysts were counted in caecal contents at day 6, 7, and 9 days post-infection. We counted oocysts in caecal contents as it was technically not feasible to collect faeces daily for oocysts counts in our isolators and to maintain germ-free conditions concomitantly. Oocyst load were severely decreased in the caeca of germ-free chickens inoculated *per os* with a dose of 1,000 oocysts compared to conventional chickens at these different time points (day 6: 1,192-fold decrease; day 7: 269-fold decrease; day 9: 129-fold decrease). Remarkably, decreasing the dose of inoculum to 100 oocysts for conventional animals was not enough to decrease their parasite load in caecal contents to the level of germ-free animals 6 days post-infection when they were inoculated *per os* 1,000 or 10,000 or even 50,000 sporulated oocysts (**Figure 1A**). However, inoculation of 10,000 sporulated oocysts led to a similar parasite load in caecal contents at day 7 post-infection for both germ-free and conventional chickens (**Figure 1A**).

Interestingly, lower parasite load in caecal tissues of germ-free chickens was already observed as soon as day 2 post-infection (**Figure 1B**). Indeed, histological analysis revealed less first-generation schizonts at day 2 post-infection and less second-generation schizonts at day 3.5 post-infection in germ-free compared to conventional chickens. At this later time point, second-generation schizonts were clearly smaller, immature and second generation merozoites were not formed yet in germ-free chickens compared to conventional chickens in which the second-generation schizonts were mature with clearly developed merozoites (**Figure 2B**). This observation suggests a delay in the beginning of the parasite replication phase in the absence of microbiota (**Figure 2B**). We next studied the expression of gamete specific genes *Etfoa1* (for microgamete) and *Etgam56* (for macrogamete) (Walker et al., 2015). For this purpose, gamete gene expressions were normalized to the parasite housekeeping genes (*Etprofilin* and *Et18S*). We observed reduced *Etfoa1* and *Etgam56* gene expressions in germ-free compared to conventional chickens at day 5.5 post-infection (**Figure 2A**). This result was corroborated by histological analysis showing a higher number of parasites in the stage of gametes in conventional compared to germ-free chickens at this time point (**Figure 2B**). At day 7 post-infection, the expression of both *Etfoa1* and *Etgam56* were similar for both groups (**Figure 2A**). Histological analysis revealed that the number of gametes decreased in conventional chickens at day 7 post-infection (**Figure 2B**) and increased in germ-free chickens. These data suggest a delay in *E. tenella* development as a result of a longer asexual phase in germ-free compared to conventional chickens.

Bile From Germ-Free Chickens Increases Sporozoite Excystation

When sporulated oocysts are ingested by chickens, mechanic and enzymatic activities such as trypsin and biliary salts are

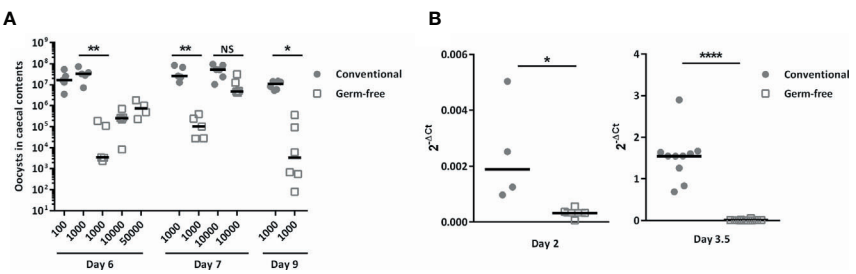

FIGURE 1 | The absence of microbiota reduced parasite load in caecal contents and in caecal tissues during infection. Conventional and germ-free chickens were orally infected with different doses of *E. tenella*. **(A)** Oocyst load in caecal contents. Oocyst load was evaluated at day 6, 7, and 9 post-infection. Medians are represented (One-Way ANOVA, Dunn's multiple comparisons test; n ≥ 4; *$P < 0.05$; **$P < 0.01$ between germ-free and conventional chickens). **(B)** The parasite load in caecal tissues is lower as soon as day 2 post-infection in germ-free chickens compared to conventional chickens. To be able to detect the parasite, conventional and germ-free chickens were orally infected with high doses of *E. tenella* (500,000 sporulated oocysts) for 2 days and 3.5 days of infection. The parasite load in caecal tissues was evaluated by RT-qPCR using the mean transcript expression of *Et18S* and *Etprofilin* relative to host housekeeping genes (*Gallus gallus gapdh* and *g10*) using the $2^{-\Delta Ct}$ formula: Ct *Et* housekeeping genes – Ct host housekeeping genes. Medians are represented (Mann-Whitney; n ≥ 4; *$P < 0.05$; ****$P < 0.0001$ between germ-free and conventional chickens).

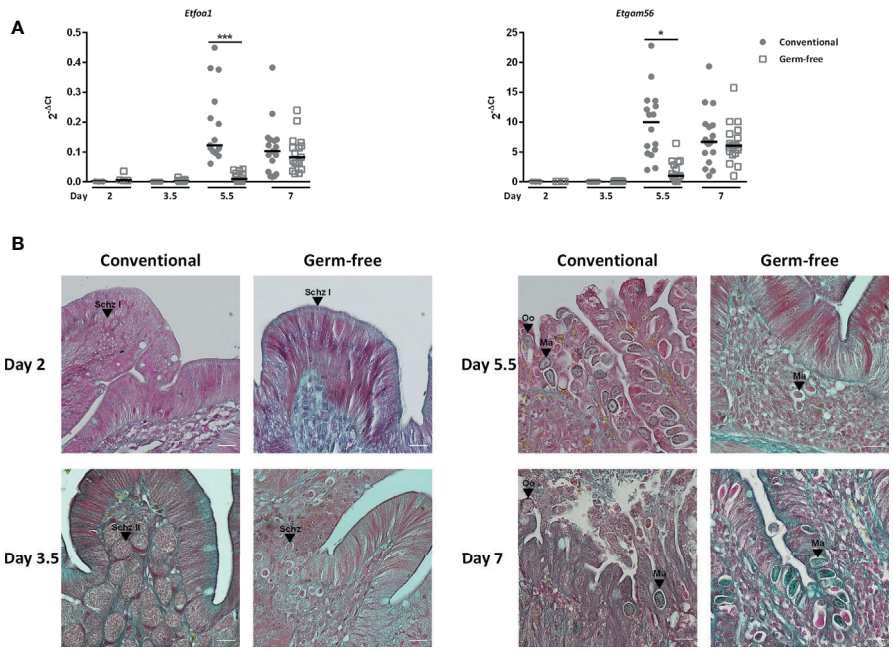

FIGURE 2 | The presence of immature second generation schizonts in germ-free chickens at day 3.5 post-infection suggests a delay in the development of the parasite. **(A)** Gametocyte gene expressions are delayed in germ-free chickens. Sporulated oocysts were orally inoculated to germ-free and conventional chickens (500,000 for 2 days and 10,000 for 3.5, 5.5, and 7 days of infection). Gametocyte gene expressions were detected by RT-qPCR on caecal tissues. The expression of microgamete and macrogamete specific genes (*Etfoa1* and *Etgam56)* were determined by RT-qPCR and expressed relative to *E. tenella* housekeeping genes (*Et18S* and *Etprofilin*) at day 2, 3.5, 5.5, and 7 post-infection using the $2^{-\Delta Ct}$ formula: Ct *Et* gametocyte specific gene – Ct *Et* housekeeping genes. Medians are represented (One-Way ANOVA, Dunn's multiple comparisons test; n ≥ 3; **P< 0.05; ***P <0.001* between germ-free and conventional chickens). **(B)** Representative histological images showing a delay in parasite development in germ-free chickens. Histological analysis was performed on tissue sections stained with Masson-Goldner Trichrome. Scale = 20 µm; Schz, schizont; Ma, macrogamete; Oo, oocyst.

necessary for sporozoite excystation. Sporozoites are then able to invade intestinal epithelial cells in which the parasite develops. Since lower parasite development in germ-free chickens may have resulted from a decrease in the excystation efficiency, we investigated the ability of sporozoites to excyst in the presence of intestinal contents and bile extracts from conventional and germ-free chickens. We then tested the activities of intestinal contents from specific segments of the gut and bile obtained from the gall bladder from germ-free and conventional chickens. We observed a higher excystation efficiency with duodenal and ileal supernatants combined with bile from germ-free chickens (**Figure 3**). To clarify the respective contribution of the intestinal content and the bile in this higher excystation efficiency, we used duodenal contents from germ-free or conventional chickens supplemented with bile from conventional, germ-free, or the standard excystation medium as a control. In these conditions, we observed a higher excystation efficiency when using duodenal contents from germ-free or conventional chickens combined with bile from germ-free chickens (**Figures 4A, B**). This result demonstrates that the higher excystation efficiency was likely to be related to the bile composition of germ-free chickens. However, this data cannot explain the lower parasite load observed caecal contents from germ-free compared to conventional chickens as a higher efficiency of excystation in germ-free chickens would be expected to lead to a higher infection rate.

The Absence of Gut Microbiota Alters the Development of the Parasite but Not Its Capacity to Invade the Caecal Mucosa

In order to study the effect of the absence of microbiota on sporozoite invasion *in vivo*, without the influence of the bile on the excystation efficiency, we shunted this process by cloacally infecting chickens with sporozoites excysted *in vitro*. Using *E. tenella* sporozoites expressing the *nano luciferase* reporter gene, we were able to determine parasite invasion level and showed that there was no difference in parasite invasion between conventional and germ-free chickens (**Figure 5A**). However, in the same experimental conditions when the animals were kept until day 7 post-infection, a decrease in oocyst load in caecal contents (280-fold) and in tissue parasite load revealed by RT-qPCR and histological analysis were observed in germ-free compared to conventional chickens (**Figures 5B, C**). These results suggest a major role of the microbiota on the development of the parasite after the invasion process but not on the parasite invasion itself.

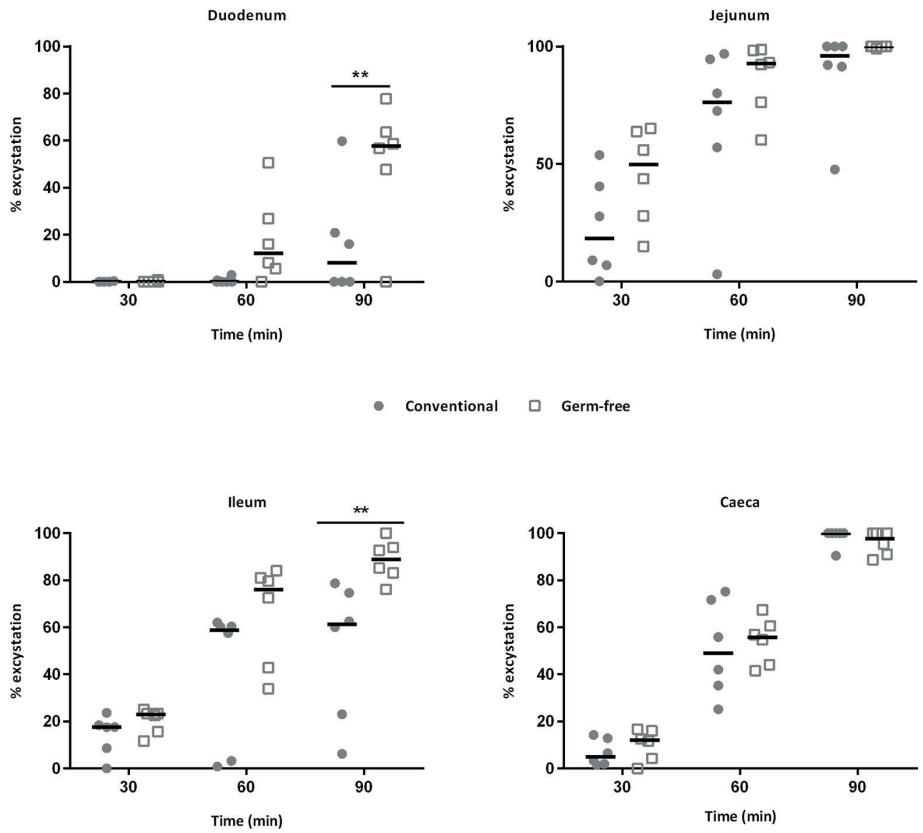

FIGURE 3 | The sporozoite excystation efficiency is increased with bile and duodenum or ileum contents from germ-free chickens. Sporozoites were excysted using contents of different segments of the intestine and bile from the same animals (germ-free and conventional chickens). The excystation efficiency of sporozoites is higher when incubating sporocysts with duodenal, ileal contents and bile from germ-free chickens. Medians are represented (Two-Way ANOVA, Sidak multiple comparisons test; n = 6; $^{**}P < 0.01$ between germ-free and conventional chickens).

DISCUSSION

To study the effect of the microbiota on *E. tenella* infection, we used an original model of germ-free broilers that we recently developed in our facilities (Guitton et al., 2020). A previous study reported that a high dose of *E. tenella* inoculum administered *per os* (>10,000 sporulated oocysts) led to similar oocyst load in caecal contents in germ-free and conventional chickens (Visco and Burns, 1972a). This observation may have resulted from a crowding effect resulting in maximal oocyst production. Indeed, we confirmed these findings, but we observed that with a lower inoculation dose of 1,000 sporulated oocysts administered *per os*, germ-free chickens presented a significantly lower load in oocysts in caecal contents at three different time points over a 3 days period. A lengthening of the parasite life cycle was observed and characterized by a delay in the formation of first and second generation schizonts. In germ-free chickens, at day 3.5 post-infection, second generation schizonts were small and immature with merozoites that were not formed yet while in conventional chickens, second generation schizonts were large and mature with clearly developed merozoites as revealed by histological analysis. Consequently, this delay in the asexual phase development led to a delay in the formation of gametocytes. This delay observed by histological analysis was confirmed by the expression of gametocyte specific genes, *Etgam56* for macrogametes and *Etfoa1* for a flagellar outer arm protein 1 specific to microgametes at day 5.5 post-infection (Walker et al., 2015). This result suggests that a delay in the appearance of the gamogony stage associated to a reduced number of sexual stages most probably will result in a delayed and decreased oocyst load in germ-free chickens.

As we observed lower parasite load in caecal tissues at day 2 post-infection in germ-free chickens, we hypothesized that there could be an effect of the microbiota on the excystation step and/or in the invasion process. As excystation media used in laboratory to artificially excyst sporozoites from sporocyst contains biliary acids, we used bile from each animal. When assessing the ability of sporozoites to excyst from sporocysts, an increased excystation efficiency was observed when using bile from germ-free chickens suggesting a difference in its

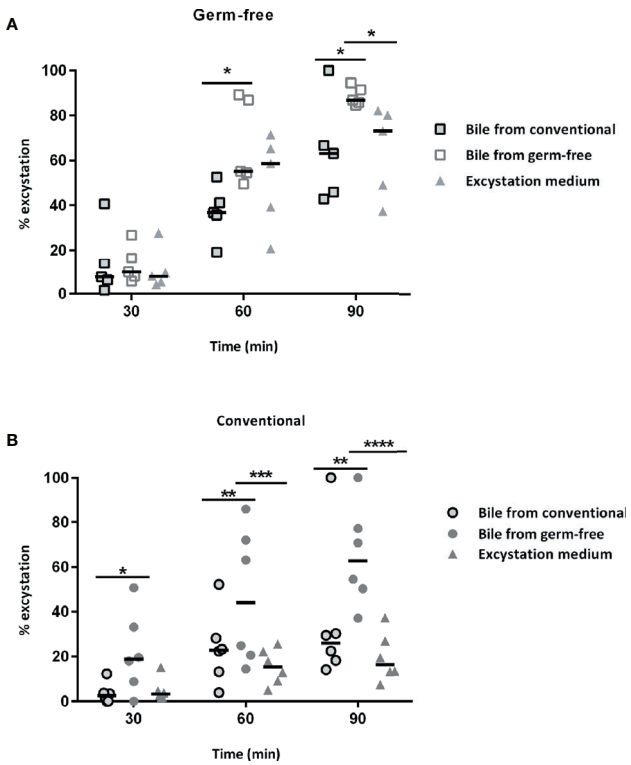

FIGURE 4 | The bile from germ-free chickens is responsible for the increase in the sporozoite excystation efficiency. **(A)** Bile from germ-free chicken leads to a higher excystation efficiency of sporozoites when incubating sporocysts with duodenal contents from germ-free chickens. Sporozoites were excysted when incubating sporocysts with duodenal contents from germ-free chickens and bile from conventional, germ-free chickens or excystation medium. Medians are represented (Two-Way ANOVA, Tukey multiple comparisons test; n = 5; **P < 0.05).*
(B) Bile from germ-free chicken leads to a higher excystation efficiency of sporozoites when incubating sporocysts with duodenal contents from conventional chickens. Sporozoites were excysted when incubating sporocysts with duodenal contents from conventional chickens and bile from conventional, germ-free chickens or the standard excystation medium. Medians are represented (Two-Way ANOVA, Tukey multiple comparisons test; n = 6; **P < 0.05; **P < 0.01; ***P < 0.001; ****P < 0.0001*).

composition. In animals, biliary acids are synthetized from cholesterol in the liver. Conjugated bile acids (primary bile acids) are secreted in the intestine and are involved in lipid absorption. The presence of bacteria in the luminal content leads to deconjugation and dehydroxylation reactions and then to the formation of unconjugated bile acids and secondary bile acids (Long et al., 2017). Consequently, in the absence of a microbiota, the composition of the bile is different with mainly conjugated bile acids found in caeca of germ-free animals. (Madsen et al., 1976). This change in the bile composition and in particular of the biliary acids may explain the higher efficiency of excystation of sporozoites in the presence of bile from germ-free chickens. However, higher excystation efficiency in the absence of microbiota cannot explain the lower parasite load in caecal contents and in tissues found in germ-free compared to conventional chickens.

We then sought to investigate the ability of sporozoites to invade the caecal mucosa of germ-free or conventional chickens by using cloacal inoculation with sporozoites in order to shunt the excystation step. The microbiota helps in the appropriate development and maturation of the gut-associated lymphoid organs in chickens (Hegde et al., 1982). However, we observed lower parasite load in caecal contents and in tissues in germ-free chickens suggesting that the lack of maturation of the immune system in the absence of microbiota is probably not involved. Indeed, the microbiota also leads to a mature intestinal mucosa including goblet cells and their mucin production (Rolls et al., 1978) (Cheled-Shoval et al., 2014). Despite the fact that the caecal mucosa of germ-free chickens may have different characteristics, we showed that the absence of microbiota did not modify the ability of sporozoites to invade the epithelium. However, when animals were cloacally infected and kept for 7 days, the oocyst load in caecal contents and the tissue parasite load were still lower in germ-free than in conventional chickens. Even though the dose of inoculum administered orally and cloacally cannot be easily compared, cloacal infection led to a decrease in oocyst load in caecal contents similar to the one observed with oral infection. This result demonstrates that the absence of microbiota alters the development of *E. tenella* but not the capacity of sporozoites to invade caecal epithelial cells.

The microbiota harbours a wide variety of bacteria which metabolize the nutrients of the digestive content and synthetizes metabolites that can act on the immune cells (Liu et al., 2019) and/or can be critical for parasite growth. As *Eimeria* infection disrupts carbon and nitrogen metabolism (Huang et al., 2018b), the parasite is likely to require some metabolites issued at least from these two biochemical pathways. We hypothesize that some metabolites synthetized by the microbiota might be critical substrates for parasite replication and are present in reduced amount in germ-free chickens to allow its normal growth. Alternatively, these metabolites can affect parasite host cell metabolism, the lining of intestinal epithelial cells, the mucosae and indirectly the development of the parasite. Further studies will be performed to compare the precise composition of metabolites in caecal contents from germ-free and conventional chickens and to identify molecules that are important for the development of the parasite.

In conclusion, we revealed that the absence of microbiota alters the development of *E. tenella*. Strategies to modulate the composition of the microbiota and its metabolism would be of interest to inhibit parasite replication and/or to stimulate the immune response. As nutrition factors can play a major role in intestinal health and more particularly on its microbiota, it could have a beneficial effect on the outcome of the disease. Notably, innovative nutritional approaches or probiotics are societal acceptable approaches in face of growing parasite resistance to anticoccidials and lack of cost-effective prophylaxis.

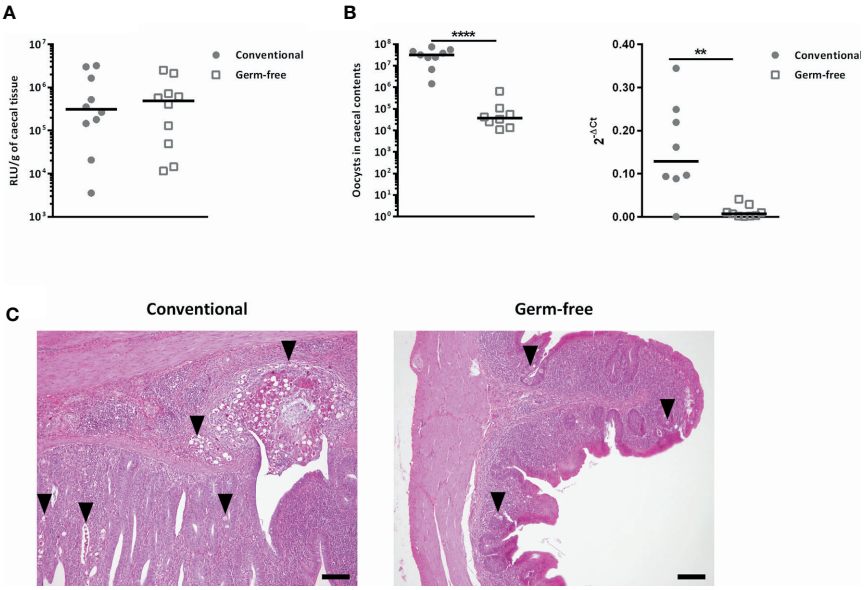

FIGURE 5 | The absence of gut microbiota has no effect on *E. tenella* sporozoite invasion capacity but alters its development. **(A)** The absence of microbiota had no effect on *E. tenella* sporozoite invasion capacity. Conventional and germ-free chickens were cloacally inoculated with *E. tenella* sporozoites expressing a *nano luciferase* reporter gene (10^6 sporozoites per animal). Caecal tissues were washed in PBS and luciferase activity was detected 16 h post-infection. Medians are represented (Mann-Whitney; n = 10; non-significant). No significant differences between germ-free and conventional chickens were observed. **(B)** The absence of microbiota alters the development of *E. tenella*. Conventional and germ-free chickens were cloacally inoculated with *Et*-INRAE sporozoites (8×10^4). *On the left panel*: Oocysts were counted in caecal contents at day 7 post-infection. *On the right panel*: the parasite load in caecal tissues at day 7 post-infection was determined by RT-qPCR. The expression of housekeeping parasite specific genes, *Et18S* and *Etprofilin* were expressed relative to *Gallus gallus* housekeeping genes *g10* and *gapdh* using the $2^{-\Delta Ct}$ formula: Ct *Et* housekeeping genes – Ct host housekeeping genes. Medians are represented (Mann-Whitney; $n \geq 8$; $^{**}P < 0.01$; $^{****}P < 0.0001$ between germ-free and conventional chickens). **(C)** Representative histological images at day 7 post-infection showing lower parasite load in caecal tissues in germ-free chickens compared to conventional chickens. Histological analysis was performed on tissue sections stained with Hemalun Eosin Saffron; scale = 100 µm.

DATA AVAILABILITY STATEMENT

The raw data supporting the conclusions of this article will be made available by the authors, without undue reservation.

ETHICS STATEMENT

The animal study was reviewed and approved by CEEA Val de Loire n°19; 2018-04-26 (APAFIS N°13904).

AUTHOR CONTRIBUTIONS

FB designed the experiments. PG, GS, GF, ASa, AN, and FB performed the experiments. EG provided the conventional and germ-free chickens. CS and NL performed the bacteriological controls. AN provided the transgenic parasite Et-INV. CR, NL, TL performed the histology on tissues. FB, PG, GS analyzed the data. FB, PG, GS, SL-L, FL, CS discussed the data. FB, GS, ASi, SL-L, FL, RG, CS, wrote and/or reviewed the manuscript. All authors contributed to the article and approved the submitted version.

FUNDING

This study was funded by the Région Centre Val de Loire, France (APR-IA "INTEGRITY" 2017-2019).

ACKNOWLEDGEMENTS

We are thankful to T. Chaumeil, M. Renouard, S. Lavillatte, P. Cousin, A. Faurie, O. Dubes, M. Girault from the Infectiology of Farm, Model and Wildlife Animals Facility (PFIE), for the animal care and skills with the animal experiments. The authors are grateful to the breeders and the society Boyé accouvage (La Boissière en Gâtine, France) for the supply of fertilized eggs. We also acknowledge Y. Le Vern for flow cytometry sorting of transgenic oocysts (INRAE, Université de Tours, UMR ISP, Platform IMI, F-37380, Nouzilly, France). We are grateful to P. Quéré (INRAE, Université de Tours, UMR ISP F-37380, Nouzilly, France) who kindly reviewed and gave suggestions for the manuscript.

REFERENCES

Al-Sheikhly, F., and Al-Saieg, A. (1980). Role of coccidia in the occurrence of necrotic enteritis of chickens. *Avian Dis.* 24, 324–333. doi: 10.2307/1589700

Blake, D. P., Knox, J., Dehaeck, B., Huntington, B., Rathinam, T., Ravipati, V., et al. (2020). Re-calculating the cost of coccidiosis in chickens. *Vet. Res.* 51, 115. doi: 10.1186/s13567-020-00837-2

Bradley, R. E., and Radhakrishnan, C. V. (1973). Coccidiosis in chickens: obligate relationship between *Eimeria tenella* and certain species of cecal microflora in the pathogenesis of the disease. *Avian Dis.* 17, 461–476. doi: 10.2307/1589145

Cheled-Shoval, S. L., Gamage, N. S., Amit-Romach, E., Forder, R., Marshal, J., Van Kessel, A., et al. (2014). Differences in intestinal mucin dynamics between germ-free and conventionally reared chickens after mannan-oligosaccharide supplementation. *Poult. Sci.* 93, 636–644. doi: 10.3382/ps.2013-03362

Cirimotich, C. M., Dong, Y., Clayton, A. M., Sandiford, S. L., Souza-Neto, J. A., Mulenga, M., et al. (2011a). Natural microbe-mediated refractoriness to *Plasmodium* infection in *Anopheles gambiae*. *Science* 332, 855–858. doi: 10.1126/science.1201618

Cirimotich, C. M., Ramirez, J. L., and Dimopoulos, G. (2011b). Native microbiota shape insect vector competence for human pathogens. *Cell Host Microbe* 10, 307–310. doi: 10.1016/j.chom.2011.09.006

Crhanova, M., Hradecka, H., Faldynova, M., Matulova, M., Havlickova, H., Sisak, F., et al. (2011). Immune response of chicken gut to natural colonization by gut microflora and to *Salmonella enterica* serovar enteritidis infection. *Infect. Immun.* 79, 2755–2763. doi: 10.1128/IAI.01375-10

Ferguson, D. J., Belli, S. I., Smith, N. C., and Wallach, M. G. (2003). The development of the macrogamete and oocyst wall in *Eimeria maxima*: immuno-light and electron microscopy. *Int. J. Parasitol.* 33, 1329–1340. doi: 10.1016/S0020-7519(03)00185-1

Ganas, P., Liebhart, D., Glosmann, M., Hess, C., and Hess, M. (2012). *Escherichia coli* strongly supports the growth of *Histomonas meleagridis*, in a monoxenic culture, without influence on its pathogenicity. *Int. J. Parasitol.* 42, 893–901. doi: 10.1016/j.ijpara.2012.07.007

Guitton, E., Faurie, A., Lavillatte, S., Chaumeil, T., Gaboriaud, P., Bussiere, F., et al. (2020). Production of germ-free fast-growing broilers from a commercial line for microbiota studies. *J. Vis. Exp.* 18 (160), e61448. doi: 10.3791/61148

Hegde, S., Rolls, B. A., Turvey, A., and Coates, M. E. (1982). Influence of gut microflora on the lymphoid tissue of the chicken (*Gallus domesticus*) and japanese quail (*Coturnix coturnix japonica*). *Comp. Biochem. Physiol.* 72A, 205–209. doi: 10.1016/0300-9629(82)90034-2

Huang, G., Tang, X., Bi, F., Hao, Z., Han, Z., Suo, J., et al. (2018a). *Eimeria tenella* infection perturbs the chicken gut microbiota from the onset of oocyst shedding. *Vet. Parasitol.* 258, 30–37. doi: 10.1016/j.vetpar.2018.06.005

Huang, G., Zhang, S., Zhou, C., Tang, X., Li, C., Wang, C., et al. (2018b). Influence of *Eimeria falciformis* infection on gut microbiota and metabolic pathways in mice. *Infect. Immun.* 86 (5), e00073-18. doi: 10.1128/IAI.00073-18

Lafont, J. P., Yvore, P., Bree, A., and Peloille, M. (1975). Pathogenic effect of *Eimeria tenella* and *Eimeria acervulina in* axenic and monoxenic chickens. *Ann. Rech. Vet.* 6 (1), 35–42.

Laurent, F., Mancassola, R., Lacroix, S., Menezes, R., and Naciri, M. (2001). Analysis of chicken mucosal immune response to *Eimeria tenella* and *Eimeria maxima* infection by quantitative reverse transcription-PCR. *Infect. Immun.* 69, 2527–2534. doi: 10.1128/IAI.69.4.2527-2534.2001

Liu, Y., Tian, X., He, B., Hoang, T. K., Taylor, C. M., Blanchard, E., et al. (2019). *Lactobacillus reuteri* DSM 17938 feeding of healthy newborn mice regulates immune responses while modulating gut microbiota and boosting beneficial metabolites. *Am. J. Physiol. Gastrointest. Liver Physiol.* 317, G824–G838. doi: 10.1152/ajpgi.00107.2019

Long, S. L., Gahan, C. G. M., and Joyce, S. A. (2017). Interactions between gut bacteria and bile in health and disease. *Mol. Aspects Med.* 56, 54–65. doi: 10.1016/j.mam.2017.06.002

Macdonald, S. E., Nolan, M. J., Harman, K., Boulton, K., Hume, D. A., Tomley, F. M., et al. (2017). Effects of *Eimeria tenella* infection on chicken caecal microbiome diversity, exploring variation associated with severity of pathology. *PloS One* 12, e0184890. doi: 10.1371/journal.pone.0184890

Madsen, D., Beaver, M., Chang, L., Bruckner-Kardoss, E., and Wostmann, B. (1976). Analysis of bile acids in conventional and germ-free rats. *J. Lipid Res.* 17, 107–111. doi: 10.1016/S0022-2275(20)36993-5

Oakley, B. B., Lillehoj, H. S., Kogut, M. H., Kim, W. K., Maurer, J. J., Pedroso, A., et al. (2014). The chicken gastrointestinal microbiome. *FEMS Microbiol. Lett.* 360, 100–112. doi: 10.1111/1574-6968.12608

Qi, Z., Shi, S., Tu, J., and Li, S. (2019). Comparative metagenomic sequencing analysis of cecum microbiotal diversity and function in broilers and layers. *3 Biotech.* 9, 316. doi: 10.1007/s13205-019-1834-1

Rolls, B. A., Turvey, A., and Coates, M. E. (1978). The influence of the gut microflora and of dietary fibre on epithelial cell migration in the chick intestine. *Br. J. Nutr.* 39, 91–98. doi: 10.1079/BJN19780015

Shirley, M. W. (1995). *Eimeria* species and strains of chicken. *Biotechnology-Guidelines Techniques Coccidiosis Res. Luxembourg Eur. Commission DGXII*, 1–24.

Stecher, B., Chaffron, S., Kappeli, R., Hapfelmeier, S., Freedrich, S., Weber, T. C., et al. (2010). Like will to like: abundances of closely related species can predict susceptibility to intestinal colonization by pathogenic and commensal bacteria. *PloS Pathog.* 6, e1000711. doi: 10.1371/journal.ppat.1000711

Swale, C., Bougdour, A., Gnahoui-David, A., Tottey, J., Georgeault, S., Laurent, F., et al. (2019). Metal-captured inhibition of pre-mRNA processing activity by CPSF3 controls *Cryptosporidium* infection. *Sci. Transl. Med.* 11 (517), eaax7161. doi: 10.1126/scitranslmed.aax7161

Visco, R. J., and Burns, W. C. (1972a). *Eimeria tenella* in bacteria-free and conventionalized chicks. *J. Parasitol.* 58, 323–331. doi: 10.2307/3278096

Visco, R. J., and Burns, W. C. (1972b). *Eimeria tenella* in bacteria-free chicks of relatively susceptible strains. *J. Parasitol.* 58, 586–588. doi: 10.2307/3278209

Walker, R. A., Sharman, P. A., Miller, C. M., Lippuner, C., Okoniewski, M., Eichenberger, R. M., et al. (2015). RNA Seq analysis of the *Eimeria tenella* gametocyte transcriptome reveals clues about the molecular basis for sexual reproduction and oocyst biogenesis. *BMC Genomics* 16, 94. doi: 10.1186/s12864-015-1298-6

Wei, S., Morrison, M., and Yu, Z. (2013). Bacterial census of poultry intestinal microbiome. *Poult. Sci.* 92, 671–683. doi: 10.3382/ps.2012-02822

Yan, W., Liu, X., Shi, T., Hao, L., Tomley, F. M., and Suo, X. (2009). Stable transfection of *Eimeria tenella*: constitutive expression of the YFP-YFP molecule throughout the life cycle. *Int. J. Parasitol.* 39, 109–117. doi: 10.1016/j.ijpara.2008.06.013

Yang, X., Brisbin, J., Yu, H., Wang, Q., Yin, F., Zhang, Y., et al. (2014). Selected lactic acid-producing bacterial isolates with the capacity to reduce *Salmonella* translocation and virulence gene expression in chickens. *PloS One* 9, e93022. doi: 10.1371/journal.pone.0093022

Conflict of Interest: The authors declare that the research was conducted in the absence of any commercial or financial relationships that could be construed as a potential conflict of interest.

frontiers in Cellular and Infection Microbiology

REVIEW
published: 22 February 2021
doi: 10.3389/fcimb.2021.634610

A Protective and Pathogenic Role for Complement During Acute *Toxoplasma gondii* Infection

Patricia M. Sikorski[1,2†], *Alessandra G. Commodaro*[1] *and Michael E. Grigg*[1*]

[1] Molecular Parasitology Section, Laboratory of Parasitic Diseases, National Institute of Allergy and Infectious Diseases, National Institutes of Health, Bethesda, MD, United States, [2] Department of Microbiology and Immunology, Georgetown University Medical Center, Georgetown University, Washington, DC, United States

OPEN ACCESS

Edited by:
Chandra Ramakrishnan, University of Zurich, Switzerland

Reviewed by:
Eric Y. Denkers, University of New Mexico, United States
Carsten Lüder, Universitätsmedizin Göttingen, Germany

***Correspondence:**
Michael E. Grigg
griggm@niaid.nih.gov

†Present address:
Patricia M. Sikorski, Department of Neurology, George Washington University, Washington, DC, United States

Specialty section:
This article was submitted to Parasite and Host, a section of the journal Frontiers in Cellular and Infection Microbiology

Received: 28 November 2020
Accepted: 06 January 2021
Published: 22 February 2021

Citation:
Sikorski PM, Commodaro AG and Grigg ME (2021) A Protective and Pathogenic Role for Complement During Acute Toxoplasma gondii Infection. Front. Cell. Infect. Microbiol. 11:634610. doi: 10.3389/fcimb.2021.634610

The infection competence of the protozoan pathogen *Toxoplasma gondii* is critically dependent on the parasite's ability to inactivate the host complement system. *Toxoplasma* actively resists complement-mediated killing in non-immune serum by recruiting host-derived complement regulatory proteins C4BP and Factor H (FH) to the parasite surface to inactivate surface-bound C3 and limit formation of the C5b-9 membrane attack complex (MAC). While decreased complement activation on the parasite surface certainly protects *Toxoplasma* from immediate lysis, the biological effector functions of C3 split products C3b and C3a are maintained, which includes opsonization of the parasite for phagocytosis and potent immunomodulatory effects that promote pro-inflammatory responses and alters mucosal defenses during infection, respectively. In this review, we discuss how complement regulation by *Toxoplasma* controls parasite burden systemically but drives exacerbated immune responses locally in the gut of genetically susceptible C57BL/6J mice. In effect, *Toxoplasma* has evolved to strike a balance with the complement system, by inactivating complement to protect the parasite from immediate serum killing, it generates sufficient C3 catabolites that signal through their cognate receptors to stimulate protective immunity. This regulation ultimately controls tachyzoite proliferation and promotes host survival, parasite persistence, and transmissibility to new hosts.

Keywords: complement, *Toxoplasma gondii*, C4BP, factor H, regulation, immune evasion

INTRODUCTION

Insect and vertebrate complement systems play critical roles in the defense against invading microbial pathogens and the regulation of inflammatory responses. Apicomplexan parasites, which comprise a diverse group of obligatory intracellular parasites, have evolved sophisticated strategies to regulate or inactivate this humoral first line of defense to promote their infection competency in both insects and mammalian hosts (Belachew, 2018; Shao et al., 2019). These parasites possess complex lifecycles consisting of both sexual and asexual stages that typically infect multiple hosts, and so, must overcome a myriad of species-specific immune defenses in order to initiate infection. The most studied among these parasites include *Toxoplasma*, *Cryptosporidium*, *Eimeria*, and *Plasmodium*, which cause various

infectious diseases of human and veterinary importance (Votýpka et al., 2017). This paper reviews the strategies employed by *Toxoplasma gondii* to both inactivate and regulate the complement cascade and highlights similar strategies employed by other Apicomplexan parasites to facilitate the establishment of a persistent, transmissible infection.

THE COMPLEMENT SYSTEM

The complement system is an evolutionarily conserved first line of defense that rapidly activates against invading pathogens. This defense system consists of a set of circulating liver-derived soluble proteins, membrane bound receptors, and regulators that function in a highly coordinated proteolytic cascade to opsonize and lyse invading microbes in addition to mobilizing the cellular arm of the immune response (**Figure 1**—schematic of complement system pathway activation and regulation). Activation of this cascade of more than 50 molecules and their complement receptors occur *via* three different pathways: the classical (CP), lectin (LP), and alternative (AP) pathways. Activation of these pathways leads to the formation of pathway-specific complexes known as C3 convertases, in which all three pathways converge to facilitate the cleavage of the central molecule C3 into effector proteins C3a and C3b. Successful complement activation culminates in the assembly of a pore-forming protein on the pathogen surface (referred to as the membrane attack complex, or MAC) that mediates pathogen lysis.

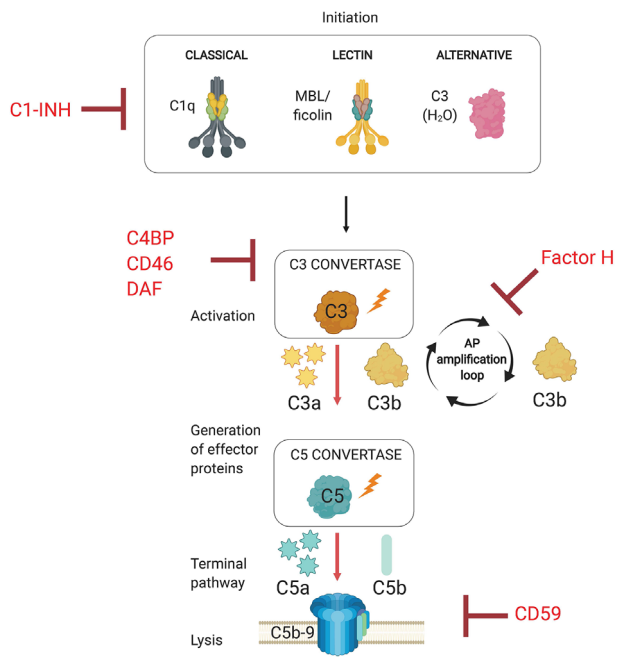

FIGURE 1 | Overview of the Complement System. The complement system is activated *via* three separate pathways (classical, lectin, and alternative) that have distinct recognition mechanisms (C1q, MBL/ficolins, and C3b(H_2O), respectively). Complement activation results in the formation of C3 convertases. All three pathways converge at C3 activation *via* C3 convertases, which generates effector molecules C3a and C3b. C3b allows for progression to the terminal pathway by forming C5 convertases, which cleave C5 into C5a and C5b. The terminal pathway requires C5 activation product C5b to initiate the assembly of the membrane attack complex (MAC, C5b-9). The pore inserts into the cell membrane and promotes pathogen lysis. Complement regulators target complement pathway initiation (C1-INH, C1 esterase inhibitor), convertase formation (C4BP, C4b-binding protein; CD46; DAF, decay accelerating factor), and the alternative pathway amplification loop (Factor H).

The complement system is activated upon detection of invading pathogens through specialized and pathway-specific recognition molecules that recognize pathogen-associated molecular patterns (PAMPs). Initiation of the classical pathway requires the recognition of pathogen bound IgM or IgG by pattern recognition molecule C1q. The lectin pathway is activated when microbial sugars are bound by the pattern recognition molecule mannose-binding lectin (MBL). The alternative pathway, however, does not rely on a recognition molecule for activation, but rather on the failure to regulate the continuous low-level spontaneous hydrolysis of C3 into C3(H_2O), which indiscriminately probes foreign and self surfaces alike. The ability of the AP to discriminate between self and non-self surfaces relies on the presence of membrane bound and soluble complement regulatory proteins. Importantly, the AP is a critical component of host defense because it amplifies the complement response independent of the pathway that initiates the response, so it represents a critical target for regulation by host and pathogens alike. Specifically, the AP utilizes CP and LP activated C3b as a platform for rapidly generating new AP C3 convertases which establishes a positive feedback loop to amplify C3 cleavage (Thurman and Holers, 2006). Due to its non-discriminatory nature and potential for rapid amplification, this process must necessarily be tightly controlled by host regulator proteins to limit inflammation and damage to host cells. Complement regulators target various points within the proteolytic cascade, which includes inactivation of proteases associated with C1q and mannose binding lectin (MBL), cleavage of active C3b into inactive iC3b and C3dg, accelerating the decay of C3 and C5 convertases, and preventing insertion of the membrane attack complex into the plasma membrane (Schmidt et al., 2016).

Protection against pathogens occurs when the complement system produces several biologically active effector molecules, which include opsonins (C3b and its catabolites iC3b, C3d and C3dg), anaphylatoxins (C3a and C5a), and the membrane attack complex (MAC). The most direct effector function is the lysis of pathogens through MAC. Because many pathogens have evolved mechanisms to limit complement activation and prevent the progression of the cascade, generation of C3b and anaphylatoxins ensure additional layers of immune defense. These effector functions are exerted by the interaction between complement split product effectors and their host receptors to facilitate biological processes such as phagocytosis, chemotaxis, and inflammation (**Figure 2A**). In the absence of antibodies, C3b and its catabolites (iC3b, C3d, and C3dg) function as major opsonins recognized by complement receptors 1, 3, and 4 (CR1, CR3, CR4) that are expressed on myeloid cells and aid in phagocytosis and pathogen

clearance. Anaphylatoxins C3a and C5a are critical danger signals that exert their function through interactions with cognate receptors C3aR and C5aR expressed on both immune and non-immune cells. Signaling through these receptors induces several critical pro-inflammatory immunological responses, including chemotaxis, oxidative burst, immune cell activation, vasodilation and induction of cytokines (Klos et al., 2009). Complement split products also play a critical role in bridging innate immunity and adaptive immunity (**Figure 2B**). For example, C3b inactivation products C3dg and C3d covalently linked to antigen are recognized by complement receptor 2 (CR2, CD21) expressed on B cells. Co-ligation of CR2 with the B cell receptor (BCR) *via* C3d-antigen complexes amplifies B cell signaling, lowers the threshold for B cell activation, and thus this interaction is critical for enhancing B cell responses (Carroll, 2008). Recent work has also implicated local intracellular complement activation and the subsequent production of anaphylatoxins (C3a, C5a) during cognate interactions between antigen presenting cells (APCs) and CD4+ T cells (Heeger et al., 2005; Strainic et al., 2008). Upregulation of and signaling through cognate receptors C3aR and C5aR have been shown to regulate T cell activation, lineage commitment and proinflammatory Th1 cytokine production (Strainic et al., 2008; Liszewski et al., 2013).

COMPLEMENT ACTIVATION AND RESISTANCE: THE APICOMPLEXA

Apicomplexan parasites, not unlike bacteria, viruses, and fungi, activate the complement system. Complement evasion is a critical step in the establishment of infection, hence parasites have evolved multiple sophisticated strategies to overcome serum killing. Mechanisms of parasite complement evasion include the recruitment of host regulators by parasite surface molecules, expression of complement regulator protein orthologs, and expression of parasite-encoded proteins that target and/or inactivate complement function (recently reviewed by Shao et al., 2019).

While parasites share common evasion strategies, these mechanisms are achieved by unique parasite-specific factors. *Plasmodium* spp. evades both mosquito and human complement systems to facilitate the survival and transmission of the parasite from vector to host. Genetic studies have identified the 6-CYS protein Pfs47 as a critical factor facilitating parasite transmission in mosquitos by its ability to regulate the insect complement-like immune system (Molina-Cruz et al., 2013). Additional recently identified parasite factors that recruit human regulator Factor H to facilitate C3b inactivation include pfGAP50 expressed by gametes in the mosquito midgut and Pf92 expressed during the blood-stage (Simon et al., 2013; Kennedy et al., 2016). In addition, parasites bind plasminogen during the intraerythrocytic stage and mediate its conversion to plasmin in order to inactivate C3b, however the parasite factor(s) that facilitate this interaction have not been determined (Reiss et al., 2021).

Complement evasion by *Cryptosporidium* and *Toxoplasma*, on the contrary, is less extensively studied. While studies have established that *Cryptosporidium parvum* binds C3 and classical (C1q) and lectin (mannose-binding lectin, MBL) pathway molecules (Petry et al., 2008), little is known about resistance mechanisms. Our group has confirmed earlier work demonstrating that *Toxoplasma* inactivates C3 (Fuhrman and Joiner, 1989; Sikorski et al., 2020) but the precise molecular details have only recently been elucidated. We utilized improved strategies to study complement interactions with *T. gondii* using flow cytometry, leading to a significant advancement in our understanding of complement activation and regulation by *T. gondii*. Our work has for the first time revealed important contributions of the lectin pathway as well as parasite genotype to

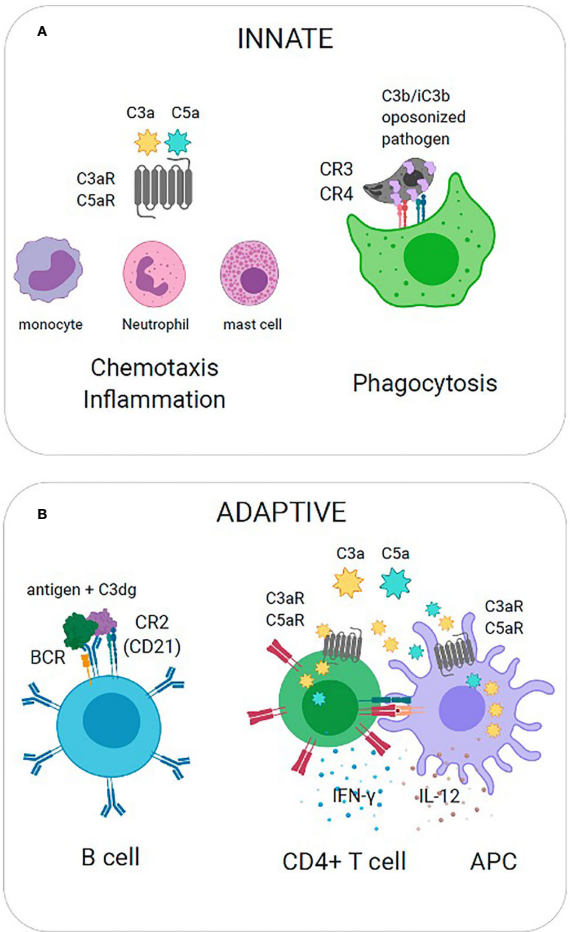

FIGURE 2 | Effector Functions of Complement Split Products. **(A)** Innate immunity. (Left) C3a is recognized by cognate receptor C3aR to mediate recruitment of innate immune cells (mast cells, monocytes, neutrophils) and promote inflammation. (Right) C3b is covalently coupled to pathogen surfaces and promotes opsonization. C3b is recognized by complement receptors (CR3, CR4) to promote phagocytosis. **(B)** Adaptive immunity. (Left) Co-ligation of complement receptor 2 with the B cell receptor (BCR) on B cells *via* C3dg-antigen complexes amplifies B cell signaling and lowers the threshold for B cell activation. (Right) The local activation and secretion of complement anaphylatoxins (C3a, C5a) and upregulation of cognate receptors (C3aR, C5aR) is triggered during T cell-APC interactions. Autocrine and paracrine signaling through C3aR and C5aR promote Th1 cytokine production (IL-12, IFN).

complement activation. Our studies showed strain-specific differences in C3b deposition between Type I and Type II strains that was partially attributed to the differences in surface glycans and lectin pathway activation, indicating that increased C3b deposition on Type II strains correlated with greater lectin binding and MBL recognition. However, despite these differences, both strains were equally capable of inactivating C3b and were resistant to serum killing. Our data showed that resistance to serum killing was due to the ability of *T. gondii* to recruit the alternative pathway regulator Factor H (FH) and classical and lectin pathway regulator C4b-binding protein (C4BP) to the parasite cell surface (Fuhrman and Joiner, 1989; Sikorski et al., 2020). The importance of the alternative pathway was highlighted by its critical role mediating serum resistance, irrespective of its limited contribution in the initiation of the complement system. Our studies demonstrated that blocking Factor H, but not C4BP, resulted in greater C5b-9 deposition and greater parasite susceptibility to serum killing, suggesting that the AP functions principally as a potent mediator that amplifies complement activation and is thus an important target for *T. gondii* regulation. Although the *T. gondii* parasite factor(s) that bind C3b, FH, and C4BP have not been identified, their discovery would directly address the role of individual and cumulative parasite factors in the molecular basis of protection against serum killing, and would further provide an opportunity to unearth potential targets for therapeutic intervention to render parasites more susceptible to complement attack. Collectively, these studies demonstrate how apicomplexan parasites employ multiple strategies to target C3 in order to successfully resist serum killing.

COMPLEMENT: PROTECTIVE AND PATHOLOGICAL ROLE DURING *T. GONDII* INFECTION

Toxoplasma gondii is a highly prevalent and successful protozoan parasite that can infect any nucleated cell in all mammals. Non felid, intermediate hosts acquire *T. gondii* by ingesting oocysts from contaminated water or food, or by eating infected meat containing tissue cysts. Upon ingestion, parasites excyst and invade the intestinal epithelium where they differentiate and rapidly replicate asexually as tachyzoites. The parasites then disseminate systemically to distal organs to mediate acute infection before establishing a chronic infection by the formation of tissue cysts (Dubey et al., 1997). The pathogenic tachyzoite form can be easily grown *in vitro* and chronic stages can be maintained in animal models, thus mice represent an experimentally tractable model system optimal for studying this host-pathogen interaction.

Until recently, *T. gondii* complement resistance mechanisms and the biological significance of the complement system *in vivo* during acute infection were unknown. The role of complement during systemic *T. gondii* intraperitoneal infection was recently evaluated using complement deficient C57BL/6 mice. In the absence of C3, mice died acutely and exhibited higher parasite loads whereas control mice survived. This study demonstrated that both the presence of C3 as well as the parasite's ability to inactivate C3 are important factors regulating parasite proliferation and contributing to host survival *in vivo* (Sikorski et al., 2020). One limitation of using C3 deficient animals is that the protective effect observed could not be specifically assigned to either C3a or C3b split product effector function (Sikorski et al., 2020). The observed reduction in *T. gondii*-specific antibodies in this model was, however, consistent with the known function of C3dg tagged antigen to enhance humoral responses (Sikorski et al., 2020), suggesting that C3b opsonization of *T. gondii* antigen is critical for priming humoral immunity. Importantly, this study suggested that *T. gondii* strikes a critical balance in fine tuning complement system activation, by evading serum killing to promote parasite persistence, while preserving the ability of complement effectors C3a and C3b to activate sufficient host immunity to regulate parasite proliferation and promote both host survival and parasite transmissibility.

Other studies have attempted to elucidate the role of anaphylatoxin signaling in acute *T. gondii* infection. Anaphylatoxin signaling has been implicated in regulating Th1 responses, which are critical in host resistance to *T. gondii* infection. The first studies demonstrated increased susceptibility of *C5ar1*$^{-/-}$ *C3ar1*$^{-/-}$ double knockout (DKO) mice to *T. gondii* infection. Intraperitoneal injection of 20 Me49 cysts resulted in acute death within 12 days in the DKO mice whereas all WT mice survived for greater than 50 days, the longest time point studied. The DKO mice had significant reductions in IL-12 and IFN-γ secretion in splenic cultures stimulated with STAg (soluble *Toxoplasma* antigen) and supported a protective role for anaphylatoxin receptor signaling (Strainic et al., 2008). These findings are consistent with an established role for locally produced C3a and C5a in regulating Th1 responses through autocrine and paracrine C3aR/C5aR receptor signaling (Strainic et al., 2008; Liszewski et al., 2013). More recently, infection studies in *C5ar1*$^{-/-}$ mice showed that these mice also die acutely, but with a much less dramatic phenotype or kinetic than the DKO mice (Briukhovetska et al., 2020). In this study, 50 cysts of the Type II strain Me49 were injected intraperitoneally. At this dose, both WT and *C5ar1*$^{-/-}$ mice were susceptible to intraperitoneal infection, with 60% of WT mice dead within 30 days compared to 80% of *C5ar1*$^{-/-}$ infected mice, which exhibited a statistically significant higher parasite load during acute disease (Briukhovetska et al., 2020). The authors argued that C3b and its degradation products likely promoted the release of the anaphylatoxin C5a that bound the C5aR1 expressed on CD8α+ dendritic cells (DCs) which were activated by *T. gondii*-induced TLR signaling to amplify IL-12 and IFN-γ production (Briukhovetska et al., 2020). Evidence for decreased levels of serum proinflammatory cytokines and increased IL-10 serum levels in *C5ar1*$^{-/-}$ mice, and the reduction of IL-12 secretion from *C5ar1*$^{-/-}$ splenic DCs in response to STAg *in vitro* suggested that complement signaling was important for priming appropriate Th1 responses to control parasite replication. Collectively, these studies suggest that loss of systemic complement and anaphylatoxin receptor signaling play a significant role in the failure to sense or initiate proper humoral and cytokine responses against acute *T. gondii* infection, respectively, which is necessary to control parasite proliferation during acute disease.

To better understand the relative and contributing roles of complement effectors C3, C3b, and associated anaphylatoxin receptor signaling on immunological priming and control of parasite proliferation, we infected C57BL/6J mice perorally with 40 cysts of the Me49 strain. C57BL/6 mice develop an acute, Th1 CD4+ T cell-mediated lethal ileitis within 8 days of *Toxoplasma* peroral infection that results in tissue destruction and necrosis of the intestinal mucosa. This immunopathology is associated with exacerbated Th1 immune responses, which include increased production of the inflammatory mediators IFNγ, TNF-α, nitric oxide (Liesenfeld et al., 1996; Khan et al., 1997; Liesenfeld et al., 1999), Th1 and Th17 cytokines (Rachinel et al., 2004; Vossenkämper et al., 2004), and shifts in the intestinal microbiota (Heimesaat et al., 2006; Molloy et al., 2013; Wang et al., 2019). Systemic complement and anaphylatoxin receptor signaling is emerging as an important component of the intestinal immune response by its ability to regulate epithelial barrier integrity, the microbiota, and oral tolerance (Pekkarinen et al., 2013; Nissilä et al., 2017; Zhang et al., 2018; Benis et al., 2019; Qi et al., 2020), however the contribution of complement in the protection of mucosal barriers during acute *T. gondii* infection has not been directly addressed.

To investigate this question, we infected C57BL/6J WT and C3 deficient animals with 40 Me49 tissue cysts perorally and assessed survival. As a control, we also infected WT and C3 deficient animals with 25 tachyzoites of the Type I RH strain intraperitoneally to demonstrate that C3 is protective during infection regardless of parasite genotype (**Figure 3A**). In stark contrast to the i.p. model in which all mice die acutely, 100% of C3 deficient mice survived *T. gondii* infection whereas all WT mice died acutely, within 10 days (**Figure 3B**). Histologic examination of the spleen and intestines at days 4, 6, and 8 (**Figures 3C, D**) post infection showed striking differences in pathology, highlighted by areas of necrosis in the white pulp of the spleen of infected WT mice compared to $C3^{-/-}$ mice, and a severe necrosis of the ilea, predominantly within the villi, with significant inflammation, a loss of columnar epithelial cells and a large accumulation of granulocytes that was largely absent in the $C3^{-/-}$ infected mice. Parasite load was determined by plaquing a portion of the spleen and small intestine of WT versus C3 deficient mice at day 6 post infection and showed a similar level of parasites present (with no significant difference detected in the tissues examined; data not shown).

Consistent with phenotypes observed in other murine models of inflammatory-driven acute colitis, complement deficient mice were protected from *T. gondii*-induced lethal ileitis and survived. We hypothesize that dysregulation of the local complement response contributed detrimental inflammation and led to the pathogenesis of acute infection. Similar phenotypes have previously been observed in perorally infected mice deficient in the inducible NO synthetase enzyme ($iNOS^{-/-}$) and may suggest that complement likewise plays an analogous role by exacerbating the immunopathology observed in this oral model of acute ileitis. Nitric oxide is an important mediator restricting intracellular pathogen growth. $iNOS^{-/-}$ mice exhibited greater dissemination and parasite burden but survived significantly longer than control mice infected perorally (Khan et al., 1997; Scharton-Kersten et al., 1997). Whereas control mice exhibited exacerbated cytokine production and necrosis, the prolonged survival of $iNOS^{-/-}$ mice was attributed to control of the dysregulated inflammatory response that occurs in B6 mice. Unlike the C3 deficient mice, $iNOS^{-/-}$ mice eventually succumb to infection, largely the result of their inability to control parasite proliferation (Khan et al., 1997). These studies indicated that iNOS and NO production is critical for parasite killing. Further, these findings suggest that acute ileitis is critically dependent on the level of IL-10 present, a critical meditator of immune homeostasis during proinflammatory Th1 responses, both in genetically susceptible C57BL/6 mice and resistant BALB/c. Indeed, mice deficient in IL-10 show an increased susceptibility to *T. gondii* infection compared to control animals (Gazzinelli et al., 1996; Suzuki et al., 2000). The increased susceptibility was not attributed to increases in parasite burden, but rather to the inability to control the pro-inflammatory response. Together, the studies highlighted illustrate that several immunological factors contribute toward tipping the balance towards immunopathology in *T. gondii*-induced ileitis, and further investigations are required to determine how protective versus pathological roles of complement contribute to the immunopathology associated with oral infection of genetically susceptible C57BL/6 mice. In the next section, we discuss how studies addressing the role of complement in other intestinal inflammatory disorders may provide insight into the observed dichotomous role for complement in the pathogenesis of acute *T. gondii* peroral infection.

ADDITIONAL INSIGHTS AND OUTSTANDING QUESTIONS

The intestinal pathology induced by oral *T. gondii* infection shares similarities with human inflammatory bowel disease (IBD) (Liesenfeld, 2002). Recent studies in the IBD field support a model in which complement has both a pathogenic and a protective role and specifically, that local complement production plays a central role in the pathophysiology of these inflammatory diseases, including the established experimental mouse model of acute dextran-sulfate induced (DSS) colitis, a model for human inflammatory bowel disease. Complement is also produced extra-hepatically by immune cells and epithelial cells, including intestinal enterocytes, and may have specific functions at local sites (Morgan and Gasque, 1997; Lubbers et al., 2017). Mice deficient in C3 or Factor B were protected from acute colitis induction 5 days post DSS treatment and exhibited improved clinical outcome (Elvington et al., 2015). In contrast to previous studies (Lu et al., 2010), complement deficient mice unexpectedly died within 5 days of the DSS recovery period, indicating a protective role for complement after induction of colitis (Schepp-Berglind et al., 2012). Mortality was attributed to impaired epithelial barrier function in the absence of complement, leading to translocation of commensals

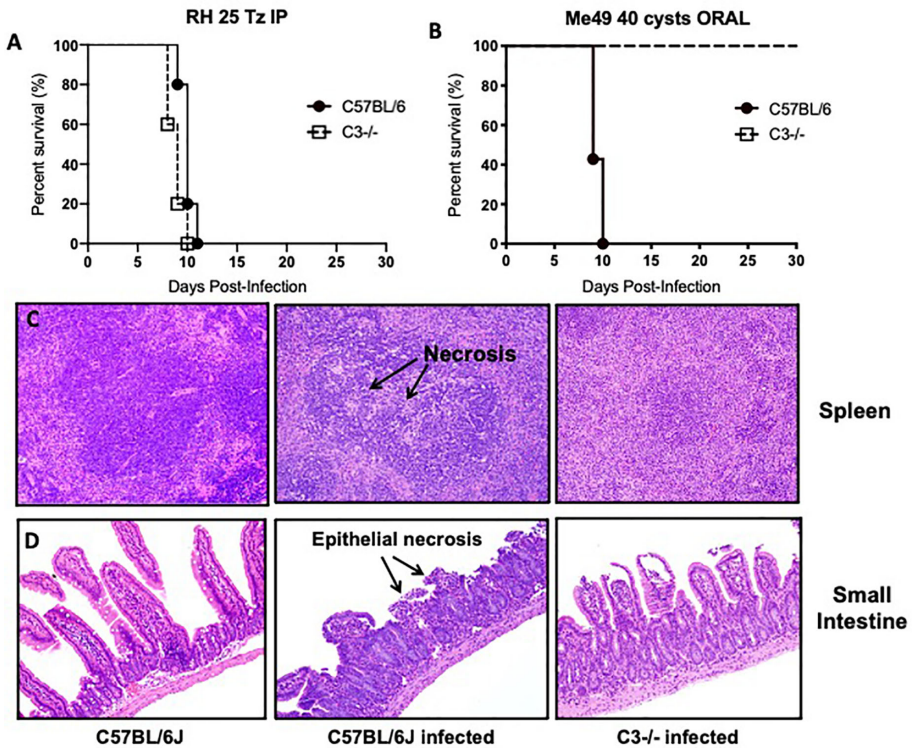

FIGURE 3 | Lethal ileitis in *Toxoplasma gondii* perorally infected C57BL/6J mice is dependent on C3. **(A)** Survival of 6- to 8-week-old C57BL6/J (n = 5, closed circle) and $C3^{-/-}$ (n=5, open square) female mice infected with 25 tachyzoites injected intraperitoneally of the RH strain of *Toxoplasma gondii*. Data shown are for one of two independently performed experiments. **(B)** Survival of 6- to 8-week-old C57BL6/J (n=5, closed circle) and $C3^{-/-}$ (n=5, open square) female mice infected by oral gavage with 40 cysts of the Me49 strain of *Toxoplasma gondii*. Data shown are for one of two independently performed experiments. **(C)** Histological examination of the spleen of C57BL6/J or $C3^{-/-}$ mice stained with hematoxylin-eosin (HE) at day 8 post-infection with 40 cysts of Me49 by oral gavage. **(D)** Histological examination of the small intestine of C57BL6/J or $C3^{-/-}$ mice stained with hematoxylin-eosin (HE) at day 8 post-infection with 40 cysts of Me49 by oral gavage.

and increased endotoxins, and reduction of mucosal tissue proliferation during the repair process (Schepp-Berglind et al., 2012; Elvington et al., 2015). C5 deficiency in an earlier study was also shown to make mice more susceptible to colitis after 10 days, supporting this protective role (Deguchi et al., 2005). Reported discrepancies in phenotypes across various studies are likely due to differences in disease severity attributed to dose of DSS and mouse genotype. Thus, understanding the contributions of complement to dual protective and pathogenic functions in *T. gondii* infection may not only rely on host genotypes but also parasite genotype and dose and thus requires further study.

Anaphylatoxin receptor signaling has also been shown to play a role in regulating pro-inflammatory responses at the intestinal barrier. Reports of a pathogenic role for C5a in colitis models are supported by the amelioration of disease pathology in mice and rats using C5aR deficient animals (Johswich et al., 2009), C5a blockade (Chen et al., 2011) or treatment with C5a agonists (Woodruff et al., 2003). Complement activation also contributed to the development of colitis-associated colorectal cancer (CAC), supported by tumor repression in complement deficient mice (C3, C5, or C5aR) (Ning et al., 2015). Mechanistic studies revealed that complement deficiency reduced proinflammatory cytokine production produced by neutrophils (IL-1β and IL-17) in the colonic tissues, indicating that C5a is a potent inducer of this response. While C3aR deficiency in BALB/c was partially protective in DDS-induced colitis, there was no significant effect observed in C57BL/6 mice (Wende et al., 2013), indicating that differences between these two mice strains are important factors in these phenotypes. Given this evidence and the recently demonstrated role of C5aR signaling in systemic *T. gondii* infection (Briukhovetska et al., 2020), it is highly likely that anaphylatoxins play an important role in promoting inflammation in the gut during *T. gondii* infection.

It is tempting to speculate that complement at mucosal barriers may need greater regulation. IBD in humans and mice is associated with increased complement activation (Ahrenstedt et al., 1990; Elvington et al., 2015; Preisker et al., 2019) and reduced expression of complement regulatory proteins in the gut epithelium (Berstad and Brandtzaeg, 1998; Scheinin et al., 1999). Accordingly, mice deficient in DAF (CD59) are more susceptible to DSS-induced colitis (Lin et al., 2004). In the previously discussed studies, while complement deficient mice died by day 5 after DSS recovery, the wild type mice treated with complement inhibitors survived the DSS treatment, suggesting complement

regulation or inhibition over deficiency is more protective and may have important therapeutic implications for inflammatory conditions (Schepp-Berglind et al., 2012; Elvington et al., 2015).

Lastly, the interaction between intestinal complement, commensal bacteria, and *Toxoplasma* during acute infection remains to be fully elucidated. *T. gondii* infection is associated with microbial dysbiosis (Molloy et al., 2013; Wang et al., 2019) and emerging evidence for the role complement plays in maintaining gut homeostasis and regulating commensal microbiota is a factor that must be carefully evaluated (Benis et al., 2019; Qi et al., 2020). Equally important is to consider whether the interaction of *T. gondii* with complement and its regulators may contribute adversely to the outcome of this complex environment. Our previous work has shown that parasite genotype impacts complement deposition. Additional studies are required to test if the capacity of Type II strains, that show greater C3b deposition (Sikorski et al., 2020) could potentially induce greater local levels of C3a and C5a, which play a role in pro-inflammatory signaling by their cognate anaphylatoxin receptors. It is also possible that greater opsonization of Type II strains may contribute to the increased internalization of Type II strains *via* phagocytosis. Recent studies have shown that avirulent Type II strains preferentially enter macrophages through phagocytosis but avoid elimination by escaping the phagolysosome in murine macrophages (Zhao et al., 2014), in which the authors hypothesized this mode of entry promotes an enhanced immune stimulation and greater control of acute infection.

The identification of parasite factors that activate and regulate complement are critical for determining whether direct parasite activation and regulation of the complement system is occurring *in vivo*. Studies from the *Plasmodium* field have identified several developmentally regulated 6-CYS surface proteins that regulate complement in both the mosquito and human host (Molina-Cruz et al., 2013; Kennedy et al., 2016). Comparative modeling studies and the crystal structure of *Pf12* has determined that the 6-CYS proteins share tertiary structural homology with *T. gondii* SRS (SAG-1 related sequences) surface proteins (He et al., 2002; Gerloff et al., 2005; Arredondo et al., 2012; Tonkin et al., 2013). This evidence points to a potential role for the structurally homologous *T. gondii* SRS surface proteins (Gerloff et al., 2005; Tonkin et al., 2013) to possess an analogous role. Though the mechanism for Factor H recruitment by the *Plasmodium* 6-CYS protein *Pf92* remains elusive, it is well established that FH is recruited to host cell surfaces through its ability to bind host ligands such as sialic acid and sulfated proteoglycans (SPGs) (Blaum, 2017). *Toxoplasma* is known to interact with both sialic acid and SPGs *via* microneme proteins 1 and 4 (MIC1, MIC4) and SRS57, and thus these proteins are prime candidates for future study to determine their capacity in recruiting FH (Ortega-Barria and Boothroyd, 1999; Dzierszinski et al., 2000; Jacquet et al., 2001; Sardinha-Silva et al., 2019). Interestingly, recent analyses done in our lab have determined that the developmentally regulated SRS superfamily of surface proteins are significantly expanded in *T. gondii* (Jung et al., 2004; Wasmuth et al., 2012). While the biological significance of this expansion remains elusive, it is tempting to speculate that the SRS superfamily plays a role in overcoming immunological barriers to establish successful infection in a wide host range. Specifically, are there stage-specific surface or secreted proteins that activate or regulate complement in a species-specific manner, *i.e.* intermediate versus definitive host, or does a universally expressed SRS protein facilitate this process across several species? All of these intriguing questions require additional studies.

CONCLUDING REMARKS

The data presented in this review highlight a protective and pathogenic role for the complement system during acute *T. gondii* infection, depending on the route of infection. We are just beginning to understand how parasite modulation of complement activation may impact complement effector functions required to strike the optimal balance in the intermediate host. Evading serum killing ensures parasite survival, persistence and transmission to new hosts, while maintaining the generation of critical effector proteins (iC3b, C3a, C5a) that are required for stimulating sufficient humoral and Th1 immunity to regulate tachyzoite proliferation. We argue that future investigations will further unravel the immunomodulatory role of complement activation and regulation during *T. gondii* infection in the gut. Additional studies into the parasite factors that interact with and regulate complement are required to better understand the dynamics that occur between parasite and host systemically and locally in the gut.

AUTHOR CONTRIBUTIONS

Review topic was solicited by MG, PS, and AC. PS wrote the first draft with editing from MG and AC. All authors contributed to the article and approved the submitted version.

FUNDING

This work was supported by the Intramural Research Program of the National Institute of Allergy and Infectious Diseases (NIAID) at the National Institutes of Health.

REFERENCES

Ahrenstedt, Ö, Knutson, L., Nilsson, B., Nilsson-Ekdahl, K., Odlind, B., and Hällgren, R. (1990). Enhanced Local Production of Complement Components in the Small Intestines of Patients with Crohn's Disease. *New Engl. J. Med.* 322 (19), 1345–1349. doi: 10.1056/NEJM199005103221903

Arredondo, S. A., Cai, M., Takayama, Y., MacDonald, N. J., Anderson, D. E. , Aravind, L., et al. (2012). Structure of the Plasmodium 6-cysteine s48/45 domain. *Proc. Natl. Acad. Sci.* 109 (17), 6692–6697. doi: 10.1073/pnas.1204363109

Belachew, E. B. (2018). Immune Response and Evasion Mechanisms of Plasmodium falciparum Parasites. *J. Immunol. Res.* 2018:6529681. doi: 10.1155/2018/6529681

Benis, N., Wells, J. M., Smits, M. A., Kar, S. K., van der Hee, B. , dos Santos, V. A. P. M., et al. (2019). High-level integration of murine intestinal transcriptomics data highlights the importance of the complement system in mucosal homeostasis. *BMC Genomics* 20 (1), 1028. doi: 10.1186/s12864-019-6390-x

Berstad, A. E., and Brandtzaeg, P. (1998). Expression of cell membrane complement regulatory glycoproteins along the normal and diseased human gastrointestinal tract. *Gut* 42 (4), 522–529. doi: 10.1136/gut.42.4.522

Blaum, B. S. (2017). The lectin self of complement factor H. *Curr. Opin. Struct. Biol.* 44, 111–118. doi: 10.1016/j.sbi.2017.01.005

Briukhovetska, D., Ohm, B., Mey, F. T., Aliberti, J., Kleingarn, M., Huber-Lang, M., et al. (2020). C5aR1 Activation Drives Early IFN-γ Production to Control Experimental Toxoplasma gondii Infection. *Front. Immunol.* 11:1397 (1397), 1–15. doi: 10.3389/fimmu.2020.01397

Carroll, M. C. (2008). Complement and humoral immunity. *Vaccine* 26 Suppl 8 (0 8), I28–I33. doi: 10.1016/j.vaccine.2008.11.022

Chen, G., Yang, Y., Gao, X., Dou, Y., Wang, H., Han, G., et al. (2011). Blockade of complement activation product C5a activity using specific antibody attenuates intestinal damage in trinitrobenzene sulfonic acid induced model of colitis. *Lab. Invest.* 91 (3), 472–483. doi: 10.1038/labinvest.2010.183

Deguchi, Y., Andoh, A., Inatomi, O., Araki, Y., Hata, K., Tsujikawa, T., et al. (2005). Development of dextran sulfate sodium-induced colitis is aggravated in mice genetically deficient for complement C5. *Int. J. Mol. Med.* 16 (4), 605–608. doi: 10.3892/ijmm.16.4.605

Dubey, J. P., Speer, C. A., Shen, S. K., Kwok, O. C., and Blixt, J. A. (1997). Oocyst-induced murine toxoplasmosis: life cycle, pathogenicity, and stage conversion in mice fed Toxoplasma gondii oocysts. *J. Parasitol.* 83 (5), 870–882. doi: 10.2307/3284282

Dzierszinski, F., Mortuaire, M., Cesbron-Delauw, M. F., and Tomavo, S. (2000). Targeted disruption of the glycosylphosphatidylinositol-anchored surface antigen SAG3 gene in Toxoplasma gondii decreases host cell adhesion and drastically reduces virulence in mice. *Mol. Microbiol.* 37 (3), 574–582. doi: 10.1046/j.1365-2958.2000.02014.x

Elvington, M., Schepp-Berglind, J., and Tomlinson, S. (2015). Regulation of the alternative pathway of complement modulates injury and immunity in a chronic model of dextran sulphate sodium-induced colitis. *Clin. Exp. Immunol.* 179 (3), 500–508. doi: 10.1111/cei.12464

Fuhrman, S. A., and Joiner, K. A. (1989). Toxoplasma gondii: mechanism of resistance to complement-mediated killing. *J. Immunol.* 142 (3), 940–947.

Gazzinelli, R. T., Wysocka, M., Hieny, S., Scharton-Kersten, T., Cheever, A., Kühn, R., et al. (1996). In the absence of endogenous IL-10, mice acutely infected with Toxoplasma gondii succumb to a lethal immune response dependent on CD4+ T cells and accompanied by overproduction of IL-12, IFN-gamma and TNF-alpha. *J. Immunol.* 157 (2), 798–805.

Gerloff, D. L., Creasey, A., Maslau, S., and Carter, R. (2005). Structural models for the protein family characterized by gamete surface protein Pfs230 of <em>Plasmodium falciparum</em&gt. *Proc. Natl. Acad. Sci. U. States America* 102 (38), 13598–13603. doi: 10.1073/pnas.0502378102

He, X.-l., Grigg, M. E., Boothroyd, J. C., and Garcia, K. C. (2002). Structure of the immunodominant surface antigen from the Toxoplasma gondii SRS superfamily. *Nat. Struct. Biol.* 9 (8), 606–611. doi: 10.1038/nsb819

Heeger, P. S., Lalli, P. N., Lin, F., Valujskikh, A., Liu, J., Muqim, N., et al. (2005). Decay-accelerating factor modulates induction of T cell immunity. *J. Exp. Med.* 201 (10), 1523–1530. doi: 10.1084/jem.20041967

Heimesaat, M. M., Bereswill, S., Fischer, A., Fuchs, D., Struck, D., Niebergall, J., et al. (2006). Gram-negative bacteria aggravate murine small intestinal Th1-type immunopathology following oral infection with Toxoplasma gondii. *J. Immunol.* 177 (12), 8785–8795. doi: 10.4049/jimmunol.177.12.8785

Jacquet, A., Coulon, L., De Nève, J., Daminet, V., Haumont, M., Garcia, L., et al. (2001). The surface antigen SAG3 mediates the attachment of Toxoplasma gondii to cell-surface proteoglycans. *Mol. Biochem. Parasitol.* 116 (1), 35–44. doi: 10.1016/s0166-6851(01)00297-3

Johswich, K., Martin, M., Bleich, A., Kracht, M., Dittrich-Breiholz, O., Gessner, J. E., et al. (2009). Role of the C5a receptor (C5aR) in acute and chronic dextran sulfate-induced models of inflammatory bowel disease. *Inflammation Bowel Dis.* 15 (12), 1812–1823. doi: 10.1002/ibd.21012

Jung, C., Lee, C. Y., and Grigg, M. E. (2004). The SRS superfamily of Toxoplasma surface proteins. *Int. J. Parasitol.* 34 (3), 285–296. doi: 10.1016/j.ijpara.2003.12.004

Kennedy, A. T., Schmidt, C. Q., Thompson, J. K., Weiss, G. E., Taechalertpaisarn, T., Gilson, P. R., et al. (2016). Recruitment of Factor H as a Novel Complement Evasion Strategy for Blood-Stage Plasmodium falciparum Infection. *J. Immunol.* 196 (3), 1239–1248. doi: 10.4049/jimmunol.1501581

Khan, I. A., Schwartzman, J. D., Matsuura, T., and Kasper, L. H. (1997). A dichotomous role for nitric oxide during acute Toxoplasma gondii infection in mice. *Proc. Natl. Acad. Sci. U. S. A.* 94 (25), 13955–13960. doi: 10.1073/pnas.94.25.13955

Klos, A., Tenner, A. J., Johswich, K.-O., Ager, R. R., Reis, E. S., and Köhl, J. (2009). The role of the anaphylatoxins in health and disease. *Mol. Immunol.* 46 (14), 2753–2766. doi: 10.1016/j.molimm.2009.04.027

Liesenfeld, O., Kosek, J., Remington, J. S., and Suzuki, Y. (1996). Association of CD4+ T cell-dependent, interferon-gamma-mediated necrosis of the small intestine with genetic susceptibility of mice to peroral infection with Toxoplasma gondii. *J. Exp. Med.* 184 (2), 597–607. doi: 10.1084/jem.184.2.597

Liesenfeld, O., Kang, H., Park, D., Nguyen, T. A., Parkhe, C. V., Watanabe, H., et al. (1999). TNF-alpha, nitric oxide and IFN-gamma are all critical for development of necrosis in the small intestine and early mortality in genetically susceptible mice infected perorally with Toxoplasma gondii. *Parasite Immunol.* 21 (7), 365–376. doi: 10.1046/j.1365-3024.1999.00237.x

Liesenfeld, O. (2002). Oral Infection of C57BL/6 Mice with Toxoplasma gondii: A New Model of Inflammatory Bowel Disease? *J. Infect. Dis.* 185 (Supplement_1), S96–S101. doi: 10.1086/338006

Lin, F., Spencer, D., Hatala, D. A., Levine, A. D., and Medof, M. E. (2004). Decay-accelerating factor deficiency increases susceptibility to dextran sulfate sodium-induced colitis: role for complement in inflammatory bowel disease. *J. Immunol.* 172 (6), 3836–3841. doi: 10.4049/jimmunol.172.6.3836

Liszewski, M. K., Kolev, M., Le Friec, G., Leung, M., Bertram, P. G., Fara, A. F., et al. (2013). Intracellular complement activation sustains T cell homeostasis and mediates effector differentiation. *Immunity* 39 (6), 1143–1157. doi: 10.1016/j.immuni.2013.10.018

Lu, F., Fernandes, S. M., and Davis, A. E. ,. 3. (2010). The role of the complement and contact systems in the dextran sulfate sodium-induced colitis model: the effect of C1 inhibitor in inflammatory bowel disease. *Am. J. Physiol. Gastrointest. Liver Physiol.* 298 (6), G878–G883. doi: 10.1152/ajpgi.00400.2009

Lubbers, R., van Essen, M. F., van Kooten, C., and Trouw, L. A. (2017). Production of complement components by cells of the immune system. *Clin. Exp. Immunol.* 188 (2), 183–194. doi: 10.1111/cei.12952

Molina-Cruz, A., Garver, L. S., Alabaster, A., Bangiolo, L., Haile, A., Winikor, J., et al. (2013). The human malaria parasite Pfs47 gene mediates evasion of the mosquito immune system. *Sci. (New York N.Y.)* 340 (6135), 984–987. doi: 10.1126/science.1235264

Molloy, M. J., Grainger, J. R., Bouladoux, N., Hand, T. W., Koo, L. Y., Naik, S., et al. (2013). Intraluminal containment of commensal outgrowth in the gut during infection-induced dysbiosis. *Cell Host Microbe* 14 (3), 318–328. doi: 10.1016/j.chom.2013.08.003

Morgan, B. P., and Gasque, P. (1997). Extrahepatic complement biosynthesis: where, when and why? *Clin. Exp. Immunol.* 107 (1), 1–7. doi: 10.1046/j.1365-2249.1997.d01-890.x

Ning, C., Li, Y. Y., Wang, Y., Han, G. C., Wang, R. X., Xiao, H., et al. (2015). Complement activation promotes colitis-associated carcinogenesis through activating intestinal IL-1β/IL-17A axis. *Mucosal Immunol.* 8 (6), 1275–1284. doi: 10.1038/mi.2015.18

Nissilä, E., Korpela, K., Lokki, A. I., Paakkanen, R., Jokiranta, S., de Vos, W. M., et al. (2017). C4B gene influences intestinal microbiota through complement activation in patients with paediatric-onset inflammatory bowel disease. *Clin. Exp. Immunol.* 190 (3), 394–405. doi: 10.1111/cei.13040

Ortega-Barria, E., and Boothroyd, J. C. (1999). A Toxoplasma lectin-like activity specific for sulfated polysaccharides is involved in host cell infection. *J. Biol. Chem.* 274 (3), 1267–1276. doi: 10.1074/jbc.274.3.1267

Pekkarinen, P. T., Vaali, K., Jarva, H., Kekäläinen, E., Hetemäki, I., Junnikkala, S., et al. (2013). Impaired intestinal tolerance in the absence of a functional complement system. *J. Allergy Clin. Immunol.* 131 (4), 1167–1175. doi: 10.1016/j.jaci.2012.09.004

Petry, F., Jakobi, V., Wagner, S., Tessema, T. S., Thiel, S., and Loos, M. (2008). Binding and activation of human and mouse complement by Cryptosporidium parvum (Apicomplexa) and susceptibility of C1q- and MBL-deficient mice to

infection. *Mol. Immunol.* 45 (12), 3392–3400. doi: 10.1016/j.molimm.2008.04.010

Preisker, S., Brethack, A. K., Bokemeyer, A., Bettenworth, D., Sina, C., and Derer, S. (2019). Crohn's Disease Patients in Remission Display an Enhanced Intestinal IgM$^+$ B Cell Count in Concert with a Strong Activation of the Intestinal Complement System. *Cells* 8 (1), 1–13. doi: 10.3390/cells8010078

Qi, H., Wei, J., Gao, Y., Yang, Y., Li, Y., Zhu, H., et al. (2020). Reg4 and complement factor D prevent the overgrowth of E. coli in the mouse gut. *Commun. Biol.* 3 (483), 1–15. doi: 10.1038/s42003-020-01219-2

Rachinel, N., Buzoni-Gatel, D., Dutta, C., Mennechet, F. J., Luangsay, S., Minns, L. A., et al. (2004). The induction of acute ileitis by a single microbial antigen of Toxoplasma gondii. *J. Immunol.* 173 (4), 2725–2735. doi: 10.4049/jimmunol.173.4.2725

Reiss, T., Theis, H. I., Gonzalez-Delgado, A., Vega-Rodriguez, J., Zipfel, P. F., Skerka, C., et al. (2021). Acquisition of human plasminogen facilitates complement evasion by the malaria parasite Plasmodium falciparum. *Eur. J. Immunol.* 51, 490–493. doi: 10.1002/eji.202048718

Sardinha-Silva, A., Mendonça-Natividade, F. C., Pinzan, C. F., Lopes, C. D., Costa, D. L., Jacot, D., et al. (2019). The lectin-specific activity of Toxoplasma gondii microneme proteins 1 and 4 binds Toll-like receptor 2 and 4 N-glycans to regulate innate immune priming. *PloS Pathog.* 15 (6), e1007871–e1007871. doi: 10.1371/journal.ppat.1007871

Scharton-Kersten, T. M., Yap, G., Magram, J., and Sher, A. (1997). Inducible Nitric Oxide Is Essential for Host Control of Persistent but Not Acute Infection with the Intracellular Pathogen Toxoplasma gondii. *J. Exp. Med.* 185 (7), 1261–1274. doi: 10.1084/jem.185.7.1261

Scheinin, T., Böhling, T., Halme, L., Kontiainen, S., Bjørge, L., and Meri, S. (1999). Decreased expression of protectin (CD59) in gut epithelium in ulcerative colitis and Crohn's disease. *Hum. Pathol.* 30 (12), 1427–1430. doi: 10.1016/S0046-8177(99)90163-6

Schepp-Berglind, J., Atkinson, C., Elvington, M., Qiao, F., Mannon, P., and Tomlinson, S. (2012). Complement-dependent injury and protection in a murine model of acute dextran sulfate sodium-induced colitis. *J. Immunol. (Baltimore Md. 1950)* 188 (12), 6309–6318. doi: 10.4049/jimmunol.1200553

Schmidt, C. Q., Lambris, J. D., and Ricklin, D. (2016). Protection of host cells by complement regulators. *Immunol. Rev.* 274 (1), 152–171. doi: 10.1111/imr.12475

Shao, S., Sun, X., Chen, Y., Zhan, B., and Zhu, X. (2019). Complement Evasion: An Effective Strategy That Parasites Utilize to Survive in the Host. *Front. Microbiol.* 10:532. doi: 10.3389/fmicb.2019.00532

Sikorski, P. M., Commodaro, A. G., and Grigg, M. E. (2020). Toxoplasma gondii Recruits Factor H and C4b-Binding Protein to Mediate Resistance to Serum Killing and Promote Parasite Persistence in vivo. *Front. Immunol.* 10:3105. doi: 10.3389/fimmu.2019.03105

Simon, N., Lasonder, E., Scheuermayer, M., Kuehn, A., Tews, S., Fischer, R., et al. (2013). Malaria parasites co-opt human factor H to prevent complement-mediated lysis in the mosquito midgut. *Cell Host Microbe* 13 (1), 29–41. doi: 10.1016/j.chom.2012.11.013

Strainic, M. G., Liu, J., Huang, D., An, F., Lalli, P. N., Muqim, N., et al. (2008). Locally produced complement fragments C5a and C3a provide both costimulatory and survival signals to naive CD4+ T cells. *Immunity* 28 (3), 425–435. doi: 10.1016/j.immuni.2008.02.001

Suzuki, Y., Sher, A., Yap, G., Park, D., Neyer, L. E., Liesenfeld, O., et al. (2000). IL-10 is required for prevention of necrosis in the small intestine and mortality in both genetically resistant BALB/c and susceptible C57BL/6 mice following peroral infection with Toxoplasma gondii. *J. Immunol.* 164 (10), 5375–5382. doi: 10.4049/jimmunol.164.10.5375

Thurman, J. M., and Holers, V. M. (2006). The Central Role of the Alternative Complement Pathway in Human Disease. *J. Immunol.* 176 (3), 1305–1310. doi: 10.4049/jimmunol.176.3.1305

Tonkin, M. L., Arredondo, S. A., Loveless, B. C., Serpa, J. J., Makepeace, K. A., Sundar, N., et al. (2013). Structural and biochemical characterization of Plasmodium falciparum 12 (Pf12) reveals a unique interdomain organization and the potential for an antiparallel arrangement with Pf41. *J. Biol. Chem.* 288 (18), 12805–12817. doi: 10.1074/jbc.M113.455667

Vossenkämper, A., Struck, D., Alvarado-Esquivel, C., Went, T., Takeda, K., Akira, S., et al. (2004). Both IL-12 and IL-18 contribute to small intestinal Th1-type immunopathology following oral infection with Toxoplasma gondii, but IL-12 is dominant over IL-18 in parasite control. *Eur. J. Immunol.* 34 (11), 3197–3207. doi: 10.1002/eji.200424993

Votýpka, J., Modrý, D., Oborník, M., Šlapeta, J., Lukeš, J., and Chapman, D. J. (2017). "Apicomplexa," in *Handbook of the Protists*. Eds. J. M. Archibald, A. G. B. Simpson, C. H. Slamovits, L. Margulis, M. Melkonian and J. O. Corliss (Cham: Springer International Publishing), 1–58.

Wang, S., El-Fahmawi, A., Christian, D. A., Fang, Q., Radaelli, E., Chen, L., et al. (2019). Infection-Induced Intestinal Dysbiosis Is Mediated by Macrophage Activation and Nitrate Production. *mBio* 10 (3):e00935-19, 1–13. doi: 10.1128/mBio.00935-19

Wasmuth, J. D., Pszenny, V., Haile, S., Jansen, E. M., Gast, A. T., Sher, A., et al. (2012). Integrated Bioinformatic and Targeted Deletion Analyses of the SRS Gene Superfamily Identify SRS29C as a Negative Regulator of Toxoplasma Virulence. *mBio* 3 (6), e00321–e00312. doi: 10.1128/mBio.00321-12

Wende, E., Laudeley, R., Bleich, A., Bleich, E., Wetsel, R. A., Glage, S., et al. (2013). The complement anaphylatoxin C3a receptor (C3aR) contributes to the inflammatory response in dextran sulfate sodium (DSS)-induced colitis in mice. *PloS One* 8 (4), e62257. doi: 10.1371/journal.pone.0062257

Woodruff, T. M., Arumugam, T. V., Shiels, I. A., Reid, R. C., Fairlie, D. P., and Taylor, S. M. (2003). A potent human C5a receptor antagonist protects against disease pathology in a rat model of inflammatory bowel disease. *J. Immunol.* 171 (10), 5514–5520. doi: 10.4049/jimmunol.171.10.5514

Zhang, J., Ye, J., Ren, Y., Zuo, J., Dai, W., He, Y., et al. (2018). Intracellular activation of complement C3 in Paneth cells improves repair of intestinal epithelia during acute injury. *Immunotherapy* 10 (15), 1325–1336. doi: 10.2217/imt-2018-0122

Zhao, Y., Marple, A. H., Ferguson, D. J. P., Bzik, D. J., and Yap, G. S. (2014). Avirulent strains of Toxoplasma gondii infect macrophages by active invasion from the phagosome. *Proc. Natl. Acad. Sci.* 111 (17), 6437. doi: 10.1073/pnas.1316841111

Conflict of Interest: The authors declare that the research was conducted in the absence of any commercial or financial relationships that could be construed as a potential conflict of interest.

frontiers in Cellular and Infection Microbiology

ORIGINAL RESEARCH
published: 22 February 2021
doi: 10.3389/fcimb.2020.610368

Harmonization of Protocols for Multi-Species Organoid Platforms to Study the Intestinal Biology of *Toxoplasma gondii* and Other Protozoan Infections

David Holthaus[†], *Estefanía Delgado-Betancourt*[†], *Toni Aebischer*, *Frank Seeber and Christian Klotz*[*]

FG 16: Mycotic and Parasitic Agents and Mycobacteria, Robert Koch-Institute, Berlin, Germany

OPEN ACCESS

Edited by:
Chandra Ramakrishnan, University of Zurich, Switzerland

Reviewed by:
Janine Laura Coombes, University of Liverpool, United Kingdom
Antonio Barragan, Stockholm University, Sweden
Mette Myrmel, Norwegian University of Life Sciences, Norway

***Correspondence:**
Christian Klotz
KlotzC@rki.de

[†]*These authors have contributed equally to this work*

Specialty section:
This article was submitted to Parasite and Host, a section of the journal Frontiers in Cellular and Infection Microbiology

Received: *25 September 2020*
Accepted: *30 December 2020*
Published: *22 February 2021*

Citation:
Holthaus D, Delgado-Betancourt E, Aebischer T, Seeber F and Klotz C (2021) Harmonization of Protocols for Multi-Species Organoid Platforms to Study the Intestinal Biology of Toxoplasma gondii and Other Protozoan Infections. Front. Cell. Infect. Microbiol. 10:610368. doi: 10.3389/fcimb.2020.610368

The small intestinal epithelium is the primary route of infection for many protozoan parasites. Understanding the mechanisms of infection, however, has been hindered due to the lack of appropriate models that recapitulate the complexity of the intestinal epithelium. Here, we describe an *in vitro* platform using stem cell-derived intestinal organoids established for four species that are important hosts of Apicomplexa and other protozoa in a zoonotic context: human, mouse, pig and chicken. The focus was set to create organoid-derived monolayers (ODMs) using the transwell system amenable for infection studies, and we provide straightforward guidelines for their generation and differentiation from organ-derived intestinal crypts. To this end, we reduced medium variations to an absolute minimum, allowing generation and differentiation of three-dimensional organoids for all four species and the subsequent generation of ODMs. Quantitative RT-PCR, immunolabeling with antibodies against marker proteins as well as transepithelial-electrical resistance (TEER) measurements were used to characterize ODM's integrity and functional state. These experiments show an overall uniform generation of monolayers suitable for *Toxoplasma gondii* infection, although robustness in terms of generation of stable TEER levels and cell differentiation status varies from species to species. Murine duodenal ODMs were then infected with *T. gondii* and/or *Giardia duodenalis*, two parasites that temporarily co-inhabit the intestinal niche but have not been studied previously in cellular co-infection models. *T. gondii* alone did not alter TEER values, integrity and transcriptional abundance of tight junction components. In contrast, in *G. duodenalis*-infected ODMs all these parameters were altered and *T. gondii* had no apparent influence on the *G. duodenalis*-triggered phenotype. In conclusion, we provide robust protocols for the generation, differentiation and characterization of intestinal organoids and ODMs from four species. We show their applications for comparative studies on parasite-host interactions during the early phase of a *T. gondii* infection but also its use for co-infections with other relevant intestinal protozoans.

Keywords: intestinal epithelium, host-pathogen interactions, epithelial barrier function, intestinal organoid, protozoa, *Toxoplasma gondii*, *Giardia* spp.

INTRODUCTION

Toxoplasma gondii and *Giardia duodenalis* are two of the most common parasites associated with protozoan disease in humans and animals (Taylor and Webster, 1998; Dubey, 2010; Cacciò and Sprong, 2011; Geurden and Olson, 2011; Torgerson and Macpherson, 2011; Kirk et al., 2015; Torgerson et al., 2015; Cacciò et al., 2018). Both parasites are zoonotic pathogens and share the same route of infection by oral uptake, and both organisms initiate infection in the small intestine, thus temporarily sharing the same habitat. However, reports on the impact of potential co-infections are scarce and have been limited by difficulties in translation of animal experiments or adequate *in vitro* model systems. In general, despite the impact and frequency of these diseases, research mostly relies on animal models or cancer cell lines that mostly do not recapitulate the situation of naturally occurring infections (Klotz et al., 2012; Delgado Betancourt et al., 2019).

The intestinal epithelium is characterized by a villus-crypt axis that is in constant cell renewal, with cells migrating from the crypt to the tip of the villi while differentiating. Beside stem cells, five major cell types can be distinguished: the absorptive enterocyte and cells of the secretory lineage such as Paneth, goblet, enteroendocrine, and Tuft cells. Mimicking this complex environment is key in understanding intestinal homeostasis and disease (Clevers, 2016). Three-dimensional (3D) organoids are *in vitro*-generated stem cell-based multicellular models that replicate the organ-specific architecture and functionality (Clevers, 2016). They are *in vitro* systems that promise to improve the reliability of host-pathogen models and consequently are currently used to study host interactions with pathogens, including protozoa (Dutta and Clevers, 2017; Hill and Spence, 2017; Heo et al., 2018; Luu et al., 2019; Martorelli Di Genova et al., 2019; Wilke et al., 2019; Kraft et al., 2020). Embedded in an extracellular matrix and supplemented with growth factors, organoids allow almost indefinite propagation of healthy and diseased primary tissues of various hosts (Sato et al., 2011a; VanDussen et al., 2015; Derricott et al., 2019).

For infection of 3D organoids various techniques have been reported (Hill et al., 2017; Williamson et al., 2018; Co et al., 2019; Luu et al., 2019). All of them have shortcomings that can limit translational success and relevance, including the difficulty of accessing the lumen, decreased viability and lower infection yields. To address some of these drawbacks, two-dimensional organoid-derived monolayers (ODMs) have been developed (Moon et al., 2014; VanDussen et al., 2015). By seeding fragmented organoids or single cells on top of pre-coated transwell filters, it is possible to generate compartmentalized infection models that possess most of the advantages of 3D organoid models while also being easily up-scalable and accessible. The use of ODMs has already enabled elementary breakthroughs in apicomplexan research such as *in vitro* sexual reproduction of *Cryptosporidium* sp. (Heo et al., 2018; Wilke et al., 2019).

T. gondii is capable of infecting virtually any nucleated cell of vertebrate hosts, including humans, rodents, birds and livestock (Lindsay and Dubey, 2007). Approximately 30% of the human population is infected with the parasite (Montoya and Liesenfeld, 2004), and more than 50% of *T. gondii* infections are associated with the consumption of contaminated meat products from wildlife and livestock (Dubey and Jones, 2008; Kijlstra and Jongert, 2008; Stelzer et al., 2019). The life cycle is complex and encompasses an asexual cycle of fast replicating tachyzoite and dormant tissue cysts comprising of bradyzoites, and sexual development in the feline definite host producing dormant oocysts comprising infectious sporozoites. After ingestion, bradyzoites and sporozoites encounter the intestinal epithelium where they disseminate to different tissues throughout the body (Delgado Betancourt et al., 2019). Frequency of gastrointestinal symptoms is unclear as they may not be recognized, but if so, appear unspecific including abdominal pain and diarrhea (Glover et al., 2017). However, in animals, in particular in laboratory mice, gastrointestinal immunopathology caused by severe inflammation is frequently observed (Schreiner and Liesenfeld, 2009). The exact interaction of the parasite with the intestinal epithelial layer is still unclear (Barragan et al., 2005; Lambert and Barragan, 2010; Gregg et al., 2013), although the parasite is reported to exploit several mechanisms to penetrate the epithelium, such as transepithelial migration (Barragan and Sibley, 2002; Barragan et al., 2005) and modulation of junctional proteins (Weight and Carding, 2012; Weight et al., 2015; Briceño et al., 2016). However, most of these observations have been performed using immortalized cell lines, which in many cases lack the architecture and properties of the cell populations found in the intestine (Pageot et al., 2000; Balimane and Chong, 2005; Hill and Spence, 2017). We and others have therefore proposed the use of intestinal organoids as potentially more relevant cellular systems to study these early events of infection (Klotz et al., 2012; Delgado Betancourt et al., 2019; Luu et al., 2019).

G. duodenalis is a species complex with zoonotic potential that infects multiple species of mammals including humans (Cacciò et al., 2018). Parasite prevalence depends largely on hygiene standards but may reach very high numbers of more than 50% in the studied animal or human population (Cacciò and Sprong, 2011; Geurden and Olson, 2011; Helmy et al., 2018). It is therefore likely that initial infection with *T. gondii* frequently coincides with *G. duodenalis* infection. Moreover, recent evidence of co-occurrence of environmental stages of *G. duodenalis* and *T. gondii* in water samples (Pineda et al., 2020) suggests the possibility of simultaneous co-infection of hosts with these two parasites. After ingestion of *G. duodenalis* cysts, trophozoites excyst and are released in the intestinal lumen where the infection is established. *G. duodenalis* trophozoites colonize and replicate in close proximity to the intestinal epithelium. Yet, in contrast to the invasive *T. gondii* stage, *Giardia* parasites attach extracellularly to the luminal part of the intestinal cell layer. This physical interaction is thought to modulate the intestinal barrier function as a proposed pathophysiological mechanism of disease, however, the detailed mechanisms remain largely unknown (Kraft et al., 2017; Allain and Buret, 2020; Kraft et al., 2020). The symptomatology and ultimate disease outcomes of giardiasis can be broad, and

generally include both asymptomatic carriage as well as various gastro-intestinal complaints such as diarrhea and nausea (Allain and Buret, 2020).

The goal of the present study was to provide protocols for the establishment of 3D intestinal organoid cultures and organoid-derived monolayers (ODM) of various host species with zoonotic relevance for *T. gondii* transmission to omnivores. By minimizing the variation of medium composition and step-by-step instructions we provide a robust protocol for establishment of 3D as well as ODM cultures for murine, human, porcine and avian hosts, as these are important habitats for zoonotic parasites such as *T. gondii* and *Giardia* spp. Additionally, we provide an infection model in murine ODMs that allows studying *T. gondii* and *G. duodenalis* co-infection in a relevant primary intestinal tissue.

METHODS

General Remarks

A detailed list of all medium components, supplements, reagents, kits and cell lines, including respective suppliers, is provided in **Supplementary Table 1**. Antibody suppliers and dilutions used in the study can be found in **Supplementary Table 2**. Primer sequences are given in **Supplementary Table 3**. For gene and protein nomenclature, we followed the international nomenclature guidelines for the respective species. However, in cases where the same molecule of different species was discussed we exemplary followed the nomenclature for vertebrates.

Establishment and Culture of 3D Organoids

Human, chicken, mouse and porcine crypts were isolated as described previously (Sato et al., 2011a; Mahe et al., 2015). The isolation and establishment of organoids from the human duodenal specimen were described before (Kraft et al., 2020) and were approved by the ethical committee of the Charite, Berlin (#EA4-015-13). For porcine samples, duodenal crypts were isolated from a 10-week old piglet (*Sus scrofa*, kindly provided by Svenja Steinfelder, Institute of Immunology, Freie Universität Berlin, animal license T0002/17). Chicken duodenal crypts were isolated from intestine of a 14-day-old female chicken (*Gallus gallus*, kindly provided by Luca Bertzbach & Benedikt Kaufer, Institute of Virology, Freie Universität Berlin, animal license T0245/14). The mouse duodenal sample derived from a female C57/Bl6 mouse from an RKI in-house bred colony (animal license T0173/14).

Intestinal sections were opened longitudinally and the intestinal content was removed by washing with ice-cold PBS. The tissue was cut into 5-mm sections and washed in ice-cold PBS until the suspension remained clear. The tissue fragments were incubated on ice in chelating buffer (PBS containing 2% sorbitol, 1% sucrose, 0.05 mM DTT, 10 mM EDTA, 10 µg/ml Fungin, 10 µg/ml tetracycline and 100 µg/ml gentamicin) for 30 min. After settling down of the fragments, the buffer was removed and the fragments were pipetted up and down 10 times in 3 to 5 ml chelating buffer without EDTA. Supernatant was harvested and collected in a sample tube. This step was repeated six more times. The isolated crypts were pelleted by centrifugation at 300*g* for 5 min, 4°C, and resuspended with Advanced DMEM/F12 supplemented with penicillin/streptomycin (P/S, added as standard supplement for Advanced DMEM/F12). After an additional centrifugation step at 300*g* for 5 min, 4°C, crypts were resupended in 1 ml Advanced DMEM/F12 and mixed 1:2 with Matrigel and seeded in 24-well plates as individual 50-µl droplets, comprising between 50 and 100 crypts. Matrigel was incubated at 37°C for ~30 min to allow polymerization before growth medium was added. The medium was exchanged every 2 to 3 days.

Organoid cultures were passaged every 3 to 7 days following the guidelines by Mahe et al. (2015). Chicken organoids were mechanically disrupted by pipetting up and down with a 200-µl pipette tip for 1 min. Human, mouse and porcine organoids were first enzymatically digested with TrypLE Express (5 min at 37°C) and mechanically disrupted by forcing the suspension through a blunt 18G needle. Cells of all species were then washed with Advanced DMEM/F12 and organoids were re-embedded in Matrigel at a 1:2 ratio.

Media Conditions

Three-dimensional intestinal epithelial cell cultures are first generated by incubating the crypt tissue in an environment that resembles the intestinal crypt condition. These culture conditions support a high proliferative capacity by maintaining stemness of the intestinal crypt base (referred to as *WERN condition*). These conditions promote growth mainly of so-called spheroids that are stem cell-enriched, three-dimensional spherical structures that can be maintained almost indefinitely (Sato et al., 2011a; Miyoshi and Stappenbeck, 2013; VanDussen et al., 2015). To induce differentiation of spheroids into organoids, i.e., structures containing multiple primary epithelial cell types, 3D spheroids were cultured in medium deficient of several stem cell-enriching factors (referred to as *ERN condition*, leaving out Wnt3a) to transform into differentiated organoids.

3D culture was performed using base medium with supplementation of small molecules and inhibitors as summarized in **Table 1**. Base medium (WERN) consisted of 50% L-WRN-conditioned media [CM, L-WRN ATCC CRL-3276; VanDussen et al. (2019)], 20% R-Spondin1 CM [293T cells stably expressing RSpo1-Fc (Kim et al., 2005), a kind gift from Calvin Kuo, Stanford University], 10% Noggin CM (293T cells stably expressing mNoggin-Fc, a kind gift from Hans Clevers, Utrecht University), 50 ng/ml EGF, 1 mM HEPES, 2 mM GlutaMax, 1× P/S, 1× N2, 1× B27, 1 mM N-acetylcysteine 10 mM nicotinamide, 500 nM A83-01 (TGF-β inhibitor) and 1 µM SB202190 (p38 inhibitor) in Advanced DMEM/F12. Pig organoids were cultured in base organoid medium with additional 10 µM rho-associated, coiled-coil-containing protein kinase 1 (ROCK1)-inhibitor Y-27632, and chicken organoid cultures were supplemented with further 10 µM prostaglandin E2 and 3 µM CHIR99021 (GSK-3 inhibitor). For cryopreservation, organoids from four wells were harvested, washed and resuspended in 1 ml freezing medium consisting of 10% DMSO, 10% fatty acid

TABLE 1 | Medium conditions for organoid culture.

Host	L-WRN CM* (50%)	Rspo1 CM** (20%)	Noggin CM***(10%)	EGF (50 ng/ml)	NAC (1 mM)	NIC (10 mM)	SB-202190 (1 μM)	A83-01 (500 nM)	Y-27632 (10 μM)	CHIR (3 μM)	PGE2 (10 μM)
Three-dimensional organoids											
Mouse	X	X	X	Mouse	X	X	X	X			
Human	X	X	X	Human	X	X	X	X			
Pig	X	X	X	Mouse	X	X	X	X	X		
Chicken	X	X	X	Human + Mouse	X	X	X	X	X	X	X
Organoid-derived monolayers											
All	(Initially)	X	X	X	X	X			(Initially)		

L-WRN conditioned medium corresponds to 100 ng/ml recombinant Wnt3A.
R-spondin1 conditioned medium corresponds to 1 μg/ml recombinant R-spondin.
Noggin conditioned medium corresponds to 100 ng/ml recombinant Noggin.
NAC, N-acetylcysteine; NIC, nicotinamide.

free BSA in Advanced DMEM/F12 and placed in cryovials. The vials were slowly frozen down at −80°C in a CoolCell LX container for 24 h before long-term storage in liquid nitrogen. Passage number never exceeded 30 passages for all species.

3D differentiation medium (ERN) consisted of 5% R-Spondin-1 CM, 5% Noggin CM, 1 mM HEPES, 2 mM GlutaMax, 1× P/S, 1× N2, 1× B27, 1 mM N-acetylcysteine and 50 ng/ml EGF in Advanced DMEM/F12 for mouse, human and porcine organoids. As the induced differentiation resulted in fast apoptosis in chicken organoids, spheroids were incubated with a differentiation medium consisting of 20% FCS, 2 mM GlutaMax, 1× P/S and 10 μM ROCK1 inhibitor Y-27632 in Advanced DMEM/F12. Mouse, porcine, and chicken organoids were kept in differentiation medium for three days; human organoids for five. Spheroids were cultured in parallel during differentiation experiments to serve as a control, since degradation of the extracellular matrix could also drive differentiation.

ODM medium consisted of 20% R-Spondin1 CM, 10% Noggin CM, 50 ng/ml EGF, 1 mM HEPES, 2 mM GlutaMax, 1× P/S, 1× N2, 1× B27, 1 mM N-acetylcysteine, and 10 mM nicotinamide in Advanced DMEM/F12 for all species.

Establishment of Organoid-Derived Monolayers (ODMs)

ODMs were established on 0.33 cm^2 (PET) or 0.6 cm^2 (polycarbonate) pre-coated transwell filters (0.4 μm pores). For coating, transwell inserts were chilled at −20°C for 20 min. In the meantime, Matrigel was mixed 1:10 with Advanced DMEM/F12. 150 μl were then pipetted into each of the upper compartments of a transwell insert and incubated for at least 16 h at 4°C. Before seeding, the supernatant was removed and the plate was incubated at 37°C for 30 min. After mechanical disruption (as described for passaging) and washing, singularized cells were collected in a single tube in pre-warmed ODM medium with 50% WRN CM supplemented with 10 μM Y-27632 and directly added onto the transwell inserts (approximately 2–3 × 10^6 cells per cm^2 transwell surface). The WRN content was reduced to 5% on day 1 and 0% on day 2, following general guidelines described by Moon et al. (2014) and VanDussen et al. (2015). Y-27632 was withdrawn from cultures on day 2 for all species. The medium was subsequently exchanged three times a week.

Immunofluorescence Assays (IFAs) and Microscopic Analyses

The ODM medium was removed and cells were subsequently fixed with 4% pre-warmed paraformaldehyde (PFA) in PBS (20 min at RT) or −20°C cold methanol (20 min at −20°C), depending on the primary antibody used (**Supplementary Table 2**) and processed within 7 days after fixation. Cells were permeabilized with 0.1 M glycine, 0.2% Triton X-100 in TBS and incubated in blocking buffer consisting of 3% BSA, 1% normal goat serum, 0.2% Triton-X-100 in TBS (50 mM Tris-Cl, pH 7.5, 150 mM NaCl) for 3 h at RT. Primary antibodies were added for incubation at 4°C overnight in blocking buffer and ODMs were washed the next day four times with 0.2% Triton-X100 in TBS. Secondary antibodies and 0.2 μg/ml DAPI or DRAQ5 as nuclear stains were added, kept for 1 h at RT in the dark, followed by three additional washing steps with TBS. The transwell inserts were washed once with deionized water and the filter surfaces with attached monolayers were then cut out from their frames using a scalpel. They were then mounted with Fluoromount-G on glass slides.

The 3D organoids were harvested and washed once in PBS, then incubated in cell-recovery solution for 30 min, followed by an additional wash with PBS, and fixed for 30 min in 4% PFA. Organoids were permeabilized and blocked as mentioned above, incubated for 2 h with Alexa 488-conjugated phalloidin and DAPI in blocking buffer. This was followed by three washing steps in 0.2% Triton-X100 in TBS and organoids were finally mounted with non-hardening IBIDI mounting medium onto glass slides.

Brightfield images were acquired using an Axio Z1 Observer microscope system (Zeiss). Images were contrast-adjusted with Zeiss ZEN software (blue edition). Fluorescence-microscopic images were taken by a Zeiss LSM 780 confocal laser scanning microscope, equipped with Plan-Apochromat 20×/0.8 M27 and C-Apochromat 40×/1.20 water M27 objectives and analyzed with ZEN software (blue edition) and ImageJ version 1.52a (Schneider et al., 2012). Panel composition and annotations were performed using Adobe Illustrator software. Secondary antibody controls are summarized in **Supplementary Figure 5**. All microscopy experiments were performed at least twice unless otherwise stated.

To quantify *T. gondii* load in infected murine ODMs, projections of z-stacks were generated and channels were separated. Number of nuclei of the parasites and host cells were quantified after size separation using the tool "Analyze particles" implemented in ImageJ. Parasite ratio to host cell was calculated by dividing the number of parasites counted by the number of nuclei counted per field. For each timepoint, three replicates were generated and three microscopic fields per filter were scanned per experiment.

RT-qPCR Analyses

To remove remaining traces of Matrigel, 3D organoids were excessively washed with ice-cold PBS before RNA extraction. RNA was extracted from 3D organoids and ODMs using Direct-zol RNA Microprep kit including an on-column DNase I treatment. RNA was quantified by 260/280 nm absorption measurement, with an Infinite M200 Pro reader (TECAN). The High Capacity RNA-to-cDNA Kit was used for cDNA synthesis with 200 to 500 ng RNA in 20 µl volume per reaction. qPCR was performed with a BioRad C1000 cycler with CFX96 system with a minimum of 5 ng cDNA per reaction. The qPCR included an initial 10 min enzyme activation step at 95°C, followed by 40 cycles of 20 s at 95°C, 30 s at 60°C, and 20 s at 72°C. To verify amplicon specificity, melting curve analysis was performed in CFX Maestro software. The ΔΔCt method was used to calculate relative expression of transcripts to housekeeping transcripts and, in comparison to spheroid or uninfected conditions, respectively.

Transepithelial-Electric Resistance (TEER) Measurements

To evaluate the barrier integrity and monolayer formation, TEER measurements were conducted. For this, a Millicell ERS-2 Voltohmmeter and a chopstick Ag/AgCl electrode (STX01) were used. For normalization, blank electric resistance (cell-free, coated transwell insert) was subtracted from raw resistance values and standardized for 1 cm^2 surface area. All measurements were conducted on a preheated 37°C heating block. For TEER measurements 12 to 36 filter inserts per species were analyzed.

Maintenance of *T. gondii* and *G. duodenalis* Parasites

T. gondii type 1 RH strain tachyzoites stably expressing mitochondrial GFP (Thomsen-Zieger et al., 2003), were maintained by continuous passage in confluent monolayers of human foreskin fibroblasts (HFF; BJ-5ta, ATCC CRL-4001) in DMEM supplemented with 2% FBS at 37°C in 5% CO_2.

G. duodenalis WB6 (ATCC 50803) trophozoites were cultured at 37°C in flat-sided 10 ml cell culture tubes in Keister's modified TYI-S-33 medium (Keister, 1983), supplemented with 10% adult bovine serum (ABS), 100 µg/mL streptomycin & 100 U/ml penicillin, and 0.05% bovine/ovine bile. For passaging, culture tubes were incubated on ice for 30 min to facilitate trophozoite detachment from the surface. Trophozoites were passaged 3 times a week at a ~1:100 ratio. For infection experiments, parasites were passaged the day before infection to guarantee logarithmic growth phase.

Infection of ODMs

For *G. duodenalis* infection, it was necessary to incubate ODMs with apical TYI-S-33 medium, as trophozoites survival is not supported in DMEM-based medium (Nash, 2019). As TYI-S-33 is a reducing, cysteine-rich medium, the confluent ODMs were incubated with TYI-S-33 medium in the apical compartment the evening before infection to allow equilibration. Before infection, TEER was measured again to ensure proper epithelial integrity. All infection experiments were conducted with TYI-S-33 medium in the apical compartment and ODM medium in the basal compartment.

For infection with *T. gondii*, HFF cells were scraped from T25 cell culture flasks and passed through a 23G blunt needle. To remove cell debris, the supernatant was collected and centrifuged at 100 *g* for 5 min. The pellet was discarded and the supernatant was then transferred to a new centrifuge tube and spun at 300*g* for 10 min. Tachyzoites were counted in a disposable Neubauer counting chamber and their number was adjusted to 1×10^8/ml in DMEM. TYI-S-33 was aspirated from the apical compartment before an appropriate amount of *T. gondii* in 100 µl DMEM was added on top of the monolayer. After 1 h, DMEM was replaced again by TYI-S-33 and ODMs were either left untouched or co-infected with *G. duodenalis* trophozoites.

G. duodenalis trophozoites were detached by chilling on ice, counted and subsequently centrifuged at 1,000*g* for 5 min at 4°C. The pellet was resuspended, their number was adjusted to 1×10^8/ml in TYI-S-33 and parasites were added into the ODM-containing transwell inserts.

For the determination of an infectious dose (ID), we assumed a density of 3×10^5 cells per cm^2 of a transwell filter, a cell number that was determined in previous experiments. For *T. gondii* infection, we added 25 tachyzoites per host cell (ID 25) and for *G. duodenalis* infection we added 3 trophozoites per host cell (ID 3).

Immunoblotting

Confluent monolayers of HFFs were detached with a cell scraper and pelleted at 500 *g*. Human organoids were harvested and prepared as for IFAs. *T. gondii* tachyzoites and *G. duodenalis* trophozoites were prepared as described above and then pelleted by centrifugation. All cells were then lysed with RIPA-buffer (50 mM Tris-HCl pH 8.0, 1% w/v NP-40, 0.5% w/v sodium deoxycholate, 0.1% w/v SDS, 150 mM NaCl, and 5 mM EDTA) containing cOmplete protease inhibitor cocktail. Protein concentrations were quantified using a Pierce BCA Protein Assay. For immunoblotting, 2× Laemmli sample buffer (4% w/v SDS, 20% v/v glycerol, 0.004% w/v bromophenol blue, and 0.125 M Tris–HCl (pH 6.8) with 10% v/v 2-mercaptoethanol) was added to the samples and boiled for 5 min. SDS-PAGE in Tris-glycine/SDS running buffer and immunoblotting on nitrocellulose membranes followed standard techniques, with 20 µg protein loaded per lane. Total protein on blots was visualized using DB71 staining (Hong et al., 2000) prior to the antibody incubation. HRP signal was detected using ECL Plus Western Blotting Detection Reagents on a Vilber Fusion FX Western blot and chemiluminescence imaging system.

Statistical Testing

Basic calculations were performed with MS EXCEL 2010 (Microsoft). Figures were plotted in Prism 8.4 (GraphPad). Quantitative results are presented as mean (± 95% CI). Significance was tested by two-way ANOVA with Dunnett's correction for multiple testing, and p values ≤ 0.05 were considered as statistically significant. Asterisks indicate statistical significance values as follows: * $p < 0.05$ ** $p < 0.01$, *** $p < 0.001$, **** $p < 0.0001$.

RESULTS

Characterization of Three-Dimensional Duodenal Organoid Cultures From Human, Mouse, Pig, and Chicken

The overall aim of this study was to define experimental parameters for the generation and maintenance of intestine-derived organoids from different host species that are robust but at the same time vary minimally in medium composition and culture conditions.

We could establish and maintain human, mouse, pig, and chicken duodenal spheroid cultures by a medium that required only a few general adaptations from previous media conditions defined for human spheroids (**Table 1**, **Figures 1A, B**, WERN). First, we found it essential to provide autologous EGF for optimal growth conditions because of the species-specific variability of the protein sequence in the receptor binding site (**Supplementary Figure 1**). Nevertheless, conveniently, pig EGF could be replaced by mouse EGF and chicken EGF could be replaced by a combination of mouse and human EGF. Of note, growth factors for species other than mouse or human are not readily available, or are prohibitively expensive for high throughput use. Second, to maintain chicken spheroids it was necessary to inhibit glycogen synthase kinase-3 (GSK-3) activity by the inhibitor CHIR99021 in order to maintain stemness conditions by potentiating the β-catenin/Wnt signaling axis as previously described by Li et al. (2018).

Next, we examined the ability of stem cell-enriched spheroid cultures to develop into differentiated epithelial organoids. After incubation in differentiation medium (ERN), spheroids of all species changed in appearance and developed into organoid structures with typical morphological signs of differentiation (**Figure 1B**, ERN). To differing degrees all cultures started to show both budding and the creation of small crypt-like structures that included pronounced apoptotic cell debris accumulating in the inner part of these structures (organoid lumen). Additionally, all cultures developed thicker epithelial layers, and cells grew more columnar in comparison with stem-cell enriched spheroids (WERN) grown in parallel (**Figure 1B**).

To confirm the changes in cell type composition, we analyzed by RT-qPCR the expression of several established marker genes characteristic for the different cell types of the intestinal epithelia, such as enteroendocrine cells, Paneth cells, goblet cells, stem cells and enterocytes (**Figure 1C**, **Supplementary Figure 2**). We compared spheroids (WERN condition) with differentiated organoids (ERN condition), and spheroids that were kept under stem cell-enriching media conditions (WERN) for the same time as organoids in ERN condition, as the degradation of the extracellular matrix may also drive differentiation. Spheroids of all four species differentiated into cell types known to be present in the intestinal epithelium, as judged by the up-regulation of transcripts for respective marker genes. One exception was the lack of enteroendocrine cells in human duodenal organoids (**Figure 1C**). It also appeared that expression of enterocyte markers such as fatty acid-binding protein (*FABP*), peptide transporter 1 (*PEPT1/SLC15A1*) and sucrose isomaltase (*SI*) were particularly elevated in response to the differentiation medium. In contrast, stem cell-associated transcripts generally decreased under differentiation medium conditions, except for mouse organoids.

To characterize the orientation and polarity of the epithelium, we performed fluorescence analysis of spheroids/organoids by labeled phalloidin staining of F-actin to highlight the intestinal brush border (**Figure 2**). As expected, all stages possessed a brush border orientated towards the lumen of the spheroid/organoid structure, thereby exposing the basal side to the surrounding medium. Additionally, under differentiation conditions columnar enlargement of the cells in the organoid walls could be observed.

Generation of Organoid-Derived, Polarized, Epithelial Monolayers Suitable for Parasite Infection

Given the constraints of limited access to the apical side in 3D organoids for infection, we established conditions for a cellular system that provides easily accessible but functionally separated apical and basolateral compartments. To this end, we seeded singularized 3D spheroid-derived cells onto transwell filters. To start differentiation, we withdrew the stem cell-promoting factors Wnt3a, A83-01 (TGF-beta inhibitor), and SB202190 (p38 inhibitor) from the medium.

For all four species we could observe that both confluent and polarized epithelial monolayers developed (**Figure 3A**). We recently reported that human ODMs developed a columnar shape with an average thickness of ~20 μm over time (Kraft et al., 2020) (**Figure 3A**, **Supplementary Figure 3**), reflecting polarized epithelial differentiation. In contrast, murine, porcine and chicken ODMs remained comparatively flat, with a thickness of < 10 μm (**Figure 3A**, **Supplementary Figure 3**). Importantly, however, cells of all species were able to generate an electrophysiologically tight epithelium, as indicated by TEER measurements (**Figure 3B**). While the human ODMs reached a plateau at ~220 $\Omega^{*}cm^2$ after approximately 8 to 10 days, murine, porcine and chicken ODMs formed a tight epithelium already after 3 to 5 days. It is also noteworthy that porcine ODMs collapsed after 6 to 9 days after establishment whereas ODMs of all other species could be maintained for at least 3 weeks (data not shown).

To compare cell differentiation in ODMs in comparison with the initial spheroid-derived cell cultures, we followed the changes of cell marker transcripts over time. As shown in **Figure 4**, the

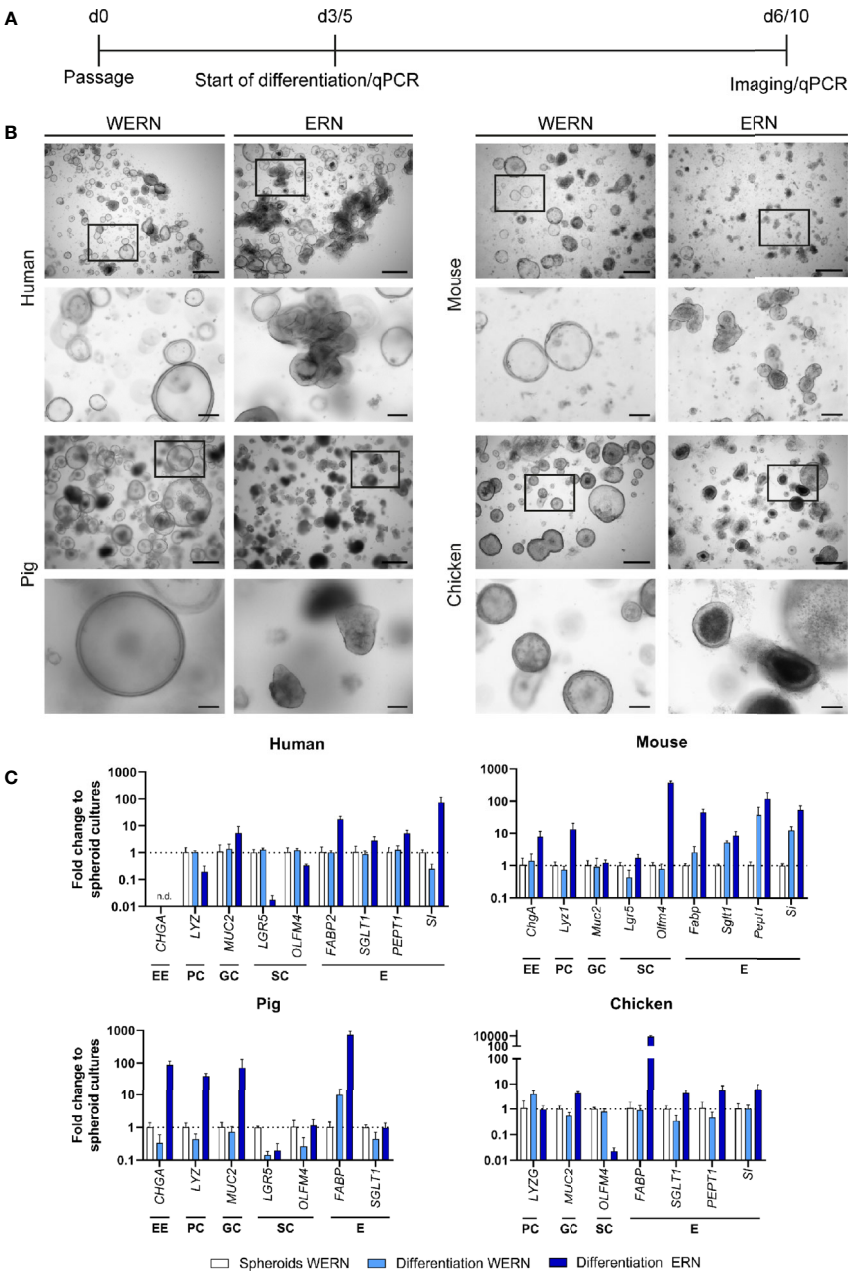

FIGURE 1 | Characterization and differentiation of 3D spheroids/organoids from human, mouse, pig and chicken origin. **(A)** A new spheroid culture was cultured for 3 days (5 days for human) in WERN medium and then spheroids were either maintained in WERN medium or differentiated in ERN medium for further 3 days (human for 5 days). At indicated time points, spheroids/organoids were imaged and/or harvested for RNA extraction and transcriptional analysis by RT-qPCR. **(B)** Representative brightfield microscopic images of spheroids/organoids. Scale bars represent 500 µm (upper panel in each species) and 100 µm (lower panel in each species). **(C)** Quantification of marker genes specific for various intestinal cell types by RT-qPCR. Note that the data are normalized to the transcript abundance of 3/5 day WERN spheroid culture. EE, enteroendocrine cell; PC, Paneth cell; GC, goblet cell; SC, stem cell; E, enterocyte. RT-qPCR experiments show mean (± 95% CI) of ≥ 4 technical replicas of at least two independent biological replicates. n.d., not detectable.

overall transcriptional pattern changed in all species from crypt-based stem cell/Paneth cell signatures [reflected by lower abundance of Leucine-rich repeat-containing G-protein coupled receptor 5 (*LGR5*), olfactomedin 4 (*OLFM4*), and lysozyme (*LYZ*)] to more villus-like enterocyte/goblet cell signatures [higher abundance of Mucin 2 (*MUC2*) and enterocyte transporters such as *PEPT1*, *FABP*, sodium-glucose linked transporter 1 (*SGLT1*) and *SI*]. However, it is important to note that abundance of specific transcripts differed from species to species, indicating different grades of differentiation (**Figure 4**,

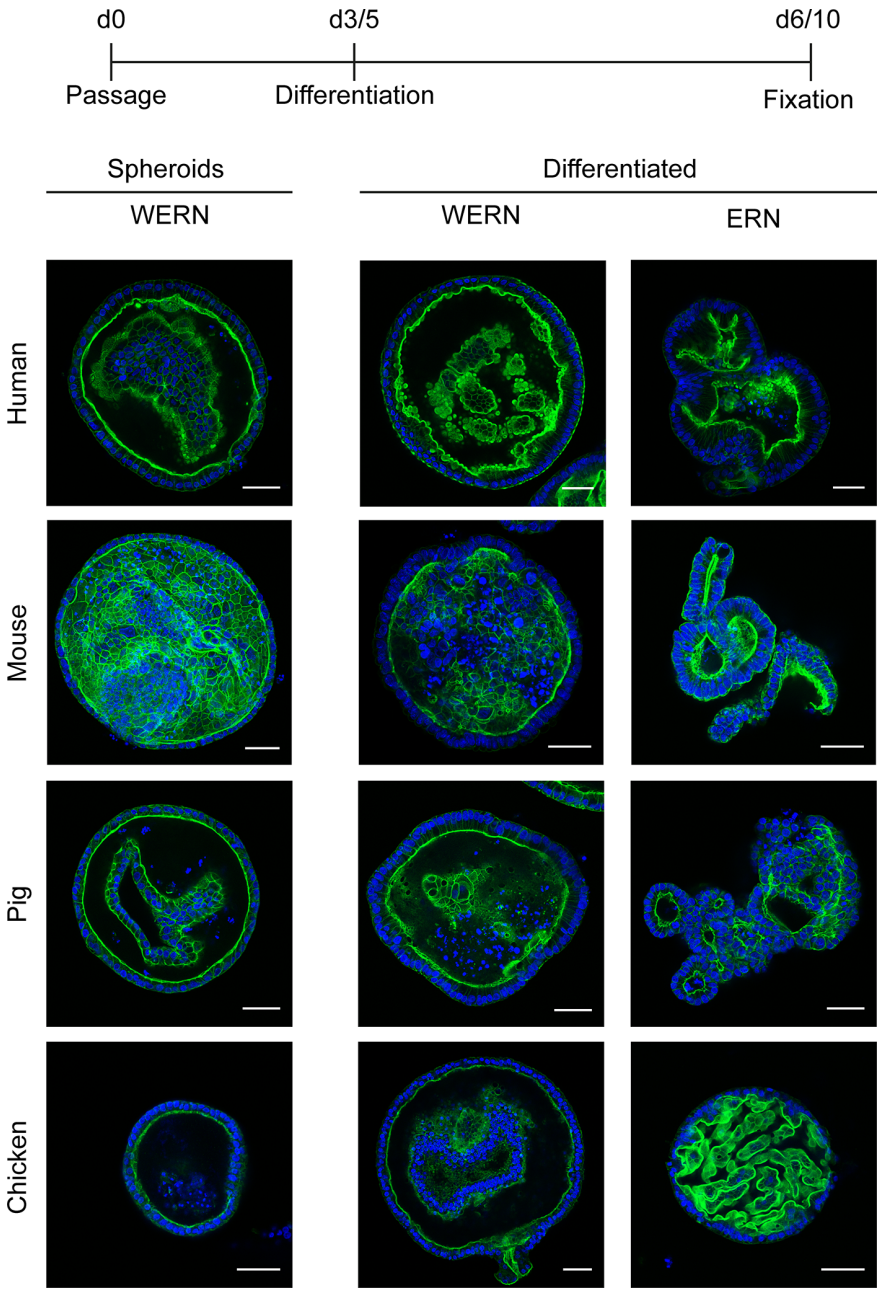

FIGURE 2 | Fluorescence analysis of brush border localization in 3D spheroids/organoids from human, mouse, pig and chicken origin. A new spheroid passage was cultured for 3 days (5 days for human) in WERN medium and then spheroids were either maintained in WERN medium or differentiated in ERN medium for further 3 days (human for 5 days). As a control, 3/5 day spheroids in WERN were also assessed in parallel. Subsequently spheroids/organoids were fixed and F-actin in the microvilli of the luminal brush border was visualized by staining with Phalloidin iFluor-488 (green). Cell nuclei were stained with DAPI (blue). Note, video composition of z-stacks are also provided as **Supplementary Material**. Scale bars represent 50 µm. All experiments were performed twice with similar results.

Supplementary Figure 2). In particular, the murine ODMs revealed still high expression of stem cell markers but also increased Pept1 expression,

To further characterize the cell lineages, we performed IFAs with antibodies directed against the essential brush border formation protein Ezrin (EZR/VIL2), Angiotensin-converting enzyme 2 (ACE2, the SARS-CoV-2 receptor) and sodium–hydrogen exchanger 3 (NHE3/SLC9A3) that are primarily expressed in enterocytes. The results were consistent with the development of both polarized and differentiated ODMs, as EZR and enterocyte markers accumulated at the apical tip of the monolayer cells (**Figure 5A**, **Supplementary Figure 4**). The

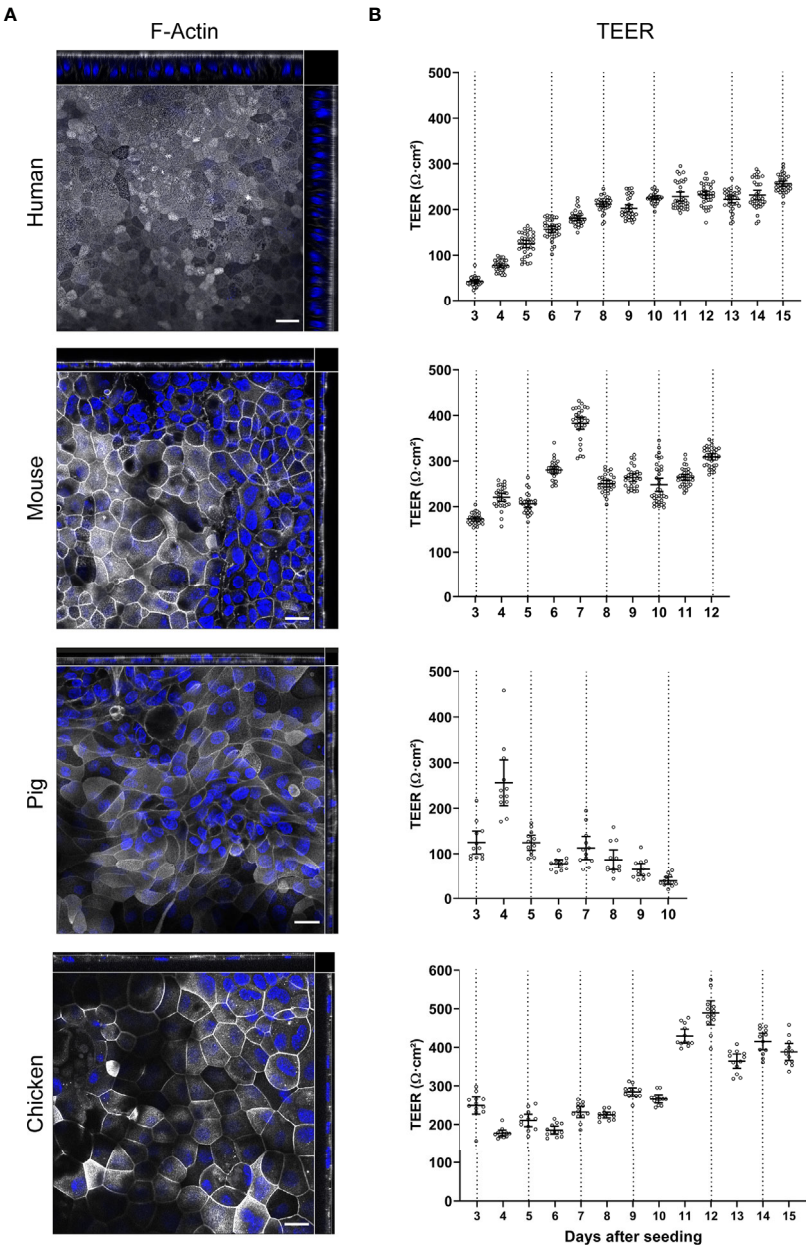

FIGURE 3 | Characterization of TEER development and brush border orientation of ODMs from human, mouse, pig and chicken origin. Spheroids of all four species were seeded on transwell inserts and cultured in differentiation media. **(A)** Representative orthogonal images of z-stacks showing F-actin accumulation in the apical brush border of ODMs. ODMs were fixed after 10 (human), 12 (mouse), 6 (pig) and 15 (chicken) days and F-actin was visualized using phalloidin (white) and nuclei using DAPI (blue). Scale bars represent 20 µm. All experiments were performed twice with similar results. **(B)** ODMs of all four species developed electrophysiologically tight barriers as indicated by TEER analysis. Dashed lines represent medium exchanges. Experiments show mean (± 95% CI) of 12–36 filter inserts per species.

general picture of a more enterocyte-guided differentiation by our transcriptional analysis was supported by the identification of NHE3- and/or ACE2-positive cells in human, mouse and chicken ODMs. Of note, pig ODMs lacked antibody binding for NHE3 and ACE2, which can also reflect missing conservation of epitopes between species (**Figure 5A**, **Supplementary Figure 4**). We also observed the presence of SRY-Box Transcription Factor 9 (SOX9) in ODMs from human, mouse and chicken, which is an indicator for the presence of proliferative cells in these ODMs (Blache et al., 2004) (**Figure 5A**, **Supplementary Figure 4**).

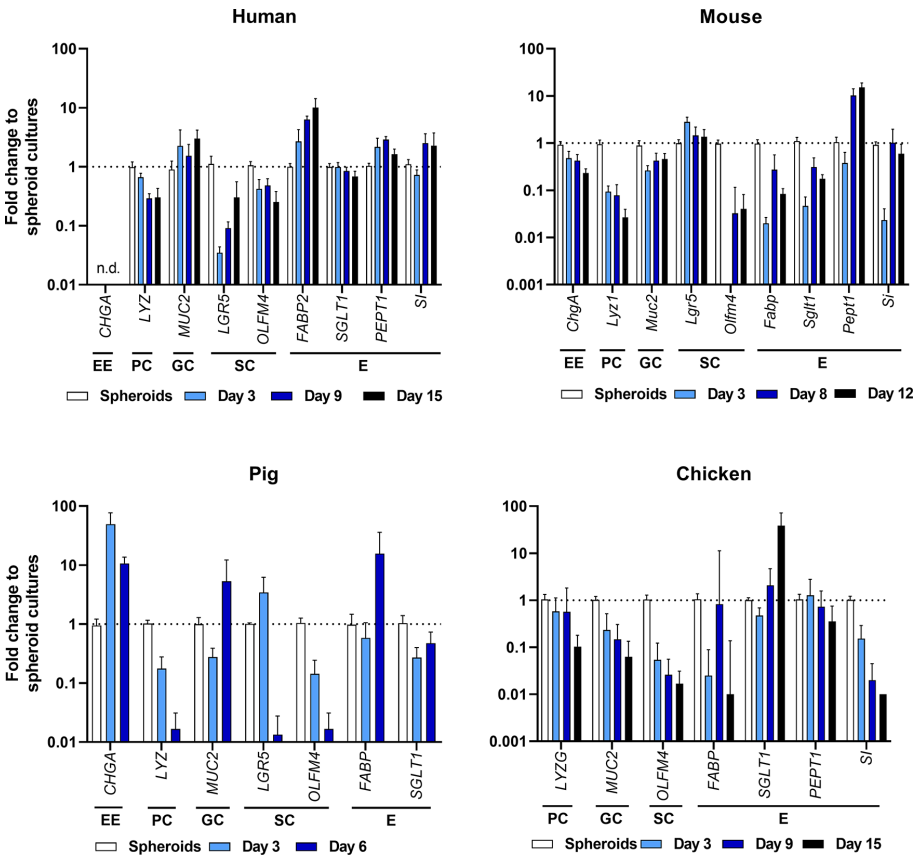

FIGURE 4 | Expression profiling of intestinal cell types by RT-qPCR of ODMs from human, mouse, pig and chicken origin. Indicated markers represent EE, enteroendocrine cells; PC, Paneth cells; GC, goblet cells; SC, stem cells; and E, enterocytes. RT-qPCR experiments show mean (± 95% CI) of ≥ 4 technical replicas of at least two independent biological replicates. n.d., not detectable.

Effects of Infection and Co-Infection With *T. gondii* and *G. duodenalis* on Barrier Function of Murine ODMs

The house mouse is an important natural host for *T. gondii* and also the prime experimental host model, not the least due to numerous knock-out mouse strains available that allow detailed studies on host-parasite interaction. In this paper, we therefore focused on the establishment of conditions for infection experiments of murine ODMs. Having a shared interest in the two parasites *T. gondii* and *G. duodenalis*, we also wanted to exploit the challenges given by their different growth conditions in this cellular system to study co-infections. Both parasites infect the same site of the gut, albeit with different modes of infection, and both have a wide and overlapping host range, including mice. However, co-infection studies have been very rarely reported.

We have recently shown that *G. duodenalis* alters the junctional integrity in human ODMs that leads to de-localization and disruption of the junctional complex (Kraft et al., 2020). *T. gondii* has also been proposed to modulate barrier dysfunction in Caco-2 cells (Briceño et al., 2016). We therefore wanted to examine whether similar adverse effects on tight junction integrity could be seen in *T. gondii* infections, alone and also in co-infection with *G. duodenalis*. In the latter case, the presence of tachyzoites might be able to modulate *G. duodenalis*' effect on barrier function, given the known influence of *T. gondii* on host cell transcription in general (Hakimi et al., 2017).

G. duodenalis infection requires incubation of the ODMs with a cysteine-rich medium—Keister's modified TYI-S-33 medium (Keister, 1983)—that contains bile salts and thereby resembles duodenal conditions. This medium is toxic to commonly-used immortalized cell lines such as Caco-2 cells (Kraft et al., 2017; Nash, 2019), but we have recently shown that these conditions are tolerated by human ODMs (Kraft et al., 2020). We have also shown that incubation of *G. duodenalis* in TYI-S-33 in the apical compartment of transwell inserts supports parasite growth for > 72 h (Kraft et al., 2020) while incubation with DMEM-based media is known to compromise *G. duodenalis* viability (Nash, 2019). As a first step to co-infection, we ensured that both the epithelial monolayers of mouse, pig and chicken, as well as *T. gondii* tachyzoites were tolerant to incubation in TYI-S-33. Incubation with this medium in the apical compartment was tolerated by ODMs of all four species, as determined by analysis of TEER (data not shown). We also observed that the use of TYI-S-33 allowed reproducible replication of RH strain tachyzoites in

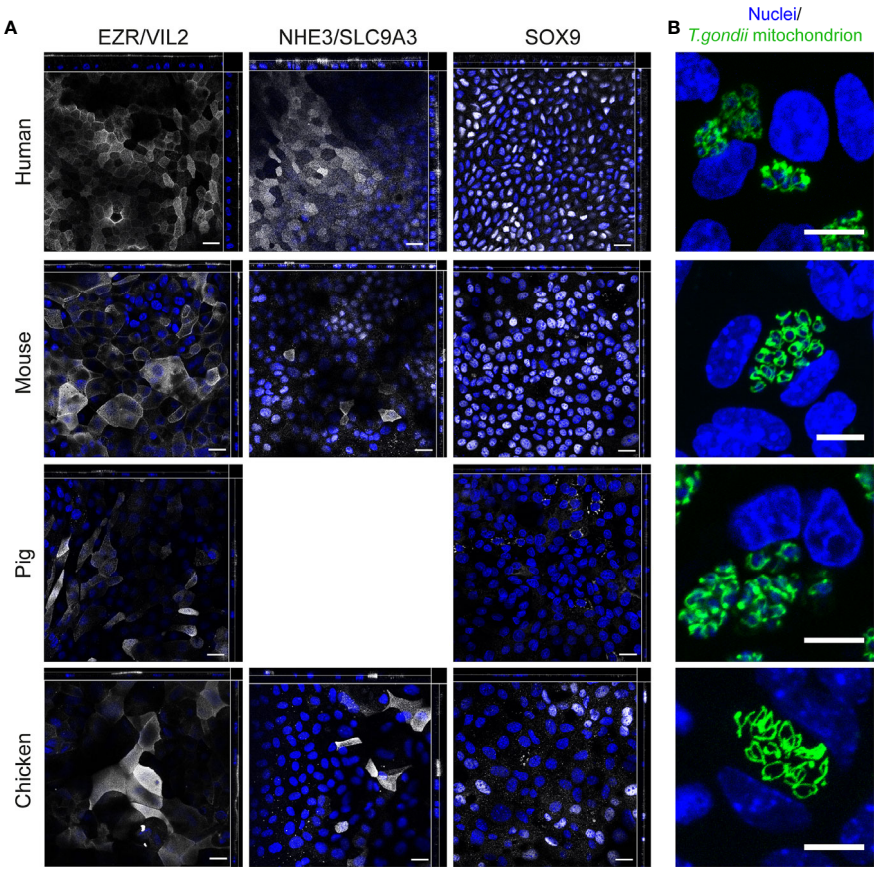

FIGURE 5 | Immunofluorescence analysis of ODMs from human, mouse, pig and chicken origin. **(A)** Orthogonal stacks for brush border protein EZR, enterocyte marker NHE3, and SOX9. ODMs were cultured as described and fixed after 10 (human), 12 (mouse), 6 (pig) and 15 (chicken) days. Note, NHE3 analysis for pig was excluded as suitability of the antibody for IFA staining in this species is questionable (see **Supplementary Figure 6**). Suitability of the SOX9 antibody for IFA staining for pig is also questionable, however, the analysis was included as the antibody target sequences are highly similar between species (see **Supplementary Figure 6**). Representative fluorescent orthogonal stacks of ODMs are shown. Scale bars represent 20 µm. **(B)** Representative confocal image projections of ODMs infected for 48 h with *T. gondii* (distinguished by its GFP-tagged green tubular mitochondria) in TYI-S-33 medium. Scale bar 10µm. All experiments were performed at least twice with similar results.

ODMs of all four species (**Figure 5B**). Quantification of *T. gondii* tachyzoite growth in murine ODMs is shown in **Supplementary Figure 7**.

Having established conditions suitable for co-infection, we next designed an experiment using murine ODMs as host system. To this end, ODMs were first infected with *T. gondii* tachyzoites for 1 h and subsequently co-cultured with or without *G. duodenalis* trophozoites for 48 h. As representative protein components of the intra- and intercellular tight junction complex, we choose zona occludens 1 (Zo-1/Tjp1) and occludin (Ocln) and evaluated by IFA whether infection with the parasites alone or in co-infection lead to alterations in barrier integrity (**Figure 6A**). While *T. gondii* showed no apparent effect on the ODMs' tight junction proteins, *G. duodenalis*' influence was striking (**Figure 6A**). Infection resulted in severe delocalization and destruction of the tight junctional integrity of murine ODMs. Still, we could identify several cells infected with *T. gondii* in the vicinity of *G. duodenalis* parasites, indicating tachyzoite replication. Overall, co-infection recapitulated the phenotype of the *G. duodenalis* infected condition with no exacerbating or dampening effect by *T. gondii* co-infection (**Figure 6A**). Notably, one report using m-ICc12 cells described a re-localization of occludin at the parasites′ point of entry and co-localization of occludin with the parasite (Weight et al., 2015). In our experiments with murine ODMs, we also observed some staining of tachyzoites in the IFAs with the same antibody (**Figure 6A**). However, Western blot analysis revealed that this reactivity is most likely due to an unrelated *T. gondii* protein cross-reacting with the respective commercial anti-occludin antibody (**Supplementary Figures 8** and **9**).

We also quantified the disturbance of the barrier function using TEER measurements. Using identical IDs as shown in **Figure 6A** *T. gondii* infection alone did not lead to a decrease in epithelial resistance, while the TEER of *G. duodenalis* infected ODMs was significantly deviating from the control conditions after 32 and 48 h

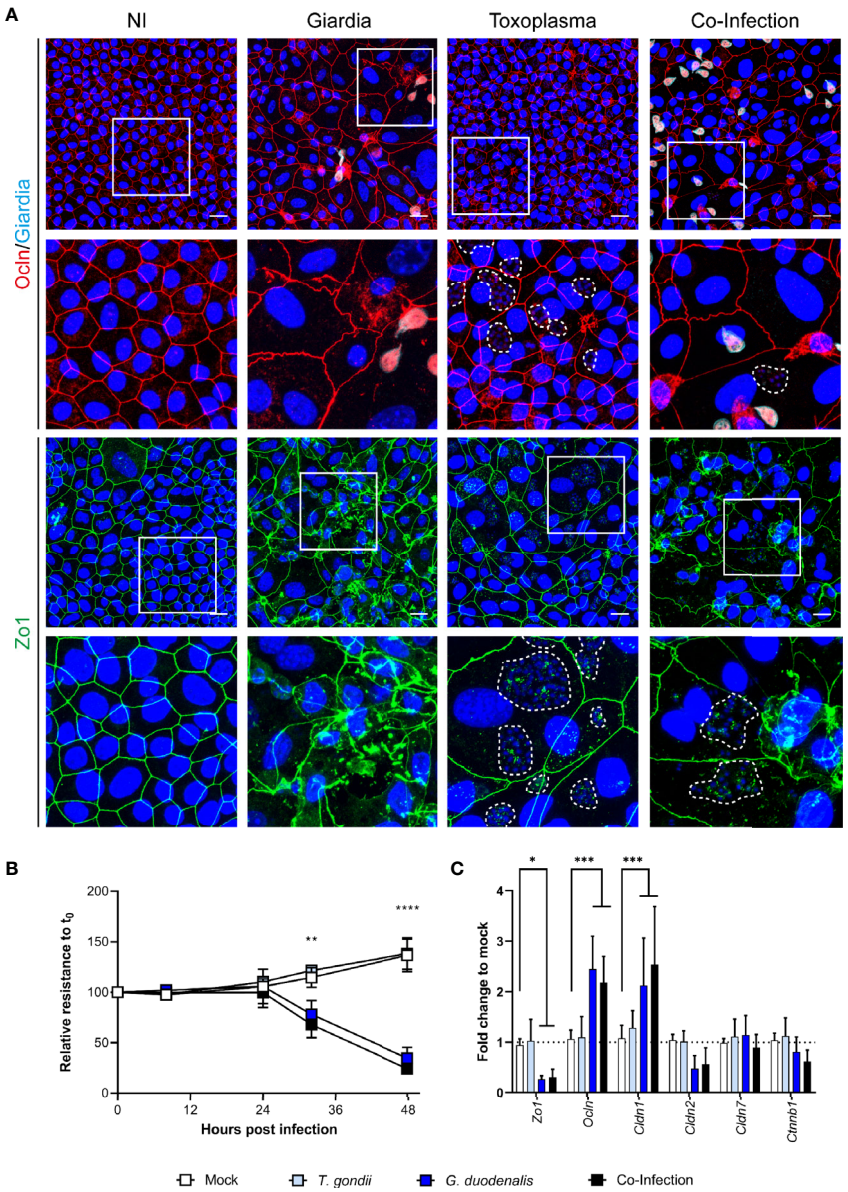

FIGURE 6 | Co-infection of murine ODMs with *T. gondii* and *G. duodenalis*. Murine ODMs were infected with either an ID of 3 (*G. duodenalis* strain WB6 trophozoites) or an ID of 25 (*T. gondii* strain RH tachyzoites), or both and monitored for 48 h post infection. **(A)** Representative projections of immunofluorescence Z-stack images of Zo-1 and occludin of non-infected (NI), *G. duodenalis, T. gondii* and co-infected murine ODMs after 48 h. *T. gondii*'s mitochondrial GFP fluorescence was lost due to methanol fixation; instead, dashed lines indicate *T. gondii* vacuoles including parasite nuclei (blue). Scale bars represent 20 µm. All experiments were performed twice with similar results **(B)** TEER monitoring of infected murine ODMs. Data are presented as mean (± 95% CI) of four independent experiments with three filters per experiment. Statistical significance between infection and mock controls was determined using a Two-Way ANOVA with Dunnett's correction for multiple testing. $^{**}p < 0.01$, $^{****}p < 0.0001$ **(C)** Transcriptional changes of indicated tight junctional components in infected ODMs. Data are presented as mean (± 95% CI) of three independent experiments with three filters per experiment. Statistical significance was determined using a Two-Way ANOVA with Dunnett's correction for multiple testing. $^{*}p < 0.05$, $^{***}p < 0.001$.

post infection (**Figure 6B**). Similar results were obtained for co-infection. RT-qPCR analysis of transcripts of components of tight junctions corroborated these findings. While no significant changes compared to non-infected control conditions could be observed in *T. gondii*-infected ODMs, those containing *G. duodenalis* showed differentially altered tight junction genes *Zo-1* ($p < 0.05$), occludin ($p < 0.001$) and claudin-1 (*Cldn1*, $p < 0.001$, **Figure 6C**). Taken together, in this ODM co-culture system, *G. duodenalis*' detrimental effect on barrier function is not altered by a concomitant *T. gondii* infection.

DISCUSSION

Here we provide robust protocols to establish and maintain stem-cell enriched spheroid cultures of four relevant host species that are subsequently used to generate electrophysiologically tight and differentiated ODMs suitable for *T. gondii* infections, alone or together with other relevant intestinal protozoa. We further provide evidence that *T. gondii* infection has, in contrast to *G. duodenalis*, no detrimental effect on TEER and tight junction integrity of murine ODMs. We anticipate that this ODM platform will help to uncover early events in infection of *T. gondii* and other relevant intestinal parasites in the intestinal epithelia in the zoonotic context.

In recent years, the organoid model has been used to overcome limitations of immortalized cell lines, as for example their inability to represent the different cell types of the primary epithelium (Klotz et al., 2012). Beginning with the intestinal adult stem cell-derived mouse organoids (Sato et al., 2009; Sato et al., 2011a), the generation of intestinal organoids has been reported from numerous other species such as mice, humans, cats, dogs, rat, cattle, pigs, birds, and even reptiles (Sato et al., 2011b; Gonzalez et al., 2013; Powell and Behnke, 2017; Chandra et al., 2019; Derricott et al., 2019; Martorelli Di Genova et al., 2019; Ambrosini et al., 2020; Hedrich et al., 2020; Post et al., 2020). Their resemblance to *in vivo* tissue, i.e., the presence of multiple cell types and tissue specific organization, makes organoids more complete and thus superior cellular systems to what most current cell line-based models are able to provide. Consequently, organoids have enabled previously unseen progress in many fields, one of them being infection biology, in particular for bacteria and viruses [reviewed in Hill and Spence (2017) and Artegiani and Clevers (2018)]. The organoid model has enabled advances in the field of parasitology with infection studies on *Cryptosporidium* (Heo et al., 2018; Wilke et al., 2019), *T. gondii* (Derricott et al., 2019; Luu et al., 2019; Martorelli Di Genova et al., 2019), *G. duodenalis* (Kraft et al., 2020) and helminths (Eichenberger et al., 2018; Duque-Correa et al., 2020).

The primary motivation for this study was to develop straightforward protocols for the generation of 3D-organoids and ODMs of different hosts to facilitate the *in vitro* evaluation of host-parasite interactions in the intestinal epithelium (Delgado Betancourt et al., 2019; Hares et al., 2020). As with any other cellular model system, the standardization of reagents, materials and experimental execution is critical in order to provide robust and reproducible results (**Supplementary Tables 2** and **3**). This is even more important for 3D-organoids and ODMs, as small changes in growth and differentiation factors or growth conditions can lead to different cellular compositions. This, in turn, may lead to corresponding differences in parasite behavior. In this context, it must be emphasized that for economic reasons, we used supernatants from cell cultures expressing the three most important (and most expensive) growth factors Wnt3a, R-Spondin1/3 and Noggin, which require careful activity testing and quantification prior to their use to guard from batch-to-batch variation (VanDussen et al., 2019).

Only a few other examples show similar comparisons of organoids from different vertebrate species other than mouse and human to study pathogen interaction in the zoonotic context. Derricott et al. (2019) compared mouse 3D-organoids with those from porcine and bovine origin and compared the morphology as well as selected proteins by mass spectrometry in order to confirm the presence of differentiated cells in the generated cultures (Derricott et al., 2019; Hares et al., 2020). They also showed susceptibility of these 3D organoids to *Salmonella* and *T. gondii* infection, but did neither report quantitative and functional data upon infection nor did they establish monolayer cultures. Culture conditions were different for bovine and porcine cultures, as bovine cultures did not survive in IntestiCult medium (commercial medium optimized to support mouse organoids) alone and required addition of Wnt3a CM. Another group described the formation of porcine ileum 3D cultures and transwell monolayers and used a similar medium containing Wnt3a, as described in the present work for 3D organoids (van der Hee et al., 2018; van der Hee et al., 2020). A further comparative study on 3D cultures from large farm and small companion animals also showed the suitability of WRN CM medium to support growth of organoids from various mammalian species (Powell and Behnke, 2017). Species-specific media components have been extensively described for the mouse and human organoid system (Sato et al., 2011a; VanDussen et al., 2019). For the monolayer system, the requirements are less defined. For example, for mouse and human, the use of 5% WRN CM and 20% FBS has been reported (Moon et al., 2014; VanDussen et al., 2015), whereas Kozuka et al. (2017) report medium requirements without Wnt3a and additional FBS, depending on species and tissue section. Of note, in the murine ODM system, our protocol maintained a high level of stem cell marker expression and induced expression of enterocyte marker Pept1. This might be a result of nicotinamide in the differentiation medium that has been shown to be critical for maintaining prolonged cultures of human organoids (Sato et al., 2011a). How the differentiation status possibly affects infection with *T. gondii* or *G. duodenalis* has not been investigated in the present work. This should be addressed in future studies, including the use of different media conditions as exemplary described above.

For porcine monolayers a medium containing 30% Wnt with additional 20% FBS was used, and measurement of TEER until 72 h after seeding showed an increase of epithelial resistance (van der Hee et al., 2018; van der Hee et al., 2020). However, whether TEER would decline after extended culture times, as observed in our study, was not reported. The observed breakdown of the barrier function in the pig ODMs might be a result of the deprivation of stem cells and the strong epithelial differentiation in these cultures.

Our ODM medium was not supplemented with Wnt3a or FBS, and we have not compared the influence of these factors on the ODMs of the various species. Nonetheless, it also supported ODM culture from chicken that have, to our knowledge, not been reported before. Thus, our protocol provides a reasonable starting point and, if required, may be further optimized.

We have focused on murine, human, porcine and avian models as a starting point for evaluating intestinal interactions with parasites such as *T. gondii* and *Giardia* spp., as these zoonotic parasites are commonly encountered in these host

populations. Moreover, while mice are the most studied species as a host for *T. gondii*, pigs, chickens, and cattle are important meat sources for humans. Studying the early phase of infection with *T. gondii* comparatively in these different host organoids might reveal similarities and differences that could lead to new insights on infection routes and early events affecting susceptibility to infection in different species. For instance, the influence of higher temperature (41°C) on the parasitic infection process can be studied with chicken organoids where this temperature is physiological.

Notably, infections initiated with either bradyzoites or oocyst-derived sporozoites, which are the *T. gondii* stages that actually come into contact with the intestinal epithelium in any host (Delgado Betancourt et al., 2019), could be developed using this ODM platform. Most prior investigations of host-pathogen interactions employ tachyzoites, as the other developmental stages are scarce resources. It thus remains an open question whether infections initiated with the different stages results in obvious differences in infection dynamics using intestinal organoids. Furthermore, it is known that the tissue migratory capacity of *T. gondii* varies between strains (Barragan and Sibley, 2002), with type I strains (used in this study) having a better migratory capacity compared to type II and type III strains. The presented models will allow the comparison of infections with *T. gondii* strains of different genetic backgrounds under standardized conditions (infection dose, timing, nutritional composition, etc).

Of course, the absence of microbiota and immune cells in this system has to be taken into account and its pros and cons and the possibilities to supplement the organoid system with these important players have been described recently (Noel et al., 2017; Williamson et al., 2018; Bar-Ephraim et al., 2020; Min et al., 2020). There are other limitations of organoids in general. For example, cell compositions of these cultures will vary not only from host-to-host but also between individuals reflecting e.g. genetic variability, unless this variation is known, comparative studies and data have to be interpreted with caution. Another limitation relates to the lack of standardized culture conditions between laboratories. However, the field is not yet at this stage. Providing a point of departure towards comparability has been a motivation for this work, though. Another limitation relates to the difference in longevity of the differentiated cultures. Although indefinite proliferation is generally achieved under Wnt-supplemented conditions, the differentiated organoids, in particular under monolayer conditions, are less stable in certain species and medium conditions. Not surprisingly, most publications describe monolayer systems used for time frames of 1 to 6 days after seeding (Moon et al., 2014; VanDussen et al., 2015; Kozuka et al., 2017), enough to show appropriate differentiation of the major cell types of the epithelium. Our main goal was to find conditions that provided stable monolayer conditions — that is maintenance of TEER — suitable for "longer" experiments. Our culture conditions indeed provided stable TEER values until 3 weeks after seeding (except for porcine ODMs). Depending on the question, media conditions need to be adapted as described above and by others (Kozuka et al., 2017).

While the dynamics of invasion and dissemination of *T. gondii* in the lamina propria are better studied, the cellular mechanisms of initial epithelial invasion still remain to be elucidated (Delgado Betancourt et al., 2019). Typically, previous infection models merely simulate the architecture of the intestinal epithelium, using intestinal cell lines such as murine m-ICc12 (Rachinel et al., 2004), human Caco-2 (Briceño et al., 2016; Ross et al., 2019), and rat IEC-6 cells (Weight et al., 2015). However, with respect to differentiation-related marker protein expression, these immortalized cell lines often retain a memory of their tissue origin and do not have the potential to reflect the complexity of the epithelium, i.e. the heterogeneity of cell populations found throughout the intestinal crypt-villus axis (Pageot et al., 2000; Balimane and Chong, 2005; Hill and Spence, 2017).

It has been suggested that *T. gondii* moves through the epithelial junctions for transepithelial migration and penetrates the lamina propria without altering paracellular barrier functions such as TEER or the permeability of higher molecular weight fluid-phase markers such as dextran (Barragan and Sibley, 2002; Barragan et al., 2005; Lambert and Barragan, 2010; Weight et al., 2015). Measurements of these parameters during infections were performed over short durations of time [90 min, Barragan et al. (2005); Ross et al. (2019) or 2 h (Weight et al., 2015)] to determine the effect during transmigration. Such short observational time points, however, may be insufficient to show the modulation of the tight junction barrier upon infection and intracellular growth of the parasite. In a study by Briceño et al. (2016), a decrease in TEER after 20 and 24 h of infection in Caco-2 cells was reported, pointing toward a modulation of barrier function during the intracellular growth phase. Moreover, studies on the junctional complex in retinal epithelial cells (Song et al., 2017) or human endothelial HUVEC cells (Franklin-Murray et al., 2020) support a similar TEER effect after a 24 h or 18h time point, respectively. In contrast, several groups have analyzed the distribution of junctional proteins during paracellular transmigration of tachyzoites in short term experiments (up to 6 h) and during intracellular growth with different cellular systems with partly conflicting results. For example, Briceño et al. (2016) used Caco-2 cells and reported the redistribution and decrease of Zo-1 after 24 h post infection (p.i.) whereas studies in MDCK (Barragan et al., 2005), m-ICc12 cells (Weight et al., 2015) and Caco2 or murine brain endothelial cells (Ross et al., 2019) showed no alterations in the distribution of this protein after 2 to 6 h p.i. With the longer time points of these studies in mind, we extended TEER measurements, RT-qPCR, and the IFA of tight junction components to 48 h. Notably, we observed no significant TEER changes or tight junction alterations in ODMs in *T. gondii* single infections. A moderate TEER decrease was observed only at much longer time points (>96h) and required higher parasite doses (ID > 50, data not shown). We have not further investigated whether this was due to cell lysis of the monolayers or other mechanisms. We speculate that the complexity of the ODM system and its proliferative capacity is partly responsible for the observed differences to traditional models based on immortalized cell lines. Understanding these differences will be insightful in future comparative studies using ODMs of different hosts.

As for *T. gondii*, most research focusing on the pathogenicity of *G. duodenalis* is performed using immortalized cell lines. To our knowledge this is the first time *G. duodenalis* infection, and

co-infection with *T. gondii*, is reported on murine organoid-derived layers. Changes of the epithelial junctional complexes have also been reported in response to *G. duodenalis* infection (Koh et al., 2013; Ma'ayeh et al., 2018). However, in a similar manner to *T. gondii* infections, most studies are inconsistent and observed this change at very early time points of infection (Chin et al., 2002; Ma'ayeh et al., 2018). The exact mechanisms of tight junction breakdown and subsequent TEER decrease *in vitro* are not fully understood. The activation of caspases is reported to lead to apoptosis (Chin et al., 2002) or to the restructuring of the cytoskeleton *via* MLCK (Bhargava et al., 2015) as the main driver in cell line-derived epithelium. While this is superficially supported with our findings (**Figure 6**), we have described elsewhere that tight junction breakdown occurs *via* a different series of events in human duodenal ODMs (Kraft et al., 2020). ODMs thus have reproduced much closer the situation found *in vivo* as reported by Troeger et al. (2007). Here, we also show differential expression of tight junction components in murine ODMs after *G. duodenalis* infection, which partly differed to the response seen in the human ODM system. This indicates species-specific responses, however, the net effect on tight junction barrier impairment as determined by TEER reduction revealed similar kinetics as compared to the human ODM system. Future studies will be necessary to dissect common and species-specific responses.

In conclusion, we provide straightforward protocols to establish and maintain stem-cell enriched primary intestinal epithelial cultures of four relevant host species and their adaptation to generate differentiated monolayer cultures suitable for *T. gondii* infections or co-infections with other relevant intestinal protozoa. The possibility of expansion of the organoid micro-architecture by additional factors such as microbiota and immune cells may aid in understanding infection and disease. In addition, the organoid system is amenable for genetic engineering which might help to identify cell type targeted pathogenic effects. In future studies these systems are therefore suitable to discover host-specific or common factors important for host-parasite relationship in the relevant primary intestinal epithelial tissue.

DATA AVAILABILITY STATEMENT

The original contributions presented in the study are included in the article/**Supplementary Material**. Further inquiries can be directed to the corresponding author.

ETHICS STATEMENT

The isolation and establishment of organoids from the human duodenal specimen were described before (Kraft et al., 2020) and were approved by the ethical committee of the Charité, Berlin (#EA4-015-13). The donors of human material provided their written informed consent to participate in this study. For porcine samples, duodenal crypts were isolated from a 10-week old piglet (Sus scrofa, kindly provided by Svenja Steinfelder, Institute of Immunology, Freie Universitat Berlin, animal license T0002/17). Chicken duodenal crypts were isolated from intestine of a 14-day-old female chicken (Gallus gallus, kindly provided by Luca Bertzbach & Benedikt Kaufer, Institute of Virology, Freie Universitat Berlin, animal license T0245/14). The mouse duodenal sample derived from a female C57/Bl6 mouse from an RKI in-house bred colony (animal license T0173/14). The animal studies were reviewed and approved by the Landesamt für Gesundheit und Soziales (LAGeSo) Berlin.

AUTHOR CONTRIBUTIONS

Study concept and design: all authors. Experiments and analysis of data: DH and ED-B. Interpretation of data: all authors. Drafting the manuscript: all authors. Critical revision of the manuscript for important intellectual content: all authors. All authors contributed to the article and approved the submitted version.

FUNDING

Financial support was provided by the Deutsche Forschungsgemeinschaft, DFG *via* GRK 2046 Parasite Infections to TA, FS, and CK. DH and ED-B were funded by GRK2046. Work by TA, FS, and CK cited is supported by the Robert Koch-Institute. FS is a also a member of IRTG 2029 (supported by the German Research Council, DFG), and of TOXOSOURCES (supported by funding from the European Union's Horizon 2020 Research and Innovation programme under grant agreement No 773830: One Health European Joint Programme).

ACKNOWLEDGMENTS

We thank Luca Bertzbach and Benedikt Kaufer at Freie Universität Berlin for the provision of intestinal chicken samples and assembly of a library of intestinal marker primer sequences. We also thank Svenja Steinfelder at Freie Universität Berlin for the provision and extraction of porcine intestinal crypts. We also want to highlight the excellent technical assistance by Gudrun Kliem and Antonia Müller. We thank Scott C. Dawson for proofreading the manuscript and valuable discussions. The Zo-1 hybridoma developed by D.A. Goodenough (Harvard Medical School) was obtained from the Developmental Studies Hybridoma Bank, created by the NICHD of the NIH and maintained at The University of Iowa, Department of Biology, Iowa City, IA 52242.

SUPPLEMENTARY MATERIAL

The Supplementary Material for this article can be found online at: https://www.frontiersin.org/articles/10.3389/fcimb.2020.610368/full#supplementary-material

Supplementary Video 1 | Differentiated mouse organoid.

Supplementary Video 2 | Differentiated pig organoid

Supplementary Video 3 | Differentiated chicken organoid.

Supplementary Video 4 | Differentiated human organoid.

REFERENCES

Allain, T., and Buret, A. G. (2020). Pathogenesis and post-infectious complications in giardiasis. *Adv. Parasitol.* 107, 173–199. doi: 10.1016/bs.apar.2019.12.001

Ambrosini, Y. M., Park, Y., Jergens, A. E., Shin, W., Min, S., Atherly, T., et al. (2020). Recapitulation of the accessible interface of biopsy-derived canine intestinal organoids to study epithelial-luminal interactions. *PloS One* 15 (4), e0231423. doi: 10.1371/journal.pone.0231423

Artegiani, B., and Clevers, H. (2018). Use and application of 3D-organoid technology. *Hum. Mol. Genet.* 27 (R2), R99–R107. doi: 10.1093/hmg/ddy187

Balimane, P. V., and Chong, S. (2005). Cell culture-based models for intestinal permeability: a critique. *Drug Discovery Today* 10 (5), 335–343. doi: 10.1016/s1359-6446(04)03354-9

Bar-Ephraim, Y. E., Kretzschmar, K., and Clevers, H. (2020). Organoids in immunological research. *Nat. Rev. Immunol.* 20 (5), 279–293. doi: 10.1038/s41577-019-0248-y

Barragan, A., Brossier, F., and Sibley, L. D. (2005). Transepithelial migration of *Toxoplasma gondii* involves an interaction of intercellular adhesion molecule 1 (ICAM-1) with the parasite adhesin MIC2. *Cell Microbiol.* 7 (4), 561–568. doi: 10.1111/j.1462-5822.2005.00486.x

Barragan, A., and Sibley, L. D. (2002). Transepithelial migration of *Toxoplasma gondii* is linked to parasite motility and virulence. *J. Exp. Med.* 195 (12), 1625–1633. doi: 10.1084/jem.20020258

Bhargava, A., Cotton, J. A., Dixon, B. R., Gedamu, L., Yates, R. M., and Buret, A. G. (2015). Giardia duodenalis Surface Cysteine Proteases Induce Cleavage of the Intestinal Epithelial Cytoskeletal Protein Villin via Myosin Light Chain Kinase. *PloS One* 10 (9), e0136102. doi: 10.1371/journal.pone.0136102

Blache, P., van de Wetering, M., Duluc, I., Domon, C., Berta, P., Freund, J. -N., et al. (2004). SOX9 is an intestine crypt transcription factor, is regulated by the Wnt pathway, and represses the CDX2 and MUC2 genes. *J. Cell. Biol.* 166 (1), 37–47. doi: 10.1083/jcb.200311021

Briceño, M. P., Nascimento, L. A., Nogueira, N. P., Barenco, P. V., Ferro, E. A., Rezende-Oliveira, K., et al. (2016). *Toxoplasma gondii* Infection Promotes Epithelial Barrier Dysfunction of Caco-2 Cells. *J. Histochem. Cytochem.* 64 (8), 459–469. doi: 10.1369/0022155416656349

Cacciò, S. M., Lalle, M., and Svärd, S. G. (2018). Host specificity in the Giardia duodenalis species complex. *Infect. Genet. Evol.* 66, 335–345. doi: 10.1016/j.meegid.2017.12.001

Cacciò, S. M., and Sprong, H. (2011). Epidemiology of Giardiasis in Humans, in *Giardia: A Model Organism*. Eds. H. D. Luján and S. Svärd (Vienna: Springer Vienna), 17–28.

Chandra, L., Borcherding, D. C., Kingsbury, D., Atherly, T., Ambrosini, Y. M., Bourgois-Mochel, A., et al. (2019). Derivation of adult canine intestinal organoids for translational research in gastroenterology. *BMC Biol.* 17 (1), 33. doi: 10.1186/s12915-019-0652-6

Chin, A. C., Teoh, D. A., Scott, K. G., Meddings, J. B., Macnaughton, W. K., and Buret, A. G. (2002). Strain-dependent induction of enterocyte apoptosis by Giardia lamblia disrupts epithelial barrier function in a caspase-3-dependent manner. *Infect. Immun.* 70 (7), 3673–3680. doi: 10.1128/iai.70.7.3673-3680.2002

Clevers, H. (2016). Modeling Development and Disease with Organoids. *Cell* 165 (7), 1586–1597. doi: 10.1016/j.cell.2016.05.082

Co, J. Y., Margalef-Català, M., Li, X., Mah, A. T., Kuo, C. J., Monack, D. M., et al. (2019). Controlling Epithelial Polarity: A Human Enteroid Model for Host-Pathogen Interactions. *Cell Rep.* 26 (9), 2509–2520.e2504. doi: 10.1016/j.celrep.2019.01.108

Delgado Betancourt, E., Hamid, B., Fabian, B. T., Klotz, C., Hartmann, S., and Seeber, F. (2019). From Entry to Early Dissemination—*Toxoplasma gondii*'s Initial Encounter With Its Host. *Front. Cell Infect. Microbiol.* 9, 46. doi: 10.3389/fcimb.2019.00046

Derricott, H., Luu, L., Fong, W. Y., Hartley, C. S., Johnston, L. J., Armstrong, S. D., et al. (2019). Developing a 3D intestinal epithelium model for livestock species. *Cell Tissue Res.* 375 (2), 409–424. doi: 10.1007/s00441-018-2924-9

Dubey, J. (2010). *Toxoplasmosis of Animals and Humans* (Boca Raton: CRC Press).

Dubey, J. P., and Jones, J. L. (2008). *Toxoplasma gondii* infection in humans and animals in the United States. *Int. J. Parasitol.* 38 (11), 1257–1278. doi: 10.1016/j.ijpara.2008.03.007

Duque-Correa, M. A., Schreiber, F., Rodgers, F. H., Goulding, D., Forrest, S., White, R., et al. (2020). Development of caecaloids to study host-pathogen interactions: new insights into immunoregulatory functions of Trichuris muris extracellular vesicles in the caecum. *Int. J. Parasitol.* 50 (9), 707–718. doi: 10.1016/j.ijpara.2020.06.001

Dutta, D., and Clevers, H. (2017). Organoid culture systems to study host-pathogen interactions. *Curr. Opin. Immunol.* 48, 15–22. doi: 10.1016/j.coi.2017.07.012

Eichenberger, R. M., Ryan, S., Jones, L., Buitrago, G., Polster, R., Montes de Oca, M., et al. (2018). Hookworm Secreted Extracellular Vesicles Interact With Host Cells and Prevent Inducible Colitis in Mice. *Front. Immunol.* 9, 850. doi: 10.3389/fimmu.2018.00850

Franklin-Murray, A. L., Mallya, S., Jankeel, A., Sureshchandra, S., Messaoudi, I., and Lodoen, M. B. (2020). *Toxoplasma gondii* Dysregulates Barrier Function and Mechanotransduction Signaling in Human Endothelial Cells. *mSphere* 5 (1), e00550-00519. doi: 10.1128/mSphere.00550-19

Geurden, T., and Olson, M. (2011). "Giardia in Pets and Farm Animals, and Their Zoonotic Potential," in *Giardia: A Model Organism*. Eds. H. D. Luján and S. Svärd (Vienna: Springer Vienna), 71–92.

Glover, M., Tang, Z., Sealock, R., and Jain, S. (2017). Diarrhea as a Presenting Symptom of Disseminated Toxoplasmosis. *Case Rep. Gastrointest. Med.* 2017:3491087. doi: 10.1155/2017/3491087

Gonzalez, L. M., Williamson, I., Piedrahita, J. A., Blikslager, A. T., and Magness, S. T. (2013). Cell Lineage Identification and Stem Cell Culture in a Porcine Model for the Study of Intestinal Epithelial Regeneration. *PloS One* 8 (6), e66465. doi: 10.1371/journal.pone.0066465

Gregg, B., Taylor, B. C., John, B., Tait-Wojno, E. D., Girgis, N. M., Miller, N., et al. (2013). Replication and distribution of *Toxoplasma gondii* in the small intestine after oral infection with tissue cysts. *Infect. Immun.* 81 (5), 1635–1643. doi: 10.1128/iai.01126-12

Hakimi, M. A., Olias, P., and Sibley, L. D. (2017). Toxoplasma Effectors Targeting Host Signaling and Transcription. *Clin. Microbiol. Rev.* 30 (3), 615–645. doi: 10.1128/cmr.00005-17

Hares, M. F., Tiffney, E.-A., Johnston, L. J., Luu, L., Stewart, C. J., Flynn, R. J., et al. (2020). Stem cell-derived enteroid cultures as a tool for dissecting host-parasite interactions in the small intestinal epithelium. *Parasite Immunol.*, e12765. doi: 10.1111/pim.12765

Hedrich, W. D., Panzica-Kelly, J. M., Chen, S.-J., Strassle, B., Hasson, C., Lecureux, L., et al. (2020). Development and characterization of rat duodenal organoids for ADME and toxicology applications. *Toxicology* 446, 152614. doi: 10.1016/j.tox.2020.152614

Helmy, Y. A., Spierling, N. G., Schmidt, S., Rosenfeld, U. M., Reil, D., Imholt, C., et al. (2018). Occurrence and distribution of Giardia species in wild rodents in Germany. *Parasit. Vectors* 11 (1), 213. doi: 10.1186/s13071-018-2802-z

Heo, I., Dutta, D., Schaefer, D. A., Iakobachvili, N., Artegiani, B., Sachs, N., et al. (2018). Modelling Cryptosporidium infection in human small intestinal and lung organoids. *Nat. Microbiol.* 3 (7), 814–823. doi: 10.1038/s41564-018-0177-8

Hill, D. R., Huang, S., Nagy, M. S., Yadagiri, V. K., Fields, C., Mukherjee, D., et al. (2017). Bacterial colonization stimulates a complex physiological response in the immature human intestinal epithelium. *Elife* 6, e29132. doi: 10.7554/eLife.29132

Hill, D. R., and Spence, J. R. (2017). Gastrointestinal Organoids: Understanding the Molecular Basis of the Host-Microbe Interface. *Cell Mol. Gastroenterol. Hepatol.* 3 (2), 138–149. doi: 10.1016/j.jcmgh.2016.11.007

Hong, H.-Y., Yoo, G.-S., and Choi, J.-K. (2000). Direct Blue 71 staining of proteins bound to blotting membranes. *Electrophoresis* 21 (5), 841–845. doi: 10.1002/(SICI)1522-2683(20000301)21:5<841::AID-ELPS841>3.0.CO;2-4

Keister, D. B. (1983). Axenic culture of Giardia lamblia in TYI-S-33 medium supplemented with bile. *Trans. R Soc. Trop. Med. Hyg.* 77 (4), 487–488. doi: 10.1016/0035-9203(83)90120-7

Kijlstra, A., and Jongert, E. (2008). Control of the risk of human toxoplasmosis transmitted by meat. *Int. J. Parasitol.* 38 (12), 1359–1370. doi: 10.1016/j.ijpara.2008.06.002

Kim, K. A., Kakitani, M., Zhao, J., Oshima, T., Tang, T., Binnerts, M., et al. (2005). Mitogenic influence of human R-spondin1 on the intestinal epithelium. *Science* 309 (5738), 1256–1259. doi: 10.1126/science.1112521

Kirk, M. D., Pires, S. M., Black, R. E., Caipo, M., Crump, J. A., Devleesschauwer, B., et al. (2015). World Health Organization Estimates of the Global and Regional Disease Burden of 22 Foodborne Bacterial, Protozoal, and Viral Disease: A Data Synthesis. *PloS Med.* 12 (12), e1001921. doi: 10.1371/journal.pmed.1001921

Klotz, C., Aebischer, T., and Seeber, F. (2012). Stem cell-derived cell cultures and organoids for protozoan parasite propagation and studying host-parasite interaction. *Int. J. Med. Microbiol.* 302 (4-5), 203–209. doi: 10.1016/j.ijmm.2012.07.010

Koh, W. H., Geurden, T., Paget, T., O'Handley, R., Steuart, R. F., Thompson, R. C., et al. (2013). Giardia duodenalis assemblage-specific induction of apoptosis and tight junction disruption in human intestinal epithelial cells: effects of mixed infections. *J. Parasitol.* 99 (2), 353–358. doi: 10.1645/ge-3021.1

Kozuka, K., He, Y., Koo-McCoy, S., Kumaraswamy, P., Nie, B., Shaw, K., et al. (2017). Development and Characterization of a Human and Mouse Intestinal Epithelial Cell Monolayer Platform. *Stem Cell Rep.* 9 (6), 1976–1990. doi: 10.1016/j.stemcr.2017.10.013

Kraft, M. R., Klotz, C., Bücker, R., Schulzke, J. D., and Aebischer, T. (2017). Giardia's Epithelial Cell Interaction In Vitro: Mimicking Asymptomatic Infection? *Front. Cell Infect. Microbiol.* 7, 421. doi: 10.3389/fcimb.2017.00421

Kraft, M., Holthaus, D., Krug, S., Holland, G., Schulzke, J.-D., Aebischer, T., et al. (2020). Dissection of barrier dysfunction in organoid-derived human intestinal epithelia induced by Giardia duodenalis. *bioRxiv*, 2020.2011.2017.384537. doi: 10.1101/2020.11.17.384537

Lambert, H., and Barragan, A. (2010). Modelling parasite dissemination: host cell subversion and immune evasion by *Toxoplasma gondii*. *Cell Microbiol.* 12 (3), 292–300. doi: 10.1111/j.1462-5822.2009.01417.x

Li, J., Li, J.Jr., Zhang, S. Y., Li, R. X., Lin, X., Mi, Y. L., et al. (2018). Culture and characterization of chicken small intestinal crypts. *Poult. Sci.* 97 (5), 1536–1543. doi: 10.3382/ps/pey010

Lindsay, D. S., and Dubey, J. P. (2007). "6 - Toxoplasmosis in Wild and Domestic Animals," in *Toxoplasma gondii*. Eds. L. M. Weiss and K. Kim (London: Academic Press), 133–152.

Luu, L., Johnston, L. J., Derricott, H., Armstrong, S. D., Randle, N., Hartley, C. S., et al. (2019). An Open-Format Enteroid Culture System for Interrogation of Interactions Between *Toxoplasma gondii* and the Intestinal Epithelium. *Front. Cell Infect. Microbiol.* 9, 300. doi: 10.3389/fcimb.2019.00300

Mahe, M. M., Sundaram, N., Watson, C. L., Shroyer, N. F., and Helmrath, M. A. (2015). Establishment of Human Epithelial Enteroids and Colonoids from Whole Tissue and Biopsy. *JoVE* 97), e52483. doi: 10.3791/52483

Ma'ayeh, S. Y., Knörr, L., Sköld, K., Garnham, A., Ansell, B. R. E., Jex, A. R., et al. (2018). Responses of the Differentiated Intestinal Epithelial Cell Line Caco-2 to Infection With the Giardia intestinalis GS Isolate. *Front. Cell Infect. Microbiol.* 8, 244. doi: 10.3389/fcimb.2018.00244

Martorelli Di Genova, B., Wilson, S. K., Dubey, J. P., and Knoll, L. J. (2019). Intestinal delta-6-desaturase activity determines host range for Toxoplasma sexual reproduction. *PloS Biol.* 17 (8), e3000364. doi: 10.1371/journal.pbio.3000364

Min, S., Kim, S., and Cho, S.-W. (2020). Gastrointestinal tract modeling using organoids engineered with cellular and microbiota niches. *Exp. Mol. Med.* 52 (2), 227–237. doi: 10.1038/s12276-020-0386-0

Miyoshi, H., and Stappenbeck, T. S. (2013). In vitro expansion and genetic modification of gastrointestinal stem cells in spheroid culture. *Nat. Protoc.* 8 (12), 2471–2482. doi: 10.1038/nprot.2013.153

Montoya, J. G., and Liesenfeld, O. (2004). Toxoplasmosis. *Lancet* 363 (9425), 1965–1976. doi: 10.1016/s0140-6736(04)16412-x

Moon, C., VanDussen, K. L., Miyoshi, H., and Stappenbeck, T. S. (2014). Development of a primary mouse intestinal epithelial cell monolayer culture system to evaluate factors that modulate IgA transcytosis. *Mucosal Immunol.* 7 (4), 818–828. doi: 10.1038/mi.2013.98

Nash, T. E. (2019). Long-term Culture of Giardia lamblia in Cell Culture Medium Requires Intimate Association with Viable Mammalian Cells. *Infect. Immun.* 87 (11), e00639–19. doi: 10.1128/iai.00639-19

Noel, G., Baetz, N. W., Staab, J. F., Donowitz, M., Kovbasnjuk, O., Pasetti, M. F., et al. (2017). A primary human macrophage-enteroid co-culture model to investigate mucosal gut physiology and host-pathogen interactions. *Sci. Rep.* 7 (1), 45270. doi: 10.1038/srep45270

Pageot, L. P., Perreault, N., Basora, N., Francoeur, C., Magny, P., and Beaulieu, J. F. (2000). Human cell models to study small intestinal functions: recapitulation of the crypt-villus axis. *Microsc. Res. Tech.* 49 (4), 394–406. doi: 10.1002/(sici)1097-0029(20000515)49:4<394::aid-jemt8>3.0.co;2-k

Pineda, C. O., Leal, D. A. G., Fiuza, V. R. D. S., Jose, J., Borelli, G., Durigan, M., et al. (2020). *Toxoplasma gondii* oocysts, Giardia cysts and Cryptosporidium oocysts in outdoor swimming pools in Brazil. *Zoonoses Public Health.* 67 (7), 785–795. doi: 10.1111/zph.12757

Post, Y., Puschhof, J., Beumer, J., Kerkkamp, H. M., de Bakker, M. A. G., Slagboom, J., et al. (2020). Snake Venom Gland Organoids. *Cell* 180 (2), 233–247.e221. doi: 10.1016/j.cell.2019.11.038

Powell, R. H., and Behnke, M. S. (2017). WRN conditioned media is sufficient for in vitro propagation of intestinal organoids from large farm and small companion animals. *Biol. Open* 6 (5), 698–705. doi: 10.1242/bio.021717

Rachinel, N., Buzoni-Gatel, D., Dutta, C., Mennechet, F. J., Luangsay, S., Minns, L. A., et al. (2004). The induction of acute ileitis by a single microbial antigen of *Toxoplasma gondii*. *J. Immunol.* 173 (4), 2725–2735. doi: 10.4049/jimmunol.173.4.2725

Ross, E. C., Olivera, G. C., and Barragan, A. (2019). Dysregulation of focal adhesion kinase upon *Toxoplasma gondii* infection facilitates parasite translocation across polarised primary brain endothelial cell monolayers. *Cell Microbiol.* 21 (9), e13048. doi: 10.1111/cmi.13048

Sato, T., Vries, R. G., Snippert, H. J., van de Wetering, M., Barker, N., Stange, D. E., et al. (2009). Single Lgr5 stem cells build crypt-villus structures in vitro without a mesenchymal niche. *Nature* 459 (7244), 262–265. doi: 10.1038/nature07935

Sato, T., Stange, D. E., Ferrante, M., Vries, R. G., Van Es, J. H., Van den Brink, S., et al. (2011a). Long-term expansion of epithelial organoids from human colon, adenoma, adenocarcinoma, and Barrett's epithelium. *Gastroenterology* 141 (5), 1762–1772. doi: 10.1053/j.gastro.2011.07.050

Sato, T., van Es, J. H., Snippert, H. J., Stange, D. E., Vries, R. G., van den Born, M., et al. (2011b). Paneth cells constitute the niche for Lgr5 stem cells in intestinal crypts. *Nature* 469 (7330), 415–418. doi: 10.1038/nature09637

Schneider, C. A., Rasband, W. S., and Eliceiri, K. W. (2012). NIH Image to ImageJ: 25 years of image analysis. *Nat. Methods* 9 (7), 671–675. doi: 10.1038/nmeth.2089

Schreiner, M., and Liesenfeld, O. (2009). Small intestinal inflammation following oral infection with *Toxoplasma gondii* does not occur exclusively in C57BL/6 mice: review of 70 reports from the literature. *Mem. Inst. Oswaldo Cruz* 104 (2), 221–233. doi: 10.1590/s0074-02762009000200015

Song, H. B., Jun, H. O., Kim, J. H., Lee, Y. H., Choi, M. H., and Kim, J. H. (2017). Disruption of outer blood-retinal barrier by *Toxoplasma gondii*–infected monocytes is mediated by paracrinely activated FAK signaling. *PloS One* 12 (4), e0175159. doi: 10.1371/journal.pone.0175159

Stelzer, S., Basso, W., Benavides Silván, J., Ortega-Mora, L. M., Maksimov, P., Gethmann, J., et al. (2019). *Toxoplasma gondii* infection and toxoplasmosis in farm animals: Risk factors and economic impact. *Food Waterborne Parasitol.* 15:e00037. doi: 10.1016/j.fawpar.2019.e00037

Taylor, M. A., and Webster, K. A. (1998). Recent advances in the diagnosis in livestock of Cryptosporidium, Toxoplasma, Giardia and other protozoa of veterinary importance. *Res. Vet. Sci.* 65 (3), 183–193. doi: 10.1016/s0034-5288(98)90141-2

Thomsen-Zieger, N., Schachtner, J., and Seeber, F. (2003). Apicomplexan parasites contain a single lipoic acid synthase located in the plastid. *FEBS Lett.* 547 (1-3), 80–86. doi: 10.1016/s0014-5793(03)00673-2

Torgerson, P. R., Devleesschauwer, B., Praet, N., Speybroeck, N., Willingham, A. L., Kasuga, F., et al. (2015). World Health Organization Estimates of the Global and Regional Disease Burden of 11 Foodborne Parasitic Disease: A Data Synthesis. *PloS Med.* 12 (12), e1001920. doi: 10.1371/journal.pmed.1001920

Torgerson, P. R., and Macpherson, C. N. (2011). The socioeconomic burden of parasitic zoonoses: global trends. *Vet. Parasitol.* 182 (1), 79–95. doi: 10.1016/j.vetpar.2011.07.017

Troeger, H., Epple, H. J., Schneider, T., Wahnschaffe, U., Ullrich, R., Burchard, G. D., et al. (2007). Effect of chronic Giardia lamblia infection on epithelial transport and barrier function in human duodenum. *Gut* 56 (3), 328–335. doi: 10.1136/gut.2006.100198

van der Hee, B., Loonen, L. M. P., Taverne, N., Taverne-Thiele, J. J., Smidt, H., and Wells, J. M. (2018). Optimized procedures for generating an enhanced, near physiological 2D culture system from porcine intestinal organoids. *Stem Cell Res.* 28, 165–171. doi: 10.1016/j.scr.2018.02.013

van der Hee, B., Madsen, O., Vervoort, J., Smidt, H., and Wells, J. M. (2020). Congruence of Transcription Programs in Adult Stem Cell-Derived Jejunum

Organoids and Original Tissue During Long-Term Culture. *Front. Cell Dev. Biol.* 8, 375. doi: 10.3389/fcell.2020.00375

VanDussen, K. L., Marinshaw, J. M., Shaikh, N., Miyoshi, H., Moon, C., Tarr, P. I., et al. (2015). Development of an enhanced human gastrointestinal epithelial culture system to facilitate patient-based assays. *Gut* 64 (6), 911–920. doi: 10.1136/gutjnl-2013-306651

VanDussen, K. L., Sonnek, N. M., and Stappenbeck, T. S. (2019). L-WRN conditioned medium for gastrointestinal epithelial stem cell culture shows replicable batch-to-batch activity levels across multiple research teams. *Stem Cell Res.* 37, 101430. doi: 10.1016/j.scr.2019.101430

Weight, C. M., Jones, E. J., Horn, N., Wellner, N., and Carding, S. R. (2015). Elucidating pathways of *Toxoplasma gondii* invasion in the gastrointestinal tract: involvement of the tight junction protein occludin. *Microbes Infect.* 17 (10), 698–709. doi: 10.1016/j.micinf.2015.07.001

Weight, C. M., and Carding, S. R. (2012). The protozoan pathogen *Toxoplasma gondii* targets the paracellular pathway to invade the intestinal epithelium. *Ann. N Y Acad. Sci.* 1258, 135–142. doi: 10.1111/j.1749-6632.2012.06534.x

Wilke, G., Funkhouser-Jones, L. J., Wang, Y., Ravindran, S., Wang, Q., Beatty, W. L., et al. (2019). A Stem-Cell-Derived Platform Enables Complete Cryptosporidium Development In Vitro and Genetic Tractability. *Cell Host Microbe* 26 (1), 123–134.e128. doi: 10.1016/j.chom.2019.05.007

Williamson, I. A., Arnold, J. W., Samsa, L. A., Gaynor, L., DiSalvo, M., Cocchiaro, J. L., et al. (2018). A High-Throughput Organoid Microinjection Platform to Study Gastrointestinal Microbiota and Luminal Physiology. *Cell Mol. Gastroenterol. Hepatol.* 6 (3), 301–319. doi: 10.1016/j.jcmgh.2018.05.004

Conflict of Interest: The authors declare that the research was conducted in the absence of any commercial or financial relationships that could be construed as a potential conflict of interest.

frontiers in Cellular and Infection Microbiology

ORIGINAL RESEARCH
published: 01 March 2021
doi: 10.3389/fcimb.2021.604129

Using scRNA-seq to Identify Transcriptional Variation in the Malaria Parasite Ookinete Stage

Kathrin Witmer[1], Farah Aida Dahalan[2], Tom Metcalf[1], Arthur M. Talman[1,3], Virginia M. Howick[1,4,5†] and Mara K. N. Lawniczak[1*†]*

[1] Parasites and Microbes Programme, Wellcome Sanger Institute, Hinxton, United Kingdom, [2] Department of Life Sciences, Imperial College London, London, United Kingdom, [3] MIVEGEC, IRD, CNRS, University of Montpellier, Montpellier, France, [4] Institute of Biodiversity, Animal Health and Comparative Medicine, College of Medical Veterinary and Life Sciences, University of Glasgow, Glasgow, United Kingdom, [5] Wellcome Centre for Integrative Parasitology, College of Medical Veterinary and Life Sciences, University of Glasgow, Glasgow, United Kingdom

OPEN ACCESS

Edited by:
Nicholas Charles Smith, University Technology Sydney, Australia

Reviewed by:
Elena Gómez-Díaz, Instituto de Parasitología y Biomedicina López-Neyra (IPBLN), Spain
Chandra Ramakrishnan, University of Zurich, Switzerland

***Correspondence:**
Virginia M. Howick
virginia.howick@glasgow.ac.uk
Mara K. N. Lawniczak
mara@sanger.ac.uk

†These authors have contributed equally to this work

Specialty section:
This article was submitted to Parasite and Host, a section of the journal Frontiers in Cellular and Infection Microbiology

Received: 08 September 2020
Accepted: 15 January 2021
Published: 01 March 2021

Citation:
Witmer K, Dahalan FA, Metcalf T, Talman AM, Howick VM and Lawniczak MKN (2021) Using scRNA-seq to Identify Transcriptional Variation in the Malaria Parasite Ookinete Stage. Front. Cell. Infect. Microbiol. 11:604129. doi: 10.3389/fcimb.2021.604129

The crossing of the mosquito midgut epithelium by the malaria parasite motile ookinete form represents the most extreme population bottleneck in the parasite life cycle and is a prime target for transmission blocking strategies. However, we have little understanding of the clonal variation that exists in a population of ookinetes in the vector, partially because the parasites are difficult to access and are found in low numbers. Within a vector, variation may result as a response to specific environmental cues or may exist independent of those cues as a potential bet-hedging strategy. Here we use single-cell RNA-seq to profile transcriptional variation in *Plasmodium berghei* ookinetes across different vector species, and between and within individual midguts. We then compare our results to low-input transcriptomes from individual *Anopheles coluzzii* midguts infected with the human malaria parasite *Plasmodium falciparum*. Although the vast majority of transcriptional changes in ookinetes are driven by development, we have identified candidate genes that may be responding to environmental cues or are clonally variant within a population. Our results illustrate the value of single-cell and low-input technologies in understanding clonal variation of parasite populations.

Keywords: ookinete, *Plasmodium*, scRNA-seq, transcriptomics, malaria, *Anopheles*

INTRODUCTION

Malaria is a devastating mosquito-borne disease caused by single-celled apicomplexan parasites belonging to the *Plasmodium* genus. Transmission begins with ingestion of an infectious blood meal by the mosquito. This initiates the most extreme population bottleneck in the parasite's life cycle, where sexual stage parasites must rapidly undergo fertilization, develop into invasive ookinetes, and transit through the midgut epithelium of the mosquito before beginning sporogonic development. Only a small proportion of ookinetes will successfully cross the midgut (Smith et al., 2014). Although the ookinete stage is a critical bottleneck in the life cycle, relatively little is known about

the molecular and population-level processes that drive successful midgut invasion of ookinetes. We also lack information on how this life stage copes with the variable environment it encounters including for example potentially highly diverged mosquito species and also highly variable microbiota between individual mosquitoes.

Variation between individuals provides necessary material for natural selection when environmental conditions change. Perhaps the most extreme environmental changes the malaria parasite experiences in its life cycle are the transitions between mammalian and mosquito vector hosts. Additionally, the parasite must be able to cope with unpredictable variation within and between hosts in order to survive. *Plasmodium falciparum* blood stage parasite populations can deal with this host environmental variation through rapid response to cues or alternatively through phenotypic diversification or bet-hedging independently of these cues (Llorà-Batlle et al., 2019). There is evidence that malaria parasites use bet-hedging strategies in the blood stage forms to optimize survival in face of variation in the mammalian host immune response and potentially during conversion to the sexual transmissible stage parasites through epigenetic regulation that results in transcriptional variation within a clonal population (Rovira-Graells et al., 2012; Brancucci et al., 2014; Voss et al., 2014; Waters, 2016; Fraschka et al., 2018). Other work has shown that the vector plays a role in modulating virulence repertoires *via* a transcriptional reset after transmission through the mosquito (Spence et al., 2013). The examination of whether parasites employ bet-hedging strategies in the mosquito host has been less well studied.

Single-cell technologies provide the possibility to understand clonally variant transcriptional patterns in unicellular parasites by deconvoluting the contribution of each individual and allowing for precise ordering of parasites in developmental time (Poran et al., 2017; Brancucci et al., 2018; Nötzel et al., 2018; Reid et al., 2018; Howick et al., 2019). In *Plasmodium*, a large proportion of the transcriptome is differentially expressed between parasite stages through tight regulation of transcription *via* a small number of ApiAP2 transcription factors (Bozdech et al., 2003; Modrzynska et al., 2017). These large changes in expression make it difficult to understand what proportion of variation observed is a result of developmental heterogeneity in a sample versus variable patterns of expression at a single point along this developmental trajectory when using bulk transcriptomic approaches (Llorà-Batlle et al., 2019). In this study, we built a framework to minimize the effects of development in single-cell RNA-seq data by identifying the most mature populations of parasites and statistically controlling for developmental timing in our analyses.

Using this framework, we investigate variable patterns of gene expression in *Plasmodium berghei* ookinetes across two vector species as well as within and between individual mosquito midguts (**Table 1**). We identify genes that are differentially expressed across these environments as well as a subset of genes that are highly variably expressed independent of developmental time and the vector host. We then revisit bulk RNA-seq data from individual vector midguts from mated or virgin *Anopheles coluzzii* infected with *P. falciparum* (Dahalan et al., 2019) and identify variable genes that may be responding to vector host physiological factors. We find that ookinetes display subtle differences in gene expression not only based on the vector species, mating status or antibiotic treatment, but also within one mosquito individual. Our findings suggest that a fine balance between adaptive gene expression and intrinsic variant gene expression act together to ensure successful gut colonization.

MATERIALS AND METHODS

Retrieval and scRNA-seq of *P. berghei* Ookinetes

P. berghei parasites were propagated in female 6- to 8-week-old Theiler's Original outbred mice supplied by Envigo UK. The clonal *P. berghei* RMgm-928 strain (Burda et al., 2015), which expresses mCherry under the control of the hsp70 promoter throughout the life cycle, was used for all *P. berghei* transcriptomic data. A Hap2 knock-out *P. berghei* strain in the RMgm-928::mCherry background, which does not produce male gametocytes, was used as a control for FACS gating (Howick et al., 2019). Mosquito infections were performed in two- to five-day-old *Anopheles stephensi* or *An. coluzzii* through direct feed on mice.

TABLE 1 | Overview of data sets and differential gene expression (DE) analysis performed in this study.

Data Set	*Plasmodium* species	*Anopheles* species	Sample collection	# midguts	Method	Cells/samples passing QC	DE comparison
Pb vector species	*P. berghei*	*An. coluzzii* *An. stephesi*	Pooled guts	5 per pool	Single-cell	253	Mosquito species
Pb single-gut	*P. berghei*	*An. stephensi*	Single guts	4	Single-cell	58; 67; 88; 91	Individual guts Within a gut
Pf bulk	*P. falciparum*	*An. coluzzii*	Single guts	24	Bulk	22	Mating status Antibiotics Individual guts

We analyzed three different data sets. First, data from the Malaria Cell Atlas (Howick et al., 2019) consisting of single cell P. berghei ookinetes collected from pooled An.stephensi midguts was compared to a data set collected simultaneously but from An. coluzzii midguts that we called Pb vector species data set. Second, we analyzed single cell P. bergheiookinetes that were collected from four individual An. coluzzii midguts and named this data set Pb single gut data set. Third, we used P. falciparum bulk RNA-seq data from a previously published data set (Dahalan et al., 2019) that investigated P. falciparum infection in An. coluzzii in mated compared to virgin females. We named this data set Pf bulk data set.

P. berghei parasites were isolated from the mosquito blood bolus at 18 or 24 h post infectious feed as previously described (Howick et al., 2019). Briefly, each midgut was dissected and a lateral incision was made along the gut epithelium to release the contents of the bolus into a small drop of PBS and the midgut tissue was further rinsed with a syringe. The released contents were transferred to an Eppendorf tube stored on ice. Each sample was diluted in an additional 400 µl of PBS, filtered with a 20 µm filter, and stained with SYBR green (1:5,000) prior to FACS. For the *Pb vector species data set*, the contents of five boli were pooled prior to sorting at 18 h (*An. stephensi*) and 24 h (*An. stephensi* and *An. coluzzii*). The 18 h time point was included in our analysis to inform developmental trajectory inference. For the *Pb single-gut data set*, parasites were collected from each gut at 24 h post-infection and maintained and sorted as separate samples. Parasites were sorted into lysis buffer in 96-well plates using an Influx cell sorter (BD Biosciences) with a 70 µm nozzle. Sorted plates were spun at 1,000 g for 10 s and placed immediately on dry ice.

Library Preparation and Sequencing

Reverse transcription, PCR, and library preparation were performed as detailed previously (Reid et al., 2018; Howick et al., 2019) using a modified Smart-seq2 (Picelli et al., 2014) protocol with a non-anchored oligoDT and 25 PCR cycles. Libraries were multiplexed up to 384 and sequenced on a single lane of HiSeq 2500 v4 with 75 bp paired-end reads.

scRNA-seq Mapping and Analysis

Mapping and Read Counting of Single-Cell Transcriptomes

Transcriptomes were mapped using HISAT2 (v 2.0.0-beta) (Kim et al., 2015) to the *P. berghei* v3 genome (https://www.sanger.ac.uk/resources/downloads/protozoa/, October 2016) using default parameters and summed against genes HTseq (v 0.6.0) (Anders et al., 2015) as described in (Reid et al., 2018).

Quality Control and Normalization

Low quality cells were identified based on the distribution of total reads and number of genes detected per cell (**Figure S1**). Cells with fewer than 500 genes per cell and 10,000 reads per cell were removed. Additionally, cells with greater than 3,000 genes per cell were removed from the *Pb single-gut data set*. Transcriptomes were normalized by calculating the base 2 logarithm of the counts per million (CPM) for each cell.

Parasite Stage Assignment and Pseudotime of the Pb Vector Species Data Set

Dimensionality reduction was performed using PCA in scater (v 1.16.0) based on the log CPM expression values of the top 500 variable features (McCarthy et al., 2017). To separate potential different developmental stages, we used k-means clustering using SC3 (v 1.16.0) (Kiselev et al., 2017) to assign each cell to a cluster (**Table S1**). Clusters were assigned cell-types based on marker gene expression and by using scmap (v 1.10.0) (Kiselev et al., 2018) *via* the scmapCell() function with the Malaria Cell Atlas *P. berghei* Smart-seq2 data as a reference index (Howick et al., 2019). Pseudotime was calculated using untransformed counts in monocle (Trapnell et al., 2014). For this, we selected the unsupervised procedure "dpFeature" and selected genes that are expressed in at least 10% of all cells. 528 genes with qval<0.01 were selected as ordering genes for the pseudotime.

Parasite Stage Assignment and Pseudotime of the Pb Single-Gut Data Set

Dimensionality reduction was performed using tSNE in scater (v 1.16.0) based on the log CPM expression values of the top 500 variable features (McCarthy et al., 2017). We then used scmap (v 1.10.0) (Kiselev et al., 2018) to assign parasite stage and order cells in developmental time. The pseudotime value and parasite stage of the matched cell in the reference Malaria Cell Atlas data was given to the query cell in the single gut ookinete data.

Analysis of Development-Independent Gene Expression Variability

To identify genes that varied in expression independently of developmental progression, we used a generalized linear model to regress out the effect of pseudotime as described in (Howick et al., 2019). We then used M3Drop (Andrews and Hemberg, 2018) on this corrected expression matrix to identify genes that still showed a variable pattern of expression (qval < 0.05). This method was used prior to differential expression analysis as a feature selection process to reduce the signal to noise ratio and identify genes that are likely to be biologically relevant. To identify genes that were variable independent of the midgut environment and could be potential bet-hedging genes, we used this method in the *Pb single-gut data set* by selecting features that were highly variable within each gut and identifying the intersection of the highly variable features across all four guts.

Differential Expression

Differential expression between ookinetes from different vector species and across individual vector guts was performed in monocle (v 2.16.0) using the differentialGeneTest function (Trapnell et al., 2014). To control for the effect of development, we included pseudotime in both the full and reduced model formulas. Only features that were expressed in more than ten cells and were identified as highly variable were included.

Bulk RNA-seq Mapping and Analysis (Pf Bulk Data Set)

Mapping

Transcriptomes from individual *Anopheles* midguts infected with *P. falciparum* from a previous study (Dahalan et al., 2019) were mapped to the *P. falciparum* v3 genome (http://www.genedb.org/Homepage/Pfalciparum, October 2016) with HISAT2 (v 2.1.0) (Kim et al., 2015) using *hisat2 –rna-strandness RF –max-intronlen 5000 p 12.* Reads were summed against transcripts using featureCounts in the Subread package (v 2.0.0) (Liao et al., 2014) using *featureCounts -p -t CDS -g transcript_id -s 2*. Two samples that had fewer than 5,000 reads were removed.

Bulk Deconvolution

The proportion of different parasite stages in each bulk sample was estimated using CIBERSORTx (Newman et al., 2019). A signature matrix was built using *P. falciparum* ookinete, gametocyte and asexual scRNA-seq data from (Reid et al., 2018; Real et al., 2020). Cell fractions in each bulk sample were imputed based on 100 permutations.

Identification of Differentially Expressed and Highly Variable Genes

A minimal pre-filtering of features was performed to keep only transcripts that have at least 10 reads in total. We then performed differential gene expression analysis using Deseq2 (Love et al., 2014) with a design that included mating status, antibiotic treatment, and the proportion of ookinetes as factors in the model.

Highly variable features were identified using the Brennecke method (Brennecke et al., 2013) in M3drop (Andrews and Hemberg, 2018) after correcting the expression matrix for the proportion of ookinetes in each sample using a generalized linear model.

RESULTS

Ookinetes Adjust Gene Expression Dependent on Vector Species

In order to understand if ookinetes can respond to the host environment, we compared single-cell transcriptomes collected from *An. coluzzii* and *An. stephensi* midgut blood boli using our *Pb vector species data set*. Cells originating from *An. stephensi* midguts are originally from the Malaria Cell Atlas data set (Howick et al., 2019) and were collected 18 and 24 h after mosquito infection. Cells collected from *An. coluzzii* midguts were collected only at 24 h after mosquito infection. Out of 286 single-cells sequenced, 253 passed quality control (**Table 1**, **Figure S1**). Parasite transcriptomes were visualized using the first two components of principal components analysis (PCA) (**Figure 1**). K-means clustering identified 5 clusters of cells based on gene expression profile (**Figure S2**). Clusters were assigned cell-types based on marker gene expression and mapping to the Malaria Cell Atlas data. Seven hundred fifty-nine marker genes were identified across all clusters and visual inspection of the top twenty marker genes for each cluster revealed that mature ookinetes belong to cluster 1, with the ookinete-specific *Pbs25*, *soap*, *cap380* and *warp* genes among the marker genes with a total of 114 cells (**Table S1**). Additionally, we staged the data using the Malaria Cell Atlas (Howick et al., 2019) as a reference index for scmap (Kiselev et al., 2018). We found that cluster 1 represents ookinetes, while the other four clusters represented a variety of different stages including asexual blood stages, male gametocytes, (unfertilized) female gametocytes, and possible retorts (**Figure S2**, **Figure 1B**).

For the remainder of our analyses, we focused only on cluster 1 cells that we identified as ookinetes (30 from *An. coluzzii* and 84 from *An. stephensi*). To control for developmental differences within the identified ookinetes, we first calculated pseudotime and then corrected the expression values using a generalized linear model with pseudotime as a covariate in the model (**Figure 1C**). Indeed, using this approach revealed that the ookinetes can be further divided into three subgroups (i.e. cluster 1.1, cluster 1.2 and cluster 1.3) (**Figure 1D**). We continued our analysis with cluster 1.3 that contained 49 mature ookinetes from both mosquito species (27 from *An. stephensi* and 22 *An. coluzzii*) as they represented the most mature ookinetes according to pseudotime and had the highest proportion of cells that were collected at 24 h. To identify genes that had an altered expression profile based on vector species, we first identified 159 genes to be highly variably expressed using M3drop (qval < 0.05) (**Table S2**). We used these 159 genes as an input to identify differentially expressed genes based on mosquito host species with pseudotime as a covariate in the model. We found 11 genes that appeared to be differentially expressed depending on the mosquito species the parasite was sampled from (qval < 0.01) (**Table S2**). Expression profiles of all 11 genes are shown in **Figures S3**, **S4**. While some differential expression of genes may be driven by expression in a small number of cells, most genes show a robust bias towards one vector species that is independent of development. One of the most prominent examples is PBANKA_1338900, the putative glideosome associated protein with multiple membrane spans 1 (GAPM1) also known as PSOP23 (Ecker et al., 2008) (**Figure 1E**). GAPM1 is predominantly expressed in ookinetes collected from *An. coluzzii* midguts but nearly completely absent in the context of an *An. stephensi* midgut. In *P. falciparum* erythrocytic stages, GAPM1 is part of the inner membrane complex (IMC) and seems to be essential for asexual proliferation in both *P. falciparum* and *P. berghei* (Bullen et al., 2009). The ubiquitin fusion degradation protein (UFD1) (PBANKA_1024700) shows a very similar pattern being predominantly expressed in ookinetes collected from *An. coluzzii* midguts, suggesting ubiquitination could support differential protein regulation between the two species. Interestingly, the inner membrane complex sub-compartment protein 3 (ISP3) (PBANKA_1324300), another IMC-related protein (Kono et al., 2012) is almost exclusively expressed in ookinetes originating from *An. stephensi* midguts.

Taken together, although the differences are mainly subtle, we find two IMC-related genes that are significantly differentially expressed in ookinetes depending on the species of the vector host, suggesting the machinery supporting ookinete motility and invasion may be able to display adaptive features in response to a varying vector species.

Ookinetes Display Variant Gene Expression Depending on Mosquito Individual

Above, we identify differences in ookinete gene expression based on the species of mosquito from which the ookinetes were sampled. We next addressed whether ookinetes exhibit differences in gene expression when infecting different mosquito individuals all from the same mosquito species. Here, we used the *Pb single-gut data set* comprising 310 *P. berghei* single-cell transcriptomes that were collected from four

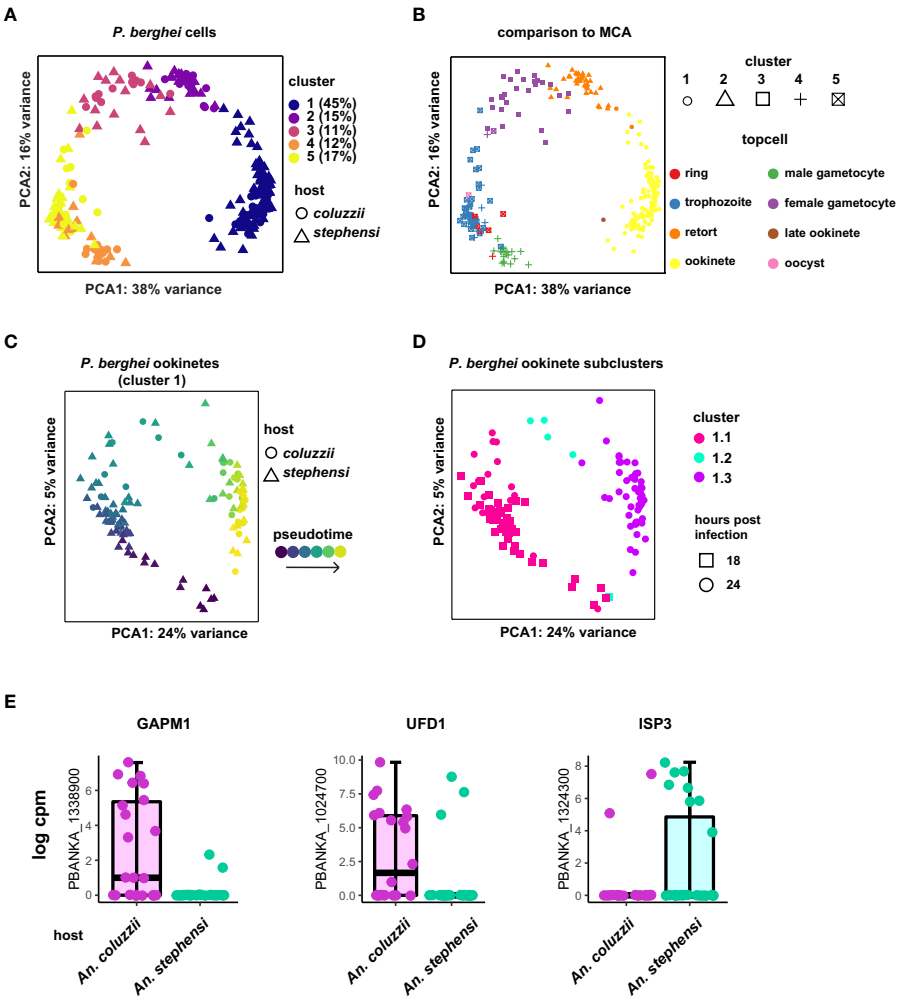

FIGURE 1 | Approach to find differentially expressed genes in *P. berghei* ookinetes dependent on vector species. **(A)** Five cell clusters were identified according to marker genes for the cells collected from *An. stephensi* and *An. coluzzii* midguts, with cluster 1 representing mature ookinetes, based on marker genes expressed in this cluster (**Figure S2**, **Table S1**). Percentage of total cells for each cluster are indicated. **(B)** Cells were staged using the Malaria Cell Atlas (MCA) data as a reference index for scmap-cell. Cluster 1 represents mature ookinetes. Each stage is indicated in different colors (topcell). **(C)** Ookinetes from cluster 1 with pseudotime-corrected gene expression show additional details. **(D)** Ookinetes from cluster 1 can be clustered into three additional clusters after pseudotime correction. Cluster 1.3 was used for the analysis to investigate the effect of vector species on gene expression, as it mostly contained the ookinetes that were collected 24 h post feeding. **(E)** Selection of the three most prominent ookinete genes that are variantly expressed depending on vector host. GAPM1 (glideosome associated protein with multiple membrane spans 1), also known as PSOP23, ISP3 (inner membrane complex sub-compartment protein 3) and UFD1 (ubiquitin fusion degradation protein).

individual *An. stephensi* midgut boli 24 h after infection. Initial t-SNE analysis did not reveal any clustering of cells based on midgut origin (**Figure 2A**) suggesting that ookinetes tend to display overall largely consistent gene expression between different mosquito individuals from the same species. To further investigate more subtle patterns of expression differences, we staged the ookinetes using the Malaria Cell Atlas data (Howick et al., 2019) as a reference index for scmap (Kiselev et al., 2018). 86% of cells mapped to ookinetes (**Figure 2B**), suggesting a much more homogenous population of parasites compared to the *Pb vector species data set*. Additional comparison of the two data sets with PCA confirmed the vast majority of single-gut ookinetes overlap with cluster 1 from the *vector species data set* (**Figure S5**). Cells that mapped to asexual stages (trophozoites and schizonts) were removed from further analyses (**Figure 2B**). We next assigned a pseudotime value to each cell based on the scmap assignment and found that there were no differences in developmental timing of the parasites across the four mosquito individuals (ANOVA: $p > 0.05$, **Figures 2C, D**). We subsetted the most mature ookinetes based on the pseudotime distribution to use for further analysis (**Figures 2D, E**). Although the financial cost associated with single-cell RNA-seq limited our study to only four mosquitoes, each individual yielded more than 50 high-quality

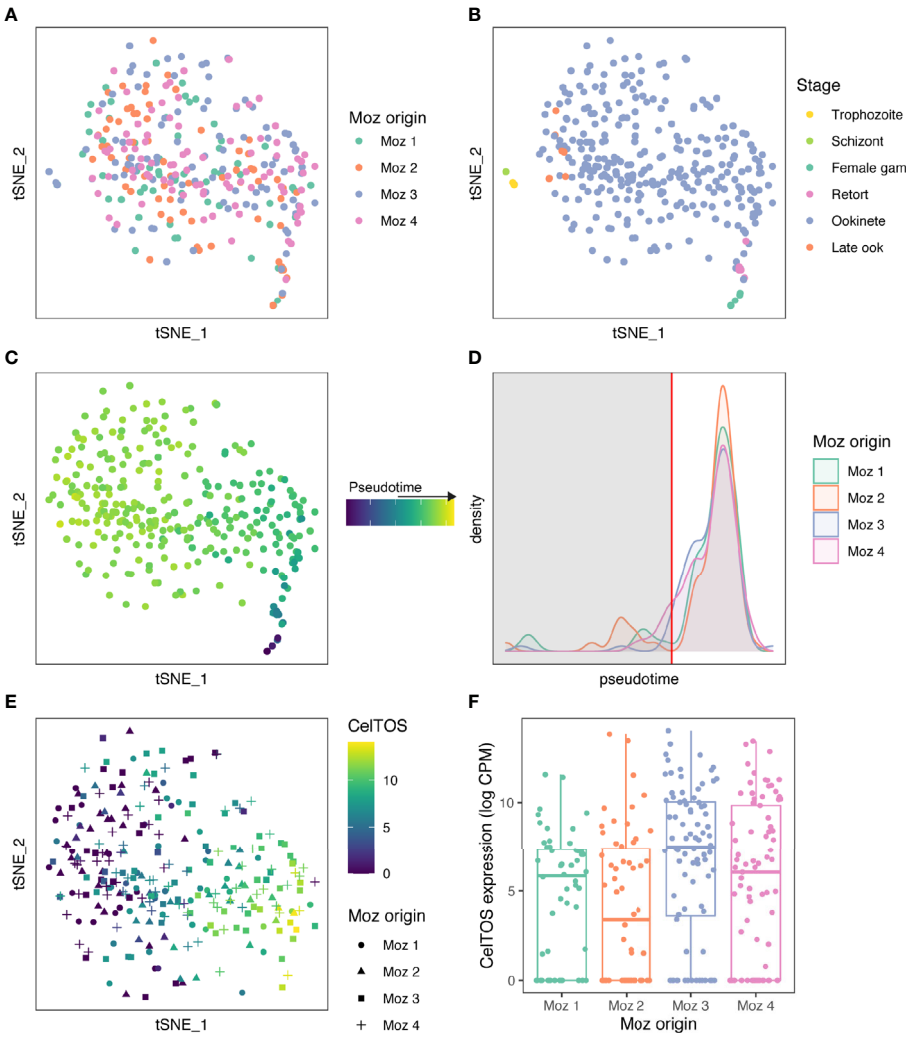

FIGURE 2 | Ookinetes display variant gene expression depending on the mosquito individual. **(A)** A tSNE of 310 high-quality cells collected from four *An. stephensi* blood boli at 24 h after infectious blood meal. Cells are colored by individual mosquito origin. **(B)** Cells were staged using the Malaria Cell Atlas data as a reference index for scmap-cell. Cells that mapped to asexual stages (trophozoites and schizonts) were removed for further analyses. **(C)** 304 cells that matched ookinetes, possible retorts, or female gametocytes were ordered in pseudotime based on their scmap-cell assignment from the Malaria Cell Atlas. **(D)** A density plot of the distribution of cells over pseudotime from each mosquito. There was no difference in ookinete maturation across the 4 individual mosquitoes (ANOVA, $p > 0.05$). Immature ookinetes were removed based on the distribution for further analysis (cut off at red vertical line). In total, 275 mature ookinetes were used for further analysis. **(E)** CelTOS was one of 12 genes identified as a highly variable gene across all cells and was differentially expressed across the four midguts. Expression of CelTOS (log CPM) is shown on the tSNE. **(F)** A boxplot of CelTOS expression (log CPM) by mosquito origin. Expression of all 12 genes differentially expressed across midguts can be found in **Figure S6** and **S7**.

transcriptomes from mature ookinetes allowing us to understand patterns of variability both within and between vector hosts.

To identify genes that displayed different expression profiles between the midguts, we identified 682 genes that were highly variable after controlling for pseudotime. (**Table S2**). We then performed differential expression analysis on these genes and identified 12 genes that vary depending on midgut origin (qval <0.01, **Table S3**, **Figure S6**, **S7**). These 12 genes included PBANKA_1432300 (Cell-traversal protein for ookinetes and sporozoites, CelTOS) (**Figures 2E, F**) and PBANKA_1006300 (perforin-like protein 1, PLP1), which are both known to play a role in cell traversal (Ishino et al., 2005; Kariu et al., 2006). This suggests that a particular vector environment may elicit a transcriptional response, including in midgut traversal genes, which may help to maximize transmission in a context-specific manner. We also identified three genes from multigene families that were differentially expressed in ookinetes originating from individual mosquitoes: a *clag* gene (PBANKA_1400600); LAP4, an LCCL domain containing protein that regulates cell division in the oocyst (PBANKA_1319500) (Saeed et al., 2018); and a CPW-WPC containing protein (PBANKA_1245200). In asexual blood stage parasites, intra-stage variation is driven by transcriptional variation

in large multigene families that are involved in host-parasite interactions (Rovira-Graells et al., 2012). For example, members of the CLAG family have been implicated in invasion, cytoadherence and nutrient uptake, which are likely to be processes where optimal function may vary across host environments (Gupta et al., 2015). Multigene family genes are often heterochromatically regulated; however, none of the differentially expressed genes we identified are from heterochromatic regions, potentially because expression of heterochromatic genes was lower in ookinetes relative to other parasite stages (**Figure S8**). Additionally, we did not find any differentially expressed ApiAP2 transcription factors (**Figure S9**), making it unclear how the identified genes are differently regulated.

Identification of Potential Bet-Hedging Genes

We were next interested in identifying patterns of expression that are consistent with a bet-hedging strategy. Bet-hedging refers to an adaptive strategy that relies on pre-existing diversity within populations to survive potentially unknown environments. Single-cell RNA-seq allows us to understand what genes are transcriptionally variable in a population, which could indicate their role in this process. In contrast to the differential expression analysis where we were specifically interested in genes that had different expression patterns between midguts, here we were interested in genes that showed a similar pattern of variability independently of the midgut environment. To do this, we first corrected the ookinete gene counts for pseudotime, and then created a gene list of highly variable genes for the ookinetes within each individual mosquito (qval < 0.05) (**Table S3**). Looking at the intersection of these four lists, we found a total of 28 ookinete genes that are consistently highly variable (hvg) in all of our mosquitoes. Interestingly, we find several genes that encode proteins with a role in the inner membrane complex (IMC) such as photosensitized INA-labeled protein (PhIL1, PBANKA_0204600) (Saini et al., 2017) and the alveolin IMC1i (PBANKA_0707100) (Kaneko et al., 2015) and ISP3 (PBANKA_1324300), which localizes to the apical anterior apical end of the parasite where IMC organization is initiated (Poulin et al., 2013). In addition, CelTOS is highly variable in this gene set as well. Looking at pseudotime-corrected gene expression, we find that the majority of the 28 highly variant genes display a huge variety of expression between different ookinetes, compared to a control group of highly expressed ookinete-specific genes (**Figure 3A**). Looking at the correlation of these 28 genes, we find that some of these genes are indeed co-expressed, including several genes involved in the IMC and the apical end of the ookinete (**Figure 3B**). Functional work to understand the fitness of parasites that are co-expressing these genes would be necessary to validate their role in bet-hedging. For example, are the subset of cells expressing the identified IMC genes more likely to cross the midgut and develop as an oocyst compared to parasites that are not? Whilst this work is beyond the scope of this study, we have developed a framework that allowed for identification of patterns of expression that are consistent with bet-hedging. We found that a compelling proportion of variant genes encode IMC-related and apically localizing proteins suggesting that these genes may contribute to a bet-hedging strategy that involves the invasion machinery.

Variation in *P. falciparum* Gene Expression Depending on Host Physiological Status and Midgut Origin

Although model systems, such as *P. berghei*, are key to understanding parasite biology and genetics, they may not fully capture the transcriptional variation that exists in malaria parasites infecting humans because of different biological processes and/or lack of orthology across species, especially in clonally variant gene families. To begin to understand how *P. falciparum* varies in gene expression in a host individual- and host physiological-dependent manner, we revisited the *Pf bulk RNA-seq data set* from (Dahalan et al., 2019). In this study, transcriptomes of individual *An. coluzzii* midguts 24 h after a *P. falciparum* (NF54) infectious blood meal were profiled using standard RNA-seq. The experiment was a 2x2 factorial design with both mated/virgin and antibiotic treated/untreated mosquitoes. The antibiotics included a cocktail of gentamycin, penicillin and streptomycin, which decreased the vector microbiota. The original use of the data set focused on questions around vector gene expression. Here we explore parasite gene expression from within the vector midguts. Mapping the reads to the *P. falciparum* genome revealed significant coverage of parasite genes with a mean of 2.6 x 10^4 mapped parasite reads and 2,543 genes per gut after quality control (**Figure S1**). Principal component analysis revealed subtle separation of transcriptomes based on mating status and antibiotic treatment along PC1 and PC2 (**Figure 4A**).

To confirm that the majority of the transcriptional signature we detect at 24 h post bloodmeal originated from ookinetes, we deconvoluted the samples into cell-types using *P. falciparum* single-cell data from ookinetes, gametocytes and asexual blood stages (Reid et al., 2018; Real et al., 2020). Indeed, ookinetes made up the largest proportion of cells in all bulk samples ranging from 73 to 99% of the total composition with a median of 93% (**Figure S10**). Female gametocytes made up the second largest proportion of cells with a median of 5%. We found the proportion of ookinetes increased along PC1 (**Figure 4B**), suggesting the relative ratios of stages across the samples was driving the variation in gene expression observed. The proportion of ookinetes in each sample was also dependent on mating status and to a lesser extent antibiotic treatment and the interaction between status and antibiotic treatment (**Figures 4B, C**, **Figure S10**) (ANOVA; antibiotic treatment: F=8.01, p=0.01; mating status: F=21.91, $p < 0.001$; interaction: F=8.06 p=0.01). Midguts from virgin mosquitoes that were not treated with antibiotics had the lowest proportion of ookinetes, which corresponds with a lower intensity of infection in virgin relative to mated individuals seen at the oocyst stage (Dahalan et al., 2019). This suggests that the lower susceptibility seen in virgin individuals may be a result of inhibition of ookinete development instead of, or in combination with, an increased failure rate in ookinetes crossing the midgut epithelium.

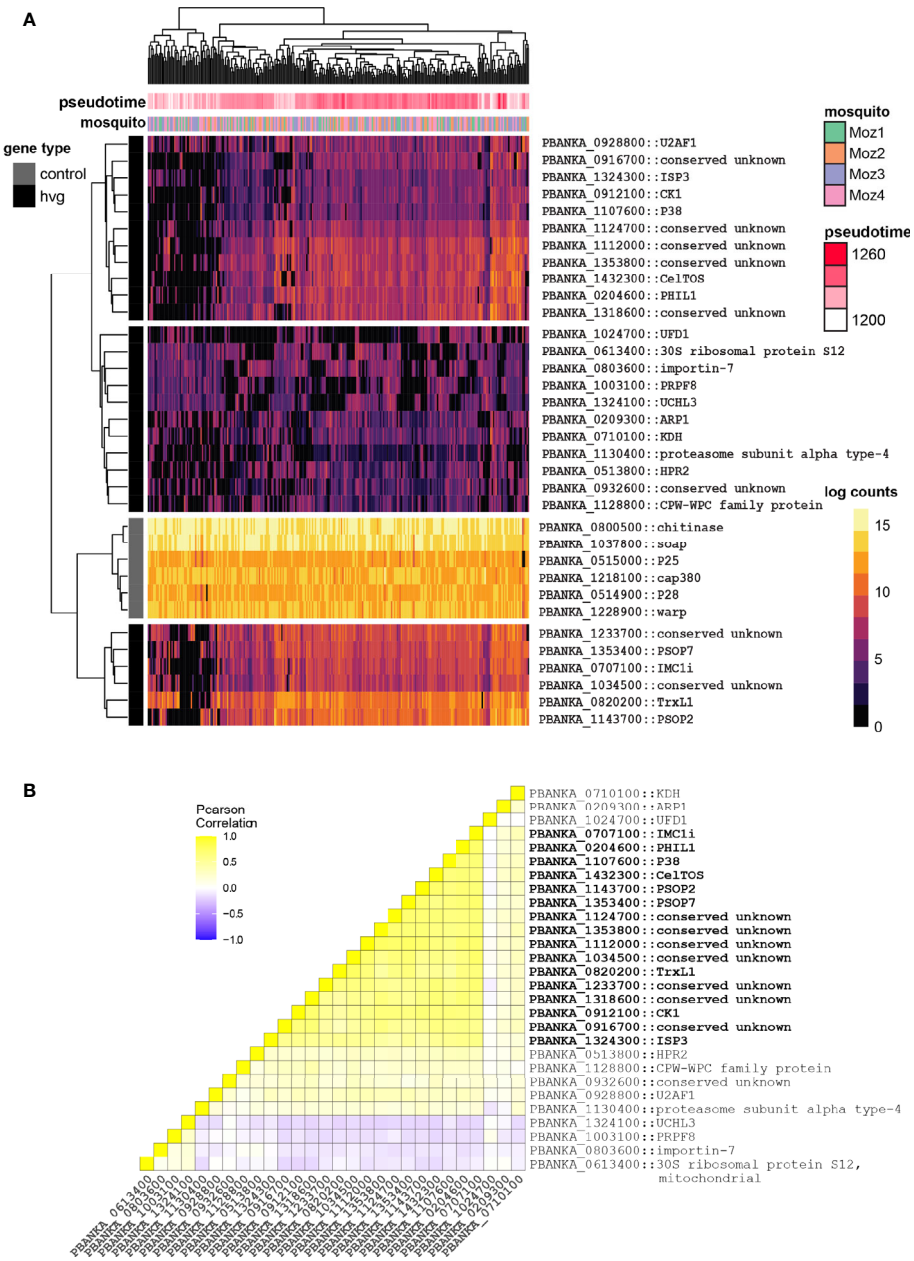

FIGURE 3 | Identification of potential bet-hedging genes in ookinetes. **(A)** Heatmap of all 28 genes that are highly variably expressed in every gut from the *Pb single-gut data set*, plotted alongside six ookinete-specific genes as comparison. Each row represents a gene, and its short name is indicated if available. Values represent pseudotime-corrected log counts to control for developmental expression patterns. Black and grey lines indicate if the genes are from the highly variant gene set (hvg) or from the control gene set. For each cell, the mosquito origin is shown. Each ookinete's coordinates along pseudotime (development) are indicated in pink. **(B)** Correlation heatmap of all 28 genes that are highly variably expressed in every gut from the *Pb single-gut data set*. IMC-related and apical genes are co-regulated in ookinetes and highlighted in bold.

We next asked if parasites showed differential expression based on their host's mating status or antibiotic treatment. We included the proportion of ookinetes as a covariate in the design to correct for differences in expression that were a result of different cell-type ratios. We identified 2 genes differentially expressed based on mating status and 24 differentially expressed based on antibiotic treatment (FDR < 0.05) (**Figures S11**, **S12**). The set of genes that changed with antibiotic treatment were enriched for those associated with the microneme and parasite cell surface (GO:0020009,

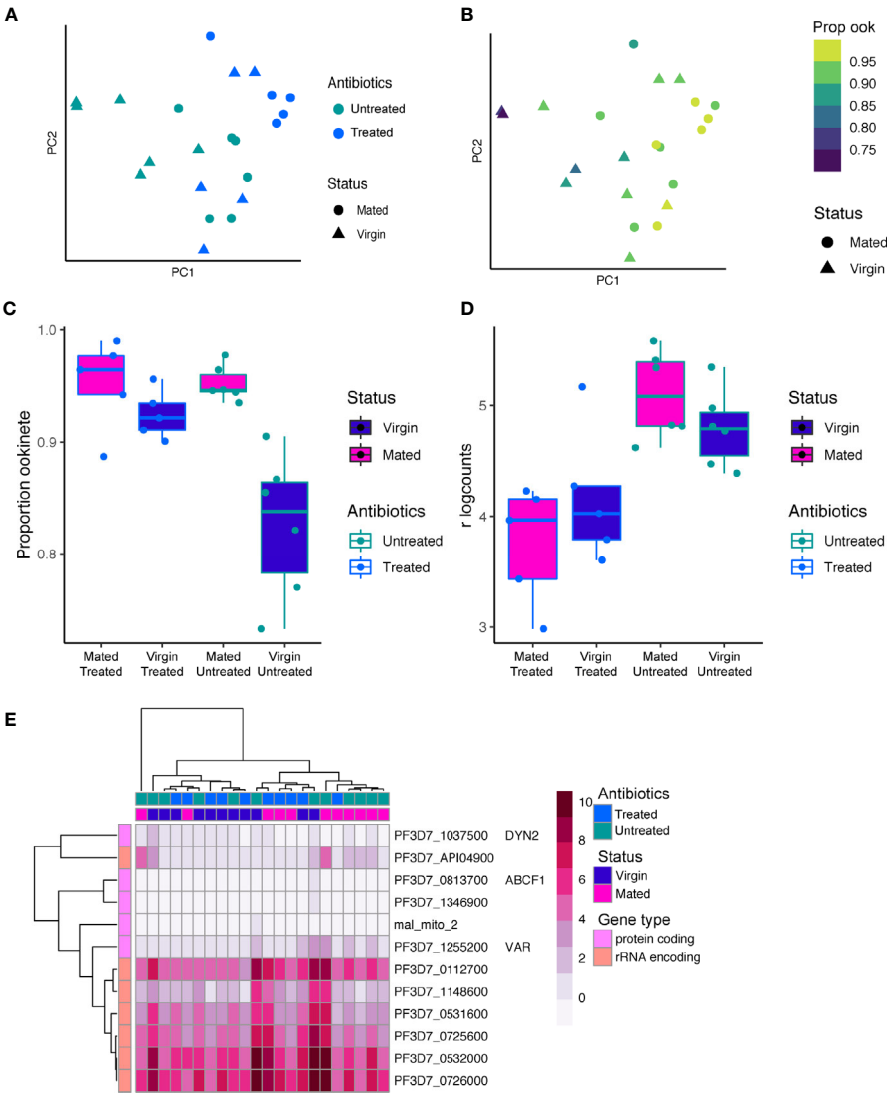

FIGURE 4 | *P. falciparum* gene expression in individual midgut transcriptomes 24 h post-infection. **(A)** PCA of 22 P. *falciparum* transcriptomes from individual *Anopheles* midguts. Points are colored by antibiotic treatment and shaped by mating status. **(B)** The PCA colored by the proportion of ookinetes in each sample based on bulk deconvolution. The proportion of ookinetes increases along PC1. **(C)** A boxplot of the proportion of ookinetes in each sample by mating status and antibiotic treatment. Both antibiotic treatment, mating status, and the interaction between the two significantly impacted the proportion of ookinetes observed in each sample (ANOVA, $p < 0.05$ for each model term). **(D)** Expression of PF3D7_1216600 (CelTOS) in bulk RNAseq data from individual *An. coluzzii* midguts with blood boli. CelTOS was more highly expressed in the antibiotic untreated condition. **(E)** The 12 genes that were identified as highly variable after correcting for the proportion of ookinetes observed are shown in a heatmap of the regularized log counts from DEseq2. Many of the highly variable genes were rRNA encoding genes. Other variable genes of more moderate expression included the *var* gene PF3D7_1255200 which has been shown to be the primary *var* in transmission stages (Gómez-Díaz et al., 2017).

GO:0009986) Benjamini p<0.05). These included PF3D7_1216600 (CelTOS), and PF3D7_1449000 (GEST, gamete egress and sporozoite traversal protein) and PF3D7_1030900 (P28), which were all upregulated in untreated individuals (**Figure S12**). CelTOS and GEST both play a role in cell traversal at multiple stages in the life cycle (Kariu et al., 2006; Talman et al., 2011; Jimah et al., 2016), suggesting the microbiota composition may influence cell traversal strategy. CelTOS was also observed to be differentially expressed at the single-cell level in *P. berghei* between individuals, which potentially could be driven by variation in the microbiota, indicating a conserved response to the midgut environment across *Plasmodium* species.

Finally, we asked which *P. falciparum* genes show a highly variable pattern of expression across individual midguts. Using the Brennecke method (Brennecke et al., 2013), we identified 12 genes that have significant biological variation (FDR < 0.05) (**Figure 4C**, **Table S4**). Seven of these genes were highly

expressed rRNA encoding genes (**Figure 4D**). The active rRNA subunits switch between the mammalian and vector host across *Plasmodium* species (Waters et al., 1989), and their expression pattern may represent inter-vector individual variation in this process driven by selection of different parasite clones or a response to the environment. We also identified a single gene PF3D7_1255200 from the clonally variant *var* gene family which encodes the virulence factor Erythrocyte Membrane Protein 1 (PfEMP1). This particular *var* gene has previously been identified as the primary *var* expressed in transmission stages originating from field samples (Gómez-Díaz et al., 2017).

DISCUSSION

Here, we used a combined approach of single-cell sequencing together with bulk sequencing of both *P. berghei* and *P. falciparum* ookinete stages to address variance of expression in this stage. We find that single-cell sequencing is a powerful tool to address transcriptional variance in ookinetes, a stage where the common consensus is that little to no transcriptional variance occurs. Previous studies indicated that the ookinete transcriptome is somewhat "hard-wired" and made up of a mixture of derepressed maternally inherited transcripts together with new transcripts that are controlled by the ookinete-specific transcription factor AP2-O (Yuda et al., 2009; Kaneko et al., 2015). Although the vast majority of transcriptional variation observed resulted from developmental differences in individual parasites, we developed a framework that allowed us to identify a small number of genes that do display variable expression patterns that are responsive to the host condition.

We identify differentially expressed ookinete genes in *P. berghei* using a nested approach by identifying highly variable genes and using them as the input for further analysis in order to minimize potential noise in the data. Using this approach, we identify 11 genes showing expression dependent on vector species and 12 genes showing expression dependent on vector individuals. Additionally, we identify 28 potential bet-hedging genes, which show a variable pattern of expression independent of the vector individual. For the *P. falciparum* samples, we performed the differential expression and highly variable gene search independently due to the bulk data collection and found 2 genes showing expression dependent on vector mating status, 24 genes showing expression dependent on vector antibiotic treatment, and 12 that show a highly variable pattern of expression. Only three genes were identified in more than one analysis. UFD1 and ISP3 were differentially expressed in the *Pb vector species data set* and identified as potential bet-hedging genes in the *single-gut ookinete data set*. CelTOS was identified as both differentially expressed and a potential bet-hedging gene in the *single-gut ookinete data set.* Additionally, it was differentially expressed in *P. falciparum* in response to antibiotic treatment in the *Pf bulk data set*.

Our analysis highlighted several genes that appear to be clonally variantly expressed that are involved in invasion and located in euchromatic regions of the genome. This is in contrast to patterns of heterochromatin observed in asexual blood stages and transmission stages, where multigene families and some invasion pathways are clonally variant and regulated by heterochromatin (Flueck et al., 2009; Lopez-Rubio et al., 2009; Salcedo-Amaya et al., 2009; Crowley et al., 2011; Brancucci et al., 2014; Fraschka et al., 2018; Witmer et al., 2020). None of the genes we identified overlapped with those found to be heterochromatic regions in either *P. berghei* asexual blood stages or ookinetes (Fraschka et al., 2018; Witmer et al., 2020) (**Figure S8**). In general, we find that heterochromatic genes are largely silenced in ookinetes. In contrast, we find that in ookinetes variant gene expression is not necessarily a yes or no decision (as seen with heterochromatic genes in other life stages) but manifests as variable expression levels of non-heterochromatic genes. This is in stark contrast to how variegated gene expression is driven by heterochromatin in asexual blood stages. One limitation of this study is that clonally variant expression of preceding or subsequent stages for each experiment is unknown as we only sampled ookinetes. However, we do know that heterochromatic *pir* genes are highly variable in male gametocytes (Reid et al., 2018) and both male and females show higher expression of heterochromatic genes (**Figure S8**), but notably these data are from a different experimental infection and should be carefully interpreted. Still, the majority of the genes detected in our study are ookinete-specific and euchromatic, supporting a model of variegated expression in the invasive ookinete stage that is not driven/controlled by heterochromatin formation.

However, it is worth noting that the *var* gene we identified to be expressed in *P. falciparum* midgut samples is the same gene that was detected in *P. falciparum* oocysts from field samples (Gómez-Díaz et al., 2017) but different from the *var* gene detected in mosquito stages in another study (Zanghì et al., 2018). Although to date it is unclear why *var* gene transcripts are found in mosquito stage parasites, as the PfEMP1 proteins they encode for have a very prominent role in antigenic variation in asexual blood stages (Scherf et al., 2008). Nonetheless, this finding suggests that there may be a favoritism of expression in *var* genes in mosquito stages and that not all *var* genes are predisposed to be expressed at this stage.

In our analyses we identify some components of the IMC supporting invasion and invasion proteins themselves to be variably expressed. Remarkably, we found variation in response to the species of mosquitoes in which ookinetes develop. In the wild, parasites can encounter many vector species, for instance *P. falciparum* can infect more than 70 *Anopheles* species (Sinka et al., 2012). Our observation raises the possibility that there exists some invasion plasticity to cater for the host environment, such a phenomenon would be an important consideration in the development of transmission blocking vaccines. For example, *P. berghei* infections in *An. stephensi* are more intense (*i.e.* have more oocysts) than in *An. coluzzii* (Alavi et al., 2003). The differentially expressed genes identified here may be actively involved in modulating infection intensity or may be differentially expressed *via* selection on the

parasite population. Secondly, we found invasion related variation in response to the mosquito environment within the same species suggesting that there is also fine tuning in response to more minor variations in the mosquito environment to potentially enhance transmission. A particularly interesting transcript identified in several of our analyses is CelTOS, a protein essential for invasion that actively takes part in membrane disruption during pore formation of the midgut epithelial cells in order for the ookinete to reach the basal lamina (Kariu et al., 2006; Jimah et al., 2016). Although CelTOS is essential for ookinete invasion, lysis of the enterocyte can also have a deleterious effect on epithelial integrity of the gut and vector survival. It may therefore be advantageous for the parasite to modulate such lytic factors to maximize invasion whilst limiting host death in response to environment or as a population wide bet-hedging strategy to limit the number of invasion events within a single gut. Although such hypotheses would require much deeper validation, our data is suggestive of adaptive phenotypic plasticity of the parasite invasion machinery in response to environmental changes.

It is important to note that this study provides a first overview of variant gene expression in individual ookinetes but is limited in the fact that it contains descriptive data. Further experimental validation is needed to confirm the individual involvement of candidate genes. Nonetheless, this study gives good insight into ookinete biology and will prove valuable for the community.

DATA AVAILABILITY STATEMENT

The data sets generated for this study can be found in ENA at: https://www.ebi.ac.uk/ena/browser/text-search?query=ERP123837.

ETHICS STATEMENT

All animal experimental procedures were reviewed and approved by the Animal Welfare and Ethical Review Body (AWERB) and the United Kingdom Home Office. These procedures were in accordance with the Animal Scientifics Procedures Act 1986, under the UK Home Office License P64F4ADF7.

AUTHOR CONTRIBUTIONS

ML and VH conceived of and designed the study. VH and AT performed *P. berghei* experiments. TM performed mouse work for *P. berghei* experiments. FD performed *P. falciparum* experiments. KW and VH analyzed the data. KW, AT, VH, and ML wrote the manuscript with contributions from other authors. All authors contributed to the article and approved the submitted version.

FUNDING

The Wellcome Sanger Institute is funded by the Wellcome Trust (grant 206194/Z/17/Z), which supports ML. ML is supported by an MRC Career Development Award (G1100339). VH is supported by a Sir Henry Dale Fellowship jointly funded by the Wellcome Trust and the Royal Society (grant 220185/Z/20/Z).

ACKNOWLEDGMENTS

The authors would like to thank the staff of the core cytometry and pipelines sequencing teams at the Wellcome Sanger Institute for their contribution and Till Voss for critically reading the manuscript.

SUPPLEMENTARY MATERIAL

The Supplementary Material for this article can be found online at: https://www.frontiersin.org/articles/10.3389/fcimb.2021.604129/full#supplementary-material

REFERENCES

Alavi, Y., Arai, M., Mendoza, J., Tufet-Bayona, M., Sinha, R., Fowler, K., et al. (2003). The dynamics of interactions between Plasmodium and the mosquito: a study of the infectivity of Plasmodium berghei and Plasmodium gallinaceum, and their transmission by Anopheles stephensi, Anopheles gambiae and Aedes aegypti. *Int. J. Parasitol.* 33, 933–943. doi: 10.1016/S0020-7519(03)00112-7

Anders, S., Pyl, P. T., and Huber, W. (2015). HTSeq–a Python framework to work with high-throughput sequencing data. *Bioinformatics* 31, 166–169. doi: 10.1093/bioinformatics/btu638

Andrews, T. S., and Hemberg, M. (2018). M3Drop: Dropout-based feature selection for scRNASeq. *Bioinformatics* 35(16):2865–7. doi: 10.1093/bioinformatics/bty1044

Bozdech, Z., Llinás, M., Pulliam, B. L., Wong, E. D., Zhu, J., and DeRisi, J. L. (2003). The transcriptome of the intraerythrocytic developmental cycle of Plasmodium falciparum. *PloS Biol.* 1, E5. doi: 10.1371/journal.pbio.0000005

Brancucci, N. M. B., Bertschi, N. L., Zhu, L., Niederwieser, I., Chin, W. H., Wampfler, R., et al. (2014). Heterochromatin protein 1 secures survival and transmission of malaria parasites. *Cell Host Microbe* 16, 165–176. doi: 10.1016/j.chom.2014.07.004

Brancucci, N. M. B., De Niz, M., Straub, T. J., Ravel, D., Sollelis, L., Birren, B. W., et al. (2018). Probing Plasmodium falciparum sexual commitment at the single-cell level. *Wellcome Open Res.* 3, 70. doi: 10.12688/wellcomeopenres.14645.4

Brennecke, P., Anders, S., Kim, J. K., Kołodziejczyk, A. A., Zhang, X., Proserpio, V., et al. (2013). Accounting for technical noise in single-cell RNA-seq experiments. *Nat. Methods* 10, 1093–1095. doi: 10.1038/nmeth.2645

Bullen, H. E., Tonkin, C. J., O'Donnell, R. A., Tham, W.-H., Papenfuss, A. T., Gould, S., et al. (2009). A novel family of Apicomplexan glideosome-associated proteins with an inner membrane-anchoring role. *J. Biol. Chem.* 284, 25353–25363. doi: 10.1074/jbc.M109.036772

Burda, P.-C., Roelli, M. A., Schaffner, M., Khan, S. M., Janse, C. J., and Heussler, V. T. (2015). A Plasmodium phospholipase is involved in disruption of the liver stage parasitophorous vacuole membrane. *PloS Pathog.* 11, e1004760. doi: 10.1371/journal.ppat.1004760

Crowley, V. M., Rovira-Graells, N., Ribas de Pouplana, L., and Cortés, A. (2011). Heterochromatin formation in bistable chromatin domains controls the epigenetic repression of clonally variant Plasmodium falciparum genes linked to erythrocyte invasion. *Mol. Microbiol.* 80, 391–406. doi: 10.1111/j.1365-2958.2011.07574.x

Dahalan, F. A., Churcher, T. S., Windbichler, N., and Lawniczak, M. K. N. (2019). The male mosquito contribution towards malaria transmission: Mating influences the Anopheles female midgut transcriptome and increases female susceptibility to human malaria parasites. *PloS Pathog.* 15, e1008063. doi: 10.1371/journal.ppat.1008063

Ecker, A., Bushell, E. S. C., Tewari, R., and Sinden, R. E. (2008). Reverse genetics screen identifies six proteins important for malaria development in the mosquito. *Mol. Microbiol.* 70, 209–220. doi: 10.1111/j.1365-2958.2008.06407.x

Flueck, C., Bartfai, R., Volz, J., Niederwieser, I., Salcedo-Amaya, A. M., Alako, B. T. F., et al. (2009). Plasmodium falciparum heterochromatin protein 1 marks genomic loci linked to phenotypic variation of exported virulence factors. *PloS Pathog.* 5, e1000569. doi: 10.1371/journal.ppat.1000569

Fraschka, S. A., Filarsky, M., Hoo, R., Niederwieser, I., Yam, X. Y., Brancucci, N. M. B., et al. (2018). Comparative Heterochromatin Profiling Reveals Conserved and Unique Epigenome Signatures Linked to Adaptation and Development of Malaria Parasites. *Cell Host Microbe* 23, 407–420.e8. doi: 10.1016/j.chom.2018.01.008

Gómez-Díaz, E., Yerbanga, R. S., Lefèvre, T., Cohuet, A., Rowley, M. J., Ouedraogo, J. B., et al. (2017). Epigenetic regulation of Plasmodium falciparum clonally variant gene expression during development in Anopheles gambiae. *Sci. Rep.* 7, 40655. doi: 10.1038/srep40655

Gupta, A., Thiruvengadam, G., and Desai, S. A. (2015). The conserved clag multigene family of malaria parasites: essential roles in host-pathogen interaction. *Drug Resist Updat* 18, 47–54. doi: 10.1016/j.drup.2014.10.004

Howick, V. M., Russell, A. J. C., Andrews, T., Heaton, H., Reid, A. J., Natarajan, K., et al. (2019). The Malaria Cell Atlas: Single parasite transcriptomes across the complete Plasmodium life cycle. *Science* 365(6455):eaaw2619. doi: 10.1126/science.aaw2619

Ishino, T., Chinzei, Y., and Yuda, M. (2005). A Plasmodium sporozoite protein with a membrane attack complex domain is required for breaching the liver sinusoidal cell layer prior to hepatocyte infection. *Cell. Microbiol.* 7, 199–208. doi: 10.1111/j.1462-5822.2004.00447.x

Jimah, J. R., Salinas, N. D., Sala-Rabanal, M., Jones, N. G., Sibley, L. D., Nichols, C. G., et al. (2016). Malaria parasite CelTOS targets the inner leaflet of cell membranes for pore-dependent disruption. *Elife* 5, e20621. doi: 10.7554/eLife.20621

Kaneko, I., Iwanaga, S., Kato, T., Kobayashi, I., and Yuda, M. (2015). Genome-Wide Identification of the Target Genes of AP2-O, a Plasmodium AP2-Family Transcription Factor. *PloS Pathog.* 11, e1004905. doi: 10.1371/journal.ppat.1004905

Kariu, T., Ishino, T., Yano, K., Chinzei, Y., and Yuda, M. (2006). CelTOS, a novel malarial protein that mediates transmission to mosquito and vertebrate hosts. *Mol. Microbiol.* 59, 1369–1379. doi: 10.1111/j.1365-2958.2005.05024.x

Kim, D., Langmead, B., and Salzberg, S. L. (2015). HISAT: a fast spliced aligner with low memory requirements. *Nat. Methods* 12, 357–360. doi: 10.1038/nmeth.3317

Kiselev, V. Y., Kirschner, K., Schaub, M. T., Andrews, T., Yiu, A., Chandra, T., et al. (2017). SC3: consensus clustering of single-cell RNA-seq data. *Nat. Methods* 14, 483–486. doi: 10.1038/nmeth.4236

Kiselev, V. Y., Yiu, A., and Hemberg, M. (2018). scmap: projection of single-cell RNA-seq data across data sets. *Nat. Methods* 15, 359–362. doi: 10.1038/nmeth.4644

Kono, M., Herrmann, S., Loughran, N. B., Cabrera, A., Engelberg, K., Lehmann, C., et al. (2012). Evolution and architecture of the inner membrane complex in asexual and sexual stages of the malaria parasite. *Mol. Biol. Evol.* 29, 2113–2132. doi: 10.1093/molbev/mss081

Liao, Y., Smyth, G. K., and Shi, W. (2014). featureCounts: an efficient general purpose program for assigning sequence reads to genomic features. *Bioinformatics* 30, 923–930. doi: 10.1093/bioinformatics/btt656

Llorà-Batlle, O., Tintó-Font, E., and Cortés, A. (2019). Transcriptional variation in malaria parasites: why and how. *Brief Funct. Genomics* 18, 329–341. doi: 10.1093/bfgp/elz009

Lopez-Rubio, J.-J., Mancio-Silva, L., and Scherf, A. (2009). Genome-wide analysis of heterochromatin associates clonally variant gene regulation with perinuclear repressive centers in malaria parasites. *Cell Host Microbe* 5, 179–190. doi: 10.1016/j.chom.2008.12.012

Love, M.II, Huber, W., and Anders, S. (2014). Moderated estimation of fold change and dispersion for RNA-seq data with DESeq2. *Genome Biol.* 15, 550. doi: 10.1186/s13059-014-0550-8

McCarthy, D. J., Campbell, K. R., Lun, A. T. L., and Wills, Q. F. (2017). Scater: pre-processing, quality control, normalization and visualization of single-cell RNA-seq data in R. *Bioinformatics* 33, 1179–1186. doi: 10.1093/bioinformatics/btw777

Modrzynska, K., Pfander, C., Chappell, L., Yu, L., Suarez, C., Dundas, K., et al. (2017). A Knockout Screen of ApiAP2 Genes Reveals Networks of Interacting Transcriptional Regulators Controlling the Plasmodium Life Cycle. *Cell Host Microbe* 21, 11–22. doi: 10.1016/j.chom.2016.12.003

Newman, A. M., Steen, C. B., Liu, C. L., Gentles, A. J., Chaudhuri, A. A., Scherer, F., et al. (2019). Determining cell type abundance and expression from bulk tissues with digital cytometry. *Nat. Biotechnol.* 37, 773–782. doi: 10.1038/s41587-019-0114-2

Nötzel, C., Poran, A., and Kafsack, B. F. C. (2018). Single-Cell Transcriptome Profiling of Protozoan and Metazoan Parasites. *Trends Parasitol.* 34, 731–734. doi: 10.1016/j.pt.2018.04.009

Picelli, S., Faridani, O. R., Björklund, Å.K., Winberg, G., Sagasser, S., and Sandberg, R. (2014). Full-length RNA-seq from single cells using Smart-seq2. *Nat. Protoc.* 9, 171–181. doi: 10.1038/nprot.2014.006

Poran, A., Nötzel, C., Aly, O., Mencia-Trinchant, N., Harris, C. T., Guzman, M. L., et al. (2017). Single-cell RNA sequencing reveals a signature of sexual commitment in malaria parasites. *Nature* 551, 95–99. doi: 10.1038/nature24280

Poulin, B., Patzewitz, E.-M., Brady, D., Silvie, O., Wright, M. H., Ferguson, D. J. P., et al. (2013). Unique apicomplexan IMC sub-compartment proteins are early markers for apical polarity in the malaria parasite. *Biol. Open* 2, 1160–1170. doi: 10.1242/bio.20136163

Real, E., Howick, V. M., Dahalan, F., Witmer, K., Cudini, J., Andradi-Brown, C., et al. (2020). A single-cell atlas of Plasmodium falciparum transmission through the mosquito. *Cold Spring Harbor Lab.* 2020. doi: 10.1101/2020.10.11.333179

Reid, A. J., Talman, A. M., Bennett, H. M., Gomes, A. R., Sanders, M. J., Illingworth, C. J. R., et al. (2018). Single-cell RNA-seq reveals hidden transcriptional variation in malaria parasites. *Elife* 7, e33105. doi: 10.7554/eLife.33105

Rovira-Graells, N., Gupta, A. P., Planet, E., Crowley, V. M., Mok, S., Ribas de Pouplana, L., et al. (2012). Transcriptional variation in the malaria parasite Plasmodium falciparum. *Genome Res.* 22, 925–938. doi: 10.1101/gr.129692.111

Saeed, S., Tremp, A. Z., and Dessens, J. T. (2018). The Plasmodium LAP complex affects crystalloid biogenesis and oocyst cell division. *Int. J. Parasitol.* 48, 1073–1078. doi: 10.1016/j.ijpara.2018.09.002

Saini, E., Zeeshan, M., Brady, D., Pandey, R., Kaiser, G., Koreny, L., et al. (2017). Photosensitized INA-Labelled protein 1 (PhIL1) is novel component of the inner membrane complex and is required for Plasmodium parasite development. *Sci. Rep.* 7, 15577. doi: 10.1038/s41598-017-15781-z

Salcedo-Amaya, A. M., van Driel, M. A., Alako, B. T., Trelle, M. B., van den Elzen, A. M. G., Cohen, A. M., et al. (2009). Dynamic histone H3 epigenome marking during the intraerythrocytic cycle of Plasmodium falciparum. *Proc. Natl. Acad. Sci. U. S. A.* 106, 9655–9660. doi: 10.1073/pnas.0902515106

Scherf, A., Lopez-Rubio, J. J., and Riviere, L. (2008). Antigenic variation in Plasmodium falciparum. *Annu. Rev. Microbiol.* 62, 445–470. doi: 10.1146/annurev.micro.61.080706.093134

Sinka, M. E., Bangs, M. J., Manguin, S., Rubio-Palis, Y., Chareonviriyaphap, T., Coetzee, M., et al. (2012). A global map of dominant malaria vectors. *Parasitol. Vectors* 5, 69. doi: 10.1186/1756-3305-5-69

Smith, R. C., Vega-Rodríguez, J., and Jacobs-Lorena, M. (2014). The Plasmodium bottleneck: malaria parasite losses in the mosquito vector. *Mem. Inst. Oswaldo Cruz* 109, 644–661. doi: 10.1590/0074-0276130597

Spence, P. J., Jarra, W., Lévy, P., Reid, A. J., Chappell, L., Brugat, T., et al. (2013). Vector transmission regulates immune control of Plasmodium virulence. *Nature* 498, 228–231. doi: 10.1038/nature12231

Talman, A. M., Lacroix, C., Marques, S. R., Blagborough, A. M., Carzaniga, R., Ménard, R., et al. (2011). PbGEST mediates malaria transmission to both

mosquito and vertebrate host. *Mol. Microbiol.* 82, 462–474. doi: 10.1111/j.1365-2958.2011.07823.x

Trapnell, C., Cacchiarelli, D., Grimsby, J., Pokharel, P., Li, S., Morse, M., et al. (2014). The dynamics and regulators of cell fate decisions are revealed by pseudotemporal ordering of single cells. *Nat. Biotechnol.* 32, 381–386. doi: 10.1038/nbt.2859

Voss, T. S., Bozdech, Z., and Bártfai, R. (2014). Epigenetic memory takes center stage in the survival strategy of malaria parasites. *Curr. Opin. Microbiol.* 20, 88–95. doi: 10.1016/j.mib.2014.05.007

Waters, A. P., Syin, C., and McCutchan, T. F. (1989). Developmental regulation of stage-specific ribosome populations in Plasmodium. *Nature* 342, 438–440. doi: 10.1038/342438a0

Waters, A. P. (2016). Epigenetic Roulette in Blood Stream Plasmodium: Gambling on Sex. *PloS Pathog.* 12, e1005353. doi: 10.1371/journal.ppat.1005353

Witmer, K., Fraschka, S. A., Vlachou, D., Bártfai, R., and Christophides, G. K. An epigenetic map of malaria parasite development from host to vector. *Sci. Rep.* (2020) 10 (1), 6354. doi: 10.1038/s41598-020-63121-5

Yuda, M., Iwanaga, S., Shigenobu, S., Mair, G. R., Janse, C. J., Waters, A. P., et al. (2009). Identification of a transcription factor in the mosquito-invasive stage of malaria parasites. *Mol. Microbiol.* 17, 1402–1414. doi: 10.1111/j.1365-2958.2009.06609.x

Zanghì, G., Vembar, S. S., Baumgarten, S., Ding, S., Guizetti, J., Bryant, J. M., et al. (2018). A Specific PfEMP1 Is Expressed in P. falciparum Sporozoites and Plays a Role in Hepatocyte Infection. *Cell Rep.* 22, 2951–2963. doi: 10.1016/j.celrep.2018.02.075

Conflict of Interest: The authors declare that the research was conducted in the absence of any commercial or financial relationships that could be construed as a potential conflict of interest.

frontiers in Cellular and Infection Microbiology

ORIGINAL RESEARCH
published: 15 March 2021
doi: 10.3389/fcimb.2021.634273

Identification of Three Novel *Plasmodium* Factors Involved in Ookinete to Oocyst Developmental Transition

Chiamaka V. Ukegbu[1], *George K. Christophides*[1,2] *and Dina Vlachou*[1,2]*

[1] Department of Life Sciences, Imperial College London, London, United Kingdom, [2] The Cyprus Institute, Nicosia, Cyprus

Plasmodium falciparum malaria remains a major cause of global morbidity and mortality, mainly in sub-Saharan Africa. The numbers of new malaria cases and deaths have been stable in the last years despite intense efforts for disease elimination, highlighting the need for new approaches to stop disease transmission. Further understanding of the parasite transmission biology could provide a framework for the development of such approaches. We phenotypically and functionally characterized three novel genes, *PIMMS01*, *PIMMS57*, and *PIMMS22*, using targeted disruption of their orthologs in the rodent parasite *Plasmodium berghei*. *PIMMS01* and *PIMMS57* are specifically and highly expressed in ookinetes, while *PIMMS22* transcription starts already in gametocytes and peaks in sporozoites. All three genes show strong phenotypes associated with the ookinete to oocyst transition, as their disruption leads to very low numbers of oocysts and complete abolishment of transmission. *PIMMS22* has a secondary essential function in the oocyst. Our results enrich the molecular understanding of the parasite-vector interactions and identify *PIMMS01*, *PIMMS57*, and *PIMMS22* as new targets of transmission blocking interventions.

Keywords: ookinete development, malaria transmission, ookinete to oocyst transition, mosquito midgut invasion, *Plasmodium* sporogonic development, vector-parasite interactions

OPEN ACCESS

Edited by:
Chandra Ramakrishnan, University of Zurich, Switzerland

Reviewed by:
Katarzyna Kinga Modrzynska, University of Glasgow, United Kingdom
Rita Tewari, University of Nottingham, United Kingdom

***Correspondence:**
Dina Vlachou
d.vlachou@imperial.ac.uk

Specialty section:
This article was submitted to Parasite and Host, a section of the journal Frontiers in Cellular and Infection Microbiology

Received: *27 November 2020*
Accepted: *10 February 2021*
Published: *15 March 2021*

Citation:
Ukegbu CV, Christophides GK and Vlachou D (2021) Identification of Three Novel Plasmodium Factors Involved in Ookinete to Oocyst Developmental Transition. Front. Cell. Infect. Microbiol. 11:634273. doi: 10.3389/fcimb.2021.634273

INTRODUCTION

Malaria remains a global public health problem with 228 million cases in 2018, causing 405,000 deaths (WHO World Malaria Report 2019). This deadly disease is caused by parasites of the genus *Plasmodium* transmitted by the bite of infected female *Anopheles* mosquitoes. *P. falciparum* is the most virulent of the human malaria parasites, responsible for most of malaria-associated deaths especially of children under 5 years old and first-time pregnant women. Transmission begins upon ingestion by a female *Anopheles* mosquito of a blood meal containing male and female gametocytes from an infected human. In the mosquito midgut, the gametocytes differentiate into male and female gametes that then mate to form the zygote. Within 24 h, the zygote, through several stages of development, differentiates into a crescent shaped motile ookinete that escapes the blood bolus and its encasing peritrophic matrix and invades and traverses the midgut epithelium. On the basal side of the midgut, the ookinete transforms into a sessile, replicative oocyst where thousands of

sporozoites are produced. Oocysts burst and sporozoites released into the haemocoel reach the salivary glands from where they are transmitted to a new host during a subsequent mosquito bite.

The ookinete-to-oocyst developmental transition in the mosquito midgut is the most critical stage of the entire parasite transmission cycle. The ingested parasite populations suffer major losses during this stage resulting in very few oocysts and, in most cases, termination of transmission. This stage is therefore a good target of interventions aiming to control disease transmission (Smith et al., 2014). Genome scale transcriptomic studies have shed important insights into *Plasmodium* gene expression and regulation that accompanies developmental stage transitions and developmental processes of the parasite (Le Roch et al., 2003; Hall et al., 2005; Otto et al., 2010; Otto et al., 2014; Lasonder et al., 2016; Yeoh et al., 2017; Reid et al., 2018). We have previously used DNA microarrays to identify transcriptional profiles driving the under characterized gametocyte-ookinete-to-oocyst developmental transitions in the rodent model parasite *Plasmodium berghei* (Akinosoglou et al., 2015); and more recently single cell RNA sequencing in *P. berghei* has also revealed genes differentially expressed during ookinete-to-oocyst developmental transition (Howick et al., 2019).

While rodent models are routinely employed in study parasite development in the mosquito vector, due to their genetic accessibility and tractability, functional differences in the utilization of genes between rodent and human parasites may be important especially with regards to specific interactions with the vector (Dong et al., 2006; Simões et al., 2017). Indeed, to cope with the live and changing host environment, *Plasmodium* has evolved the ability to undertake transcriptional variation for its survival and transmission (Rovira-Graells et al., 2012; Waters, 2016). *P. falciparu*m utilizes and infects about 60–70 *Anopheles* species, therefore, there would be a necessity to adapt to the different environments of each of these mosquito species, in particular with regards to differences in mosquito immune responses, behavior, and physiology (White et al., 2011; Mitri et al., 2015; Costa et al., 2018; Lefevre et al., 2018). For these reasons, we have developed an operational framework where *P. falciparum* genes potentially involved in parasite interactions with the vector are identified using genome-wide transcriptomic studies in near field settings and then prioritized for genetic and functional characterization in laboratory mosquito infections with *P. berghei*.

Here, we selected from our dataset three *P. falciparum* genes that exhibit highly abundant transcripts 24 h post blood feeding (hpbf) in the midguts of *Anopheles coluzzii* mosquitoes. These genes have been part of a large reverse genetic *P. berghei* screen to identify genes that function during parasite infection of the mosquito midgut, designated as *Plasmodium* Infection of the Mosquito Midgut Screen (PIMMS). We have previously reported the characterization of *PIMMS2* that encodes an ookinete membrane-associated subtilisin-like protein involved in midgut traversal (Ukegbu et al., 2017) and *PIMMS43* that encodes another ookinete membrane protein aiding in resistance to responses of the mosquito complement-like system (Ukegbu et al., 2020). Now we report the identification and characterization of three additional genes, *PIMMS01*, *PIMMS57*, and *PIMMS22*, which are highly transcribed and translated in the ookinete; with *PIMMS22* also highly expressed at both the gametocyte and sporozoite stages. PIMMS01 and PIMMS57 are putatively secreted and membrane-bound proteins, respectively, while PIMMS22 does not include any known secretory or membrane association signals but localizes on the periphery of ookinetes and sporozoites, possibly the inner membrane complex. An earlier study by Zheng and colleagues designated *PIMMS57* as *PSOP26* (Zheng et al., 2016) and showed the antibodies against *P. berghei* PIMMS57 can affect ookinete maturation and malaria transmission. We demonstrate that none of these genes has a role in ookinete development but are all important for the ookinete-to-oocyst developmental transition in the midgut and disease transmission.

MATERIALS AND METHODS

Ethics Statement

Animal procedures were carried out in accordance with the Animal (Scientifics Procedures) Act 1986 under the UK Home Office Licenses PPL70/8788.

Sequence Analysis

Plasmodium protein sequences were retrieved from PlasmoDB (http://plasmodb.org/plasmo/) and apicomplexan parasite sequences were retrieved from UniProt. Alignment was carried out using Clustal Omega and visualized in the BioEdit sequence alignment editor program. Signal peptide and transmembrane domains were predicted using SignalP and Phobius (Käll et al., 2007; Armenteros et al., 2019).

P. falciparum Culturing and Mosquito Infections

P. falciparum NF54 was cultured as described previously (Habtewold et al., 2019). Briefly, ABS and gametocytes were cultured using human RBCs of various blood groups in the following order of preference: O+ male, O+ female, A+ male, and A+ female. Asexual cultures were set up in 10 ml complete medium [RPMI-1640, 0.05 g/L Hypoxanthine, 0.3 mg/L L-glutamine, 10% (v/v) sterile human serum of A+ serotype] containing a final volume of 500 µl of hRBCs (0.3%–4% infection). Cultures were gassed with "malaria gas" (3% O_2/5% CO_2/92% N_2) and incubated at 37°C. Gametocyte cultures were set up by dilution of a 3-4% ring stage asexual culture to 1% ring forms in a final volume of 8 ml complete medium and supply of fresh hRBCs. The cultures underwent daily exchange of around 75% of the media, gassed with malaria gas and incubated at 37°C until day 14. Mosquitos were infected with *P. falciparum* by SMFAs as described previously (Habtewold et al., 2019). Briefly, Giemsa staining was used to assess gametocyte density and *in vitro* exflagellation was used to assess viability of stage V male

gametocytes. In a pre-warmed tube, the gametocyte cultures were pooled in a final volume of 300 µl containing 20% (v/v) uninfected serum-free hRBCs and 50% (v/v) heat-inactivated human serum. This mixture was then transferred to pre-warmed mosquito feeders kept a constant temperature of 37°C.

P. berghei Strains and Cultivation

P. berghei lines used were the reference parent line of *P. berghei* ANKA 2.34 (*cl15cy1*) and the *507m6cl1* (*c507*) line that contains *GFP* integrated into the *230p* gene locus (*PBANKA_0306000*) without a drug selectable marker and constitutively expresses *GFP* under the control of the EF1 alpha promoter (Janse et al., 2006a). All parasite lines were maintained in 8-10-week-old CD1 and/or TO female mice by serial passaging. *P. berghei* mixed blood stages, gametocytes, and ookinetes were cultured and purified as described previously (Janse and Waters, 1995; Beetsma et al., 1998).

Quantitative RT-PCR

Total RNA was extracted from *P. berghei* and *P. falciparum* parasites or *A. coluzzii* infected with *P. berghei* or *P. falciparum* using Trizol reagent (ThermoFisher) according to the manufacturer's instructions. cDNA was synthesized using the PrimeScript Reverse Transcription Kit (Takara) after Turbo DNase (ThermoFisher) treatment. For qRT-PCR, SYBR green (Takara) and gene specific qRT-PCR primers (**Table S6**) were used according to the manufacturer's guidelines. Gene expression was normalized against *GFP* in *P. berghei* and against *P. falciparum* arginyl-tRNA synthetase in *P. falciparum* using the ΔΔCt method.

Antibody Production

Rabbit polyclonal antibodies against peptides of the deduced proteins PIMMS01 and PIMMS57 were raised and purified from the serum of an immunized rabbit (Eurogentec): α-Pfc01 targets the PfPIMMS01 peptide EKHKDSTKWDKSYSF (aa 72–86); α-Pbc57 targets the PbPIMMS57 the N-terminal peptide SNDSNYEDRDNAPNR (aa 48–62); and α-Pfc57, targets the N-terminal peptide EQRVRDEGRENNRRS (aa 111–125.)

Western Blot Analysis

Soluble cell lysates were prepared by suspending purified parasite pellets in cell lysis buffer (5 mM Tris, 150 mM NaCl) containing protease inhibitors. Triton X-100 soluble cell lysates were prepared by suspending purified parasite pellets in Triton X-100 cell lysis buffer (5 mM Tris, 150 mM NaCl, 1% v/v Triton X-100) containing protease inhibitors. Triton X-100 insoluble cell fractions/whole cell lysates were prepared by suspending parasite pellets or infected midguts in reducing (3% v/v 2-mercapthoethanol) Laemmli buffer. Protein samples were then boiled under reducing (3% v/v 2-mercapthoethanol) conditions in Laemmli buffer and separated using sodium dodecyl sulfate polyacrylamide gel electrophoresis. Separated proteins were then transferred to a PVDF membrane (GE Healthcare). Proteins were detected using Goat α-GFP (Rockland chemicals) (1:100), mouse α-tubulin (Sigma), and 3D11 mouse monoclonal α-PbCSP (Potocnjak et al., 1980) (1:1000), α-Pbc57 (1:100), α-Pfc01 (1:50), α-Pfc57 (1:50), and α-Pfs25 (Barr et al., 1991), (1:100) antibodies. Secondary horseradish peroxidase (HRP) conjugated IgG, goat α-mouse IgG antibodies (Promega), and donkey α-goat IgG (Abcam) were used at 1: 10,000 and 1: 5,000 dilutions, respectively. All primary and secondary antibodies were diluted in 3% milk-PBS-Tween (0.05% v/v) blocking buffer.

Indirect Immunofluorescence Assay

For IFAs on blood bolus parasites, the blood bolus was collected from dissected midguts of mosquitoes at 2 and 19 hpbf. The blood bolus was washed in PBS and fixed in 4% paraformaldehyde (PFA) for 10 min. The fixed parasites were smeared on a glass slide, permeabilized with 0.2% (v/v) Triton X-100, and blocked with 3% (w/v) bovine serum albumin Purified gametocytes and *in vitro* ookinetes were fixed, permeabilized and blocked as above. For IFAs on midgut sporozoites at 15 dpbf, infected midguts were dissected, and tissues were homogenized to release sporozoites. Sporozoites were fixed, blocked and permeabilized as that above. For IFAs on ookinetes invading the midgut epithelium, the midguts of mosquitoes at 26 hpbf were dissected, and the blood boluses were discarded. The midgut epithelium was fixed in 4% PFA in PBS for 45 min and washed thrice in PBS for 10 min each. Midgut epithelium was permeabilized and blocked for 1 h in 1% w/v BSA, 0.1% v/v Triton X-100 in PBS blocking solution. Samples were then stained in blocking solution with primary antibodies (α-GFP, 1:100; 13.1 mouse monoclonal α-P28 (Winger et al., 1988), 1:1000; and α-PbCSP 1:100; α-Pfc01, 1:100; α-Pfc57, 1:100; 4B7 mouse monoclonal α-Pfs25, 1:100. Alexa Fluor (488 and 568) conjugated secondary antibodies specific to goat or mouse (ThermoFisher) were used at a dilution of 1:1000. 4′,6-diamidino-2-phenylindole (DAPI) was used to stain nuclear DNA. Images were acquired using a Leica SP5 MP confocal laser-scanning microscope. Images underwent processing by deconvolution using Huygens software and were visualized using Image J.

Generation of Transgenic Parasites

For *GFP* tagging of *Pbc01* in the *2.34* line, a 603 bp ApaI/HindIII 5' and a 770 bp EcoRI/BamHI 3' homology arm region were amplified from *P. berghei 2.34* genomic DNA using the primer pairs P1/P2 and P3/P4, respectively. For *GFP* tagging of *Pbc57* in the *2.34* line, a 919 bp ApaI/SacII 5' homology arm corresponding to the most 3' region of the CDS without the stop codon and a 359 bp XhoI/XmaI 3' homology arm region corresponding to the *3' UTR* of the gene were amplified using the primer pairs P5/P6 and P7/P8, respectively. For *GFP* tagging of *Pbc22* in the *2.34* line, a 753 bp ApaI/HindIII 5' homology arm corresponding to the most 3' region of the CDS without the stop codon and a 530 bp EcoRI/BamHI 3' homology arm region corresponding to the *3' UTR* of the gene were amplified using the primer pairs P9/P10 and P11/P12, respectively. The *Pbc01* and *Pbc22* fragments were cloned into the pBS-TgDHFR vector which carries a modified *Toxoplasma gondii* dihydrofolate gene (TgDHFR/TS) cassette that confers resistance to pyrimethamine (Dessens et al., 1999). The *Pbc57* fragments were cloned into plasmid pL0035 which carries the *hDHFR* selection cassette

(Braks et al., 2006). Finally, to put *GFP* tag in frame with the 3' region of the CDS, a HindIII or SacII *GFP-P. berghei DHFR 3'UTR* fragment was amplified from the pL00018 vector (MRA-787, MR4) using primers P13/P14 or P15/P16, respectively.

For *3XHA* tagging of *Pbc01* in the c*507* line, a 687 bp ApaI/SacII 5' homology arm corresponding to the some of the *5'UTR*, the whole CDS without the stop codon and the 3XHA tag and a 2051 bp XhoI/XmaI 3' homology arm region corresponding to the *3' UTR* of the gene was amplified from genomic DNA using the Gibson assembly primer pairs P43/P44 and P45/P46, respectively. For *3XHA* tagging of *Pbc57* in the c*507* line, a 1003 bp ApaI/SacII 5' homology arm corresponding to the most 3' region of the CDS without the stop codon and the 3XHA tag and a 359 bp XhoI/XmaI 3' homology arm region corresponding to the *3' UTR* of the gene was amplified using the Gibson assembly primer pairs P47/P48 and P49/P50 respectively. The *Pbc01* and *Pbc57* fragments were cloned into plasmid pL0035 *via* Gibson assembly.

For partial disruption of *Pbc01* in the *c507* line, a 432 bp ApaI/HindIII 5' homology arm and a 1102 bp EcoRI/BamHI 3' homology arm was amplified using the primer pairs P24/P25 and P26/P27, respectively. For partial disruption of *Pbc57* in the *c507* line, a 590 bp ApaI/HindIII 5' homology arm and a 684 bp EcoRI/BamHI 3' homology arm was amplified using the primer pairs P28/P29 and P30/P31, respectively. For partial disruption of *Pbc22* in the *c507* line, a 560 bp ApaI/HindIII 5' homology arm and a 712 bp EcoRI/BamHI 3' homology arm was amplified using the primer pairs P32/P33 and P34/P35, respectively. These fragments were cloned into the pBS-TgDHFR vector. The targeting cassettes by ApaI/BamHI digestion allows knockout of 39% of *Pbc01* CDS, 70% of *Pbc57* CDS, and 80% of *Pbc22* CDS.

Transfection of linearized constructs, selection of transgenic parasites and clonal selection was carried out as described previously (Janse et al., 2006b).

Genotypic Analysis of Transgenic Parasites

Blood stage parasites were purified by removal of white blood cells using hand packed cellulose (Sigma) columns. Parasites were released using red blood cell lysis buffer (0.17 M NH_4Cl) on ice for 20 min. Genomic DNA was extracted from parasites using the DNeasy kit (Qiagen). Integration events or maintenance of the unmodified locus was detected by PCR on genomic DNA using primers listed in **Table S6**. For PFGE, blood stage parasites within agarose plugs were lysed in lysis buffer (1X TNE, 0.1 M EDTA pH 8.0, 2% (v/v) Sarkosyl, 400 μg/ml proteinase K) to release nuclear chromosomes. PFGE separated chromosomes (Run settings: 98 volts, 1–5 mins pulse time for 60 h at 14°C) were then subjected to Southern blot analysis using a probe targeting the *TgDHFR/TS-P. berghei DHFR 3'UTR*, obtained by HindIII and EcoRV digestion of the pBS-TgDHFR plasmid.

Phenotypic Assays

Exflagellation assays were performed as described previously (Akinosoglou et al., 2015). Briefly, blood from a high gametocytemic mouse was added in a 1:40 ratio to ookinete medium (RPMI 1640, 20% v/v FBS, 100 μM xanthurenic acid, pH 7.4), and exflagellation was counted in a standard hemocytometer under a light microscope. Conversion assays were performed as previously described (Akinosoglou et al., 2015). Briefly, *in vitro* cultivated ookinetes were resuspended in 50 μl of fresh ookinete and incubated with a Cy3-labeled 13.1 mouse monoclonal α-P28 (1:50 dilution) for 20 min on ice. The conversion rate was calculated as the percentage of Cy3 positive ookinetes to Cy3 positive macrogametes and ookinetes.

Ookinete motility assays were performed as described previously (Moon et al., 2009). Briefly, on a glass slide, 24 h *in vitro* ookinete culture was incubated with Matrigel (BD biosciences), and allowed to set at RT for 30 min. On a Leica DMR fluorescence microscope and a Zeiss Axiocam HRc camera controlled by the AxioVision (Zeiss) software, time-lapse images (1 frame every 5 s for 10 min) of ookinetes were obtained. Using the manual tracking plugin in the Icy software (http://icy.bioimageanalysis.org/), the speed of individual ookinetes was measured.

A. coluzzii mosquitoes were fed by direct blood feeding as previously described (Sinden, 1997) on mice with parasitemia of 4%–5% and gametocytemia of 1%–2%. Midguts tissues were dissected at 7–10 dpbf and fixed in 4% PFA in PBS and mounted in Vectashield® (VectorLabs). Oocysts or melanized ookinetes were counted using light and/or fluorescence microscopy. 25-30 P. *berghei* infected *A. coluzzii* midguts or salivary glands at 15 and 21 dpbf respectively were homogenized and oocyst and salivary gland sporozoites counted using a standard hemocytometer. Finally, in mosquito to mouse transmission assays, at least 30 P. *bergh*ei infected mosquitoes at 21 dpbf were allowed to feed on two to three anaesthetized C57/BL6 mice for 15 min. Parasitemia was monitored until 14 days post mosquito bite by Giemsa staining of blood smears.

Ookinete Injections in Mosquito Haemocoel

Ookinete injections were carried out as described previously (Bushell et al., 2009). Briefly, the concentration of ookinetes from 24 h *in vitro* cultures was adjusted with RPMI 1640, and this was injected using glass capillary needles and the Nanoject II microinjector (Drummond Scientific) into the thorax of *A. coluzzii* mosquitoes at a final concentration of 800 ookinetes per mosquito.

Gene Silencing

Total RNA extracted from *A. coluzzii* midgut infected with *P. berghei c507* at 24 hpbf was used to prepare cDNA. The cDNA was used in conjunction with primers reported in (Habtewold et al., 2008) to amplify CTL4. DsRNA was then produced using the resulting PCR product and the T7 high yield transcription kit (ThermoFisher). 0.2 μg of purified dsRNA in 69 nl was injected into the thorax of *A. coluzzii* mosquitoes using glass capillary needles and the Nanoject II microinjector. Two to three days post injected mosquitoes were then infected with *P. berghei*.

Statistical Analysis

Statistical analyses were performed using GraphPad Prism v8.0. Statistical analyses for exflagellation, ookinete conversion and motility assays were performed using a two-tailed, unpaired Student's t-test. For statistical analyses of the oocyst or melanized parasite load, P-values were calculated using the Mann-Whitney test.

RESULTS

In Silico Analysis

Based on their expression profiles in a *P. falciparum* transcriptomics dataset and mutant phenotypes in a *P. berghei* high throughput reverse genetics screen, three parasite genes were selected for further characterization, including targeted disruption and detail phenotypic analysis in *P. berghei*. These genes were *PF3D7_0112100* in *P. falciparum* and *PBANKA_*0201700 in *P. berghei*, *PF3D7_1244500* in *P. falciparum* and *PBANKA_1457700* in *P. berghei*, and *PF3D7_0814600* in *P. falciparum* and *PBANKA_1422900* in *P. berghei*; designated as *PIMMS01*, *PIMMS57*, and *PIMMS22*, respectively.

PfPIMMS01 encodes a 163 amino acid-long protein (19 kDa) with a predicted signal peptide (aa 1–27; probability according to SignalP and Phobius 0.688 and 0.904, respectively). Its *P. berghei* orthologue, *PbPIMMS01*, encodes a much shorter 85 amino acid-long protein (9 kDa) and also contains a predicted signal peptide (aa 1–26; probability according to SignalP and Phobius 0.826 and 0.978, respectively). This suggests that both proteins are putatively secreted. While the central part of the deduced protein is highly conserved between all PIMMS01 orthologues, all rodent PIMMS01 proteins are shorter than their orthologues in human parasites, lacking the entire second half of the protein (**Figure S1**). InterPro domain analysis revealed no recognizable domain, and BLAST searches showed that the protein is *Plasmodium* specific.

PfPIMMS57 encodes a 810 amino acid-long (94 kDa) protein with a predicted signal peptide (aa 1–26; probability according to SignalP and Phobius 0.697 and 0.657, respectively) that overlaps with a putative transmembrane domain albeit with low probability according to Phobius (0.343). A second transmembrane domain close to the carboxy terminus of PfPIMMS57 (aa 677–697) is predicted with very high probability (0.874). The *P. berghei* orthologue, *PbPIMMS57*, encodes a protein of 774 amino acid-long (90 kDa) protein with two putative transmembrane domains (aa 6–23 and aa 633–653) predicted with high probability (0.984 and 0.967, respectively). These data suggest that both proteins are putatively membrane-bound. Higher sequence conservation between PIMMS57 orthologues is observed in the second half of the proteins compared to the first half, pointing to a conserved functional role served by this region (**Figure S2**). A previous *in silico* analysis identified in PfPIMMS57, two *P. falciparum* serine/threonine protein phosphatase type I catalytic (PfPP1c) binding motifs, the RVxF motif, RRKVNF (aa 347–352) and the Fxx[RK]x[RK] motif, FNKILKR (aa 488–494) (Hollin et al., 2016). These motifs are not conserved in the other PIMMS57 orthologues.

Finally, *PfPIMMS22* encodes a 393 amino acid (45 kDa) protein and *PbPIMMS22* encodes a 393 aa (44 kDa) protein, both with no predicted signal peptide or transmembrane domain. The protein is highly conserved amongst *Plasmodium* orthologues with sequence identity ranging from 96% in PyPIMMS22 to 76% and 80% in PfPIMMS22 and PvPIMMS22, respectively (**Figure S3**). PyPIMMS22 (PY17X_1424900) was previously identified in salivary gland sporozoites through a subtractive hybridization (SSH) profiling and termed sporozoite protein S15 (Kaiser et al., 2004). The same protein was also identified in midgut oocyst sporozoites as an interacting partner to the apicomplexan specific RNA-binding protein, ALBA4, which is involved in mRNA regulation in gametocyte and midgut oocyst sporozoite development (Muñoz et al., 2017). PIMMS22 homologues are found in other apicomplexan parasites including *Toxoplasma gondii*, *Neospora caninum* and *Eimeria* with sequence identities to PIMMS22 ranging from 36% to 42% (**Figure S4**). InterPro domain analysis revealed no recognizable domain in PIMMS22.

Transcription Profiles

We searched a DNA microarray dataset of *A. coluzzii* midguts infected with *P. falciparum* field isolates from Burkina Faso to examine the transcriptional profiles of the three genes under study. *PfPIMMS01* and, to a lesser extent, *PfPIMMS57* were lowly transcribed 1 h post blood-feeding (hpbf) and their transcription peaked 24 hpbf, while *PfPIMMS22* expression started in gametocytes and continued at high levels 24 hpbf. We corroborated these data with quantitative real-time RT-PCR (qRT-PCR) in laboratory *P. falciparum* NF54 cultured gametocytes and in NF54 infections of *A. coluzzii* 1 and 24 hpbf (**Figure 1A**). Very low levels of *PfPIMMS01* and *PfPIMMS57* transcripts were detected in gametocytes and in *A. coluzzii* midguts 1 hpbf, peaking at 24 hpbf.

Transcription of the *P. berghei* orthologous genes was also analyzed using qRT-PCR (**Figure 1B**). In this assay, the *P. berghei* line *ANKA507m6cl1* that constitutively expresses GFP was used (Janse et al., 2006a); hereafter referred to as *c507*. *PbPIMMS01* and *PbPIMMS57* transcripts were highly abundant in purified mature ookinetes (Ook) and not detectable in mixed blood stages (MBS) and purified gametocytes. While *PbPIMMS57* appears to be specific for ookinetes, low levels of *PbPIMMS01* transcripts are also detected in mature oocysts and midgut sporozoites at 10 days and 15 days post blood-feeding (dpbf). Like *PfPIMMS22*, expression of *PbPIMMS22* starts in gametocytes and continues at high levels 24 hpbf and peaks in midgut sporozoites 15 dpbf (**Figure 1B**). Low abundance *PbPIMMS22* transcripts detected in MBS is likely due to expression in gametocytes. These results generally agree with those in published RNA-sequencing data from blood stages and ookinetes (Otto et al., 2014; Yeoh et al., 2017).

Protein Expression and Localization

Protein expression was assessed by endogenous *GFP* tagging of the three *P. berghei* genes *via* double crossover homologous

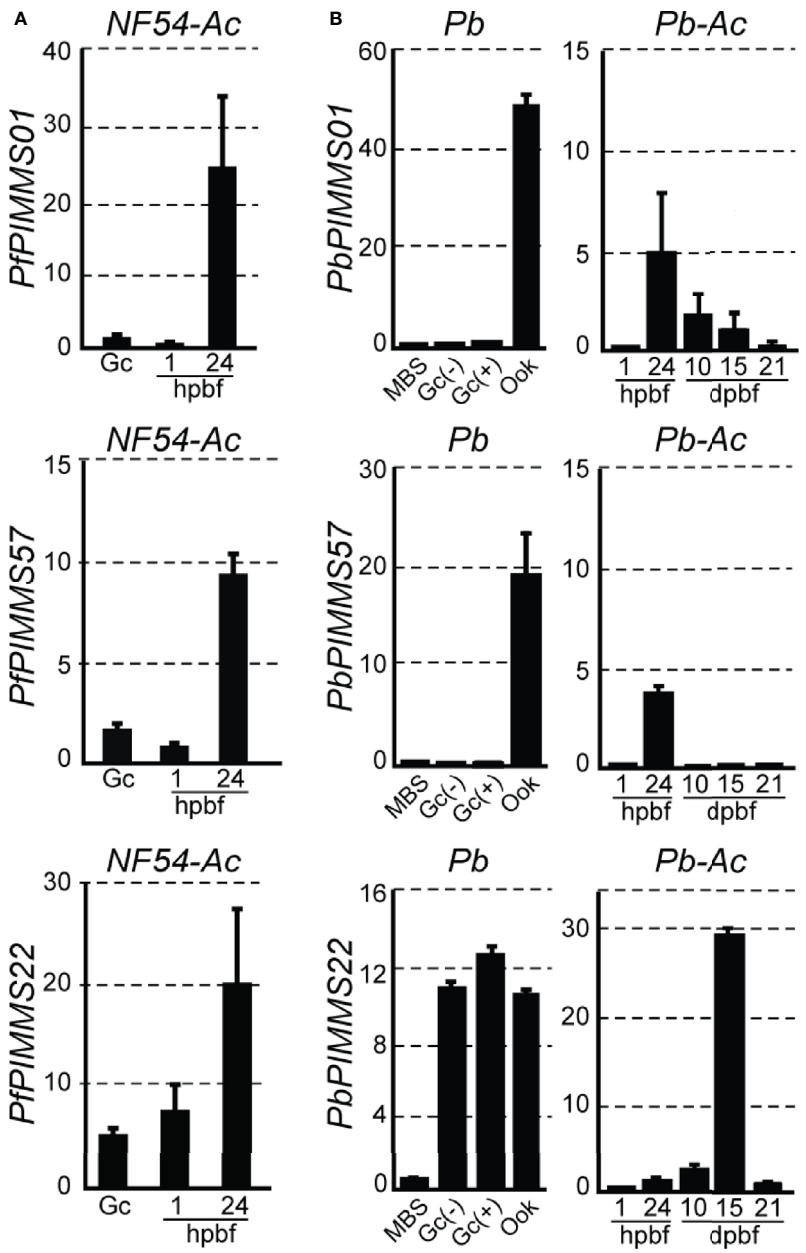

FIGURE 1 | *PIMMS01*, *PIMMS57*, and *PIMMS22* transcriptional profiles. **(A)** Relative abundance of *PfPIMMS01*, *PfPIMMS57*, and *PfPIMMS22* transcripts in purified *P. falciparum in vitro* cultured gametocytes, and *A. coluzzii* mosquito infected midguts at 1 and 24 hpbf, as determined by qRT-PCR in *NF54* parasite populations and normalized against the Arginyl-tRNA synthetase. **(B)** Relative abundance of *P. berghei PIMMS01*, *PbPIMMS57*, and *PbPIMMS22* transcripts in purified blood stages and *in vitro* produced ookinetes, and in *A. coluzzii* mosquito stages, as determined by qRT-PCR in the *c507* line and normalized against the constitutive expressed *GFP*. In all panels. each bar is the average of three biological replicates. Error bars indicate SEM. MBS, mixed blood stages; Gc, gametocytes; Gc(+), activated gametocytes; Gc(-), non-activated gametocytes; Ook, ookinetes; hpbf, hours post blood feeding; dpbf, days post blood feeding.

recombination in the ANKA 2.34 line. The generated transgenic parasites were named *c01::gfp*, *c57::gfp*, and *c22::gfp* (**Figure S5**). *P. berghei PIMMS01* and *PIMMS57* genes were also terminally tagged with the 3xHA (hemagglutinin) tag in the *c507* line, and transgenic parasites were named *c01::3xha* and *c57::3xha* (**Figure S6**). We also generated rabbit polyclonal antibodies raised against peptides of the deduced proteins in both *P. berghei* and *P. falciparum*. Of all antibodies, those that produced data and are analyzed below were: α-Pfc01, PfPIMMS01 peptide aa 72-86; α-Pbc57, PbPIMMS57 peptide aa 48-62; and α-Pfc57, PfPIMMS57 peptide aa 111–125.

Mosquito stage development of transgenic GFP-tagged *P. berghei* lines was assessed by counting midgut sporozoite numbers 15 dpbf. Amongst the three transgenic parasites, only

c22::gfp produced wild type (wt) number of midgut sporozoites (**Table S1**). Lines *c01::gfp* and *c57::gfp* yielded severely reduced sporozoite numbers, suggesting that insertion of GFP compromises the function of the two proteins. Similar to their GFP-tagged counterpart and concomitant gene knockout (see next section) parasite lines, both HA-tagged transgenic lines, showed severely reduced oocyst numbers compared to the *c507* reference parasite, as assessed by counting oocyst numbers 8 dpbf (**Table S2**). This phenotype suggests that insertion of the 3xHA tag compromises the function of the two proteins.

PIMMS01 Expression and Localization

Western blot analysis using an α-GFP antibody on the non-functional *c01::gfp* line confirmed high levels of PbPIMMS01::GFP fusion protein at the expected molecular weight (**Figure 2A**). The protein was found to be highly expressed in mature ookinetes of the *c01::gfp* line and be absent from MBS or gametocytes or any stage of the *ANKA 2.34* background parasite. Similarly, western blot analysis on the *c01::3xha* transgenic line using an α-HA antibody confirmed expression of the PbPIMMS01::3xHA fusion protein in the ookinete at the expected molecular weights and absence from gametocytes (**Figure 2B**). The protein was only detected in the Triton X-100 soluble fraction suggesting that it is not membrane associated.

Despite the strong evidence that the PbPIMMS01 GFP- and HA-tagged proteins are non-functional, these are still likely to be localised correctly. IFAs on the developmentally compromised *c01::gfp* and *c01::3xha* transgenic lines revealed strong cytoplasmic localization of both PbPIMMS01::GFP and PbPIMMS01::3xHA (**Figure 2C**), which indicates that the protein may be stuck in a secretory pathway and suggests that the native polypeptide may be associated with the ookinete outer membrane especially during invasion. Peptide antibodies raised against *P. berghei* PIMMS01 did not work in western blots and IFAs.

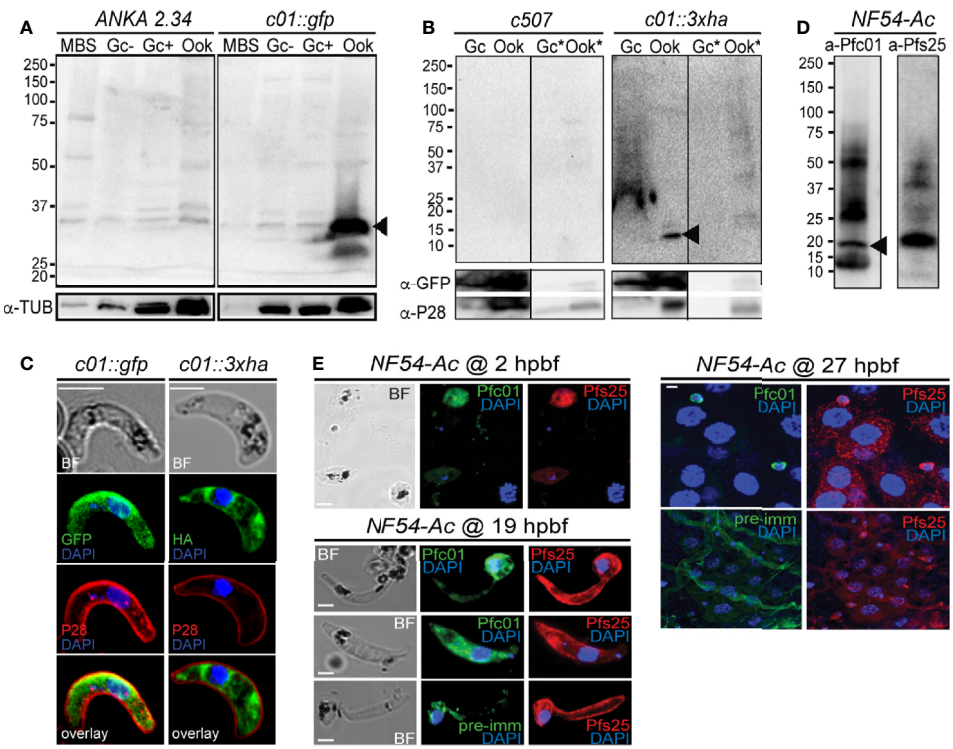

FIGURE 2 | PIMMS01 protein expression and localization. **(A)** Western blot analysis using α-GFP antibody on whole cell lysates of *P. berghei c01::gfp* parasites. The PbPIMMS01::GFP fusion protein band is indicated with a black arrowhead. The ANKA *2.34* parental parasite line was used as a negative control. Tubulin was used as a loading control. MBS, mixed blood stages; Gc(-), non-activated gametocytes; Gc(+), activated gametocytes; Ook, ookinetes. **(B)** Western blot analysis using the α-HA antibody on Triton X-100 soluble lysates of *in vitro* gametocyte (Gc) and ookinetes (Ook) and Triton X-100 insoluble lysates (Gc*, Ook*) of *c01::3xha*. The *c507* reference line (left panel) was used as a negative control. PbPIMMS01::HA fusion protein band is indicated with a black arrowhead. GFP and P28 were used as a loading and a stage specific control, respectively. **(C)** Immunofluorescence assays on ookinetes of PIMMS01 tagged with GFP (left panel) and 3xHA (right panel) stained with α-GFP or α-HA (green), respectively, as well as with the ookinete surface α-P28 (red). DNA was stained with DAPI. Images are de-convoluted projections of confocal stacks. BF, bright field; Scale bars, 5 μm. **(D)** Western blot analysis using α-Pfc01 antibody on whole cell lysates of *coluzzii* midguts at 22 h post blood feeding (hpbf). The PfPIMMS01 protein band is indicated with a black arrowhead. Tubulin was used a loading control for Gc and Sch while Pfs25 was used for 22 hpbf. **(E)** Immunofluorescence assays of *P. falciparum* NF54 parasites in mosquito blood bolus at 2 hpbf, ookinetes in mosquito blood bolus at 19 hpbf and ookinetes traversing the mosquito midgut epithelium at 27 hpbf, stained with α-Pfc01 (green) and the female gamete/zygote/ookinete α-Pfs25 (red) antibodies. Pre-immune (pre-imm) serum was used as negative control. DNA was stained with DAPI. Pre-immune serum was used as a negative control. BF, bright field; hpbf, hours post blood feeding. Scale bars, 5 μm.

In *P. falciparum*, the α-Pfc01 antibody detected a band of about 20 kDa (predicted molecular weight of PfPIMMS01 is 19 kDa) in *A. coluzzii* midguts infected 22 h earlier with *P. falciparum* NF54 (**Figure 2D**). This band was not detected in NF54 cultured schizonts or gametocytes (**Figure S7**). In indirect immunofluorescence assays (IFAs) using the α-Pfc01 antibody, PfPIMMS01 was detected in gametes/early zygotes found in the blood bolus 2 hpbf, ookinetes in the mosquito blood bolus 19 hpbf, and ookinetes crossing the mosquito midgut epithelium (**Figure 2E**). Its localization varied from cytoplasmic in early developmental stages, mostly stages III and IV of the ookinete development, to totally peripheral in mature, midgut-crossing ookinetes.

PIMMS57 Expression and Localization

Using the non-functional *c57::gfp* parasite line and the α-GFP antibody in western blot analysis, high levels of the PbPIMMS57::GFP fusion protein were detected in mature ookinetes, at the expected molecular weight of 117 kDa (**Figure 3A**). This band was not detected in MBS or gametocytes or in the *ANKA 2.34* background parasite line. Similarly, western blot analysis using the *c57::3xha* transgenic line and the α-HA antibody confirmed expression of the PbPIMMS57::3xHA protein in the ookinete at the expected molecular weight and its absence from gametocytes (**Figure 3B**). The protein was mostly detected in the Triton insoluble fraction, indicating membrane association. No band was detected in the *c507* reference line.

To validate the ookinete expression of PbPIMMS57, the α-Pbc57 peptide antibody was utilized. In westerns, the α-Pbc57 antibody detected in ookinetes a band at about 90 kDa, close to the predicted molecular weight of PbPIMMS57. This band was not seen in MBS, gametocytes and the control *Δc57* (see below) knockout parasite line (**Figure 3C**). Fractionation assays revealed that, in ookinetes, PbPIMMS57 is mostly found in the Triton X-100 insoluble fraction with low amounts also seen in the Triton X-100 soluble fraction (**Figure 3D**), suggesting that Pbc57 is membrane associated. These results agree with the prediction of transmembrane domains in this protein. The α-Pbc57 peptide antibody did not work in IFAs.

IFAs on the developmentally compromised *c57::gfp* and *c57::3xha* transgenic lines revealed cytoplasmic localization of the PbPIMMS57::GFP and PbPIMMS57::3xHA fusion proteins with bias for the ookinete convex side, especially for the former, pointing to a possible involvement of the protein with ookinete motility or invasion machinery (**Figure 3E**). However, given that both types of fusions lead to developmentally compromised parasites, these data must be interpreted with caution.

Similar analysis in *P. falciparum* using the α-Pfc57 peptide antibody detected a clear band albeit of lower-than-expected molecular weight in western blots of midgut homogenates of *A. coluzzii* mosquitoes infected 22 h earlier with *P. falciparum* NF54 cultured gametocytes (**Figure 3F**). This in conjunction with additional low molecular weight bands could be attributed to degradation in the highly proteolytic environment of the midgut blood bolus. In IFAs, the α-Pfc57 antibody showed that PfPIMMS57 is localized in the cytoplasm of gametes/early zygotes and intermediate ookinete developmental stages (mostly stages III and IV) obtained from the midgut blood bolus at 2 and 19 hpbf, respectively, with their distribution extending to the ookinete periphery (**Figure 3G**). Although it is difficult to decipher a clear membrane distribution of the signal, apparent similarities with the Pfs25 signal in the ookinete periphery makes a membrane-associated localization of PfPIMMS57 highly probable.

PIMMS22 Expression and Localization

Western blot analysis using the *c22::gfp* transgenic parasite line and α-GFP antibody revealed high levels of the PbPIMMS22::GFP fusion protein in ookinete and oocyst derived sporozoites, at the expected molecular weight of 71 kDa (**Figure 4A**). This band was not detected in the *ANKA 2.34* background parasite line. IFAs on the *c22::gfp* parasites allowed us to analyze the sub-cellular localization of the fusion protein. In Triton X-100 permeabilized blood stage gametocytes, PbPIMMS22::GFP was found to be localized on the cell periphery with the majority of the protein localizing in the cytoplasm (**Figure 4B**). Non-Triton X-100 permeabilized blood stage gametocytes are visibly less fluorescent than their Triton X-100 permeabilized counterparts. In Triton X-100 permeabilized *in vitro* ookinetes, PbPIMMS22::GFP was clearly observed on the ookinete periphery, a result that is inconsistent with the predicted absence of a signal peptide or transmembrane domain (**Figure 4C**). Additional staining on non-Triton X-100 permeabilized ookinetes show some peripheral signal albeit much weaker than its Triton X-100 permeabilized counterpart suggesting that PbPIMMS22::GFP is mainly localized on the inner surface of the ookinete and not on the plasma membrane. IFAs on *in vivo* midgut epithelium invading ookinetes at 26 hpbf also show surface localization of PbPIMMS22::GFP (**Figure 4D**). In midgut sporozoites, PbPIMMS22::GFP is found on the surface of both Triton X-100 and non-Triton X-100 permeabilized sporozoites (**Figure 4E**).

Generation and Phenotypic Analysis of *P. berghei* Mutant Parasites

Genetically modified *c507 P. berghei* lines, designated *Δc01*, *Δc57*, and *Δc22*, were generated by replacing most of the coding regions of *PbPIMMS01*, 57, and 22 with a modified *Toxoplasma gondii* pyrimethamine resistance (TgDHFR) expression cassette, respectively (**Figures S8A–C**). Integration of the disruption cassette and generation of clonal lines was confirmed by PCR and pulse field gel electrophoresis (**Figures S8D–E**).

Male gametogenesis in all three knockout parasite lines was assessed by counting exflagellation centers and found to be comparable to that of the *c507* parental line (**Figure 5A**). The macrogamete (female gamete) to ookinete conversion rates for all knockout lines were also comparable to that of the *c507* parental reference line (**Figure 5B**). These two datasets indicated that gametocyte-ookinete development is not affected in any of these knockout parasite lines.

Next, we assessed the ability of the knockout lines to complete further developmental steps in *A. coluzzii* mosquitoes that were fed on mice each infected with a knockout parasite line or the

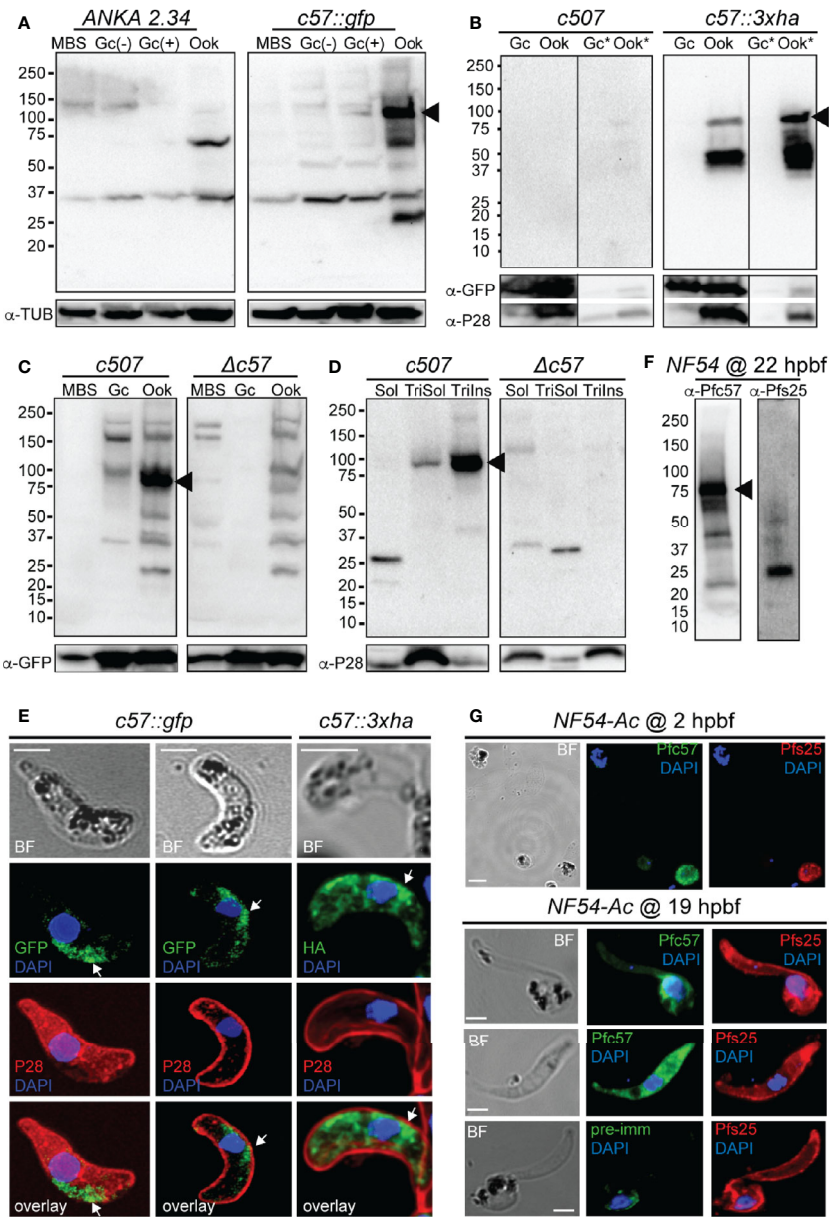

FIGURE 3 | PIMMS57 protein expression and localization. **(A)** Western blot analysis using α-GFP antibody on whole cell lysates of the *P. berghei c57::gfp* parasites. The PbPIMMS57::GFP fusion protein band is indicated with a black arrowhead. The *ANKA 2.34* parental parasite was used as a negative control. Tubulin was used a loading control. MBS, mixed blood stages; Gc(-), non-activated gametocytes; Gc(+), activated gametocytes; Ook, ookinetes. **(B)** Western blot analysis using the α-HA antibody on Triton X-100 soluble lysates of *in vitro* gametocyte (Gc) and ookinetes (Ook) and Triton X-100 insoluble lysates (Gc*, Ook*) of *c57::3xha*. The *c507* reference line (left panel) was used as a negative control. PbPIMMS57::HA fusion protein band is indicated with a black arrowhead. GFP and P28 were used as a loading and a stage specific control, respectively. **(C)** Western blot analysis using the α-Pbc57 peptide antibody on whole cell lysates of MBS, Gc, and ookinetes of the *c507* parasite line. The PbPIMMS57 protein band is indicated with a black arrowhead. *Δc57* parasites were used as a negative control. GFP was used as a loading control. **(D)** Western blot analysis using the α-Pbc57 antibody on fractionated *in vitro* ookinetes. The PbPIMMS57 protein band is indicated with a black arrowhead. *Δc57* ookinetes were used as a negative control. P28 was used as a loading control. Soluble (Sol), Triton X-100 soluble (TriSol) and Triton X-100 Insoluble (TriInso) fractions are shown. **(E)** Immunofluorescence assays on ookinetes of PbPIMMS57 tagged with GFP and 3xHA stained with α-GFP or α-HA (green; white arrows) as well as with the ookinete surface α-P28 (red). DNA was stained with DAPI. Staining of the *c507* and *ANKA 2.34* parental parasites were used as negative controls for the HA and GFP staining, respectively. Images are de-convoluted projections of confocal stacks. BF, bright field; Scale bars, 5 μm. **(F)** Western blot analysis using α-Pfc57 antibody on whole cell lysates of *A. coluzzi* midguts at 22 hpbf. The PfPIMMS57 protein band is indicated with a black arrowhead. Pfs25 was used as a loading and stage specific control for 22 hpbf. **(G)** Immunofluorescence assays of *P. falciparum* NF54 parasites in mosquito blood bolus at 2 hpbf (top) and ookinetes in mosquito blood bolus at 19 hpbf (bottom), stained with α-Pfc57 (green) and the female gamete/zygote/ookinete α-Pfs25 (red) antibodies. Pre-immune serum was used as a negative control. DNA was stained with DAPI. Staining with pre-immune serum was used as a negative control. BF, bright field; Scale bars, 5 μm.

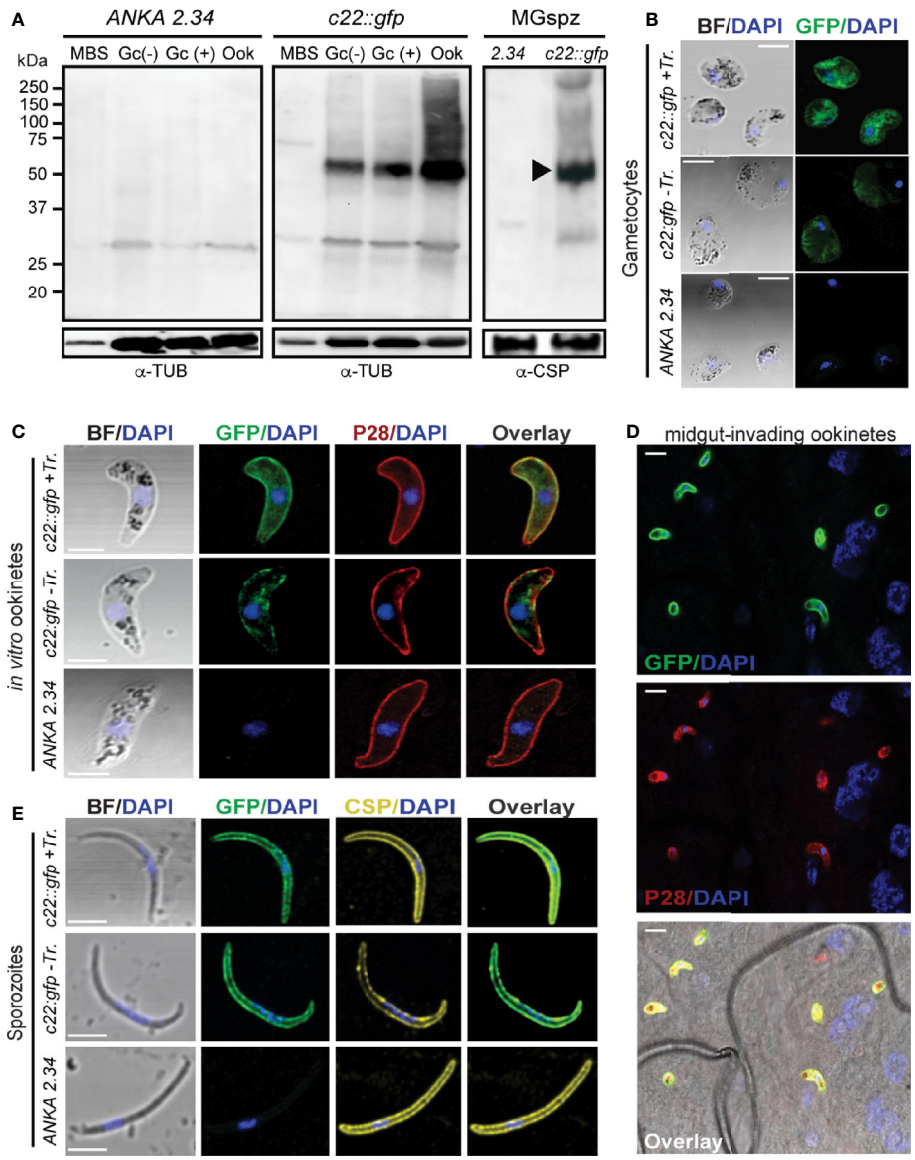

FIGURE 4 | PIMMS22 protein expression and localization. **(A)** Western blot analysis using α-GFP antibody on whole cell lysates of *P. berghei c22::gfp* parasites. The PbPIMMS22::GFP fusion protein band is indicated with a black arrowhead. The *ANKA 2.34* parental parasite line was used as a negative control. Tubulin was used a loading control in all parasite stages except from midgut sporozoites where CSP was used. MBS, mixed blood stages; Gc(-), non-activated gametocytes; Gc(+), activated gametocytes; Ook, ookinetes; MgSpz, midgut sporozoites. Immunofluorescence assays of *c22::gfp* blood stage gametocytes treated or not treated with Triton X-100 (Tr.) **(B)**, *in vitro* ookinetes **(C)**, ookinetes traversing the mosquito midgut epithelium at 26 hpbf **(D)** and midgut sporozoites at 15 dpbf **(E)**, stained with α-GFP (green), ookinete surface α-P28 (red), or sporozoite surface α-PbCSP (yellow) antibodies. DNA was stained with DAPI. Staining of the *2.34 wt* parental parasite was used as a negative control. Images are de-convoluted projections of confocal stacks. BF, bright field; Scale bars in **(A–C, E)** 5 μm; Scale bars in **(D)** 10 μm.

c507 parental line. Significant decreases in the numbers of oocysts present in the mosquito midguts at 8 dpbf were observed for all the three knockout lines compared to *c507* (**Figure 5C**, **Table S3**), indicating that ookinete to oocyst development is defective all three lines.

The ability of knockout mutant parasites to produce sporozoites was assessed by counting midgut and salivary gland sporozoites 15 and 21 dpbf, respectively. Compared to the *c507* reference line, significant decreases in midgut and salivary gland sporozoite numbers were observed for all three knockout lines (**Figure 5D**, **Table S4**). None of the three knockout parasites could be transmitted back to mice through mosquito bites carried out 21 dpbf, in all cases leading to termination in malaria transmission (**Table S4**).

Parasites displaying normal ookinete development but showing a defect during the ookinete to oocyst developmental

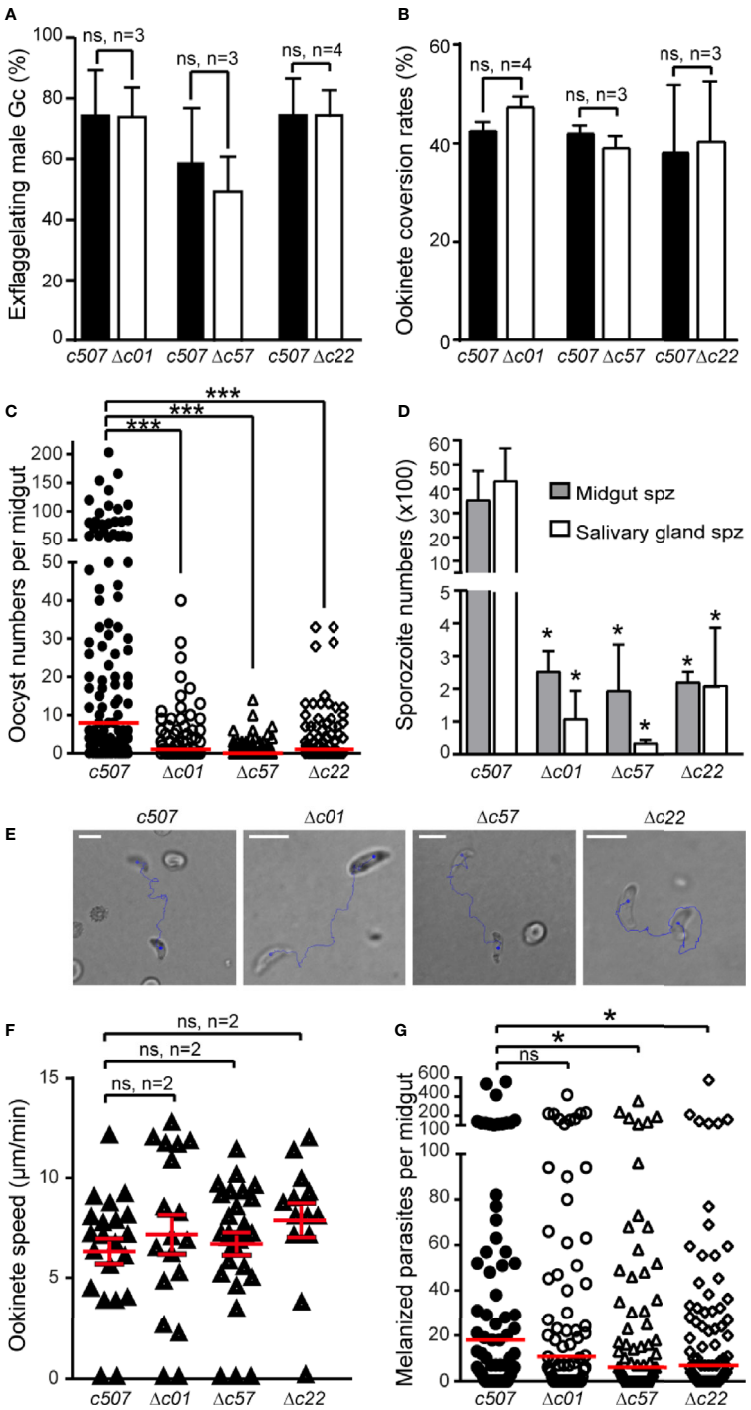

FIGURE 5 | Phenotypic analysis of *P. berghei* Δc01, Δc57, and Δc22 knockout mutants. Male gametocyte activation measured as percentage of exflagellating male gametocytes **(A)** and percentage of female gamete conversion to ookinetes **(B)** of the *c507* reference and knockout parasites. ns, not significant; n, number of biological replicates. Error bars indicate SEM. **(C)** *Δc01*, *Δc57*, and *Δc22* oocyst development at 8 dpbf in *A. coluzzii*. Red horizontal lines indicate median. ***P < 0.0001 using Mann-Whitney test. **(D)** *Δc01*, *Δc57*, and *Δc22* midgut (MgSpz) and salivary gland sporozoite (SgSpz) numbers at 15 and 21 dpbf respectively in *A. coluzzii*. **(E)** Representative instances of *c507* reference and *Δc01*, *Δc57*, and *Δc22* knockout ookinetes from gliding motility assays. Blue lines show ookinete gliding traces captured for 2 min. Note the gliding helical motility that is characteristic of *wt* ookinete observed in these ookinetes. Scale bars, 10 µm. **(F)** Speed of *c507* reference and knockout ookinetes measured from time-lapse microscopy. ns, not significant; n, number of biological replicates. Red horizontal lines indicate mean and error bars show SEM. **(G)** Melanized ookinete numbers in *CTL4* kd *A. coluzzii* infected with *c507* reference and knockout parasite lines. Red lines indicate median; ns, not significant; *P < 0.05 using Mann-Whitney test.

transition could be a result of a defect in ookinete motility and/or a midgut invasion and traversal. To investigate for motility defects, speed measurements of ookinetes were carried out. *Δc01*, *Δc57*, and *Δc22 in vitro* cultured ookinetes exhibited movements with speed not significantly different to that of the *c507 wt* ookinete (**Figures 5E, F** and **Movies S1–8**).

Next, we investigated for invasion defects by carrying out mosquito infections in *A. coluzzii* mosquitoes silenced for C-type lectin *CTL4* using RNA interference. Knockdown of *CTL4* leads to melanization of ookinetes immediately after they have traversed the midgut epithelium and been exposed to the haemocoel in the basal sub-epithelial space thereby providing a means to visualize and enumerate ookinetes that successfully traverse the midgut epithelium. The number of melanized *Δc01* parasites was not significantly different to the *c507* reference parasite line (p=0.3971) (**Figure 5G**, **Table S5**), suggesting that *Δc01* ookinetes can readily invade and traverse the midgut epithelium but are defective at the ookinete-to-oocyst transition stage resulting in the significant decrease in the oocyst numbers observed. However, compared to the *c507* parasite, significantly lower numbers of melanized *Δc57* (p=0.0337) and *Δc22* (p= 0.0487) ookinetes was observed, indicating that *Δc57* and *Δc22* ookinetes are defective in midgut invasion. However, the documented reduction in midgut invasion capacity of *Δc57* and *Δc22* ookinetes cannot fully explain the massive reduction in oocyst numbers, suggesting that like *Δc01*, *Δc57*, and *Δc22* are also defective for ookinete to oocyst transition.

The ookinete to oocyst developmental transition potential of *Δc01*, *Δc57*, and *Δc22* ookinetes was further assessed by bypassing the midgut epithelium entirely and injecting these ookinetes into the haemocoel of *A. coluzzii* mosquitoes. By skipping midgut epithelium invasion, *Δc57* ookinetes can transform to oocysts that produce salivary gland sporozoites at numbers comparable to those of the *c507* reference line (**Table 1**). These sporozoites could also be transmitted to mice in transmission experiments. In this experiment, while the mean *Δc01* salivary gland sporozoite number was significantly lower than the *c507* parasite, high *Δc01* salivary gland sporozoite numbers observed in some replicates resulted in transmission to mice while lower salivary gland sporozoite numbers resulted in no transmission suggesting that *Δc01* transmission efficiency is dependent on sporozoite numbers. For the *Δc22* parasite line, the significantly smaller number of salivary gland sporozoites produced were still not able to initiate transmission (**Table 1**).

DISCUSSION

To establish a successful infection in the mosquito, *Plasmodium* parasites must within 24 h of uptake into the mosquito midgut, fertilize to form ookinetes that have to invade and traverse the midgut epithelium and form oocysts on the basal side of the epithelium. The molecular processes driving the *Plasmodium* ookinete to oocyst developmental transition remain relatively under characterized. In this study, we have identified PIMMS01, PIMMS57, and PIMMS22 as being important factors for ookinete to oocyst transition and essential for malaria transmission. While gametocyte to ookinete development is not affected in the mutant knockout parasites, they all display severe defects in oocyst formation. The midgut invasion capabilities of these knockout parasites suggest that other factors come into play to block this ookinete to oocyst transitional step. The decrease in number of subsequent sporozoites eventually result in an abolishment of malaria transmission. The observed reduction in sporozoites may not be merely an effect of the oocyst defective phenotype. Since the gene knock out system used in this study is not regulatable, gene functions cannot be assessed past the point of their initial essential action. This means that additional functions of these genes past the ookinete to oocyst developmental transition in oocyst and sporozoite development and in malaria transmission cannot be ruled out. This is especially true for *PIMMS22* which shows peak transcript expression during oocyst sporozoite development and its concomitant protein is highly expressed also at this stage.

Amongst genes reported to function during the ookinete to oocyst developmental transition, an overwhelming defect before and at entry into the midgut is observed. The ookinete to oocyst defective mutants of *CTRP*, *PPKL*, *CDPK3*, *GCβ*, *DHHC3*, *OMD*, and the alveolins *IMC1 b* and *h* are defective in ookinete motility (Dessens et al., 1999; Siden-Kiamos et al., 2006; Tremp et al., 2008;

TABLE 1 | Sporozoite development and infectivity upon ookinete injection in the haemocoel.

	Salivary gland sporozoites		Infectivity to mice
Parasite	**Mean**	**SEM**	
c507	2,907 (3036;1888;4850;2842;2175;2650)	389	12/12 (2/2;2/2;ND;3/3;3/3;2/2)
Δc01	973 (582;683;492;2653;824;603)	310	3/12 (0/2;0/2;ND;2/3;1/3;0/2)
Δc57	3,460 (2328;6955;3864;2105;3050;2458)	680	12/12 (2/2;2/2;ND;3/3;3/3;2/2)
Δc22	501 (995;216;560;586;396;252)	107	0/12 (0/2;0/2;ND;0/3;0/3;0/2)

Mean salivary gland sporozoite numbers 21 days post A. coluzzii haemocoel inoculation with ookinetes, obtained from six biological replicates. Data from independent biological replicates are presented in brackets and are separated with semicolons. SEM represents the standard error of the mean. Infectivity of sporozoites was assessed by infected mosquito bite back experiments of C57/BL6 mice at day 21 post haemocoel inoculation. Parasitemia was monitored for 14 days post mosquito bite and the ratio of infected to all mice used is shown. ND, not determined.

Moon et al., 2009; Guttery et al., 2012; Volkmann et al., 2012; Hopp et al., 2016; Currà et al., 2019), *CHT* mutants are defective in ookinete penetration of the peritrophic matrix (Dessens et al., 2001) and *P25*, *P28*, *SOAP*, *PPLP3*, *PPLP4*, *PPLP5*, *PSOP2*, *7*, and *9* and *Enolase* mutants are defective in ookinete midgut invasion (Tomas et al., 2001; Dessens et al., 2003; Kadota et al., 2004; Ecker et al., 2007; Ecker et al., 2008; Ghosh et al., 2011; Deligianni et al., 2018). Only null mutants of *CelTOS*, *MISFIT*, *PPM5*, *AP2-O4*, *PIMMS2*, and *PIMMS43* have been identified to have a midgut invasion independent phenotype with their null mutant ookinetes able to invade the midgut epithelium but have problems in establishing an oocyst infection (Kariu et al., 2006; Bushell et al., 2009; Guttery et al., 2014; Modrzynska et al., 2017; Ukegbu et al., 2017; Ukegbu et al., 2020). Cell traversal upon midgut invasion is not compromised in *Δc01* mutant ookinetes like that observed in the oocyst formation defective *PIMMS2* and *CelTOS* mutants (Kariu et al., 2006; Ukegbu et al., 2017), as melanized *Δc01* mutant ookinetes must have traverse the midgut epithelium to reach the basal lamina where the melanization response occurs (Osta et al., 2004). In the *MISFIT* and *PPM5* mutants, the reduced number of oocysts formed are smaller and fail to complete sporulation (Bushell et al., 2009; Guttery et al., 2014). Our observations show that the small number of oocysts formed by the *Δc01*, *Δc57*, and *Δc22* parasites are morphologically normal with sizes comparable to *wt* oocysts suggesting these proteins function differently from MISFIT and PPM5.

The observation that parasite development is rescued when *Δc57* ookinetes bypass the epithelium, suggests that the viability of these ookinetes and their inherent ability to differentiate into the oocyst is not affected. This implies that the ookinete to oocyst developmental transition is only impaired when ookinetes must cross the midgut wall. This type of phenotype has been previously observed in the *SHLP1* mutant (Patzewitz et al., 2013). There, it has been suggested that developmental defects in the ookinete such as in microneme deficiency, results in a block in oocyst formation following midgut invasion which is restored if mutant ookinetes are injected into the haemocoel (Patzewitz et al., 2013). However, this may not be the case for *Δpbc57*, as ookinete microneme deficiency has been previously shown not to be essential for the ookinete transformation to oocyst (Bushell et al., 2009). Whether any ookinete morphological/developmental defects are involved with the seemingly dual phenotype of the *Δpbc57* parasite requires further investigation. Indeed, the ookinete injection experiment has shown that the reduced *Δc57* oocyst and salivary gland sporozoites obtained with the natural route of infection is a direct result of the reduced number of oocysts and not due to any additional function of PIMMS57 at the oocyst and sporozoite developmental stages.

The ookinete injection phenotypes of *Δc01* and *Δc22* indicate that the defective oocyst formation phenotypes are independent of midgut invasion suggesting that the viability of these ookinetes are overall affected *in vivo* in the mosquito. While the sporozoite numbers for *Δc01* and *Δc22* appeared to be higher than those obtained from the direct blood feeding, the observation that the sporozoite numbers produced, following injection, are on average lower than the *wt* parasite indicates that their development is still impaired. As it is impossible to accurately assess ookinete to oocyst transformation in this experiment (oocyst enumeration upon ookinete haemocoel injection is unreliable as oocysts are formed everywhere in the haemocoel-bathed tissues) (Paskewitz and Shi, 2005), it is possible that *Δc01* and *Δc22* ookinetes can transform to oocysts but the reduced sporozoite numbers are the result of impaired oocyst sporogony or defect at the transition of oocyst sporozoites to the salivary glands. As expected and has been previously observed (Churcher et al., 2017), *Δc01* salivary gland sporozoite numbers following ookinete injection significantly affects transmission. Finally, the observation that *Δc22* sporozoites produced following ookinete injection could still not be transmitted suggests putative additional functions of *PIMMS22* during this stage.

The observed impaired parasite development suggests putative roles of PIMMS01, PIMMS57, and PIMMS22 proteins in interaction with the midgut to either promote ookinete fitness or ookinete-to-oocyst differentiation. PIMMS01 and PIMMS57 are predicted to be secreted and membrane-bound, respectively, while PIMMS22 does not show any putative transmembrane domains but is clearly localized at the ookinete periphery, possibly the inner membrane complex. While the results showing that PIMMS01 and PIMMS57 are also localized at the ookinete periphery must be interpreted with caution, midgut crossing ookinetes show a clear peripheral localization of PIMMS01 and PIMMS57 has been previously also shown by others to localize on the ookinete surface (Zheng et al., 2016). All these are suggestive of a capability of these proteins to interact, directly or indirectly, with the midgut environment.

The mosquito midgut epithelium *via* effectors of the JNK pathway has been proposed to actively mark invading ookinetes for killing by the mosquito complement-like system (de Almeida Oliveira et al., 2012). The GPI-anchored ookinete surface protein Pfs47 has been suggested to protect *P. falciparum* ookinetes against attack by this system (Molina-Cruz et al., 2013), and we have previously shown that the ookinete surface protein PIMMS43 is also essential in protecting ookinetes by complement-like responses (Ukegbu et al., 2020). While PIMMS01, PIMMS57, and PIMMS22 may directly interact with the midgut, much like Pfs47 whose receptor in the midgut epithelium has been recently identified (Molina-Cruz et al., 2020) to promote ookinete survival, an alternative explanation is that loss of function of these proteins may bear a fitness cost on ookinetes. In the midgut, where oxidative stress is high due to the blood meal (Turturice et al., 2013) and *P. berghei* infection of the midgut has been shown to exacerbate the production of reactive oxygen species (ROS) (Molina-Cruz et al., 2008), ookinetes lacking such proteins are expected to be compromised.

A clue to the possible functions of these proteins is the presence of defining signatures in their amino acid sequences. Apart from the signal peptide, PIMMS01 is devoid of any other domains that could predict its putative function. The identification of putative PP1c binding motifs in *P. falciparum* PIMMS57 suggests that it may function through PP1. In eukaryotes, PP1 is essential for cell cycle progression (Bollen et al., 2009). The exact role of PP1 in *Plasmodium* has not been

deciphered yet due to its essentiality in asexual blood stages (Guttery et al., 2014). Nevertheless, the identification of several PP1c interacting proteins that can modulate the activity of this enzyme (Daher et al., 2006; Fréville et al., 2012; Hollin et al., 2016), including the gametocyte exported protein GEXP15 that is important for both blood stage development and oocyst formation (Hollin et al., 2019), could suggest additional and important roles of PP1-like activity during sexual development in the mosquito. The putative physical interaction between PfPIMMS57 and PfPP1c remains to be confirmed in functional interaction studies. The lack of PP1c binding motifs in the rest of the PIMMS57 orthologs suggest that these may function independently of PP1.

Like PIMMS01, PIMMS22 lacks any domain that could predict its putative function. Its localization and putative interacting partners could however point to the function of this protein. While we have shown PbPIMMS22 to localize at the ookinete periphery and putatively on the inner surface of the ookinete, how it achieves this without a predicted signal peptide or transmembrane domain remains to be investigated. A hypothesis is that PIMMSS22 could be interacting with other proteins located on the inner surface of the ookinete. This theory is supported by the observation that in *P. yoelii* sporozoites, PIMMS22 is found in a complex with several alveolin proteins of the subpellicular network and glideosome-associated proteins of the inner membrane complex (Muñoz et al., 2017). This interaction with the alveolin proteins could also be extended to the ookinete as some members of the SPN (subpellicular network) and IMC (inner membrane complex) are conserved and utilized across the ookinete and sporozoite stages (Morrissette and Sibley, 2002; Santos et al., 2009; Al-Khattaf et al., 2015). Proteins associated with the SPN and IMC are mostly linked to functions relating to cell motility (Tremp and Dessens, 2011; Volkmann et al., 2012; Frénal et al., 2017); however, this is not the case for PIMMS22 as no defect in ookinete motility is observed. Any putative functional interactions between PIMMS22 and proteins associated with the SPN and IMC will have to be further investigated in co-localization and pull-down experiments.

Despite the unknown exact molecular mechanisms that PIMMS01, PIMMS57, and PIMMS22 utilize to promote the ookinete to oocyst developmental transition, these proteins are good targets for the development of transmission blocking interventions. Two approaches are envisaged. First, and like the current frontline transmission blocking vaccine candidates Pfs230, Pfs48/45, and Pfs25 that target gametocyte/ookinete surface proteins, antibodies against these proteins can be generated in the human serum which, when ingested by mosquitoes together with gametocytes, interfere with the function of these proteins and block transmission to a new host (Nikolaeva et al., 2015). While this approach has been hampered by the difficulty in recombinant expression of full length and correctly folded *Plasmodium* proteins in a high throughput manner (Nikolaeva et al., 2020), the identification of small proteins that can be easily expressed such as PIMMS01 bears hopes for this approach. An alternative approach includes the creation of genetically modified mosquitoes which express single-chain antibodies that bind these proteins conferring refractoriness to infection and eventual blocking of malaria transmission (Isaacs et al., 2011; Gantz et al., 2015). These transgenes can be spread within wild mosquito populations through gene drive mechanisms (e.g. CRISPR/Cas9) leading to sustainable local malaria elimination (Carballar-Lejarazú and James, 2017).

DATA AVAILABILITY STATEMENT

The original contributions presented in the study are included in the article/**Supplementary Material**. Further inquiries can be directed to the corresponding author.

ETHICS STATEMENT

The animal study was reviewed and approved by Animal Welfare and Ethical Review Body (AWERB), Imperial College London.

AUTHOR CONTRIBUTIONS

Conceptualization, DV. Methodology, CU and DV. Formal analysis, CU and DV. Investigation, CU and DV. Resources, GC and DV. Data curation, CU and DV. Writing paper, CU, GC, and DV. Supervision, DV. Project administration, GC and DV. Funding acquisition, GC and DV. All authors contributed to the article and approved the submitted version.

FUNDING

The work was funded by a Wellcome Trust Investigator Award (107983/Z/15/Z) to GC, a Wellcome Trust Project grant (093587/Z/10/Z) to GC and DV, and a Bill and Melinda Gates Foundation grant (OPP1158151) to GC.

ACKNOWLEDGMENTS

The authors thank Temesgen M. Kebede for assistance with *P. berghei* culturing and mosquito rearing, Julia Cai for providing some *P. falciparum* NF54 RNA for qPCR assays, Maria Grazia Inghilterra for *P. falciparum* culturing and Rajeev Rai and Chrysanthi Taxiarchi for technical assistance with the ko constructs for the generation of the mutant parasites and for mosquito infections.

SUPPLEMENTARY MATERIAL

The Supplementary Material for this article can be found online at: https://www.frontiersin.org/articles/10.3389/fcimb.2021.634273/full#supplementary-material

REFERENCES

Akinosoglou, K. A., Bushell, E. S., Ukegbu, C. V., Schlegelmilch, T., Cho, J. S., Redmond, S., et al. (2015). Characterization of p lasmodium developmental transcriptomes in a nopheles gambiae midgut reveals novel regulators of malaria transmission. *Cell. Microbiol.* 17 (2), 254–268. doi: 10.1111/cmi.12363

Al-Khattaf, F. S., Tremp, A. Z., and Dessens, J. T. (2015). Plasmodium alveolins possess distinct but structurally and functionally related multi-repeat domains. *Parasitol. Res.* 114, 631–639. doi: 10.1007/s00436-014-4226-9

Armenteros, J. J. A., Tsirigos, K. D., Sønderby, C. K., Petersen, T. N., Winther, O., Brunak, S., et al. (2019). Signalp 5.0 improves signal peptide predictions using deep neural networks. *Nat. Biotechnol.* 37, 420–423. doi: 10.1038/s41587-019-0036-z

Barr, PJ, Green, KM, Gibson, HL, Bathurst, IC, Quakyi, IA, and Kaslow, DC (1991). Recombinant Pfs25 protein of Plasmodium falciparum elicits malaria transmission-blocking immunity in experimental animals. *J. Exp. Med.* 174 (5), 1203–1208. doi: 10.1084/jem.174.5.1203

Beetsma, A., van de Wiel, T. J., Sauerwein, R., and Eling, W. (1998). Plasmodium berghеianka: Purification of large numbers of infectious gametocytes. *Exp. Parasitol.* 88, 69–72. doi: 10.1006/expr.1998.4203

Bollen, M., Gerlich, D. W., and Lesage, B. (2009). Mitotic phosphatases: From entry guards to exit guides. *Trends Cell Biol.* 19, 531–541. doi: 10.1016/j.tcb.2009.06.005

Braks, J. A., Franke-Fayard, B., Kroeze, H., Janse, C. J., and Waters, A. P. (2006). Development and application of a positive–negative selectable marker system for use in reverse genetics in plasmodium. *Nucleic Acids Res.* 34, e39–e39. doi: 10.1093/nar/gnj033

Bushell, E. S., Ecker, A., Schlegelmilch, T., Goulding, D., Dougan, G., Sinden, R. E., et al. (2009). Paternal effect of the nuclear formin-like protein misfit on plasmodium development in the mosquito vector. *PLoS Pathog.* 5, e1000539. doi: 10.1371/journal.ppat.1000539

Carballar-Lejarazú, R., and James, A. A. (2017). Population modification of anopheline species to control malaria transmission. *Pathog. Global Health* 111, 424–435. doi: 10.1080/20477724.2018.1427192

Churcher, T. S., Sinden, R. E., Edwards, N. J., Poulton, I. D., Rampling, T. W., Brock, P. M., et al. (2017). Probability of transmission of malaria from mosquito to human is regulated by mosquito parasite density in naive and vaccinated hosts. *PLoS Pathog.* 13, e1006108. doi: 10.1371/journal.ppat.1006108

Costa, G., Gildenhard, M., Eldering, M., Lindquist, R., Hauser, A., Sauerwein, R., et al. (2018). Non-competitive resource exploitation within mosquito shapes within-host malaria infectivity and virulence. *Nat. Commun.* 9, 1–11. doi: 10.1038/s41467-018-05893-z

Currà, C., Kehrer, J., Lemgruber, L., Silva, P. A., Bertuccini, L., Superti, F., et al. (2019). Malaria transmission through the mosquito requires the function of the omd protein. *PLoS One* 14, e0222226. doi: 10.1371/journal.pone.0222226

Daher, W., Browaeys, E., Pierrot, C., Jouin, H., Dive, D., Meurice, E., et al. (2006). Regulation of protein phosphatase type 1 and cell cycle progression by pflrr1, a novel leucine-rich repeat protein of the human malaria parasite plasmodium falciparum. *Mol. Microbiol.* 60, 578–590. doi: 10.1111/j.1365-2958.2006.05119.x

de Almeida Oliveira, G., Lieberman, J., and Barillas-Mury, C. (2012). Epithelial nitration by a peroxidase/nox5 system mediates mosquito antiplasmodial immunity. *Science* 335, 856–859. doi: 10.1126/science.1209678

Deligianni, E., Silmon de Monerri, N. C., McMillan, P. J., Bertuccini, L., Superti, F., Manola, M., et al. (2018). Essential role of plasmodium perforin-like protein 4 in ookinete midgut passage. *PLoS One* 13, e0201651. doi: 10.1371/journal.pone.0204083

Dessens, J. T., Beetsma, A. L., Dimopoulos, G., Wengelnik, K., Crisanti, A., Kafatos, F. C., et al. (1999). Ctrp is essential for mosquito infection by malaria ookinetes. *EMBO J.* 18, 6221–6227. doi: 10.1093/emboj/18.22.6221

Dessens, J. T., Mendoza, J., Claudianos, C., Vinetz, J. M., Khater, E., Hassard, S., et al. (2001). Knockout of the rodent malaria parasite chitinase pbcht1 reduces infectivity to mosquitoes. *Infect. Immun.* 69, 4041–4047. doi: 10.1128/IAI.69.6.4041-4047.2001

Dessens, J. T., Sidén-Kiamos, I., Mendoza, J., Mahairaki, V., Khater, E., Vlachou, D., et al. (2003). Soap, a novel malaria ookinete protein involved in mosquito midgut invasion and oocyst development. *Mol. Microbiol.* 49, 319–329. doi: 10.1046/j.1365-2958.2003.03566.x

Dong, Y., Aguilar, R., Xi, Z., Warr, E., Mongin, E., and Dimopoulos, G. (2006). Anopheles gambiae immune responses to human and rodent plasmodium parasite species. *PLoS Pathog.* 2, e52. doi: 10.1371/journal.ppat.0020052

Ecker, A., Pinto, S. B., Baker, K. W., Kafatos, F. C., and Sinden, R. E. (2007). Plasmodium berghei: Plasmodium perforin-like protein 5 is required for mosquito midgut invasion in anopheles stephensi. *Exp. Parasitol.* 116, 504–508. doi: 10.1016/j.exppara.2007.01.015

Ecker, A., Bushell, E. S., Tewari, R., and Sinden, R. E. (2008). Reverse genetics screen identifies six proteins important for malaria development in the mosquito. *Mol. Microbiol.* 70, 209–220. doi: 10.1111/j.1365-2958.2008.06407.x

Frénal, K., Dubremetz, J.-F., Lebrun, M., and Soldati-Favre, D. (2017). Gliding motility powers invasion and egress in apicomplexa. *Nat. Rev. Microbiol.* 15, 645. doi: 10.1038/nrmicro.2017.86

Fréville, A., Landrieu, I., García-Gimeno, M. A., Vicogne, J., Montbarbon, M., Bertin, B., et al. (2012). Plasmodium falciparum inhibitor-3 homolog increases protein phosphatase type 1 activity and is essential for parasitic survival. *J. Biol. Chem.* 287, 1306–1321. doi: 10.1074/jbc.M111.276865

Gantz, V. M., Jasinskiene, N., Tatarenkova, O., Fazekas, A., Macias, V. M., Bier, E., et al. (2015). Highly efficient cas9-mediated gene drive for population modification of the malaria vector mosquito anopheles stephensi. *Proc. Natl. Acad. Sci.* 112, E6736–E6743. doi: 10.1073/pnas.1521077112

Ghosh, A. K., Coppens, I., Gårdsvoll, H., Ploug, M., and Jacobs-Lorena, M. (2011). Plasmodium ookinetes coopt mammalian plasminogen to invade the mosquito midgut. *Proc. Natl. Acad. Sci.* 108, 17153–17158. doi: 10.1073/pnas.1103657108

Guttery, D. S., Poulin, B., Ferguson, D. J., Szöőr, B., Wickstead, B., Carroll, P. L., et al. (2012). A unique p rotein p hosphatase with k elch-l ike domains (ppkl) in plasmodium modulates ookinete differentiation, motility and invasion. *PLoS Pathog.* 8, e1002948. doi: 10.1371/journal.ppat.1002948

Guttery, D. S., Poulin, B., Ramaprasad, A., Wall, R. J., Ferguson, D. J., Brady, D., et al. (2014). Genome-wide functional analysis of plasmodium protein phosphatases reveals key regulators of parasite development and differentiation. *Cell Host Microbe* 16, 128–140. doi: 10.1016/j.chom.2014.05.020

Habtewold, T., Povelones, M., Blagborough, A. M., and Christophides, G. K. (2008). Transmission blocking immunity in the malaria non-vector mosquito anopheles quadriannulatus species a. *PLoS Pathog.* 4, e1000070. doi: 10.1371/journal.ppat.1000070

Habtewold, T., Tapanelli, S., Masters, E. K., Hoermann, A., Windbichler, N., and Christophides, G. K. (2019). Streamlined smfa and mosquito dark-feeding regime significantly improve malaria transmission-blocking assay robustness and sensitivity. *Malaria J.* 18, 1–11. doi: 10.1186/s12936-019-2663-8

Hall, N., Karras, M., Raine, J. D., Carlton, J. M., Kooij, T. W., Berriman, M., et al. (2005). A comprehensive survey of the plasmodium life cycle by genomic, transcriptomic, and proteomic analyses. *Science* 307, 82–86. doi: 10.1126/science.1103717

Hollin, T., De Witte, C., Lenne, A., Pierrot, C., and Khalife, J. (2016). Analysis of the interactome of the ser/thr protein phosphatase type 1 in plasmodium falciparum. *BMC Genomics* 17, 246. doi: 10.1186/s12864-016-2571-z

Hollin, T., De Witte, C., Fréville, A., Guerrera, I. C., Chhuon, C., Saliou, J.-M., et al. (2019). Essential role of gexp15, a specific protein phosphatase type 1 partner, in plasmodium berghei in asexual erythrocytic proliferation and transmission. *PLoS Pathog.* 15, e1007973. doi: 10.1371/journal.ppat.1007973

Hopp, C. S., Balaban, A. E., Bushell, E. S., Billker, O., Rayner, J. C., and Sinnis, P. (2016). Palmitoyl transferases have critical roles in the development of mosquito and liver stages of plasmodium. *Cell. Microbiol.* 18, 1625–1641. doi: 10.1111/cmi.12601

Howick, V. M., Russell, A. J., Andrews, T., Heaton, H., Reid, A. J., Natarajan, K., et al. (2019). The malaria cell atlas: Single parasite transcriptomes across the complete plasmodium life cycle. *Science* 365, eaaw2619. doi: 10.1126/science.aaw2619

Isaacs, A. T., Li, F., Jasinskiene, N., Chen, X., Nirmala, X., Marinotti, O., et al. (2011). Engineered resistance to plasmodium falciparum development in transgenic anopheles stephensi. *PLoS Pathog.* 7, e1002017. doi: 10.1371/journal.ppat.1002017

Janse, C., and Waters, A. (1995). Plasmodium berghei: The application of cultivation and purification techniques to molecular studies of malaria parasites. *Parasitol. Today* 11, 138–143. doi: 10.1016/0169-4758(95)80133-2

Janse, C. J., Franke-Fayard, B., Mair, G. R., Ramesar, J., Thiel, C., Engelmann, S., et al. (2006a). High efficiency transfection of plasmodium berghei facilitates novel selection procedures. *Mol. Biochem. Parasitol.* 145, 60–70. doi: 10.1016/j.molbiopara.2005.09.007

Janse, C. J., Ramesar, J., and Waters, A. P. (2006b). High-efficiency transfection and drug selection of genetically transformed blood stages of the rodent malaria parasite plasmodium berghei. *Nat. Protoc.* 1, 346. doi: 10.1038/nprot.2006.53

Kadota, K., Ishino, T., Matsuyama, T., Chinzei, Y., and Yuda, M. (2004). Essential role of membrane-attack protein in malarial transmission to mosquito host. *Proc. Natl. Acad. Sci.* 101, 16310–16315. doi: 10.1073/pnas.0406187101

Kaiser, K., Matuschewski, K., Camargo, N., Ross, J., and Kappe, S. H. (2004). Differential transcriptome profiling identifies plasmodium genes encoding pre-erythrocytic stage-specific proteins. *Mol. Microbiol.* 51, 1221–1232. doi: 10.1046/j.1365-2958.2003.03909.x

Käll, L., Krogh, A., and Sonnhammer, E. L. (2007). Advantages of combined transmembrane topology and signal peptide prediction—the phobius web server. *Nucleic Acids Res.* 35, W429–W432. doi: 10.1093/nar/gkm256

Kariu, T., Ishino, T., Yano, K., Chinzei, Y., and Yuda, M. (2006). Celtos, a novel malarial protein that mediates transmission to mosquito and vertebrate hosts. *Mol. Microbiol.* 59, 1369–1379. doi: 10.1111/j.1365-2958.2005.05024.x

Lasonder, E., Rijpma, S. R., van Schaijk, B. C., Hoeijmakers, W. A., Kensche, P. R., Gresnigt, M. S., et al. (2016). Integrated transcriptomic and proteomic analyses of p. Falciparum gametocytes: Molecular insight into sex-specific processes and translational repression. *Nucleic Acids Res.* 44, 6087–6101. doi: 10.1093/nar/gkw536

Le Roch, K. G., Zhou, Y., Blair, P. L., Grainger, M., Moch, J. K., Haynes, J. D., et al. (2003). Discovery of gene function by expression profiling of the malaria parasite life cycle. *Science* 301, 1503–1508. doi: 10.1126/science.1087025

Lefevre, T., Ohm, J., Dabiré, K. R., Cohuet, A., Choisy, M., Thomas, M. B., et al. (2018). Transmission traits of malaria parasites within the mosquito: Genetic variation, phenotypic plasticity, and consequences for control. *Evol. Appl.* 11, 456–469. doi: 10.1111/eva.12571

Mitri, C., Bischoff, E., Takashima, E., Williams, M., Eiglmeier, K., Pain, A., et al. (2015). An evolution-based screen for genetic differentiation between anopheles sister taxa enriches for detection of functional immune factors. *PLoS Pathog.* 11, e1005306. doi: 10.1371/journal.ppat.1005306

Modrzynska, K., Pfander, C., Chappell, L., Yu, L., Suarez, C., Dundas, K., et al. (2017). A knockout screen of apiap2 genes reveals networks of interacting transcriptional regulators controlling the plasmodium life cycle. *Cell Host Microbe* 21, 11–22. doi: 10.1016/j.chom.2016.12.003

Molina-Cruz, A., DeJong, R. J., Charles, B., Gupta, L., Kumar, S., Jaramillo-Gutierrez, G., et al. (2008). Reactive oxygen species modulate anopheles gambiae immunity against bacteria and plasmodium. *J. Biol. Chem.* 283, 3217–3223. doi: 10.1074/jbc.M705873200

Molina-Cruz, A., Garver, L. S., Alabaster, A., Bangiolo, L., Haile, A., Winikor, J., et al. (2013). The human malaria parasite pfs47 gene mediates evasion of the mosquito immune system. *Science* 340, 984–987. doi: 10.1126/science.1235264

Molina-Cruz, A., Canepa, G. E., e Silva, T. L. A., Williams, A. E., Nagyal, S., Yenkoidiok-Douti, L., et al. (2020). Plasmodium falciparum evades immunity of anopheline mosquitoes by interacting with a pfs47 midgut receptor. *Proc. Natl. Acad. Sci.* 117, 2597–2605. doi: 10.1073/pnas.1917042117

Moon, R. W., Taylor, C. J., Bex, C., Schepers, R., Goulding, D., Janse, C. J., et al. (2009). A cyclic gmp signalling module that regulates gliding motility in a malaria parasite. *PLoS Pathog.* 5, e1000599. doi: 10.1371/journal.ppat.1000599

Morrissette, N. S., and Sibley, L. D. (2002). Cytoskeleton of apicomplexan parasites. *Microbiol. Mol. Biol. Rev.* 66, 21–38. doi: 10.1128/MMBR.66.1.21-38.2002

Muñoz, E. E., Hart, K. J., Walker, M. P., Kennedy, M. F., Shipley, M. M., and Lindner, S. E. (2017). Alba4 modulates its stage-specific interactions and specific mrna fates during plasmodium yoelii growth and transmission. *Mol. Microbiol.* 106, 266–284. doi: 10.1111/mmi.13762

Nikolaeva, D., Draper, S. J., and Biswas, S. (2015). Toward the development of effective transmission-blocking vaccines for malaria. *Expert Rev. Vaccines* 14, 653–680. doi: 10.1586/14760584.2015.993383

Nikolaeva, D., Illingworth, J. J., Miura, K., Alanine, D. G., Brian, I. J., Li, Y., et al. (2020). Functional characterization and comparison of plasmodium falciparum proteins as targets of transmission-blocking antibodies. *Mol. Cell. Proteomics* 19, 155–166. doi: 10.1074/mcp.RA117.000036

Osta, M. A., Christophides, G. K., and Kafatos, F. C. (2004). Effects of mosquito genes on plasmodium development. *Science* 303, 2030–2032. doi: 10.1126/science.1091789

Otto, T. D., Wilinski, D., Assefa, S., Keane, T. M., Sarry, L. R., Böhme, U., et al. (2010). New insights into the blood-stage transcriptome of plasmodium falciparum using rna-seq. *Mol. Microbiol.* 76, 12–24. doi: 10.1111/j.1365-2958.2009.07026.x

Otto, T. D., Böhme, U., Jackson, A. P., Hunt, M., Franke-Fayard, B., Hoeijmakers, W. A., et al. (2014). A comprehensive evaluation of rodent malaria parasite genomes and gene expression. *BMC Biol.* 12, 86. doi: 10.1186/s12915-014-0086-0

Paskewitz, S. M., and Shi, L. (2005). Bypassing the midgut results in development of plasmodium berghei oocysts in a refractory strain of anopheles gambiae (diptera: Culicidae). *J. Med. Entomol.* 42, 712–715. doi: 10.1603/0022-2585(2005)042[0712:BTMRID]2.0.CO;2

Patzewitz, E.-M., Guttery, D. S., Poulin, B., Ramakrishnan, C., Ferguson, D. J., Wall, R. J., et al. (2013). An ancient protein phosphatase, shlp1, is critical to microneme development in plasmodium ookinetes and parasite transmission. *Cell Rep.* 3, 622–629. doi: 10.1016/j.celrep.2013.01.032

Potocnjak, P., Yoshida, N., Nussenzweig, R. S., and Nussenzweig, V. (1980) Monovalent fragments (Fab) of monoclonal antibodies to a sporozoite surface antigen (Pb44) protect mice against malarial infection. *J. Exp. Med.* 151 (6), 1504–1513.

Reid, A. J., Talman, A. M., Bennett, H. M., Gomes, A. R., Sanders, M. J., Illingworth, C. J., et al. (2018). Single-cell rna-seq reveals hidden transcriptional variation in malaria parasites. *Elife* 7, e33105. doi: 10.7554/eLife.33105

Rovira-Graells, N., Gupta, A. P., Planet, E., Crowley, V. M., Mok, S., de Pouplana, L. R., et al. (2012). Transcriptional variation in the malaria parasite plasmodium falciparum. *Genome Res.* 22, 925–938. doi: 10.1101/gr.129692.111

Santos, J. M., Lebrun, M., Daher, W., Soldati, D., and Dubremetz, J.-F. (2009). Apicomplexan cytoskeleton and motors: Key regulators in morphogenesis, cell division, transport and motility. *Int. J. Parasitol.* 39, 153–162. doi: 10.1016/j.ijpara.2008.10.007

Siden-Kiamos, I., Ecker, A., Nybäck, S., Louis, C., Sinden, R. E., and Billker, O. (2006). Plasmodium berghei calcium-dependent protein kinase 3 is required for ookinete gliding motility and mosquito midgut invasion. *Mol. Microbiol.* 60, 1355–1363. doi: 10.1111/j.1365-2958.2006.05189.x

Simões, M. L., Dong, Y., Hammond, A., Hall, A., Crisanti, A., Nolan, T., et al. (2017). The anopheles fbn9 immune factor mediates plasmodium species-specific defense through transgenic fat body expression. *Dev. Comp. Immunol.* 67, 257–265. doi: 10.1016/j.dci.2016.09.012

Sinden, R. E. (1997). "Infection of mosquitoes with rodent malaria," in *The molecular biology of insect disease vectors* (Dordrecht: Springer), 67–91.

Smith, R. C., Vega-Rodríguez, J., and Jacobs-Lorena, M. (2014). The plasmodium bottleneck: Malaria parasite losses in the mosquito vector. *Mem. Inst. Oswaldo Cruz* 109, 644–661. doi: 10.1590/0074-0276130597

Tomas, A. M., Margos, G., Dimopoulos, G., Van Lin, L. H., de Koning-Ward, T. F., Sinha, R., et al. (2001). P25 and p28 proteins of the malaria ookinete surface have multiple and partially redundant functions. *EMBO J.* 20, 3975–3983. doi: 10.1093/emboj/20.15.3975

Tremp, A. Z., and Dessens, J. T. (2011). Malaria imc1 membrane skeleton proteins operate autonomously and participate in motility independently of cell shape. *J. Biol. Chem.* 286, 5383–5391. doi: 10.1074/jbc.M110.187195

Tremp, A. Z., Khater, E. I., and Dessens, J. T. (2008). Imc1b is a putative membrane skeleton protein involved in cell shape, mechanical strength, motility, and infectivity of malaria ookinetes. *J. Biol. Chem.* 283, 27604–27611. doi: 10.1074/jbc.M801302200

Turturice, B. A., Lamm, M. A., Tasch, J. J., Zalewski, A., Kooistra, R., Schroeter, E. H., et al. (2013). Expression of cytosolic peroxiredoxins in plasmodium berghei ookinetes is regulated by environmental factors in the mosquito bloodmeal. *PLoS Pathog.* 9, e1003136. doi: 10.1371/journal.ppat.1003136

Ukegbu, C. V., Akinosoglou, K. A., Christophides, G. K., and Vlachou, D. (2017). Plasmodium berghei pimms2 promotes ookinete invasion of the anopheles gambiae mosquito midgut. *Infect. Immun.* 85 (8), e00139–17. doi: 10.1128/IAI.00139-17

Ukegbu, C. V., Giorgalli, M., Tapanelli, S., Rona, L. D., Jaye, A., Wyer, C., et al. (2020). Pimms43 is required for malaria parasite immune evasion and sporogonic development in the mosquito vector. *Proc. Natl. Acad. Sci.* 117, 7363–7373. doi: 10.1073/pnas.1919709117

Volkmann, K., Pfander, C., Burstroem, C., Ahras, M., Goulding, D., Rayner, J. C., et al. (2012). The alveolin imc1h is required for normal ookinete and sporozoite motility behaviour and host colonisation in plasmodium berghei. *PLoS One* 7, e41409. doi: 10.1371/journal.pone.0041409

Waters, A. P. (2016). Epigenetic roulette in blood stream plasmodium: Gambling on sex. *PLoS Pathog.* 12, e1005353. doi: 10.1371/journal.ppat.1005353

White, B. J., Lawniczak, M. K., Cheng, C., Coulibaly, M. B., Wilson, M. D., Sagnon, N. F., et al. (2011). Adaptive divergence between incipient species of anopheles gambiae increases resistance to plasmodium. *Proc. Natl. Acad. Sci.* 108, 244–249. doi: 10.1073/pnas.1013648108

Winger, L. A., Tirawanchai, N., Nicholas, J., Carter, H. E., Smith, J. E., and Sinden, R. E. (1988) Ookinete antigens of Plasmodium berghei. Appearance on the zygote surface of an Mr 21 kD determinant identified by transmission-blocking monoclonal antibodies. *Parasite Immunol.* 10 (2), 193–207. doi: 10.1111/j.1365-3024.1988.tb00214.x

Yeoh, L. M., Goodman, C. D., Mollard, V., McFadden, G. I., and Ralph, S. A. (2017). Comparative transcriptomics of female and male gametocytes in plasmodium berghei and the evolution of sex in alveolates. *BMC Genomics* 18, 734. doi: 10.1186/s12864-017-4100-0

Zheng, W., Kou, X., Du, Y., Liu, F., Yu, C., Tsuboi, T., et al. (2016). Identification of three ookinete-specific genes and evaluation of their transmission-blocking potentials in plasmodium berghei. *Vaccine* 34, 2570–2578. doi: 10.1016/j.vaccine.2016.04.011

Conflict of Interest: The authors declare that the research was conducted in the absence of any commercial or financial relationships that could be construed as a potential conflict of interest.

Advantages of publishing in Frontiers

OPEN ACCESS
Articles are free to read for greatest visibility and readership

FAST PUBLICATION
Around 90 days from submission to decision

HIGH QUALITY PEER-REVIEW
Rigorous, collaborative, and constructive peer-review

TRANSPARENT PEER-REVIEW
Editors and reviewers acknowledged by name on published articles

Frontiers
Avenue du Tribunal-Fédéral 34
1005 Lausanne | Switzerland

Visit us: www.frontiersin.org
Contact us: frontiersin.org/about/contact

REPRODUCIBILITY OF RESEARCH
Support open data and methods to enhance research reproducibility

DIGITAL PUBLISHING
Articles designed for optimal readership across devices

FOLLOW US
@frontiersin

IMPACT METRICS
Advanced article metrics track visibility across digital media

EXTENSIVE PROMOTION
Marketing and promotion of impactful research

LOOP RESEARCH NETWORK
Our network increases your article's readership